STRUCTURAL STUDIES OF DNP-BINDING IMMUNOGLOBULINS

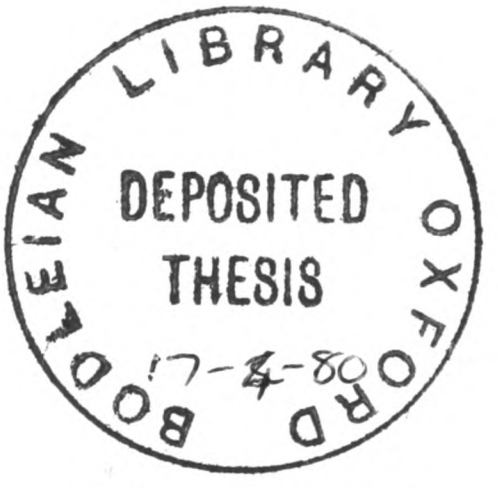

Roland Jackson
Exeter College, Oxford

A thesis submitted in partial fulfilment of the requirements for the degree of Doctor of Philosophy

September 1979

To my parents

and to Nicky.

ABSTRACT

Structural studies of DNP-binding immunoglobulins

W.R.C. Jackson, Exeter College
Submitted for the degree of D.Phil., September 1979

The importance of tryptophan in the combining sites of anti-DNP antibodies is evaluated from a series of model studies. The thermodynamic parameters characterizing the formation of a DNP/tryptophan complex are determined. The contribution of this interaction to the affinity and specificity of anti-DNP antibodies is discussed.

The accuracy of antibody combining site structures generated by model-building is examined, using available crystallographic data. The average error of alpha-carbon atom positions is estimated to be 1-2 Å.

The binding of nitrophenyl compounds to the V_L dimer of the DNP-binding mouse myeloma protein 315 is investigated by ^1H n.m.r. It is concluded that any conformational changes are small, and that the physical basis for the DNP-binding specificity of the V_L dimer is the conservation of structural features which are important in determining the specificity of the intact protein 315. A model of the combining site of the V_L dimer is described. The proposed site is a large cavity bounded by the aromatic side-chains of the Trp-93_L and Tyr-34_L residues. The structure is able to explain the large upfield chemical shift changes of the ligand resonances observed on binding. The kinetic parameters and structural extent of the pH-dependent conformational change of the V_L dimer are investigated by fluorescence and ^1H n.m.r. The transition does not obey a reversible one-step mechanism, and is limited in extent.

The involvement of two tyrosine residues in the hypervariable regions of protein 315 is investigated by specific nitration. Nitration of Tyr-34_L has no effect on the affinity of protein 315 or of the V_L dimer for several ligands. It is concluded that no hydrogen bond is formed between the phenolic group of Tyr-34_L and the 2-nitro group of the ligand. From measurements of the perturbation of the visible absorption spectrum of protein 315 nitrated at Tyr-33_H, it is concluded that this residue is in proximity to the side-chains, but not the nitrophenyl rings, of bound ligands.

Several aspects of the interaction of a homogeneous mouse anti-DNP antibody, protein A3, with nitrophenyl and similar ligands are described. The findings are discussed in relation to the heterogeneity and cross-reactivity of antisera.

CONTENTS

ACKNOWLEDGEMENTS

My supervisor, Dr. R.A. Dwek, has been a continual source of inspiration and encouragement, and I would like to thank him for three very enjoyable years. I have been greatly aided by discussions with all the members of his group, past and present - Jonathan Boyd, Steve Dower, Simon Easterbrook-Smith, Peter Gettins, Arabella Morris, Marie-Rose van Schravendijk, Simon Wain-Hobson, Keith Willan and Carolyn Wright.

I would like to thank Professor R.R. Porter for extending to me the use of the facilities of the Department of Biochemistry. I am indebted to the technical and administrative staff of the Department, without whose help this research could not have materialized.

It has also been my good fortune to benefit from the help of many other people during the course of this work. I would like to thank the following in particular:

Dr. D. Givol, for inviting me to use the facilities of the Department of Chemical Immunology, Weizmann Institute, Israel; and Dr. M. Gavish, with whom I worked on several aspects of the chemical studies described in Chapter 6.

Professor R. Huber and Dr. A. Jones, who allowed me access to the computer graphics system of protein model-building at the Max Planck Institute of Biochemistry, Munich.

Dr. B.A. Askonas, who gave me the cell line producing protein A3; and Dr. G.G.B. Klaus, who furnished me with details of his affinity purification method for protein A3, prior to publication.

Dr. A.F. Williams and his group, who helped a physical biochemist with cellular techniques; and L. Hackfath, who recloned the A3 cell line.

I would like to thank the Medical Research Council for a post-graduate training award, and Exeter College for the award of an Usher-Cunningham Studentship.

I am very grateful to my wife, Nicky, for proof-reading the entire manuscript and enduring endless attempts at the Berg piano sonata.

Lastly, my thanks to Mrs H. Holloway, who decoded my writing with apparent ease and carefully typed the manuscript.

ABBREVIATIONS

ANS	1-anilinonaphthalene-8-sulphonic acid
BBS	Borate buffered saline
BGG	Bovine gamma globulin
BSA	Bovine serum albumen
CD	Circular dichroism
δ	Chemical shift
$\Delta\delta$	Chemical shift change
DEAE	Diethylaminoethyl
DNP	2,4-dinitrophenyl
DSS	2,2-dimethyl-2-silapentane-5-sulphonate
DTT	Dithiothreitol
EDTA	Diaminoethane tetra-acetic acid
Fab, Fab'	Immunoglobulin fragments produced by papain or pepsin cleavage respectively, each containing a complete light chain and N-terminal two domains of a heavy chain
Fc	Crystallizable fragment of immunoglobulin containing the C-terminal two domains of two heavy chains
Fd	H-chain component of an Fab fragment
Fv	Immunoglobulin fragment composed of the variable domains of an H-chain and an L-chain
FCS	Foetal calf serum
HAM	Culture medium (Gibco 176)
H-chain	Heavy chain
H_1, H_2, H_3	First, second and third H-chain hypervariable loops
HEPES	4-(2-hydroxylethyl)-1-piperazine-ethane sulphonic acid
HSA	Human serum albumen
Ig	Immunoglobulin
KLH	Keyhole limpet hemocyanin
L-chain	Light chain
L_1, L_2, L_3	First, second and third L-chain hypervariable loops
NIP	4-hydroxy-5-iodo-3-nitrophenylacetyl
N.m.r.	Nuclear magnetic resonance
ORD	Optical rotatory dispersion
PBS	Phosphate buffered saline
pFc'	Immunoglobulin fragment composed of the C-terminal domains of two heavy chains
pH*	pH of ^2H_2O solution (meter reading)
p.p.m.	Parts per million

Q_{max}	Percentage of protein fluorescence quenched by saturating ligand
RAM	Rabbit anti-mouse IgG
SDS	Sodium dodecyl sulphate
SDS-PAGE	Sodium dodecyl sulphate polyacrylamide gel electrophoresis
SRBC	Sheep red blood cells
TNBS	2,4,6-trinitrobenzene sulphonic acid
TNM	Tetranitromethane
TNP	2,4,6-trinitrophenyl
Tris	Tris-(hydroxymethyl)-methylamine
T_1, T_2	Spin-lattice and spin-spin relaxation times
V_H, V_L	Variable domains of H-chain and L-chain
$V_L V_H$	Recombined Fv fragment
VS	Veronal buffered saline

Single letter amino acid code:

A - ala; B - asn/asp; C - cys; D - asp; E - glu;
F - phe; G - gly; H - his; I - ile; K - lys; L - leu;
M - met; N - asn; P - pro; Q - gln; R - arg; S - ser;
T - thr; V - val; W - trp; Y - tyr; Z - gln/glu; X - pca

CHAPTER 1

INTRODUCTION

The ability of an individual to acquire immunity against reinfection with a disease has been realised for many centuries. An important advance in the understanding of this process arose from the discovery that vertebrates are capable of producing specific antidotes to foreign substances. These antidotes, or antibodies, were shown to belong to a class of proteins called globulins, and to be present in the serum as a highly heterogeneous population of molecules. The generic term 'immunoglobulin' is now used to describe these proteins.

The primary function of antibodies is to bind to the diverse array of foreign antigens which may invade the organism. The heterogeneity of the antibody population is a consequence of this diversity of antigenic structures. Once an antigen has been bound, the antibody is involved in several secondary processes which are directed towards neutralization of the effects of the foreign material. An example is the lysis of foreign cells by the system of serum proteins known as complement. The constancy of the basic structure of all immunoglobulins, described in detail below, reflects the requirement of antibodies with many different binding specificities to activate a small number of secondary processes.

The experiments described in this thesis were designed to investigate the structural basis for the specificity of dinitrophenyl-binding immunoglobulins. It is therefore appropriate to summarize present knowledge of antibody structure, specificity and diversity.

Homogeneous immunoglobulins

Acquisition of detailed knowledge of the structural and functional properties of antibodies is greatly facilitated by the availability of homogeneous immunoglobulins. Four types of approach have been used to obtain such proteins from the normal heterogeneous population.

1. Myeloma proteins

The clonal selection theory of antibody formation (Burnet, 1959) is now generally accepted. According to this theory, a given clone of lymphocytes is committed to producing an antibody of a particular specificity. The disease myelomatosis, which is found most frequently in humans and in certain strains of mice, is associated with a neoplastic transformation of a single lymphocyte. The disease results in extensive proliferation of a single clone, and concomitant overproduction of the corresponding immunoglobulin. Since the concentration of the immunoglobulin may reach 10 mg/ml, the protein may be easily purified. Myelomatosis may be induced in certain strains of mice by injection of mineral oils (Potter, 1972). Almost all the detailed structural work to date has involved the use of myeloma proteins. Experiments using the mouse myeloma protein 315 are described in this thesis.

There is one major drawback in using myeloma proteins for the study of antibody specificity. The neoplastic process is apparently random, with the result that any binding activity of the myeloma protein has to be established by a laborious screening procedure. It is generally believed, however, that myeloma proteins are representative samples of the natural pool of antibodies (Rudikoff and Claflin, 1976; Granato et al., 1974). They have all the structural characteristics of normal immunoglobulins, and may have affinities for ligands which lie within

the range of affinities of antibodies elicited against those ligands in a normal immune response. The most compelling evidence for their equivalence to natural antibodies is that myeloma proteins with a particular specificity often share precise chemical and serological characteristics with naturally raised antibodies of the same specificity.

2. Specific immunization procedures

With a suitable choice of antigen and immunization schedule, a predominantly homogeneous response can sometimes be obtained. This approach has been particularly useful for genetic and structural studies of rabbit antibodies, since myelomatosis has not been observed in rabbits. For example, several streptococcal carbohydrates are capable of eliciting a predominantly homogeneous response in individual rabbits (Osterland et al., 1966; Schalch et al., 1979). Homogeneous responses have also been obtained to other antigens under some conditions (Keck et al., 1973; Montgomery et al., 1975). The factors most important in determining whether or not a response will be predominantly homogeneous are not clear. Hyperimmunization with a chemically simple antigen appears to produce the best results. Because of the extensive differences between individual systems, specific immunization procedures are not the methods of choice for producing antibodies for structural studies.

3. Stimulation of single clones

Two similar methods, involving transfer of limited numbers of cells into irradiated recipients, have been developed. Small splenic fragments from irradiated mice which have received about 10^6 immune spleen cells may be stimulated in vitro (Klinman, 1971; Klinman, 1972). Alternatively, splenic fragments from

mice producing a response of limited heterogeneity may be serially transferred into irradiated recipients (Askonas et al., 1970). The disadvantages of these methods are that the large amounts of protein required for structural studies are not available, and that the clones have a limited proliferative potential of about 90 generations (Williamson and Askonas, 1972).

4. Cell fusion

The recent discovery that a mouse spleen cell can be fused with a myeloma cell to give a hybrid cell or 'hybridoma', provides a powerful method for producing homogeneous antibodies (Köhler and Milstein, 1975; Köhler et al., 1976). If a non-secreting variant of the myeloma cell line is used, the hybridoma cell synthesizes the antibody originally produced by the spleen cell. However, it has the proliferative and productive characteristics of a myeloma cell, enabling the purification of large amounts of material. A single antibody of a predetermined specificity may therefore be 'immortalized' for further study. This technique has yet to be applied to its full potential by structural immunologists or by those interested in the theoretical aspects of protein-ligand interactions. Preliminary experiments on a DNP-binding hybridoma protein are described in Chapter 7.

Immunoglobulin structure

1. Basic structure and classification

Immunoglobulins are found in vertebrates, but not in invertebrates. The basic immunoglobulin structure has been conserved throughout vertebrate evolution. It consists of four polypeptide chains, of which two are termed heavy chains (H-chains, MW = 50,000-75,000) and two are termed light chains (L-chains,

MW = 22,000-23,000). A given antibody molecule contains identical H-chains and identical L-chains. The chains are held together by noncovalent forces and by disulphide bonds. The arrangement of the chains was deduced from chemical and enzymic studies. The importance of disulphide bonds and the identification of H-chains and L-chains were described by Edelman and Poulik (1961). It had been shown by Porter (1959a) that rabbit immunoglobulin G could be cleaved by crystalline papair to give two distinct fragments of MW ~50,000. One fragment, Fab, retained antigen binding activity. The other fragment, Fc, present in half the yield of the Fab fragment, was crystallizable. The relative arrangement of the two Fab fragments with one Fc fragment, and the arrangement of the H-chains and L-chains was proposed by Fleischman et al. (1962). The structure is shown in Figure 1.1, and has subsequently been confirmed by chemical and physical studies.

Despite their heterogeneity, immunoglobulins may be classified serologically into groups. Serological classification is based on the ability of an animal to make antibodies against antigenic determinants on immunoglobulins of another animal of the same species or of a different species. Determinants present on antibodies of every individual of a given species are termed isotypes. These determinants would only be recognized as foreign by heterologous antisera. H-chains are divided into classes (IgG, IgA, IgM, IgD and IgE) and sub-classes (e.g. IgG_1, IgG_{2a}, IgG_{2b} and IgG_3). L-chains are divided into types (κ and λ) and sub-types (λ_1 and λ_2). Isotypic determinants are associated with particular subclasses and subtypes. A similar classification may be made for the immunoglobulins of any species. The classification of these isotypic determinants, initially made serologically, is interpretable in terms of conserved amino acid sequences in H-

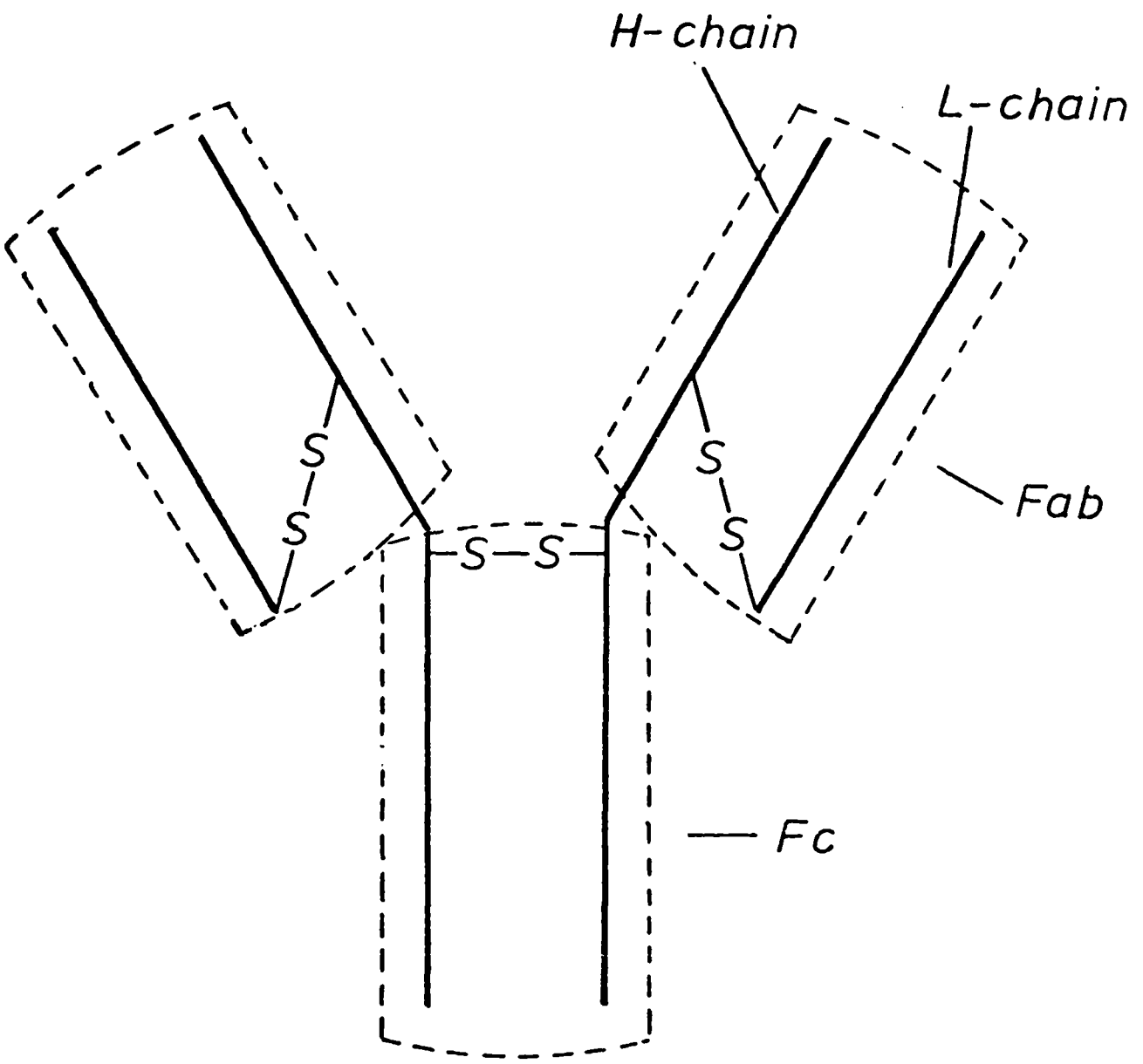

Figure 1.1 Basic immunoglobulin structure

Schematic representation of the structure of rabbit IgG, showing the relationship of the H-chains and L-chains to the Fab and Fc fragments produced by papain cleavage. After Fleischman et al. (1963).

chains and L-chains.

Immunoglobulins belonging to particular subclasses have characteristic molecular weights, inter-chain disulphide bridges and carbohydrate content. They also have distinct biological properties. Some properties of the mouse IgG subclasses are listed in Table 1.1. Mouse IgG, in common with IgG of other

Table 1.1 Some properties of mouse IgG subclasses

Subclass	Disulphide bonded structure	Fixation of Guinea Pig complement	Mediation of passive cutaneous anaphylaxis in		Transport across placenta
			Mouse	2. Guinea Pig	
IgG_1	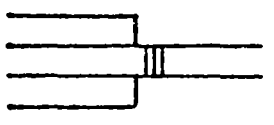	-	+	-	+
IgG_{2a}	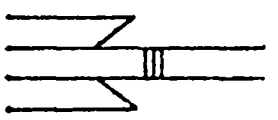	+	-	+	+
IgG_{2b}	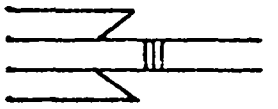	+	-	+	+
IgG_3	probably 2 H-H bonds	-	-	-	++

Data from Nisonoff et al. (1975)

species, occurs as the basic four-chain structure with a molecular weight of ~150,000, and a low carbohydrate content of 2-3%. In contrast to human IgA, which occurs in serum predominantly as a four-chain monomer with a molecular weight of ~160,000, 80% of mouse serum IgA is in the form of disulphide-linked polymers. Mouse IgA has a carbohydrate content of 7-8%. Mouse secretory IgA is similar to human secretory IgA, found for example in saliva and colostrum, in that the IgA polymer is associated with a J-chain (MW = 15,000) and a secretory piece (MW = 70,000). No secretory piece is associated with the IgA produced by mice in

ascites fluid. The IgA produced by mice of the BALB/c strain is unusual in that no H-L disulphide bond is formed, but that one is formed between the two L-chains. Mouse IgM, similar to human IgM, occurs as a high molecular weight pentamer, disulphide-bonded through the Fc regions, and associated with a J-chain. The molecular weight of the monomer is ~190,000, and the IgM has a carbohydrate content of ~10%. The majority of immunoglobulins of any species are IgG, IgA or IgM. However, the two other classes, IgE and IgD, may often be found in small amounts. IgE has been identified in mice. Mouse IgE, in common with mouse IgG_1, is capable of mediating passive cutaneous anaphylaxis in the mouse. By analogy with human IgE, mouse IgE should occur as a monomer with a molecular weight of ~190,000, and a carbohydrate content of ~10%. Evidence for IgD on the surface of mouse spleenocytes has been obtained (Melcher et al., 1974; Melcher and Uhr, 1976). It has a molecular weight of ~165,000 and probably contains more carbohydrate than IgM. It appears that any subtype of L-chain may be associated with any subclass of H-chain. However, non-random combinations do occur - for example the preponderance of λ-chains with human IgD (Fahey et al., 1968).

The genes for individual subclasses and subtypes are found to exhibit polymorphism. Corresponding antigenic determinants, known as allotypic determinants, may therefore be found in some, but not all, members of a given species (Grubb, 1956; Oudin, 1956). Allotypic determinants are inherited in strictly Mendelian fashion, although allelic exclusion occurs in individual antibody-producing cells (Pernis et al., 1965). The amino acid changes responsible for some allotypic differences have been determined.

2. Variable and constant regions

The availability of partial and complete amino acid sequences has given us enormous insight into the structure, function and genetic origin of immunoglobulins. The sequences of individual chains may be divided into sections, approximately 110 residues in length, showing homology to each other. This conclusion was originally made from studies on L-chains, which have two such sections (Hilschman and Craig, 1965). The N-terminal section was found to exhibit much more variability than the C-terminal section. These segments were termed the variable region (V-region) and constant region (C-region) respectively. It was proposed that the variability reflected different antigenic specificities, and that the V-region and C-region were encoded by separate genes (Dreyer and Bennett, 1965). The studies were extended to the H-chain, which has either four (IgG, IgA and IgD) or five (IgM and IgE) such homology regions. Again, the N-terminal region is more variable than the other three or four regions. These homology regions were proposed to fold into discrete structures, or domains, joined by more extended regions of polypeptide chain (Edelman et al., 1969). The domain hypothesis accounts for the pattern of digestion of immunoglobulins by proteases, and has been substantiated by X-ray crystallography. A diagram of the domain structure of an immunoglobulin is shown in Figure 1.2. Different functions are associated with different domains. Formal proof that antigen binding is a function of the V-domain came from the production of an immunoglobulin Fv fragment, consisting only of the V-regions, which retained full ligand binding activity (Inbar et al., 1972). The secondary functions of antibodies are associated with the C-domains, in particular with the Fc region.

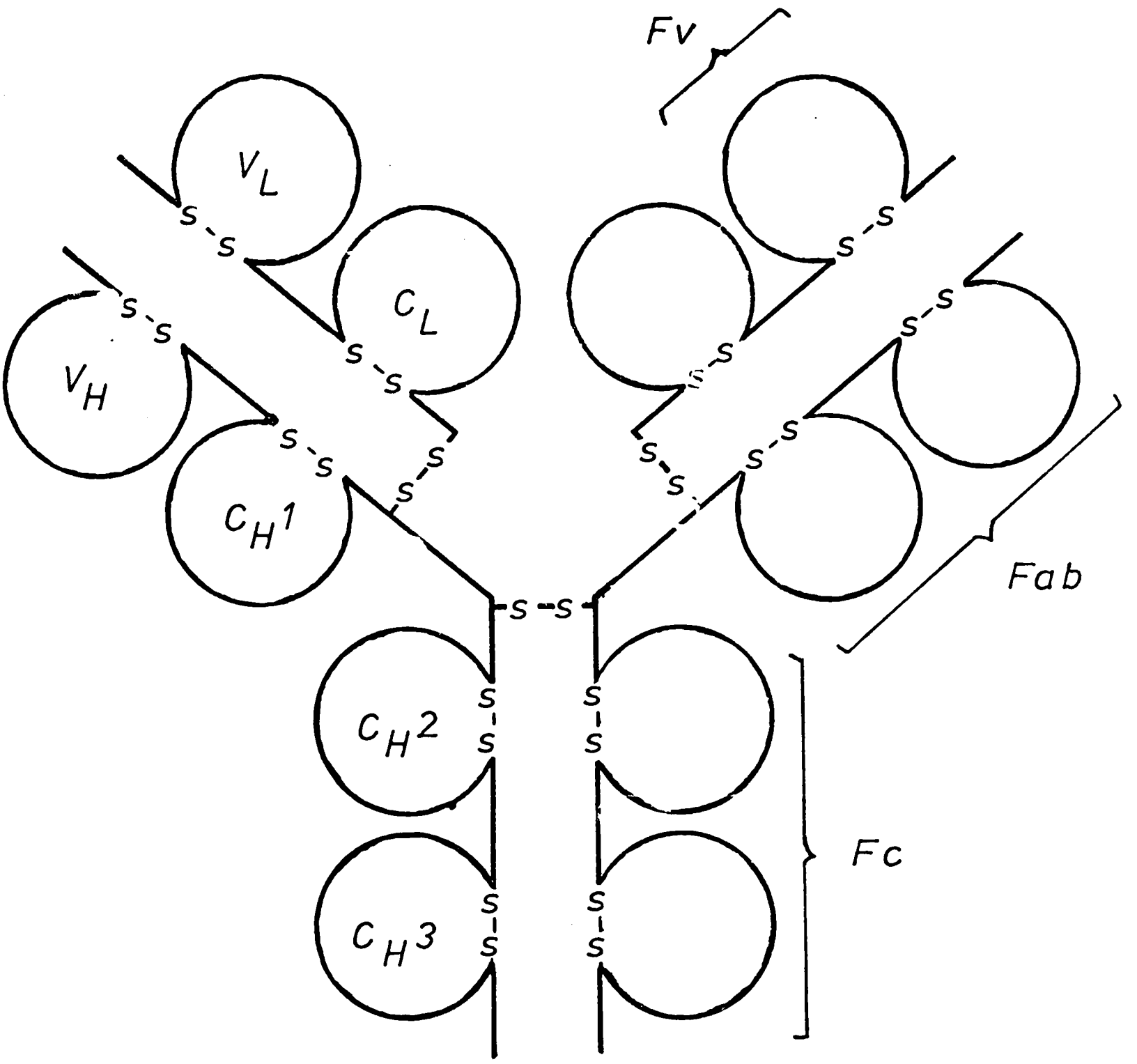

Figure 1.2 The domain structure of immunoglobulins

An illustration of the relative arrangements of the V-domains (V_H and V_L) and C-domains (C_H1, C_H2, C_H3 and C_L) to immunoglobulin fragments (Fv, Fab and Fc).

The pattern of variability in V-region sequences is not random. An extensive comparison of sequences of V-regions of immunoglobulins from the same species and from different species showed that particular positions exhibited high variability (Wu and Kabat, 1970; Kabat and Wu, 1971). These sequences were termed hypervariable regions. They are now generally referred to as 'complementarity determining' regions, since crystallographic studies have shown that six of these regions, three from the H-chain and three from the L-chain, determine the nature of the antigen binding site, as predicted by Wu and Kabat (1970). A distinct pattern of variability also extends to the nonhypervariable, or framework, regions of the V-domains. The sequences may be arbitrarily divided into subgroups of closely related sequences (Niall and Edman, 1967). Defined subgroups emerged prior to mammalian speciation, suggesting that at least one germ-line gene codes for each V-region subgroup. In addition to the isotypic and allotypic antigenic specificities exhibited by immunoglobulins, individual animals possess individual determinants which may not be shared by other individuals of the same species. These determinants are called idiotypic determinants. They are associated with the V-region (Wells et al., 1973), and in particular with the binding site. Idiotypic determinants were originally defined as determinants not observed in other immunoglobulins of the donor nor in immunoglobulins of the same antigenic specificity from other individuals of the same species (Oudin, 1966). The definition has been operationally extended to include specificities shared among antibodies of different individuals, or cross-idiotypic specificities (Kunkel, 1970). A precise understanding of the distribution and expression of idiotypic specificities will come with an understanding of the genetic

basis of antibody diversity.

3. Domain structure

X-ray crystallographic studies have shown that each immunoglobulin domain is built round a conserved structure. This structure has been termed the 'immunoglobulin fold' (Poljak et al., 1973). It consists of two layers of β-pleated sheet, one layer containing three strands of polypeptide chain, and the other having four (Fig. 1.3). The layers are joined by an intradomain disulphide bond. Amino acid residues involved in the immunoglobulin fold are highly conserved in all species. The relative arrangement of the β-pleated sheets is different in the V-domains and in the C-domains. The interdomain contacts between two C-domains are made by the four-chain layers of each domain, whereas dimerization of two V-domains occurs through the three-chain layers (Edmundson et al., 1975). As a result, a cavity, which may be capable of binding ligands, is formed between the two V-domains. The hypervariable sequences are attached to the conserved structure of the framework provided by the immunoglobulin fold. Six hypervariable loops, three from each chain, line the cavity between the V-domains and form the binding site. A conserved framework, to which the hypervariable sequences are attached, appears to be the structural mechanism used to generate the diversity of antigen binding sites. The comparison of immunoglobulin structures determined crystallographically has shown not only that the immunoglobulin fold is a conserved feature, but also that homologous hypervariable loops of the same length have similar structures (Padlan, 1977). It has therefore been considered feasible to construct models of immunoglobulins for which no X-ray data exists, on the basis of their presumed similarity to known structures (Poljak et al., 1974; Padlan et

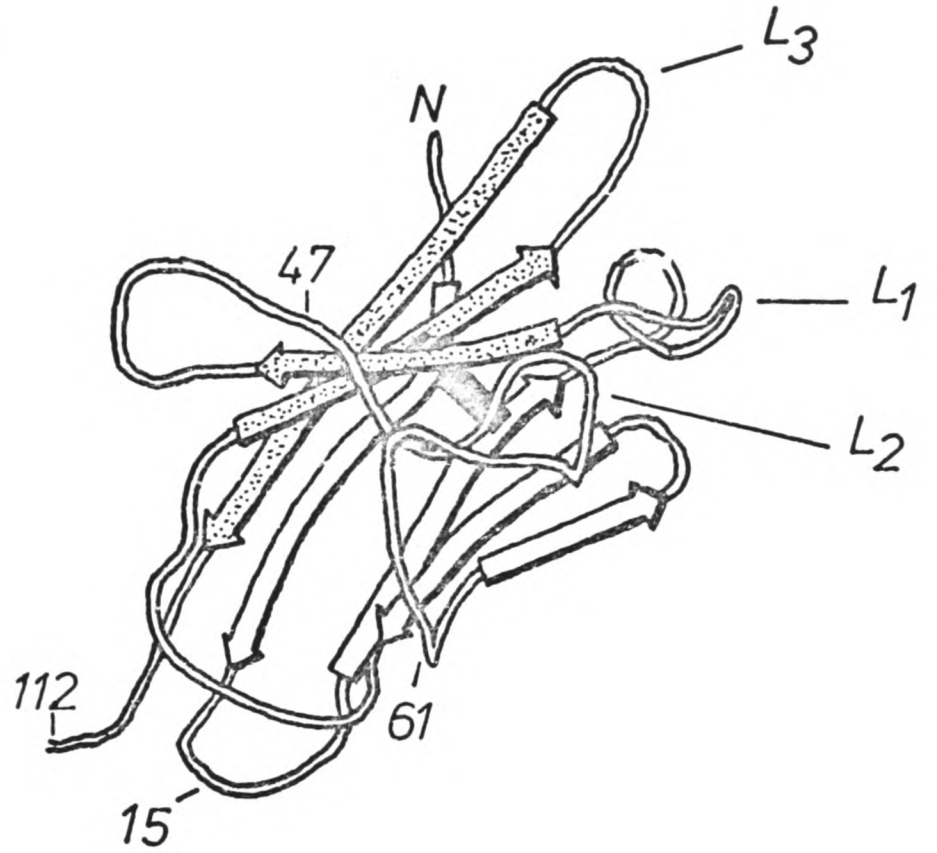

Figure 1.3 The structure of a V_L domain

The structure of the V-domain of monomer 2 of protein Mcg, showing the immunoglobulin fold. The arrows point in the C-terminal direction of the polypeptide chain. The white arrows are in the 4-chain layer, and the shaded arrows are in the 3-chain layer. The solid bar represents the intradomain disulphide bond. The positions of the hypervariable loops (L_1, L_2 and L_3) are indicated. From Schiffer et al. (1973).

al., 1976a). One such model has been constructed of the combining site of the mouse myeloma protein 315, with which this thesis is largely concerned (Padlan et al., 1976a). A quantitative assessment of the accuracy of model-building is presented in Chapter 4.

4. The antigen binding site

Before the application of X-ray crystallography, many features of the combining site had been recognized. The importance of the immunodominant group, that group the most distant from the carrier molecule used for immunization, had been realized. The size of the combining site to several antigens had been determined, generally by inhibition of precipitation using small molecular weight components of the antigen. Combining sites, although varying in size, were able to accommodate five or six linked glucose residues (Kabat, 1960), or about four amino acid residues (Schechter et al., 1966). The possibility of interaction with the carrier molecule as well as with the haptenic group was recognized many years ago (Hooker and Boyd, 1933). This property was used in experiments showing that the antibody combining site could accommodate a polypeptide with a backbone of 10 to 12 carbon atoms (Schechter et al., 1970). One can envisage two extremes of combining site shape - a surface groove, capable like that of lysozyme of binding five or six sugar residues, or a deep cavity, capable of binding less polar molecules. Anti-fluorescein antibodies would be expected to fall into the latter category. The fluorescein group probably fills the entire cavity, since no carrier effect is observed (Voss and Watt, 1977). The smaller DNP group does show a carrier effect, since DNP-lysine generally binds more tightly than the DNP group alone (Eisen and Siskind, 1964; see also Chapter 7). The depth of the DNP-binding site has been

estimated to be about 10-13 Å, both by cross-linking experiments using bifunctional haptens (Valentine and Green, 1967; Wilder et al., 1975), and by using spin-labelled derivatives of different lengths (Hsia and Piette, 1969). The involvement of hypervariable residues in the combining site had been shown by affinity labelling experiments, and the participation of both H-chain and L-chain had been shown by cross-linking the two with a bifunctional reagent (Givol et al., 1971).

The determination, by X-ray crystallography, of the structures of several antibody combining sites confirmed the previous conclusions. These findings now provide the essential starting point for a detailed understanding of the diversity of antigen binding sites. The combining sites of two myeloma proteins, containing bound hapten, are shown in Figure 1.4. Both ligands are bound in sites lined by hypervariable residues, and are in contact with side-chains from both the H-chain and the L-chain. In the case of Fab' New, the vitamin K_1 derivative binds in a shallow groove 15 Å long, 6 Å deep and about 6-7 Å wide at its centre. The napthoquinone ring interacts with the side chain of Tyr-90_L, and with two or three other amino acids. The phytyl side chain of the ligand is bound in an extended conformation, and makes contacts with several amino acids from the L-chain and H-chain (Amzel et al., 1974). The combining site of the Fab' fragment of protein 603 is much deeper than that of protein New. This increase may be attributed to an insertion of six residues in the first hypervariable region of the L-chain (the L_1 loop). The L_1 and H_3 loops may be particularly important in determining the shape and size of a combining site, since they are the most variable in length. The phosphorylcholine ligand occupies only a small region of the binding site of protein 603, allowing the

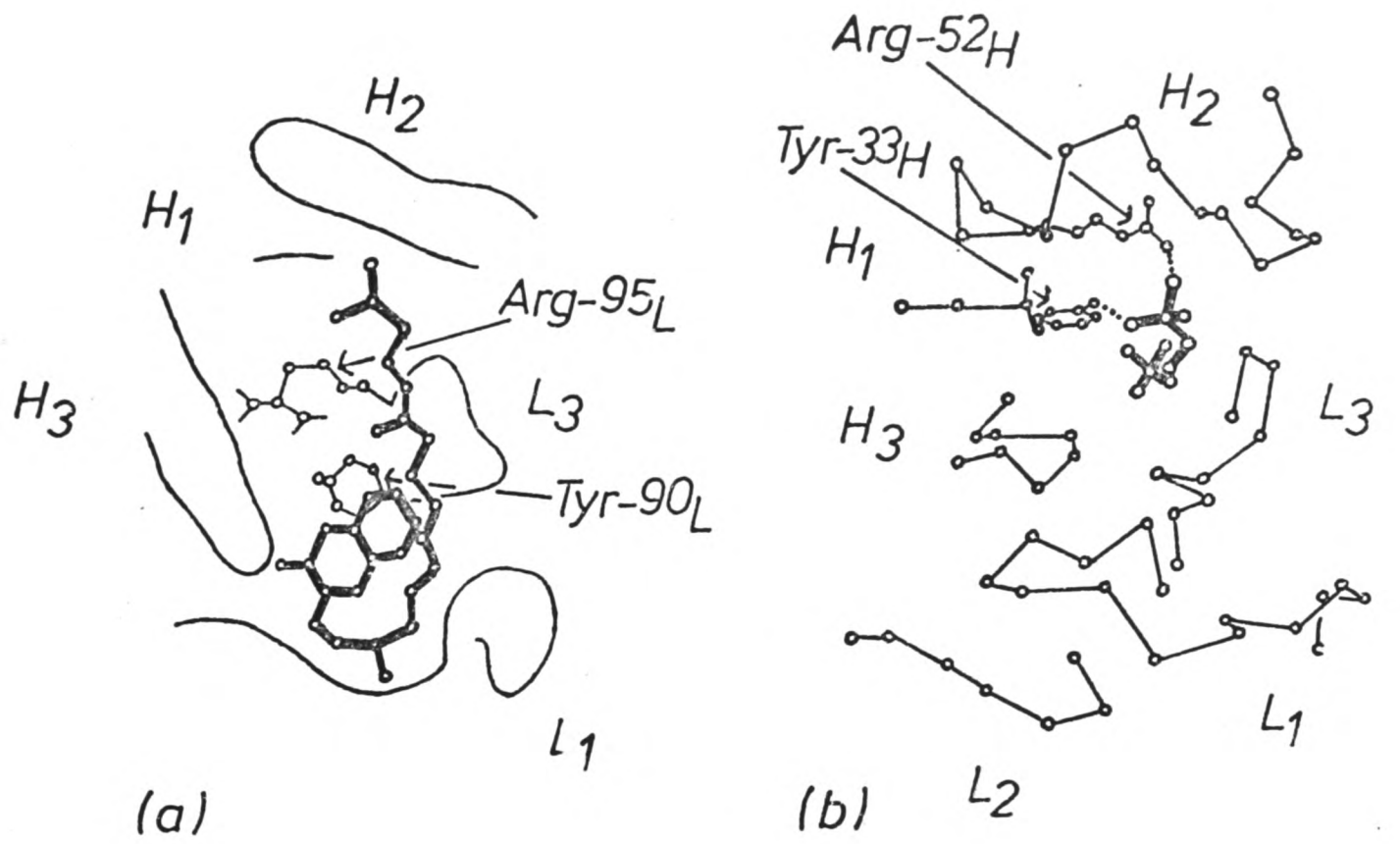

Figure 1.4 The combining sites of two immunoglobulin Fab fragments

(a) The binding site of protein New, determined from X-ray data at 3.5 Å resolution. The ligand, vitamin K_1OH is shown in bold lines. Adapted from Amzel et al. (1974).

(b) The binding site of protein 603, determined from X-ray data at 3.1 Å resolution. The site is viewed in approximately the same orientation as that of protein New. The ligand, phosphorylcholine, is shown in bold lines. Adapted from Segal et al. (1974)

binding of a much larger antigen containing the phosphorylcholine determinant. Contacts of the phosphorylcholine group are predominantly with the H-chain. These include bonding of the phosphate group to Tyr-33_H and Arg-52_H, bonding of the trimethylammonium cation to Glu-35_H and Glu-59_H, and van der Waals contacts with Trp-105_H (Padlan et al., 1976b). The important V_H contact residues are present in all mouse myeloma proteins with phosphorylcholine binding specificity. Indeed, there are similarities both in H_1 sequence and the length of the L_1 loop between these proteins and a human myeloma protein with the same specificity (Riesen et al., 1976; Riesen and Jaton, 1976).

5. Structure and flexibility of the whole immunoglobulin

Our knowledge of the overall shape of the immunoglobulin molecule, deduced from chemical and enzymic approaches, has been confirmed and greatly extended in detail through the use of electron microscopy, X-ray diffraction and other physical techniques. There is general agreement that the IgG molecule is flexible, particularly about the hinge region, and that a variety of structures from T-shaped to Y-shaped are possible (Yquerabide et al., 1970; Sarma et al., 1971; Colman et al., 1976). The relative positions of the Fab and Fc regions can change in the presence of antigen (Feinstein and Rowe, 1965; Valentine and Green, 1967).

A knowledge of the conformational properties of immunoglobulins is important for an understanding of the mechanism by which antigen binding activates secondary processes, such as the complement cascade. Three distinct models have been proposed for this mechanism. In the 'allosteric' model, ligand-induced conformational changes are produced distal to the combining site following antigen binding, and initiate the secondary function.

In the 'distortive' model, the critical factor is the ability of the immunoglobulin to be distorted to accommodate the topological distribution of antigenic determinants. This process would result in the structural alteration of the secondary effector site, or the exposure of a site previously unavailable. For the 'associative' model, it is proposed that polymerization of the antibody by a multivalent antigen is the important feature. It is very difficult to test these theories critically, and there is no reason for them all to be mutually exclusive. Although conformational changes have been detected following ligand binding, it is not clear that these are transmitted to the Fc region, nor, as predicted by the 'allosteric' model, that functional changes are stoichiometrically correlated with site occupation (Metzger, 1978). Most of the present evidence indicates that cross-linking of antibody molecules is of prime importance.

Immunoglobulin light chains

1. General properties

'On the 1st November 1845 I received from Dr. Watson the following note, with a test-tube containing a thick, yellow, semi-solid substance:- 'the tube contains urine of very high specific gravity; when boiled it becomes highly opake; on the addition of nitric acid it effervesces, assumes a reddish hue, becomes quite clear, but, as it cools, assumes the consistence and appearance which you see: heat reliquifies it. What is it?'' (H. Bence Jones, 1848). Jones found the substance to be an 'oxide of albumen', and these proteins became known as Bence-Jones proteins. They are pathological products frequently associated with the disease multiple myelomatosis, and occasionally with macroglobulinaemia and leukaemia. It was not for over a century

that Bence-Jones proteins were shown to be indistinguishable from immunoglobulin L-chains (Edelman and Gally, 1962). Because of their ready availability, Bence-Jones proteins have been extensively studied, and have provided much of our knowledge about the structure of immunoglobulins. The structures of several Bence-Jones proteins or their fragments have been determined by X-ray crystallography (Edmundson et al., 1974a; Epp et al., 1975; Fehlhammer et al., 1975; Colman et al., 1977; Wang et al., 1979).

L-chains tend to associate to form dimers. The association constant between L-L pairs is less than that between H-L pairs, and L-chains frequently occur as a mixture of monomers and dimers at concentrations of ~1mg/ml (Bernier and Putnam, 1963; Green, 1973). κ-chains have a greater tendency than λ-chains to form monomers, and λ-chains may exist as covalently linked dimers (Solomon, 1976). Bence-Jones proteins are easily cleaved in the switch region between V-domains and C-domains. The V-domain is more resistant to proteolysis and has a thermal solubility similar to that of the whole protein (Solomon and McLaughlin, 1969). The two chains of the dimer form a site, lined by hypervariable residues, analogous to the site formed by H-L pairs.

Although the secretion of large quantities of L-chains is a pathological phenomenon, free L-chains are detectable in the plasma and urine of healthy people, indicating a slight natural imbalance of H-chain and L-chain synthesis. At present, no physiological role has emerged for L-chains. It has been suggested that molecules of similar nature may form the T-cell receptor (Janeway et al., 1976). However, there is far from general agreement on this possibility (Jensenius et al., 1977).

2. Binding properties of isolated chains

The binding properties of isolated chains, and of re-recombinant H-chains and L-chains give information on the contribution of individual chains to antibody specificity. It is a general conclusion of these experiments that the major contribution to affinity comes from the H-chain rather than the L-chain. Early experiments showed that the activity of horse anti-rabbit IgG antibodies was largely maintained in isolated H-chains (Fleischman et al., 1963), and that the affinity of the isolated H-chain of rabbit anti-p-azophenyl-β-lactoside antibody was only an order of magnitude lower than that of the parent antibody (Utsumi and Karush, 1964). An extensive study of rabbit anti-DNP and anti-TNP antibodies also showed that most isolated H-chains retained a substantial fraction of the affinity of the native antibodies (Haber and Richards, 1966). Some investigators have found retention of activity in L-chains. About 10% of L-chains from horse anti-diphtheria toxoid retained activity (Raynaud and Mangalo, 1967), and L-chains of rabbit antibodies retained the ability to neutralise T_1 phage (Goodman and Donch, 1965). L-chains of rabbit antibodies to ANS were found to retain some binding activity (Yoo et al., 1967). The affinity for ANS was however very low - approximately 10^2 M^{-1}. Indeed, isolated chains often show no detectable binding activity (Hong and Nisonoff, 1966; Edelman et al., 1963). Affinities of L-chains for ligands are generally much lower than H-chains. They rarely reach values of 10^4-10^5 M^{-1}, representative of low affinity antibodies. The discoveries that the L-chain dimer and V_L dimer of protein 315 retain a substantial fraction of the affinity of the intact antibody for DNP ligands were therefore unexpected (Schechter et al., 1976; Gavish et al., 1977). Experiments

described in Chapter 4 and Chapter 5 were designed to investigate the structural basis for this retention of binding activity.

3. Conformation and flexibility

The retention of binding activity by isolated chains suggests that the conformation of an isolated chain is very similar to its conformation in the intact molecule. ORD and CD measurements on rabbit IgG show that isolated chains retain an ordered structure, although their spectra differ from those of the native molecules (Björk and Tanford, 1971a; Björk and Tanford, 1971b). These differences could well be due to the changed environment of aromatic residues at the domain interfaces rather than to a significant intradomain conformational change. The V-domain and C-domain of an L-chain are able to take up different positions with respect to each other. One chain of the Mcg dimer has a conformation similar to that of the L-chain in an intact antibody, whereas the disposition of domains in the other chain mimics that of an H-chain (Schiffer et al., 1973).

Conformational changes have been observed in L-chains, both in the presence and absence of ligands. The binding of nitro-benzoxadiazole-alanine (NBD-alanine) or DNP-lysine to the L-chain dimer of protein 315 exhibits positive cooperativity. The cooperativity was attributed to a ligand-induced conformational change (Lancet et al., 1977). No information on the extent of this conformational change was presented. Two conformational isomers of the L-chain dimer of protein Mcg have been observed by crystallographic and CD studies (Firca et al., 1978). In the presence of the ligand DNP-lysine, crystallization of only one form is observed (Ely et al., 1978). The conformational change was thought to include an alteration in the relative position of Trp-189 and Tyr-195 (Firca et al., 1978). This implies a trans-

mission of the effect of binding from the V-domains to the C-domains.

The V_L dimer of protein 315 undergoes a pH-dependent transition between two forms, associated with a fluorescence change of greater than two-fold (Gavish et al., 1978). An analysis of the kinetic parameters and structural extent of this conformational change is presented in Chapter 5. The findings are compared with the results of studies on similar systems, and a possible reason for these conformational properties of L-chains is discussed.

4. Preferential recombination

The ability of H-chains or L-chains to recombine preferentially with their original partners rather than with heterologous chains is a surprising feature of immunoglobulin structure. This property is observed both with myeloma proteins (Grey and Mannik, 1965) and with heterogeneous antisera (Roholt et al., 1965). No satisfactory explanation for this behaviour has been advanced. Preferential recombination is in apparent contradiction with the idea that H-L combinations are random, a mechanism which would greatly increase the possible number of combining sites for a given amount of genetic material. However there is no evidence at present that the synthesis of particular H-L pairs or particular V_H-V_L pairs is under strict control.

Antibody specificity

The immune system must have the ability to distinguish between self components and foreign substances. In this sense, the specificity of an antibody population resides in its ability to react against a foreign antigen, but not to trigger off a

response against any self-antigen, however similar chemically that self-antigen may be to the foreign component. The ability of an antiserum to distinguish between chemically similar compounds, for example stereoisomers of tartaric acid, is well known (Landsteiner, 1945). The composition of a serum is a complex function of the evolutionary and environmental history of any individual. Nevertheless, it is possible to identify and examine the various factors which are important in determining the specificity of any antiserum. The important factors are the affinity for the immunizing ligand, the affinity for any other related or unrelated ligand, the multivalency of the antibody and the heterogeneity of the antiserum.

The effect of heterogeneity of an antiserum is one which complicates any analysis of the physical basis of antibody specificity. There are two main consequences of heterogeneity. Firstly, it makes the analysis of kinetic, thermodynamic and structural parameters ambiguous. This point is discussed more fully in the following section. Secondly, it is possible for a heterogeneous antiserum to be more specific, in terms of its discriminatory ability, than any individual component of that antiserum present at the same total concentration. This idea was propounded by Talmage (1959). Talmage envisaged that the individual antibodies elicited against antigen 'A' would all have different patterns of reactivity against related and unrelated antigens 'B', 'C' etc. Any reactivities to antigens 'B', 'C' etc. would therefore be diluted out in the antiserum, and reaction observed only with antigen 'A'. If this mechanism is used, it has been calculated that only 10^4-10^6 distinct combining sites would be required to distinguish between an almost infinite number of haptens (Inman, 1973). It is worth remarking that the

tadpole of Rana catesbiana has only 2 x 10^6 lymphocytes in total, yet is able to raise a response against DNP and TNP compounds (Haimovich and du Pasquier, 1973). There is evidence that antisera raised in rabbits against ribonuclease contain antibodies which also bind the DNP group (Varga et al., 1973). However, many other pairs of compounds chosen at random did not show this behaviour. An extension of the Talmage theory is that antibodies are 'multispecific', and can bind structurally unrelated ligands in different regions of the combining site (Richards et al., 1975). It has been suggested that the binding sites for menadione and DNP-lysine on proteins 315 and 460 are non-overlapping (Manjula et al., 1976; Rosenstein and Richards, 1976). However, this conclusion is difficult to accept, since the two ligands are not highly dissimilar and bind competitively to the proteins studied (Michaelides and Eisen, 1974).

Even if individual antibodies do have a broad range of binding specificity, the structures of their binding sites are not necessarily different in principle from those of many enzyme active sites. The dye proflavin and the substrate analogue acetyl-tyrosine-ethyl-ester compete for the same site of chymotrypsin (Bernhard et al., 1966). Other examples of dyes binding to globular proteins in sites overlapping those of structurally dissimilar substrates or coenzymes have also been given (Glaser, 1970). Strong binding sites ($K > 10^5\ M^{-1}$) were not commonly observed. It is possible to object that anti-nitrophenyl antibodies, particularly those of low affinity, are 'nonspecific', in that they reflect the binding of an unnatural apolar group into a hydrophobic site (Parker and Osterland, 1970). However, if such antibodies are inducible they are, by definition, specific, and are indicative of the potential of the immune system to respond to

foreign antigens. The only major objection to the use of anti-nitrophenyl antibodies is that the nitrophenyl group is less likely than many other antigenic determinants, for example sugars and amino acids, to cross-react with self antigens. This possibility, together with the high reactivity of nitrophenyl groups towards proteins (Saul et al., 1978), implies that an analysis of the anti-nitrophenyl response may lead to an exaggerated view of the diversity and number of combining sites which can be produced by the immune system.

Anti-DNP and anti-TNP antibodies

Much information on the development and specificity of the immune response has been obtained from studying anti-DNP and anti-TNP responses. Immunogens containing DNP or TNP may be easily synthesized, and the nitrophenyl group has convenient spectral properties.

1. Biological aspects

The response, in all animals studied, is usually highly heterogeneous. Typical immunogens producing heterogeneous responses are DNP-KLH and DNP-BGG. The clonal repertoire of strain CBA/J or C3H/He mice against DNP is probably as great as that against the NIP determinant (Pink and Askonas, 1974). About 8000 different clones may be stimulated by NIP in CBA/H mice (Kreth and Williamson, 1973). Only a fraction of the potential contained in the strain is used by any individual mouse. This suggests either that different V-region germ-line genes are present in individuals of the same strain, or that a somatic mutation process is occurring. Homogeneous responses in individual rabbits have been observed to DNP-Gramicidin-S (Montgomery et

al., 1975), and a restricted, possibly monoclonal response has been observed to DNP-insulin (Keck et al., 1973). Carrier complexity may therefore influence the heterogeneity of the response. The immunogenicity of the response is certainly influenced by the spatial arrangement of DNP groups on a carrier (Dintzis et al., 1976).

Different mouse strains show responses of different specificity for DNP derivatives (Paul et al., 1970). This may reflect different structural V-region genes or genetic control of recognition of antigenic determinants. Differences are also observed among different species of animals and do not appear to be carrier dependent (Yoshida et al., 1970).

The average affinity of antibodies in the secondary response is higher than that in the primary response. This may reflect antigen-stimulated production of new clones, or selection of high-affinity clones. Present evidence suggests that the latter mechanism is important. High affinity antibodies against DNP have been shown to be present at the outset of the immune response both in BALB/c mice (Claflin and Merchant, 1973) and in rabbits (Haber et al., 1967). The structure of the immunogen was thought to be important in the latter experiments. Preservation of a high affinity subpopulation rather than sequential expression of low and high affinity antibodies was also indicated in the response of guinea pigs to DNP (Davie and Paul, 1972). Low doses of antigen tend to favour production of antibodies of high affinity (Eisen and Siskind, 1964; Steiner and Eisen, 1967). Indeed, tolerance may be induced selectively in cells producing high affinity antibody by high doses of antigen (Goidl et al., 1968). The class of an antibody influences its affinity. DNP-binding IgM antibodies from horse and rabbit were

shown to have a lower affinity than IgG antibodies from the same bleeding (Voss and Eisen, 1968). A continual increase in affinity is not an innate characteristic of the immune response. The response of rabbits to β-galactosidase shows cyclical changes in affinity (Macario and Conway de Macario, 1973).

The responses to DNP, TNP and similar ligands gives much information on the cross-reactivity and possible multispecificity of antibodies. The response of BALB/c neonatal mice to DNP or TNP is dominated by a few nonidentical clonotypes (Klinman and Press, 1975a). Their frequent recurrence suggests a germ-line origin. There may be a sequential, antigen-independent expression of clonotypes during ontogeny. TNP ligands can bind to the DNP clones, and DNP ligands to the TNP clones, with a decrease of affinity of about an order of magnitude with respect to the homologous ligand. However, the cells are not stimulated in vitro by the heterologous ligand (Klinman and Press, 1975b). A threshold requirement for activation is therefore clearly demonstrated. Independent clones of cells are also stimulated by DNP and TNP in the primary response of adult mice (Klinman et al., 1973) and in rabbits (Little and Eisen, 1969). The stimulation of nonoverlapping populations of cells by two such closely related ligands as TNP and DNP is difficult to reconcile with the idea of multispecificity. Such limitations are not seen in the secondary response (Klinman et al., 1973). This may reflect the higher affinity of such antibodies, so that cross-reacting ligands are more likely to reach the necessary threshold affinity. It may also reflect a difference between primary and secondary cell receptors (Klinman, 1972). The importance of the threshold requirement is demonstrated by rabbit antisera to DNP and menadione taken early or late in the response. Almost all the anti-

bodies bound both DNP and menadione. Late antisera had higher affinities than early antisera. However, the early antisera were able to discriminate better between the two ligands in the precipitin test than were the late antisera (Johnston and Eisen, 1976).

2. Structural aspects

(a) Heterogeneous antisera

Many kinetic, thermodynamic and spectroscopic experiments have been carried out on heterogeneous populations of anti-DNP and anti-TNP antibodies. Experiments on heterogeneous antisera inevitably lead to the measurement of average quantities. Important but subtle differences between antibodies may therefore be missed. Nevertheless, much useful information has emerged.

The kinetic parameters for the interaction of DNP and TNP ligands with antibodies have been measured by temperature jump and stopped flow methods. In most cases, the data are interpretable in terms of a fast bimolecular single step mechanism, probably diffusion controlled (Froese, 1968; Froese and Sehon, 1975; Barisas et al., 1975). The stability of the complex is then directly related to the off-rate. A slow, concentration-independent step was observed on the binding of a di-DNP ligand to rabbit antibodies. It was interpreted in terms of the energetically unfavourable attainment of closure of a bridged dimer (Barisas et al., 1977).

The determination of thermodynamic parameters of the interaction of nitrophenyl groups with heterogeneous antisera is beset by particular difficulties. Calculations of the average affinity of an antiserum generally assume a Gaussian distribution of affinities. Although this may be a good approximation early in the response, experiments with rabbit anti-DNP antibodies showed

that a progressive skewing towards high affinities occurred later. The distribution then became bimodal (Werblin and Siskind, 1972). The probability density of association constants is better fitted using delta functions (Erwin and Aladjem, 1976). However, this does not greatly simplify the extraction of thermodynamic parameters. Different workers, using very similar systems, can come to very different conclusions. There is general agreement that the binding of nitrophenyl groups to antibodies is characterized by a large negative enthalpy change (Barisas et al., 1971; Barisas et al., 1972; Szewczuk and Mukkur, 1977). ΔH values of about -20 kcal/mol have been measured. One report, however, gave a value of only 1.6 kcal/mol (Carsten and Eisen, 1955). It has been suggested that an interaction with tryptophan is a major source of this thermal effect (Johnston et al., 1974). This point is investigated in Chapter 3. Values reported for the heat capacity change on binding are in disagreement. Using rabbit anti-DNP antibodies, one group reported a heat capacity change of -300 cal deg^{-1} (Barisas et al., 1971) and another a change of $+472.7$ cal deg^{-1} (Szewczuk and Mukkur, 1977). This emphasizes the difficulty of working with unique and heterogeneous preparations of antibodies.

Several characteristic spectral changes associated with the nitrophenyl ring occur on binding. The interpretation of these changes in terms of specific interactions provides information on the factors determining the specificity of anti-DNP and anti-TNP antibodies. The protein fluorescence is quenched on the binding of nitrophenyl groups (Velick et al., 1960). The absorption spectrum of the nitrophenyl group undergoes a red-shift and hypochromic change on binding to specific antibodies from many species of animal (Eisen and Siskind, 1964; Little and

Eisen, 1967). The induced CD spectrum of the ligand also shows characteristic features (Glaser and Singer, 1971). All these three effects have been interpreted in terms of an interaction with tryptophan in the binding sites.

Changes of the resonance Raman bands associated with the nitro groups were seen on the binding of DNP-lysine to rabbit antibodies. The changes were consistent with a decrease in double-bond character of the nitro groups. Hydrogen bonding effects alone could not account for the changes (Carey et al., 1973).

(b) Homogeneous antibodies

Investigation of the factors influencing the specificity of antibodies is greatly simplified by the availability of homogeneous proteins. Such studies have inevitably concentrated on myeloma proteins found to have binding activity. Although several human myeloma proteins with activity have been reported, their affinities, when measured, have been low. Two examples are the $IgG_1\lambda$ protein BRY with affinity 2.3×10^4 M^{-1} for DNP-lysine (Eisen et al., 1967) and the Waldenström magroglobulin Wag with affinity 3.8×10^4 for DNP-amino-caproate (Ashman and Metzger, 1969). Both these proteins showed the red-shift and fluorescence quenching properties. The enthalpy change was measured for protein Wag and found to be -2.4 kcal/mol. The IgG was unable to precipitate DNP-HSA, although the IgM did precipitate DNP-BGG.

The most extensive studies have been performed on the mouse myeloma protein 315. The myeloma MOPC 315 was induced in a 6th generation backcross of a BALB/cAnNxC57BL/KA mouse to BALB/c mice, selecting for C57BL/KA allotypic markers. However, the BALB/c α-chain allotype was retained in the cross (Sirisinha and Eisen, 1971). A screening process revealed its ability to bind the DNP

group (Eisen et al., 1968). Protein 315 has an affinity of $\sim 3 \times 10^6$ M^{-1} for DNP-lysine, the highest affinity reported for a myeloma protein. A large body of evidence suggests that protein 315 is representative of naturally raised anti-DNP antibodies in BALB/c mice. The affinity of the protein is within the range of affinities of naturally induced antibodies. Idiotypic determinants of protein 315 have been identified on some antibodies raised against DNP compounds in BALB/c mice (Granato et al., 1974). Shared determinants were not, however, detected in a subsequent study (Helman et al., 1976). The source of the discrepancy between these results is not clear. Protein 315 has an unusual λ_2 -type L-chain. This subtype occurs as only 1% of the total proportion of L-chains in normal sera from BALB/c mice (Blaser and Eisen, 1978). However, there is a 10-fold increase of this subtype on immunization with DNP-KLH (Cotner and Eisen, 1978). The spectral changes of nitrophenyl ligands on binding to protein 315 are similar to those observed on binding to other anti-DNP and anti-TNP antibodies. These include the fluorescence quenching properties, absorption spectrum changes and induced CD changes. It has been suggested on the basis of the fluorescence quenching properties that protein 315 is more like anti-TNP antibodies than anti-DNP antibodies (Eisen et al., 1970), and on the basis of induced CD spectra that it is not characteristic of either (Glaser and Singer, 1971). These points exemplify the difficulty of comparing a homogeneous protein with a heterogeneous mixture.

The binding of DNP ligands to protein 315 and to the mouse myeloma protein 460 were found to be accompanied by large negative enthalpy changes (Johnston et al., 1974). An extensive analysis of the kinetics of ligand binding to protein 315 showed that the reaction could be represented as a single-step process (Haselkorn

et al., 1974). Although no evidence for a conformational change was detected in protein 315, such a change was seen with protein 460 by the temperature jump technique (Lancet and Pecht, 1976). Neither the generality nor significance of this effect is clear at present.

The construction of a model of the combining site of protein 315 (Padlan et al., 1976a) has enabled a detailed approach to be made towards understanding the molecular basis of the specificity of this antibody. A quantitative examination of the likely accuracy of the original model is presented in Chapter 4. The predicted site was modified according to the requirements of chemical and physical data (Dwek et al., 1977). The model of the site is shown in Figure 1.5. The DNP ring is proposed to stack with Trp-93_L. This interaction is presumed to account for the absorbance and CD changes on ligand binding. Since the possible importance of tryptophan in the combining sites of anti-DNP and anti-TNP antibodies has been stressed by so many authors, a detailed analysis of the specificity of the DNP/tryptophan interaction and of the thermodynamic parameters associated with the interaction is presented in Chapter 3. In addition to Trp-93_L, two further aromatic residues, Tyr-34_L and Phe-34_H, were positioned round the DNP ring to account for the large upfield chemical shift changes of the DNP ring proton resonances observed by ^1H n.m.r. on ligand binding (Dower et al., 1977). A further ring, Tyr-33_H, was required to account for the upfield chemical shift change observed for the side-chain resonance of DNP-glycine on binding. The proximity of Tyr-34_L to the combining site had previously been indicated by affinity labelling experiments (Haimovich et al., 1970; Goetzl and Metzger, 1970a and b). The 2-nitro group and 4-nitro group were proposed to form hydrogen

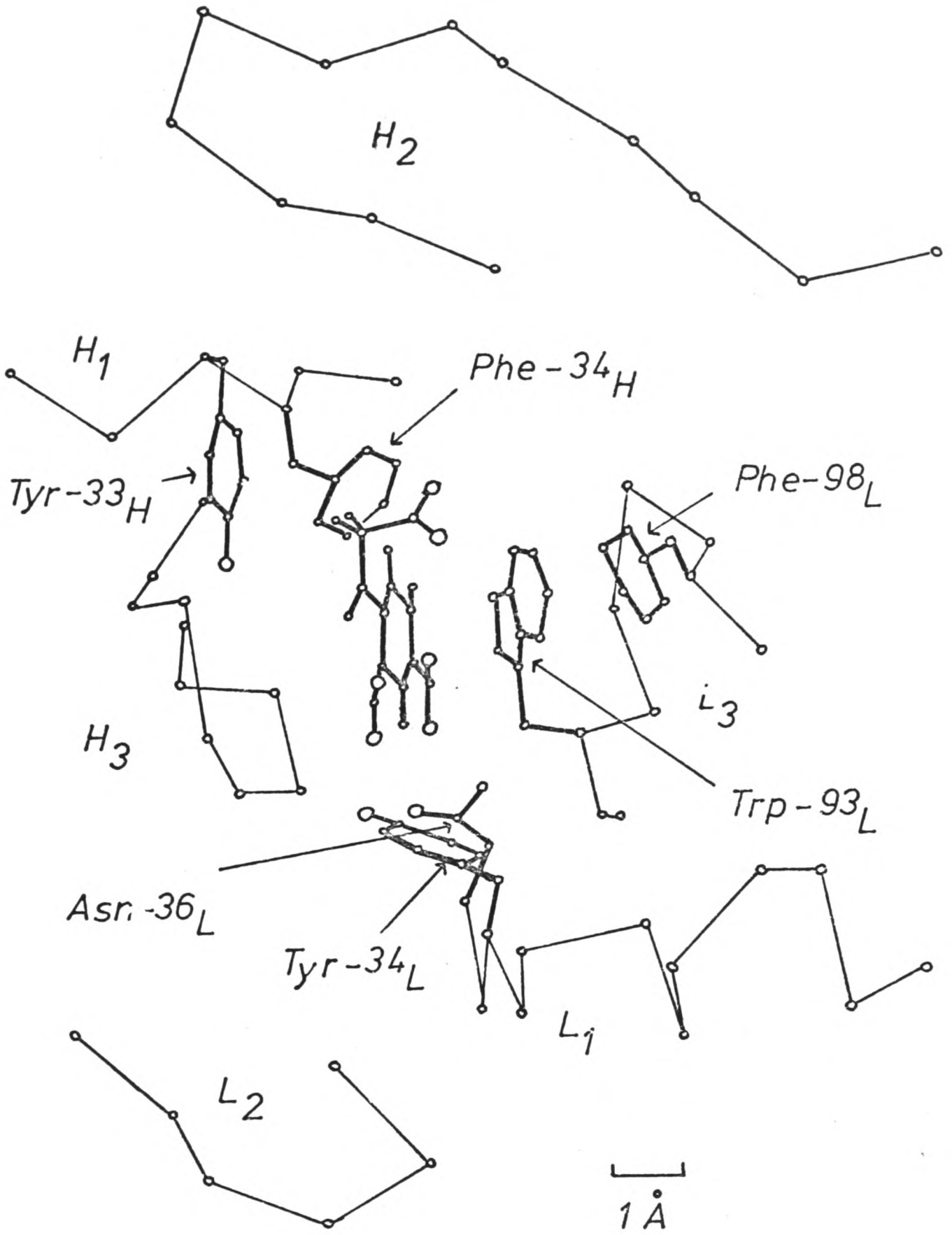

Figure 1.5 The model of the combining site of protein 315

The binding site is shown containing DNP-glycine (Dower et al., 1977), and is viewed in approximately the same orientation as the sites of proteins New and 603 (Figure 1.4).

bonds to the phenolic group of Tyr-34_L and the amido group of Asn-36_L respectively. Experiments designed to test the possibility of hydrogen bonding to Tyr-34_L and the involvement of Tyr-33_H with the side-chains of DNP and TNP ligands are described in Chapter 6. Examination of the model (Figure 1.5) shows that many contacts of the DNP group are made with L-chain residues. The importance of the L-chain in determining the specificity of protein 315 is discussed in Chapter 5.

The final chapter of this thesis is concerned with a preliminary characterization of a naturally induced homogeneous anti-DNP antibody, obtained by the cell-fusion technique.

CHAPTER 2

MATERIALS

Haptens

DNP-glycine, DNP-L-aspartic acid, ε-DNP-L-lysine, di-DNP-L-cystine, 2,4-dinitroaniline, 2,4-dinitrophenol and 2,4-dinitro-1-naphthol-7-sulphonic acid (flavianic acid) were obtained from B.D.H. 2,4-dinitro-1-naphthol was obtained from Eastman, and 2-methyl-1,4-naphthoquinone (menadione) was obtained from Sigma. DNP-aminocaproic acid (synthesized according to Porter, 1959b) and TNP-aminoethylamine (synthesized according to Haselkorn et al. 1974) were gifts from Dr. D. Givol. TNP-glycine (synthesized according to Dower et al., 1978) and TNP-aminomethylphosphonate (synthesized according to Wain-Hobson et al., 1977) were gifts from Dr. S.K. Dower. 2,4,6-trinitroaniline (synthesized according to Gettins, 1979) was a gift from P. Gettins. The syntheses of 2-chloro-4-nitrophenyl-glycine and 4-chloro-2-nitrophenylglycine are described below. ^{3}H-DNP-L-lysine (1.1 Ci/mmol) was obtained from New England Nuclear.

Miscellaneous reagents

L-tyrosine, L-phenylalanine, L-cysteine, 2,4,6-trinitrobenzene sulphonic acid (TNBS) and dithiothreitol (DTT) were obtained from B.D.H. L-tryptophan was obtained from Fisons. Tetranitromethane (TNM) and glutaraldehyde were obtained from Koch-Light. 2-chloro-4-nitroaniline, 4-chloro-2-nitroaniline, dithioerythritol, iodoacetamide and 2,6,10,14-tetramethylpentadecane (pristane) were obtained from Aldrich.

$^{2}H_2O$ (99.8% ^{2}H) and ^{2}H-acetic acid (99.5% ^{2}H) were obtained

from Ryvan. NaO^2H and ^2HCl (99+ % ^2H) were obtained from Aldrich.

Sepharose 4B, thiol-activated Sepharose 4B and Sephadex column materials were obtained from Pharmacia. DEAE-Cellulose (DE-52) was obtained from Whatman, and Dowex IX-8 from Sigma.

Sheep red blood cells in Alsevier's medium were obtained from Tissue Culture Services, Slough. HAM nutrient medium was obtained from Gibco Biocult, Glasgow.

Syntheses of glycine-N-(2-chloro-4-nitro)benzene and glycine-N-(4-chloro-2-nitro)benzene

Syntheses were carried out as described by Gettins (1979).

10g 2-chloro-4-nitroaniline (or 4-chloro-2-nitroaniline), 8g bromoacetic acid and 8g sodium acetate (trihydrate) were heated on an oil bath at 125-135°C for 45 mins. Air was passed over the reaction mixture to remove HBr. The mixture was cooled, and extracted with 30 ml hot water, adding 0.88 ammonia to keep the solution at pH 8. The clear filtrate was acidified with 5N HCl to give a yellow precipitate (2-chloro-4-nitrophenylglycine) or an orange precipitate (4-chloro-2-nitrophenylglycine). The precipitate was washed and dried. The yields achieved by this method were low (~3%).

Proteins

Protein 315 was purified from the ascites fluid produced by the appropriate myeloma cell line in D2c/F_1 mice. Mice received an injection of 0.5 ml pristane intraperitoneally, approximately two weeks before injection of the myeloma cells. The purification and preparation of fragments are described below.

The cell line producing protein A3 was a gift from Dr. B.A.

Askonas. Details of the method of propagation of the cell line, cloning and purification procedures are given in Chapter 7.

Bovine serum albumen (BSA) and hog stomach mucosa pepsin were obtained from Sigma. ^{125}I-rabbit anti-mouse IgG (RAM), 3 x 10^5 c.p.m./50 µl was a gift from Dr. A. Williams. Non-immune rabbit serum was a gift from M.-R. van Schravendijk.

Extinction coefficients

The following molar extinction coefficients were used (1 cm path length): DNP-lysine, ε_{360} = 17,400; DNP-glycine, ε_{360} = 15,890; DNP-aspartate, ε_{360} = 18,300; 2,4-dinitrophenol, ε_{360} = 14,900; 2,4-dinitroaniline, ε_{345} = 8,300; 2,4,6-trinitroaniline, ε_{325} = 9,650; TNP-glycine, ε_{360} = 11,000; TNP-aminomethylphosphonate ε_{360} = 11,000; DNP-aminocaproate, ε_{360} = 17,400; 2-chloro-4-nitrophenylglycine, ε_{392} = 15,800; 4-chloro-2-nitrophenylglycine, ε_{450} = 5,000; menadione, ε_{335} = 2200; dinitronaphthol, ε_{390} = 13,900; dinitronaphthol sulphonic acid, ε_{358} = 19,950; tryptophan, ε_{280} = 5500; phenylalanine, ε_{258} = 195.

For protein solutions of 1 mg/ml, the following extinction coefficients were used, at 280 nm: Fv fragment of protein 315, 1.5; V_L of protein 315, 1.0; L-chain of protein 315, 1.1, protein A3 (IgG_1), 1.35.

METHODS

Most of the preparative and analytical methods referred to in the text are described here. The nitrations of protein 315 are described in Chapter 6, and the preparation of protein A3 in Chapter 7.

Nuclear magnetic resonance (n.m.r.)

^{1}H n.m.r. spectra were recorded at 270 MHz using a modified Bruker spectrometer with an Oxford Instrument Company superconducting magnet and an internal ^{2}H field-frequency lock. Free induction decays were sampled at 4096 points using quadrature detection, and Fourier transformed over 8192 points by the zero-filling method to improve spectral definition. Signal-to-noise ratios were increased by convolution. Sweep widths employed were 3000 Hz (small molecules) or 4000 Hz (proteins), using a pulse angle of 70^{o} and a delay of 130-150 μs between the main pulse and the start of accumulation. Overall inter-pulse times were generally 0.7s (3000 Hz sweep width) or 0.52s (4000 Hz sweep width). Selective suppression of the solvent resonance was rarely necessary. When required, it was applied as a gated pulse of 0.4s. Chemical shift values are reported as parts per million (p.p.m.) downfield from the high field singlet resonance of sodium 2,2-dimethyl-2-silapentane-5-sulphonate (DSS) used as an external standard.

Under the conditions of the ligand binding experiments reported in this thesis, the affected resonances were found to be in fast exchange. The observed chemical shift change on binding ($\Delta\delta_{obs}$) may therefore be related to the chemical shift change between bound and unbound species ($\Delta\delta$) and to the fraction

of molecules bound (X_B) by the equation:

$$\Delta\delta_{obs} = X_B\Delta\delta$$

Two distinct types of binding processes were observed:

1. Formation of 1:1 complexes

The binding of two ligands A and B, with a dissociation constant K_{D1}, may be formulated as follows:

$$A + B \overset{K_{D1}}{\rightleftharpoons} AB$$

N.m.r. titration curves ($\Delta\delta_{obs}$ against total ligand concentration) are a function of the two parameters K_{D1} and $\Delta\delta$. If the free ligand concentration does not approximate to the total ligand concentration, the parameters may be obtained by a best fit procedure. Theoretical curves were calculated for systematically varied combinations of K_{D1} and $\Delta\delta$, and the best fit was defined as the combination giving the minimum root mean square difference between calculated and experimental values. The FORTRAN IV program written for this purpose is listed in Appendix 2.1. READ and WRITE statements are omitted. Their positions will be obvious to anyone wishing to use the method.

2. Simultaneous formation of 1:1 and 2:1 complexes

Consider the following scheme:

$$A + B \overset{K_{D1}}{\rightleftharpoons} AB$$

$$AB + B \overset{K_{D2}}{\rightleftharpoons} BAB$$

The titration curves may be described by four parameters (K_{D1}, K_{D2} and two chemical shift changes). If the two chemical shift changes are assumed to be the same, and the sites assumed to be of equal affinity, the titration curves may be expressed as a function of the two parameters K_D (intrinsic dissociation constant, $K_D = 2K_{D1} = \frac{1}{2} K_{D2}$) and $\Delta\delta$. The amounts of binary and ternary complexes formed may be calculated from the binomial distribution. Programming details are given in Appendix 2.1.

Unitary free energy

Binding energies described in this thesis are expressed in unitary terms. The necessity for the use of unitary quantities arises from the arbitrary choice of the mole per litre as the biochemical standard state (Gurney, 1953). If two molecules associate in solution, there is a net decrease in the number of particles mixing with the solvent. If the concentrations are expressed on the molar scale, and not on the mole fraction or unitary scale, there is an entropically unfavourable change on binding, since there is a net decrease of 1 mole of particles mixing with 55.6 moles of water. This 'cratic' contribution to the entropy change is simply a function of the number of particles in solution, and is independent of the forces involved in complex formation. The cratic contribution is $R\ln(x_o)$, where x_o is the mole fraction of solute when the solute concentration is 1 mole per litre, and is equal to $R\ln(^1/55.6)$ or -7.98 e.u.. The contribution to the free energy change of association at 300K is therefore +2.4 kcal mol^{-1}. It is important to realise that the unitary free energy only accounts for the thermodynamics of mixing. It does not include the change in degrees of freedom

occurring on complex formation.

Fluorescence

Measurements were made with a Perkin-Elmer/Hitachi MPF-2A spectrofluorimeter. IgG was used at a concentration of 0.02mg/ml in PBS, T = 293K. Protein fluorescence was excited at 295 nm and observed at 340 nm, with excitation and emission slit-widths of 5-6 nm. Correction for the absorption by ligand of incident and emitted radiation - the 'inner filter' effect - was made by using a tryptophan blank of similar fluorescence intensity to the protein solution. The correction factor was of the order of 1% at a ligand concentration of 1 μM.

Under the conditions of the binding experiments, the concentration of free ligand did not approximate to the total ligand concentration. The dissociation constants (K_D) and limiting fluorescence quenching values (ε) were therefore obtained by a simple best fit procedure, as described for the n.m.r. titrations (see above and Appendix 2.1).

Ultra-violet and visible absorption

Spectral measurements were made with a Gilford Model 260 spectrophotometer or a Cary Model 17 spectrophotometer.

Equilibrium dialysis

Equilibrium dialysis was performed using Lucite chambers separated by Visking dialysis membrane. 100 μl of protein solution was applied to one chamber and 100 μl of ligand solution to the other. Equilibrium was reached overnight at 4°C or at 25°C.

Where stated in the text, the binding of some ligands was measured by competition with ^{3}H-DNP-lysine. The competition

experiments were performed with concentrations of ^{3}H-DNP-lysine which gave approximately 50% occupancy of the binding sites when used as sole ligand. The concentration of bound inhibitor, $[X_2]$, and the intrinsic association constant for the inhibiting ligand, K_I, were obtained from equations (1) and (2) respectively, where [I] is the initial concentration of inhibiting ligand added to one side of the dialysis chamber, [C] is the free concentration of DNP-lysine, K is the association constant for DNP-lysine, $[X_1]$ is the bound concentration of DNP-lysine, [P] is the protein concentration and n is the number of sites.

$$[X_2] = n[P] - [X_1](1 + 1/K[C]) \qquad (1)$$

$$K_I = \frac{2[X_2]}{([I] - [X_2])(n[P] - [X_1] - [X_2])} \qquad (2)$$

These equations are derived from simple mass-action considerations and involve no approximations (Licht et al., 1977).

Polyacrylamide gel electrophoresis

Electrophoresis was performed using 7% (w/v) acrylamide gels containing 1% SDS. Reduction of protein samples was achieved by incubation with 0.05M DTT/4M urea/1% (w/v) SDS/0.1M Tris-HCl pH8 at 37°C for 30 minutes. Samples were alkylated by incubation with 0.12M iodoacetamide/4M urea/1% (w/v) SDS/0.1M Tris-HCl pH 8 at 37°C for a further 30 minutes. Gels were run using a buffer of 0.04M Tris-HCl/0.02M sodium acetate/0.002M EDTA/0.2% (w/v) SDS pH 7.4, at a current of 4mA/gel.

Protein bands were stained by incubating gels with 0.5% Coomassie Blue in methanol/acetic acid/water (5:1:5 by volume)

at 37°C for 1 hr. Destaining was effected by diffusion into methanol/acetic acid/water (2:3:35 by volume).

Preparation of DNP-lysine-Sepharose

150 ml of Sepharose 4B were diluted to 300 ml with H_2O and the pH brought to 11 with 4N NaOH. 7.5g of CNBr were added, keeping the pH at 11 with 4N NaOH, and the mixture on ice. The Sepharose was filtered and washed with 0.1M $NaHCO_3$, pH 8.5. 150 mg of DNP-lysine in 100 ml of 0.1M $NaHCO_3$, pH 8.5, were added and the Sepharose was stirred overnight in the cold room. Recently prepared DNP-lysine-Sepharose required washing with 0.05M NH_3 prior to use.

Preparation of the Fv fragment of protein 315

The method used was essentially that of Hochman et al. (1973). The salient features only are outlined. Preparation of reduced and alkylated IgA: Ascites fluid was dialysed against 0.2M Tris, 0.15M NaCl, pH 8.2 and Na_2EDTA was added to 0.002M. The preparation was reduced with 0.01M DTT at room temperature for 1 hr and alkylated with 0.03M iodoacetamide at room temperature for ½ hr. After dialysis against Tris buffer, the material was applied to a DNP-lysine-Sepharose column, eluted with DNP-glycine and passed down a Dowex IX-8 column to remove the DNP-glycine. The preparation was dialysed against 0.1M sodium acetate, 0.15M NaCl, pH 4.7 and brought to a concentration of 10 mg/ml. Digestion of IgA: Pepsin (1:50 w/w) was added, and the solution was incubated at 37°C for 3 hrs, keeping the pH above 4.5. The pH was then lowered to 3.5 with acetic acid, and the preparation was incubated for a further 2½ hrs. The Fv fragment was separated from undigested IgA and Fab fragment on a

Sephadex G-75 column in PBS.

Preparation of the V_L dimer of protein 315

The Fv fragment was separated into its constituent V_H and V_L chains according to the method of Hochman et al. (1973). The Fv fragment was dissolved in 8M urea, 0.1M Tris, pH 9.0, and applied to a column of DEAE-cellulose. The V_L chain remains in the effluent, and the V_H chain may be eluted with urea-Tris buffer containing 1M NaCl. The V_L chain dimerizes during dialysis against PBS whereas the V_H chain tends to precipitate.

Preparation of the L-chain dimer of protein 315

Reduced and alkylated IgA was dissolved in 4M urea, 1M acetic acid, and separated into H-chain and L-chain on a Sephadex G-100 column (Bridges and Little, 1971).

APPENDIX 2.1

FORTRAN IV programs

1. Calculation of parameters from n.m.r. titrations

(a) 1:1 complexes (fixed concentration of one species).

MASTER GUESS

```
C FITS DATA BY TRIAL AND ERROR TO KD1 AND Δδ.  DK, DKS,
C P0 AND POS ARE STARTING AND INCREMENTAL VALUES OF KD1
C AND Δδ RESPECTIVELY.  PT IS FIXED CONCENTRATION OF ONE
C SPECIES.  FV(I) AND HT(I) ARE MEASURED SHIFT AND
C TOTAL LIGAND CONCENTRATION FOR NP EXPERIMENTAL POINTS.
 1          DIMENSION A(20,20), FV(25), HT(25), F(25), D(20), P(20)
 2          XNP=NP
 3          D(1)=DK
 4          P(1)=P0
 5          DO 15 J=1,20
 6          IF(J.GT.1) D(J) = D(J-1) + DKS
 7          IF(J.GT.1) P(I) = P(J-1) + POS
 8       15 CONTINUE
 9          DO 100 J=1,20
10          DO 101 I=1,20
11          FX=0
12          DO 102 K =1,NP
13          PA=((HT(K)+PT+D(J))-SQRT((HT(K)+PT+D(J))**2-4.*HT(K)
               *PT))/2.
14          F(K) = (PA* P(I))/PT
15          FX=FX+(F(K)-FV(K))**2
16      102 CONTINUE
17    C BEST FIT IS MINIMUM IN MATRIX A
18          A(I,J) = SQRT(FX)/XNP
19          IF (A(I,J).GE.10.) A(I,J) = 9.99
20      101 CONTINUE
21      100 CONTINUE
22          STOP
            END
```

(b) Simultaneous formation of 1:1 and 2:1 complexes

(fixed concentration of the species with two binding sites).

DK is now the intrinsic dissociation constant

Insert after line 1 of MASTER GUESS:

```
PT = 2.*PT
```

Insert after line 13:

```
R = (2.*PA)/PT
```

Replace line 14:

```
F(K) = R*(1.-0.5*R)* P(I)+((0.5*R)**2)*2.*P(I)
```

2. Calculation of parameters from fluorescence titrations

In MASTER GUESS, P0 is now the limiting fluorescence quenching, defined as the ratio of fluorescence intensity at infinite ligand concentration to the initial fluorescence intensity. The initial fluorescence intensity must be read in first, as FV(1).

Insert after line 1 of MASTER GUESS:

```
DIMENSION FT(25)
```

Replace line 12:

```
DO 102 K = 2,NP
```

Insert after line 12:

```
FT(K) = (FV(1)-FV(K))/(FV(1)-P(I)*FV(1))
```

Replace lines 14, 15 and 18:

```
F(K) = PA/PT
FX = FX + (F(K)-FT(K))**2
A(I,J) = (10.*(SQRT(FX)))/(XNP-1.)
```

3. Calculation of parameters from pH titrations

Experimental data were fitted to a single ionization curve, expressed as a function of three variables - pK_a, shift (or absorbance) of high pH form and shift (or absorbance) difference between ionized and unionized forms. The program uses the least squares linear Taylor differential method (Cleland, 1967).

```
      MASTER PKA
C AI, BI AND CI ARE INITIAL ESTIMATES OF PKA, SHIFT OF HIGH PH
C FORM AND SHIFT RANGE.  DWE(I) AND X(I) ARE MEASURED SHIFT
C AND PH, FOR NP EXPERIMENTAL POINTS.
      DIMENSION DWEST(100), DIFF(100), XPER(100), D(100), X(100)
      DIMENSION DWE (100), DWT(100), R(100), DA(100), DB(100),
      DIMENSION DC(100)
      AI = EXP10(-AI)
      DO 100 I=1,NP
      X(I)=EXP10(-X(I))
  100 CONTINUE
  120 A=AI
      B=BI
      C=CI
      TOL=0.1
  149 CONTINUE
      LL=1
  150 DO 200 I=1,NP
      DWT(I) = B+((C*X(I))/(A+X(I)))
      R(I)=DWT(I)-DWE(I)
  200 CONTINUE
      AA=0.
      BB=0.
      CC=0.
      AB=0.
      BC=0.
      AC=0.
      AR=0.
      BR=0.
      CR=0.
      DO 300 I=1,NP
C CALCULATE PARTIAL DERIVATIVES
      DA(I)=-(C*X(I))/((A+X(I))**2)
      DB(I)=1.
      DC(I)=X(I)/(A+X(I))
  300 CONTINUE
      DO 400 I=1,NP
      AA=AA + DA(I)**2
      AB=AB+DA(I)*DB(I)
      AC=AC+DA(I)*DC(I)
      BC=BC+DB(I)*DC(I)
      BB=BB+DB(I)**2
      CC=CC+DC(I)**2
      AR=AR+DA(I)*R(I)
      BR=BR+DB(I)*R(I)
      CR=CR+DC(I)*R(I)
  400 CONTINUE
      AR=-AR
      BR=-BR
      CR=-CR
C CALCULATE CORRECTIONS TO VARIABLES
      DET1=AA*(BB*CC-BC*BC)-AB*(AB*CC-AC*BC)+AC*(AB*BC-BB*AC)
      DET2=AR*(BB*CC-BC*BC)-AB*(BR*CC-BC*CR)+AC*(BR*BC-BB*CR)
      DET3=AA*(BR*CC-BC*CR)-AR*(AB*CC-AC*BC)+AC*(AB*CR-AC*BR)
      DET4=AA*(BB*CR-BR*BC)-AB*(AB*CR-BR*AC)+AR*(AB*BC-BB*AC)
      CORRA=DET2/DET1
      CORRB=DET3/DET1
      CORRC=DET4/DET1
      A=A+CORRA
      B=B+CORRB
      C=C+CORRC
```

```
 3000 IF (LL-15) 3001, 3001, 999
C EXITS IF NO CONVERGENCE AFTER 15 ITERATIONS
 3001 LL=LL+1
      SUM = 0.
      DO 700 I = 1,NP
      DWEST(I) = B+((C*X(I))/(A+X(I))
      DIFF(I) = DWEST(I)-DWE(I)
      XPER(I) = ABS((DIFF(I)/DWE(I)))
      SUM=SUM+XPER(I)
  700 CONTINUE
      XNP=NP
      SSUM=SUM/XNP
      IF (SSUM-TOL) 2000, 2000, 150
C IF SUFFICIENT FIT, REDUCE TOLERANCE.  IF NOT, TRY AGAIN!
 2000 TOL=TOL*0.75
      GO TO 149
  999 CONTINUE
      TOL=TOL/0.75
C THIS IS SATISFIED TOLERANCE
      SIGSUM=0.
      DO 4000 I=1,NP
      SIGSUM=SIGSUM+DIFF(I)**2
 4000 CONTINUE
C CALCULATE SIGMA SQUARED, VARIANCES AND STD ERRORS
      SIGMA2-SIGSUM/(XNP-3.)
      VARA=SIGMA2*(BB*CC-BC*BC)/DET1
      VARB=SIGMA2*(AA*CC-AC*AC)/DET1
      VARC=SIGMA2*(AA*BB-AB*AB)/DET1
      SEA=SQRT(VARA)
      SEB=SQRT(VARB)
      SEC=SQRT(VARC)
      A=-ALOG10(A)
C THIS IS THE PKA
 9999 STOP
      END
```

CHAPTER 3

THE ROLE OF TRYPTOPHAN IN THE COMBINING SITES OF ANTIBODIES AGAINST THE DINITROPHENYL GROUP

INTRODUCTION

An important contribution to the specificity of anti-DNP and anti-TNP antibodies may be provided by the interaction of the nitrophenyl group with a tryptophan residue in the combining site. Evidence for such an interaction has been obtained by several means. High affinity rabbit anti-DNP antibodies contain 50% more tryptophan than low affinity antibodies (McGuigan and Eisen, 1968). This difference is associated entirely with the Fd region. It is consistent with the observation that the H-chain plays a predominant role in the binding of DNP compounds to specific rabbit antibodies (Haber and Richards, 1966). The binding of nitrophenyl compounds to antibodies results in substantial quenching of the tryptophan fluorescence (Velick et al., 1960). The ultra-violet absorption spectrum of the bound nitrophenyl group is red-shifted, and often exhibits hypochromism (Eisen et al., 1968). These absorbance changes are reproduced in aqueous solutions of tryptophan. They are not reproduced in solutions of other amino acids, nor by changes of solvent (Little and Eisen, 1967). Circular dichroism (CD) spectra of DNP and TNP ligands are induced on binding. These spectra are strongly indicative of an interaction with tryptophan (Freed et al., 1976; Orin et al., 1976). All these spectral changes, originally observed with heterogeneous antibody populations, have also been seen with myeloma proteins possessing DNP binding activity. Comparisons were first made with protein 315 (Glaser and Singer, 1971;

Michaelides and Eisen, 1974; Freed et al., 1976). They have since been extended to proteins 460 (Rockey et al., 1972) and 25 (Hardy and Richards, 1978). It has been suggested on theoretical grounds that a charge-transfer process is an important feature of the interaction (Szent-Györgi, 1960; Eisen and Siskind, 1964). A charge-transfer interaction with tryptophan has also been proposed to underlie the large exothermic heats of reaction generated on binding (Johnston et al., 1974).

The observation that the absorbance changes of nitrophenyl groups on binding to antibodies could be reproduced in aqueous solutions of tryptophan, suggests that the relative orientations of the ligand and tryptophan moieties are similar in the two cases. The elucidation of the structure of the complex of ligand and tryptophan should therefore provide information about the interaction occurring in the antibody combining site. The technique of n.m.r. is particularly suitable for studying weak complexes between aromatic molecules in solution, since the effects of ring-currents associated with such molecules can be related to the geometries of the complexes (Johnson and Bovey, 1958). N.m.r. studies on this system were first carried out in this laboratory by P. Gettins, who showed that the aromatic ^{1}H resonances of both tryptophan and DNP compounds were upfield shifted on complex formation, indicative of a stacking interaction. This chapter primarily describes a more detailed characterization, by n.m.r., of the structural and thermodynamic parameters for complexes between nitrophenyl compounds and aromatic amino acids. The evidence for the importance of tryptophan in the combining sites of anti-DNP and anti-TNP antibodies is critically assessed.

RESULTS AND DISCUSSION

Stoichiometry of complex formation

The titration of tryptophan with a solution of DNP-aspartate is shown in Figure 3.1a. Complex formation is monitored by the change in chemical shift of the tryptophan H_7 resonance. The conditions of a low concentration of tryptophan and excess DNP-aspartate were chosen to produce a large fraction of tryptophan complexed with DNP-aspartate. The converse experiment, favouring complexes of DNP-aspartate, is shown in Figure 3.1b. The chemical shift change of the DNP-aspartate H_3 resonance is followed. Simple inspection shows that the two curves are not of the same form. The formation of a 1:1 complex alone is not sufficient to explain the data. The simplest model consistent with the results involves formation of a 2:1 complex of tryptophan/DNP-aspartate in addition to the 1:1 complex. Formation of the 2:1 DNP-aspartate/tryptophan complex appears to be negligible.

Formation of 2:1 complexes has been observed in many analogous systems. For example, a 2:1 complex of tryptophan/adenosine is observed in water (Dimicoli and Hélène, 1973). Similar complexes have been observed in nonaqueous solvents (Landauer and McConnell, 1952; Ross and Labes, 1957). In each case, the 2:1 complex involves two molecules of the donor, or electron rich, species. However, 2:1 complexes are not always formed. Similar systems may form 1:1 complexes only, 2:1 complexes, or long stacks. No general rules have emerged for predicting the stoichiometries of complexes between small aromatic molecules. Many workers have used conditions which would not reveal the presence of all the complexes being formed. Generalizations become correspondingly harder to make.

Previous studies of the properties of complexes between

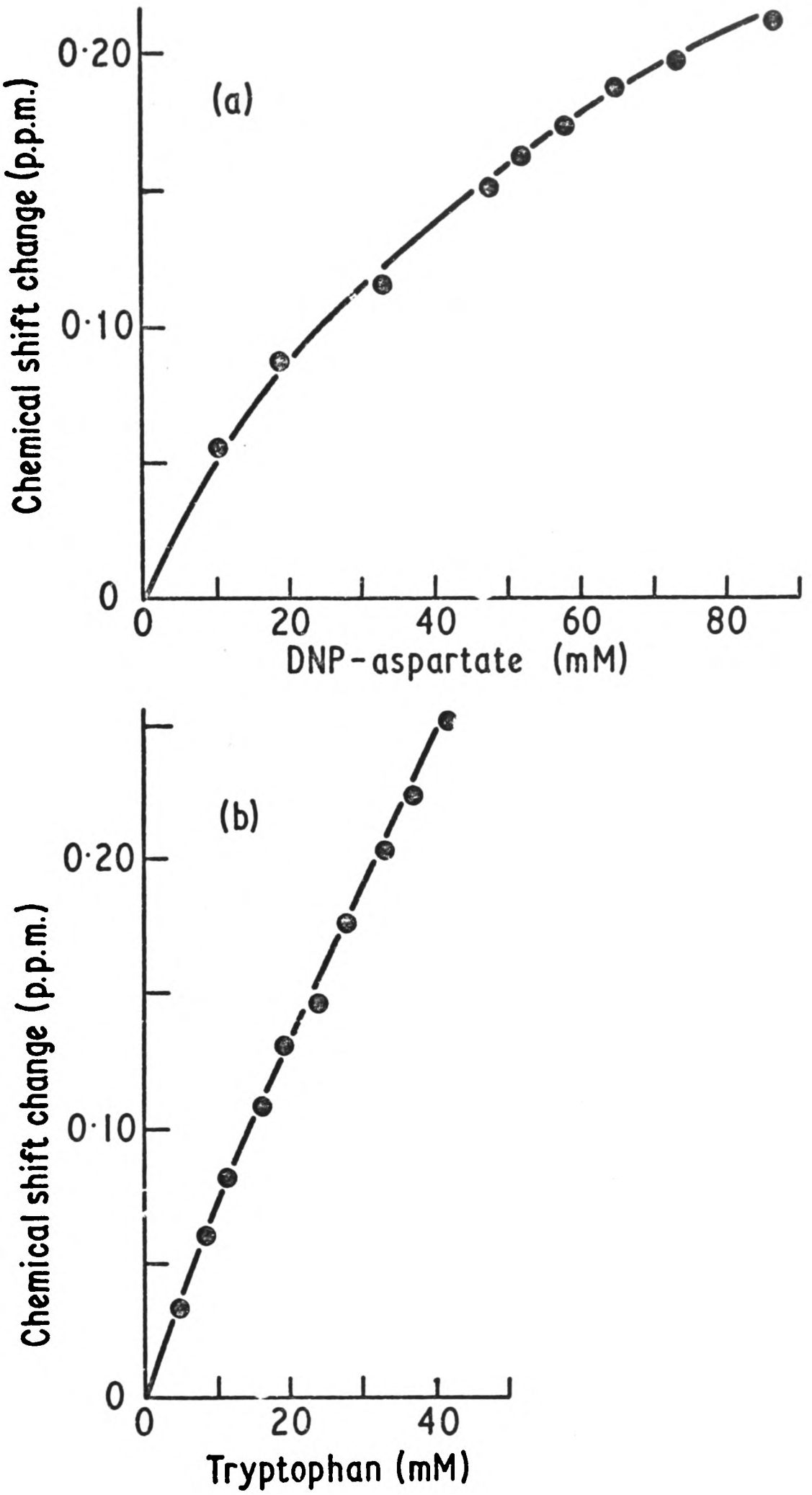

Figure 3.1 Chemical shift changes following the formation of DNP-aspartate/tryptophan complexes

Measurements were made at 270 MHz, T = 303K, with solutions in $^{2}H_{2}O$, 0.15M NaCl, pH* 6.1. (a) H_7 resonance of tryptophan (4.0 mM). (b) H_3 resonance of DNP-aspartate (4.14 mM).

tryptophan and nitrophenyl compounds in water have assumed 1:1 stoichiometry (Little and Eisen, 1967; Johnston et al., 1974). Since this assumption has been shown not to hold, a re-examination of some of the parameters of the interaction is described below.

Affinity constants of complex formation

Titrations of the type shown in Figure 3.1 were analysed on the basis of the following two equilibria:

$$\text{Trp} + \text{DNP} \overset{K_{D1}}{\rightleftharpoons} \text{Trp/DNP}$$

$$\text{Trp/DNP} + \text{Trp} \overset{K_{D2}}{\rightleftharpoons} \text{Trp/DNP/Trp}$$

Details of the procedure are given in Chapter 2. For the complexes of tryptophan with DNP-aspartate, at 303K, the value of K_{D1} was found to be 40-90 mM, and the value of K_{D2} 160-360 mM, with $K_{D2} \approx 4K_{D1}$. It has previously been shown that formation of Trp/Trp or DNP/DNP complexes is negligible (Gettins, private communication).

The possible influence of the side-chain on the structure and affinity of the complex was investigated. Titrations of DNP-glycine and DNP-aminocaproate with tryptophan are shown in Figure 3.2. The reverse experiments were not performed, because of the low solubility of DNP-glycine and DNP-aminocaproate relative to DNP-aspartate. The titration curves are very similar to those of Figure 3.1b. This implies that the major interaction occurs through the rings, with the side-chains playing a minor role in determining the affinity of binding. Some influence of the side-chain is, however, detectable. Table 3.1 shows the ratios of the

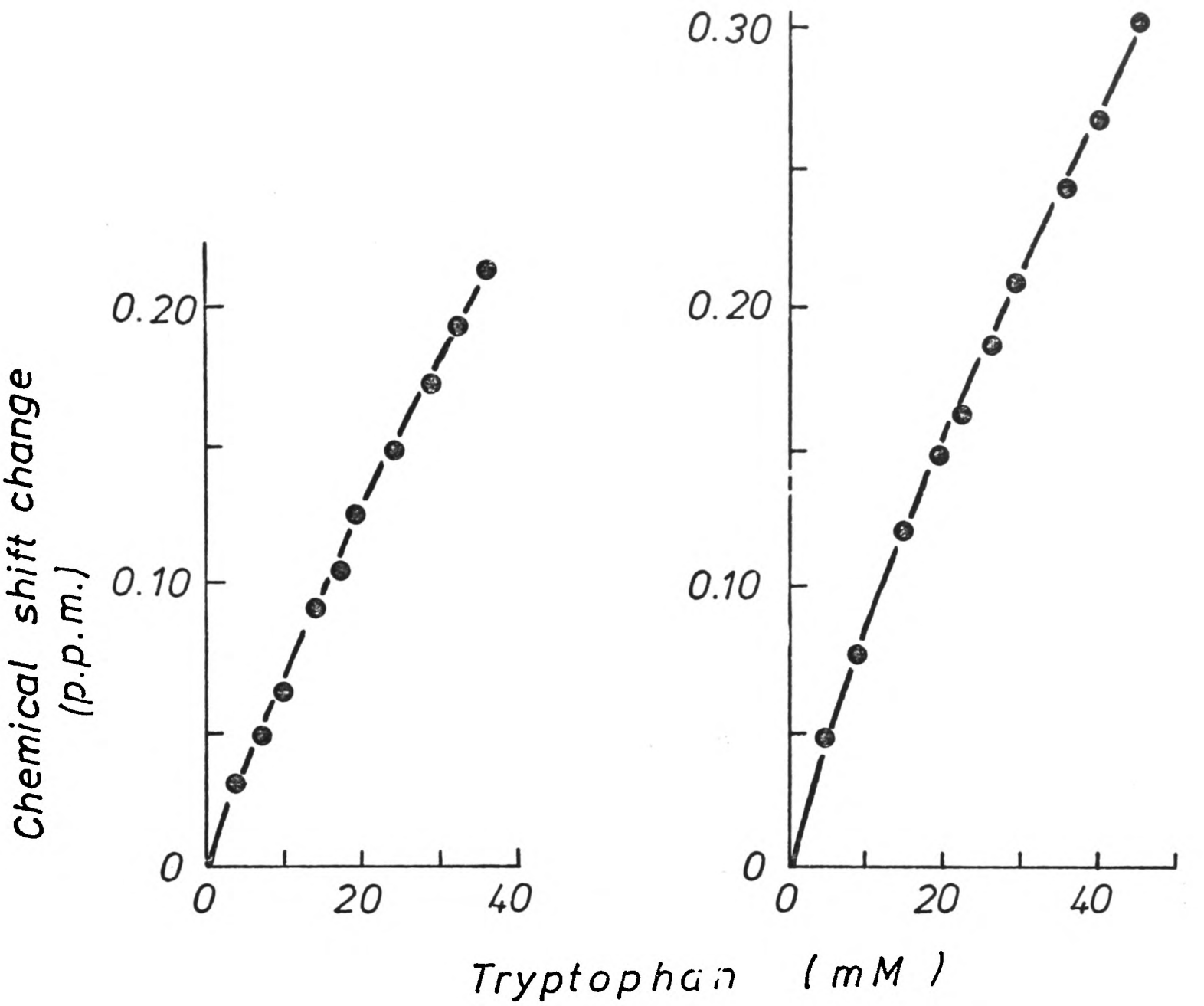

Figure 3.2 Chemical shift changes following the formation of DNP-glycine/tryptophan and DNP-aminocaproate/tryptophan complexes

Measurements were made at 270 MHz, T = 303K, with solutions in ^2H_2O, 0.15M NaCl. (a) H_3 resonance of DNP-glycine (3.63 mM), pH* 6.0. (b) H_3 resonance of DNP-aminocaproate (2.92 mM), pH* 6.8.

chemical shift changes of the three sets of DNP ^1H resonances, relative to the H_3 resonance. The small differences imply changes in the relative orientations of the DNP and tryptophan rings.

Table 3.1 Ratios of chemical shift changes of DNP resonances for DNP/tryptophan complexes

Measurements were made at 270 MHz, T = 303K, in ^2H_2O containing 0.15M NaCl, pH* = 7.0

	DNP-aspartate	DNP-aminocaproate	DNP-glycine
H_5/H_3	0.64	0.65	0.69
H_6/H_3	0.49	0.75	0.76

The intrinsic affinity for complex formation between DNP-aspartate and tryptophan, assuming equivalent sites on each DNP molecule, is given by $2K_{D1}$ (or $\frac{1}{2}$ K_{D2}). Equivalence of sites is indicated both from the finding that $K_{D2} \approx 4K_{D1}$, and from the observation that the ratios of the chemical shift changes of the DNP resonances remain constant for the course of the titration shown in Figure 3.1b. The intrinsic dissociation constant at 303K is therefore 80-180 mM. This is within the range commonly found for weak donor-acceptor complexes. The value is approximately half that derived from optical measurements (Little and Eisen, 1967). The optical measurements were carried out under conditions very similar to Figure 3.1b. It is clear that since the optical data were analysed on the assumption of 1:1 stoichiometry, the apparent binding constant would be weaker than the true binding constant. The two sets of data are therefore consistent.

Enthalpy and entropy changes on complex formation

The ΔH for association of tryptophan and DNP-aminocaproate in water has been estimated calorimetrically to lie between -3.8 and -7.4 kcal mol^{-1} (Johnston et al., 1974). However, 1:1 stoichiometry was assumed in the study although the conditions used, very similar to Figure 3.1b, favoured formation of the 2:1 complex. Because of the apparently weak binding, it was reported by the authors that the extrapolated value of ΔH was almost linearly dependent on the assumed dissociation constant.

In order to re-examine the thermodynamic parameters, conditions were chosen under which formation of the 2:1 complex is negligible. This necessitates using high DNP concentrations, and DNP-aspartate was used for the experiments since it is very soluble in water. The results presented above suggest that there will be no significant difference between the parameters obtained for DNP-aspartate or for DNP-aminocaproate.

The temperature dependence of complex formation between tryptophan and DNP-aspartate is shown in Figure 3.3. The dissociation constants and chemical shift changes for complex formation at each temperature were calculated by the best-fit procedure described in Chapter 2. The values are given in Table 3.2.

For the calculation of ΔH and ΔS for complex formation, the structure of the complex should be unchanged over the temperature range used. That the structure is constant, is shown by the small variations of the extrapolated chemical shift changes given in Table 3.2. The values for the H_7 and H_4 tryptophan resonances all lie within 11% of their respective means. A more accurate measure may be obtained from the ratios of the chemical shift changes for the five tryptophan aromatic resonances. No

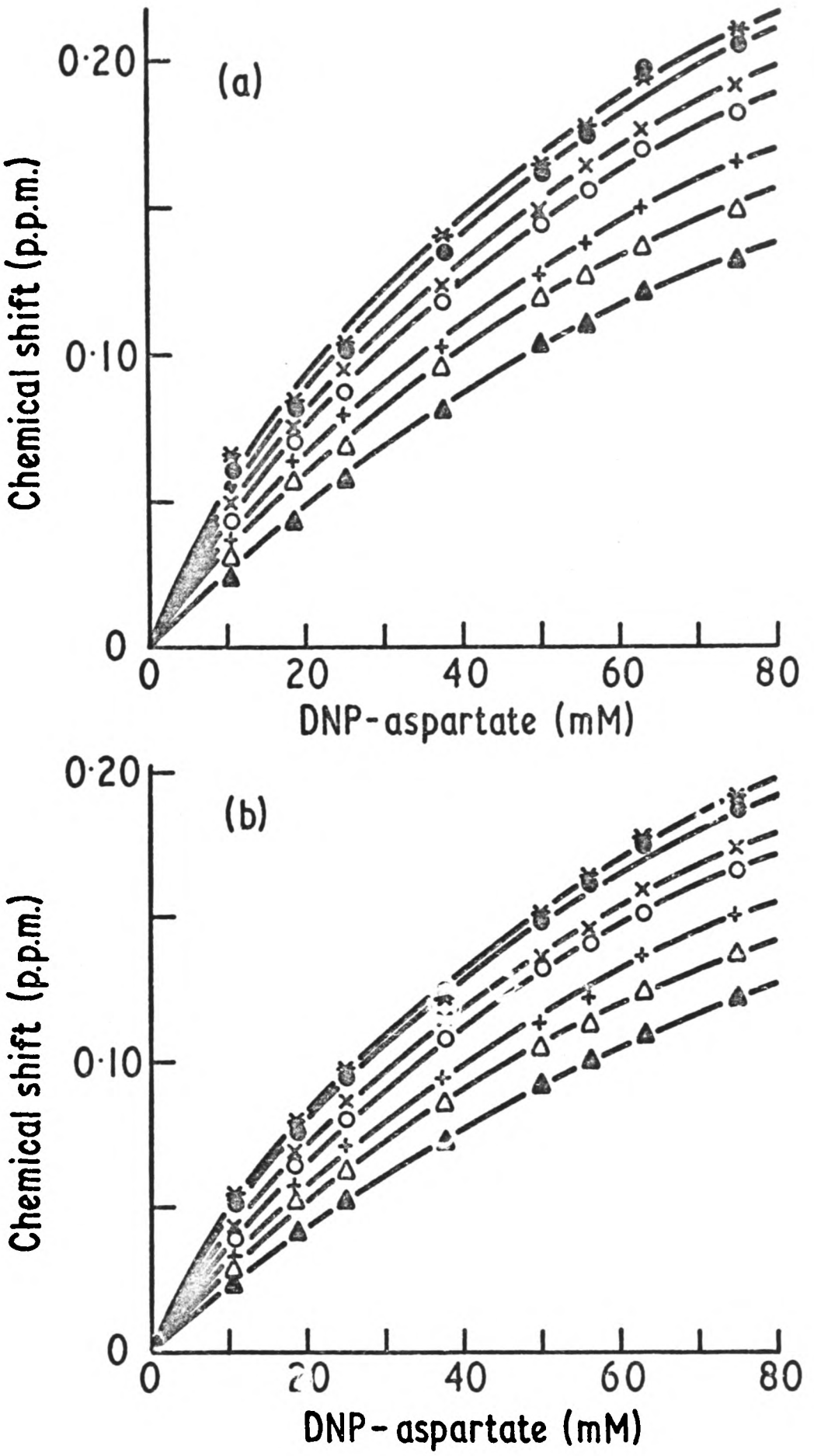

Figure 3.3 Temperature dependence of the formation of complexes between DNP-aspartate and tryptophan

Measurements were made at 270 MHz with solutions in ^2H_2O, 0.15M NaCl, pH* 7.0. The tryptophan concentration was 3.0 mM. * - 277.5K, ● - 282K, x - 292.5K, o - 302.5K, + - 312K, △ - 322K, ▲ - 332K.

differences exceeded 5%.

Table 3.2 Dissociation constants and chemical shift changes for the DNP-aspartate/tryptophan complex

Measurements were made at 270 MHz in ^2H_2O solutions containing 0.15M NaCl, pH* = 7.0

	Tryptophan resonance			
	H_7		H_4	
Temperature (K)	K_{D1} (mM)	Chemical Shift change (p.p.m)	K_{D1} (mM)	Chemical Shift change (p.p.m)
277.5	70	0.41	66	0.35
282	73	0.41	79	0.39
292.5	80	0.40	80	0.36
302.5	84	0.39	77	0.34
312	92	0.37	95	0.34
322	103	0.36	109	0.34
332	133	0.37	131	0.34

A van't Hoff plot of the binding data given in Table 3.2 is shown in Figure 3.4. The slope of the curve gives $\Delta H = -2.0$ kcal mol^{-1}. This value is much lower than the value obtained calorimetrically for the complex of tryptophan with DNP-aminocaproate (Johnston et al., 1974). This difference reflects the assumption of 1:1 stoichiometry in the calorimetric study, and the use of optically determined dissociation constants. It is therefore concluded, contrary to the previous suggestion, that the large negative enthalpy changes generally observed on the binding of nitrophenyl groups to antibodies do not predominantly arise from interactions with one or more tryptophan residues in the combining sites.

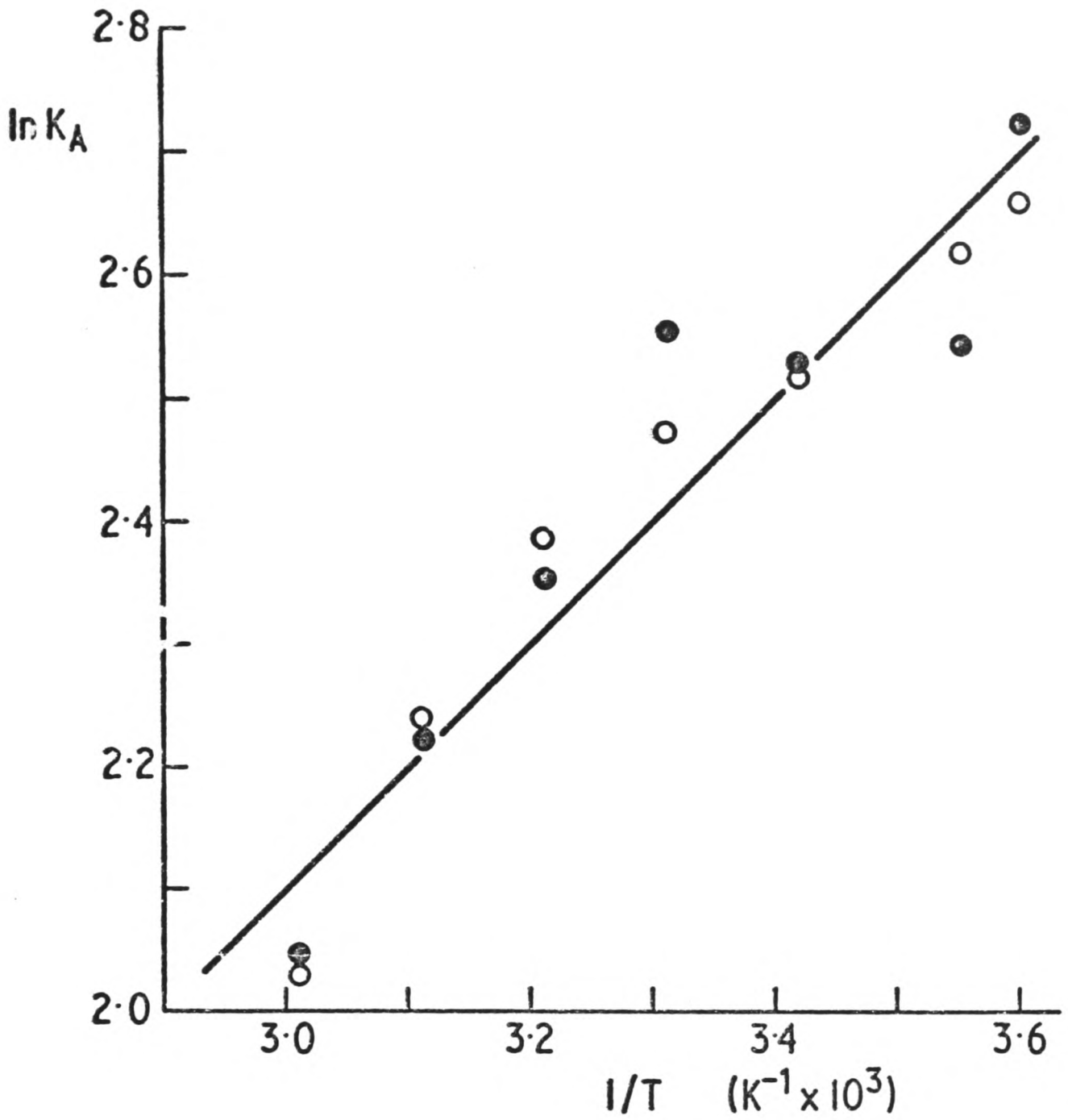

Figure 3.4 Van't Hoff plot for complex formation between DNP-aspartate and tryptophan

Association constants (K_A) were calculated from the data given in Table 3.2. o - Tryptophan H_7 resonance. ● - Tryptophan H_4 resonance.

The unitary free energy change, ΔG_u, for complex formation at 303K may be obtained from the intrinsic dissociation constant. The definition of unitary free energy has been given in Chapter 2. The value of ΔG_u is -3.5 kcal mol^{-1} at 303K, and the value of ΔS_u is therefore ~~+2.8~~ 5.0 e.u. The contribution of entropic factors to complex formation may, however, be much larger than the net entropic change suggests. This possibility arises from consideration of the loss of rotational and translational entropy on complex formation. The magnitude of these effects is very difficult to estimate, since the theoretical value for two molecules completely immobilized with respect to each other will be reduced by any residual relative motion (Page and Jencks, 1971). However, it is still expected to be significant, and could reach 30-35 e.u. (Page and Jencks, 1971; Janin and Chothia, 1978). On this basis, the driving force for association would come from an entropically favourable process, that of exclusion of solvent from the interacting surfaces (Chothia and Janin, 1975; Janin and Chothia, 1976). Any specific effect, for example a charge-transfer interaction, would provide an additional but relatively small contribution to the free energy of complex formation. Such specific interactions would influence the geometry of the complex. However, if these specific interactions contribute only a small proportion of the total binding energy, the relative positions of the DNP and tryptophan rings may be altered without a large effect on the affinity of the complex. The implications of this possibility are discussed in Chapter 5.

Chemical shift changes and the structure of the complex

The chemical shift changes for the ring proton resonances of tryptophan and DNP-aspartate on complex formation are given in

Table 3.3. Errors are quite large because of the weak binding and formation of 2:1 complexes.

Table 3.3 Chemical shift changes of DNP-aspartate and tryptophan resonances on formation of a 1:1 complex

Measurements were made at 270 MHz, T = 303K, in ^2H_2O containing 0.15M NaCl, pH* = 7.0

Resonance	Chemical shift change (p.p.m)
Trp H_7	0.26 -0.40
Trp H_4	0.23 -0.35
Trp H_6	0.19 -0.29
Trp H_2	0.19 -0.29
Trp H_5	0.18 -0.28
DNP H_3	0.35 -0.55
DNP H_5	0.22 -0.35
DNP H_6	0.17 -0.27

Since the ratios of the chemical shift changes of the DNP resonances remain constant during the titrations, the chemical shift changes of those resonances in the 2:1 complex are twice the values given in Table 3.3.

Ring current effects, rather than local solvent changes, are likely to be the most important factors in determining the chemical shift changes (Hanna and Ashbaugh, 1964; Wain-Hobson, 1977). The upfield chemical shift changes observed for all the aromatic proton resonances therefore show that a stacked complex is formed, with a large degree of overlap of the two ring systems. The structure of the complex in solution is very similar to the structures of complexes between similar molecules determined

crystallographically which also show overlap of the two ring systems in a stacked geometry (Hanson, 1964; Gartland et al., 1974).

The chemical shift changes observed on formation of the DNP-aspartate/tryptophan complex fall in the same range as those of similar weak donor-acceptor complexes. An example is the adenosine/tryptophan system (Dimicoli and Hélène, 1973). Higher values of 1-1.5 p.p.m. are often found in the earlier literature (Foster and Fyfe, 1965). These values may reflect the assumption of 1:1 stoichiometry for systems with excess of the donor species.

Absorbance studies

The characteristic absorbance changes of nitrophenyl compounds on binding to myeloma proteins or to heterogeneous antisera are generally accepted to indicate a specific interaction with tryptophan. The difference spectra obtained with a TNP ligand on binding to the Fab fragment of protein 315 or to tryptophan are shown in Figure 3.5. It is clear that these absorbance changes do reflect specific interactions rather than binding per se, or a change in the local dielectric constant. In contrast to the red shift observed on binding to antibodies, the absorption spectra undergo a blue shift on transfer from water to a less polar solvent (Little and Eisen, 1967; Schubert et al., 1960). The weak binding to BSA is also associated with a small blue shift (Carsten and Eisen, 1953).

Although the characteristic difference spectrum is produced on the binding of nitrophenyl ligands to antisera, this does not prove that all, or even the majority of antibodies constituting those antisera produce the effect. Since it is now possible to

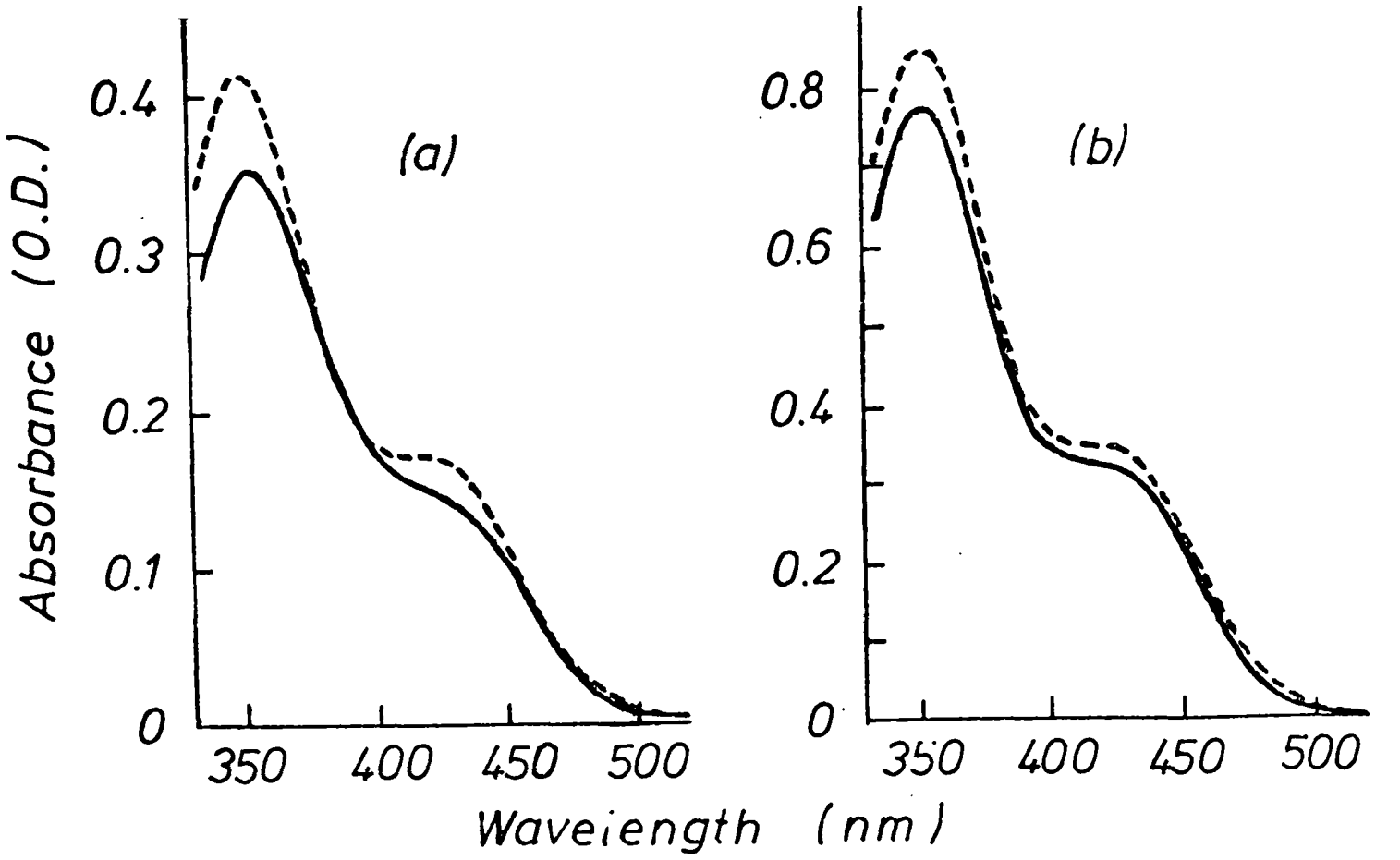

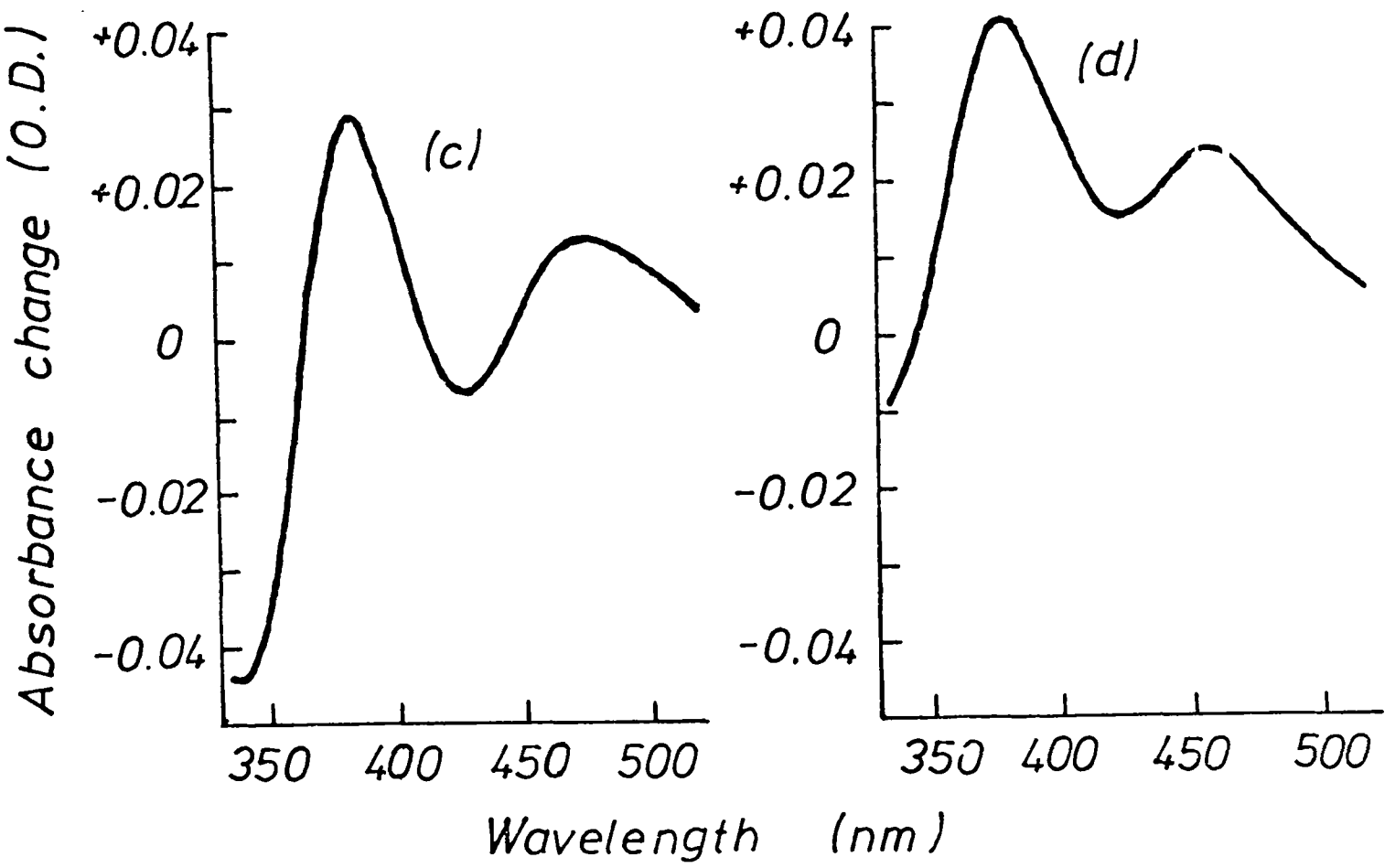

Figure 3.5 Changes of the absorption spectrum of TNP-aminomethylphosphonate following the formation of complexes

(a) Absorption spectrum of TNP-aminomethylphosphonate (9.5×10^{-5}M) in the absence (---) or presence (——) of the Fab fragment of protein 315 (6.5×10^{-5}M), in 0.01M potassium phosphate, 0.15M NaCl, pH 7.4.

(b) Absorption spectrum of TNP-aminomethylphosphonate (1.9×10^{-4}M) in the absence (---) or presence (——) of tryptophan (3.3×10^{-2}M), in 0.15M NaCl, pH 6.0.

(c) Difference spectrum with the Fab fragment.

(d) Difference spectrum with tryptophan.

purify individual antibodies from a heterogeneous antiserum using the cell fusion technique, this idea may be directly tested. The effect of the binding of one such antibody, protein A3, on the absorption spectrum of DNP-lysine is shown in Figure 3.6. The isolation and binding properties of protein A3 are described in detail in Chapter 7. The absorption spectrum is red shifted by 28 nm, and a typical difference spectrum is produced. Protein A3 therefore shares with the anti-DNP myeloma proteins the ability to produce this absorbance change. The molecular interaction underlying this absorbance change may be common to most, if not all, anti-DNP antibodies.

It is not possible at present to determine the type of spectral perturbation which would be associated with the interaction of a nitrophenyl group with tyrosine or phenylalanine rather than tryptophan. Although no perturbation by tyrosine or phenylalanine was detected in the reported study (Little and Eisen, 1967), it will be shown in the following section that complex formation is too weak to have given an observable effect. In the absence of this direct experimental test, and of a theoretical understanding of the changes observed, the conclusion that tryptophan is always involved must be questionable. Although the observation of the characteristic difference spectrum is strongly suggestive of a stacking interaction with tryptophan, it is preferable to be able to obtain independent evidence in any particular case.

The specificity of the interaction of tryptophan with DNP

It has been suggested that a charge-transfer interaction may be a factor determining the specificity of tryptophan for DNP compounds. Tryptophan has the highest ionization potential of

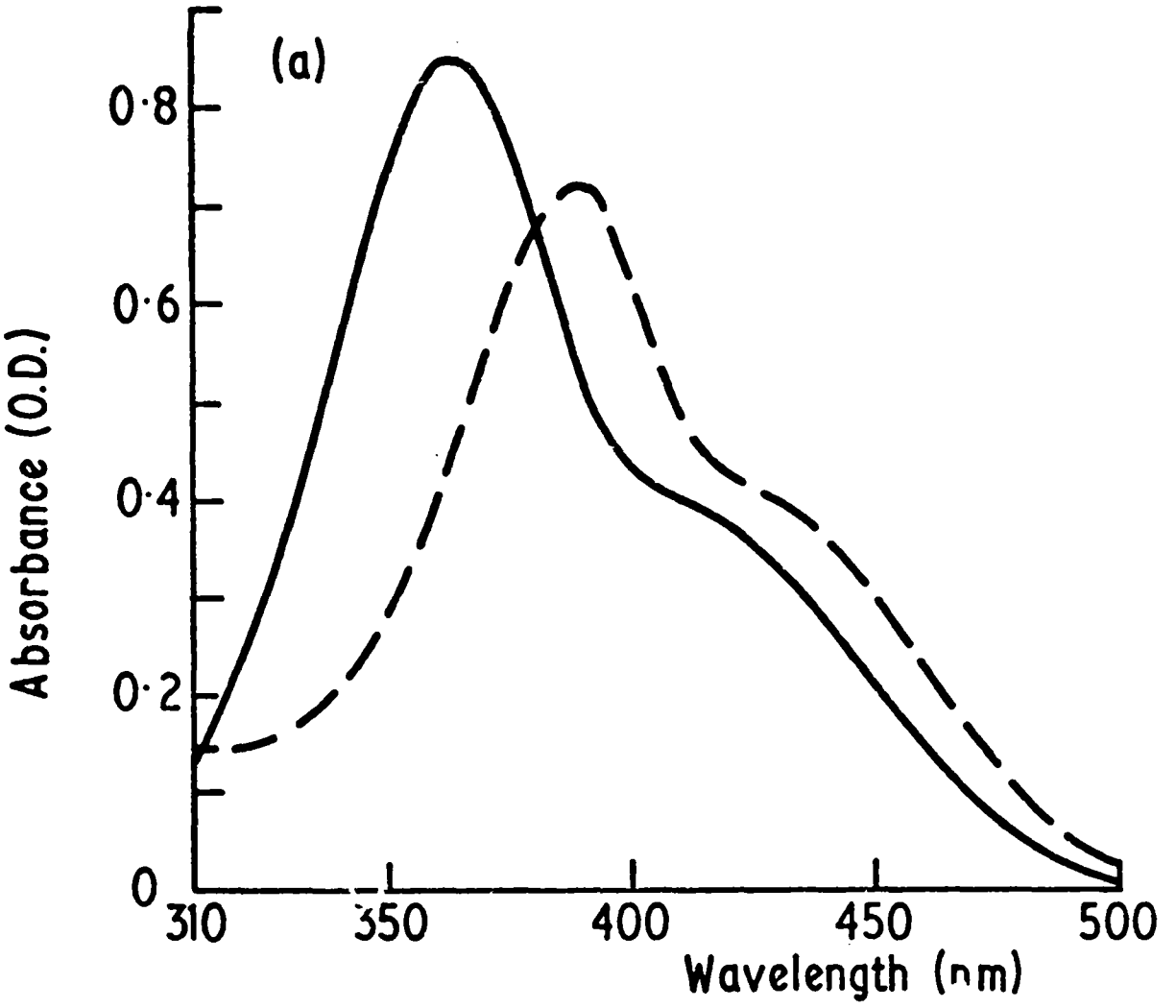

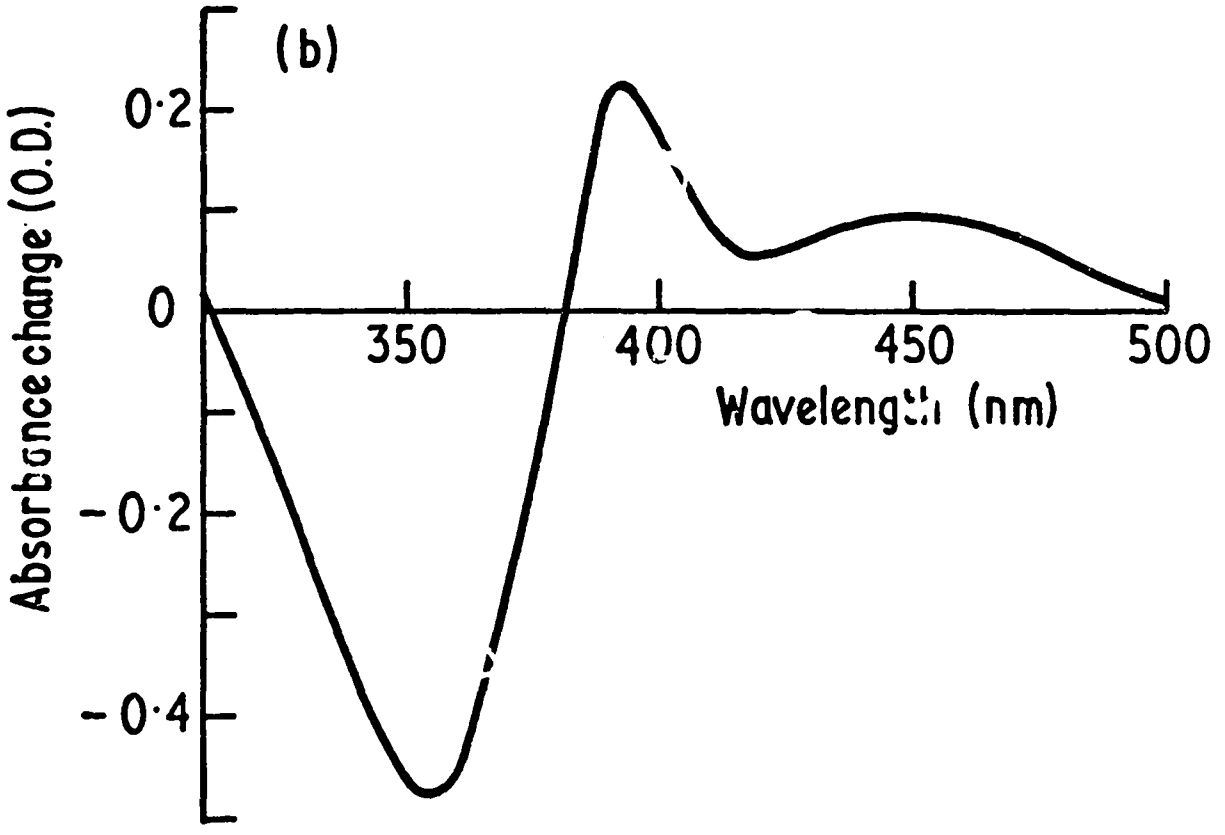

Figure 3.6 Change of the absorption spectrum of DNP-lysine following binding to protein A3.

(a) Absorption spectrum of DNP-lysine (53 μM) in the absence (——) or presence (---) of protein A3 (33 μM), in 0.015M potassium phosphate, 0.15M NaCl, pH 7.0. (b) The resulting difference spectrum.

the amino acids, and is therefore the most likely to act as an electron donor in a donor-acceptor complex (Szent-Györgyi, 1960). The term 'charge-transfer' is widely used to describe complexes of weak acceptors and donors, although transfer of charge may not provide a large proportion of the interaction energy (Foster, 1969). The spectral and thermodynamic properties of such complexes are poorly understood. Although extra absorption bands, or charge-transfer bands, are often seen in the electronic spectra of these complexes, they are generally of low intensity ($\varepsilon_{max} \approx 1000 M^{-1} cm^{-1}$) and may be masked by bands from the interacting species. No distinct band can be seen on the binding of DNP to antibodies or to tryptophan. It would be expected that the stability of a donor-acceptor complex would be affected by the ionization potential of the donor and the electron affinity of the acceptor. Although there is evidence for this in the literature, it is difficult to separate this effect quantitatively from any concomitant effects on other intermolecular forces. For example, substitution of groups of different polarizabilities may affect not only the charge-transfer interaction, but also the van der Waals dispersion forces. For this reason, the possible specificity of tryptophan for DNP is described below in a qualitative manner.

Neither the optical studies mentioned previously nor initial n.m.r. studies (Dower et al., 1977) were able to detect an interaction of DNP with tyrosine or phenylalanine. This implied an important role for tryptophan. To maximize the possibility of detecting complex formation, n.m.r. titrations were carried out with DNP-aspartate, using low concentrations (2mM) of tyrosine or phenylalanine. Titration curves are shown in Figure 3.7. All the aromatic proton resonances undergo upfield chemical shift

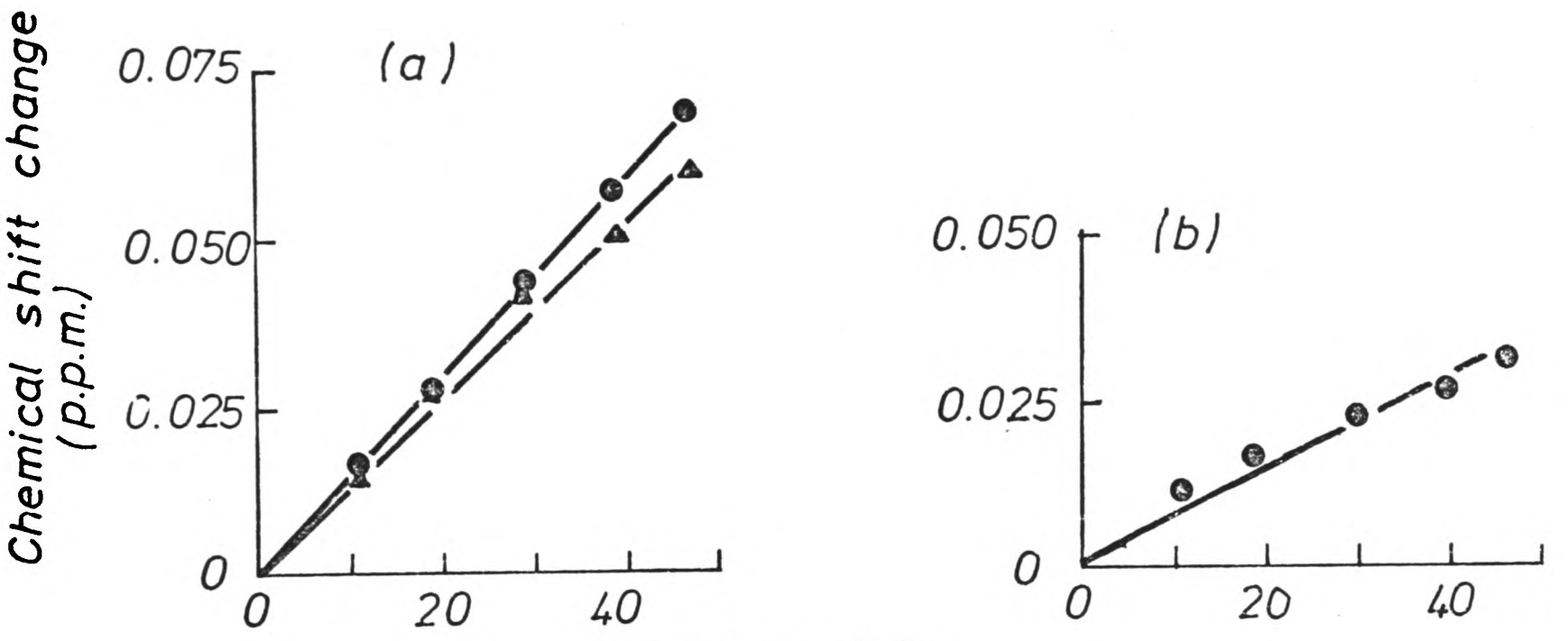

Figure 3.7 Chemical shift changes following the formation of DNP-aspartate/tyrosine and DNP-aspartate/phenylalanine complexes

Measurements were made at 270 MHz, T = 303K, with solutions in ^2H_2O, 0.15M NaCl, pH* 7.0.
(a) Tyrosine (? mM), ● - $H_{3,5}$ resonance,
▲ - $H_{2,6}$ resonance. (b) Phenylalanine (2 mM),
● - resonances at 7.33 p.p.m. and 7.46 p.p.m.

changes. Stacked complexes analogous to the complexes of DNP-aspartate with tryptophan are therefore formed with tyrosine and phenylalanine. If the changes in chemical shifts on complex formation for both the tyrosine and phenylalanine resonances are assumed to be similar in magnitude to those observed for the tryptophan system, the binding constants for the complexes with tyrosine and phenylalanine may be estimated. The affinities are approximately an order of magnitude less than that with tryptophan. Interactions were not detected by the previous absorbance or n.m.r. measurements because the fraction of complexed ligand was too low.

Since the difference in affinity between complexes of DNP-aspartate with tryptophan or with tyrosine and phenylalanine is only an order of magnitude, it seems unlikely that there is an absolute requirement for tryptophan in the combining sites of anti-nitrophenyl antibodies, particularly in low affinity antibodies.

The contribution of a DNP/tryptophan interaction to the affinity of anti-DNP antibodies

The interpretation of thermodynamic parameters in structural terms is exceedingly difficult. This is particularly applicable to the parameters ΔH and ΔS, because of the mutually compensatory relationship between enthalpy and entropy changes in water (Jencks, 1969), and because of the alterations in degrees of freedom on complex formation. The non-zero heat capacity change on binding is an additional complication. The large negative enthalpy change on the binding of DNP compounds to antibodies is therefore not explicable at present, although the studies presented in this chapter suggest that a DNP/tryptophan inter-

action does not contribute greatly to this change.

As a first step, it is necessary to evaluate the contributions of particular interactions to the unitary free energy (ΔG_u) of complex formation. The unitary free energies of the binding of DNP-lysine and of the DNP moiety alone (dinitroaniline) to protein 315 and to the homogeneous antibody protein A3 are given in Table 3.4 with the corresponding value for the DNP/tryptophan complex.

Table 3.4 Unitary free energies of binding for some complexes with DNP ligands

All measurements were made at pH 7.

Complex	Association Constant (M^{-1})	ΔG_u (kcal mol^{-1})	
DNP/tryptophan	c.3	- 3.5	(T = 303K)
DNP-lysine/315	3.3×10^6 (a)	-11.4	(T = 298K)
Dinitroaniline/315	2.9×10^5 (b)	- 9.9	(T = 293K)
DNP-lysine/A3	1.8×10^7 (c)	-12.4	(T = 293K)
Dinitroaniline/A3	1.3×10^6 (c)	-10.8	(T = 303K)

(a) Dower et al., 1978. (b) Gettins et al., 1978. (c) Chapter 7.

It can be seen from Table 3.4 that a DNP/tryptophan interaction alone could provide approximately a third of the binding energy of DNP ligands for proteins 315 and A3. This is clearly a substantial contribution to ΔG_u, and indicative of the importance of this type of interaction. The contribution would obviously be proportionally less for antibodies of very high affinity (approximately a quarter for antibodies of affinity 3×10^8 M^{-1}). The contributions of the nitro groups, in terms of van der Waals forces and hydrogen bonding, may be estimated from the effect of replacing them with chloro groups after allowing for the concomi-

tant change in the energy of the stacking interaction (Gettins et al., 1978). The effect on the affinities of protein 315 (Gettins et al., 1978) and of protein A3 (Chapter 7) is a reduction in affinity of approximately 5-fold to 10-fold per nitro group, equivalent to a ΔG of 1 to 1.4 kcal mol^{-1}. Since there is probably some residual interaction with the chloro group, the contribution of each nitro group is at least -1 to -1.4 kcal mol^{-1} to the overall free energy change. About two-thirds of the interaction energy of proteins 315 and A3 with DNP compounds is therefore accounted for by a stacking interaction with tryptophan and by interactions with the nitro groups. The remaining energy might be accounted for by the interaction of apolar protein residues with the side of the DNP ring which is not involved in the stacking interaction and with the aliphatic side chain. As discussed previously in this chapter, an important feature of the mechanism underlying these free energy changes may be the exclusion of water from the interacting surfaces of the protein and ligand (Kauzmann, 1959; Karush, 1962; Chothia and Janin, 1975). In order to produce very high affinity antibodies both the steric fit and the nature of the interacting protein residues would have to be optimized. As suggested many years ago by Karush (1962), what is required is a pure high affinity antibody to define the upper limits of the interaction. The necessary technology, in the form of the cell fusion method, now exists for the production of such antibodies.

CHAPTER 4

MODEL-BUILDING OF ANTIBODY COMBINING SITES

INTRODUCTION

It is now well established that the structures of immunoglobulin domains are very similar, and that the basis for this similarity is the conservation of a framework structure, the 'immunoglobulin fold' (Poljak et al., 1973; Davies et al., 1975a and b; Edmundson et al., 1975; Epp et al., 1975). Similarity is particularly marked when equivalent domains are compared (Padlan and Davies, 1975). It should, therefore, be possible to predict the structure of any immunoglobulin domain by aligning its amino acid sequence with that of an equivalent domain of known structure (Poljak et al., 1974; Padlan et al., 1976a). The resulting model may then be tested against physicochemical data, and modified accordingly (Dwek et al., 1977). If validated, such a procedure provides an important complementary approach to crystallographic studies, and is of particular use for proteins which cannot be crystallized, or for which high-resolution X-ray data cannot be collected.

To construct a model of an immunoglobulin V-domain, the framework is assumed to be identical in conformation to that of a known structure, and the hypervariable loops are attached to this framework with appropriate allowances for insertions and deletions (Padlan et al., 1976a). It is apparent from known structures that homologous hypervariable loops of the same length have similar structures (Padlan, 1977). However, no quantitative measure of their differences, and hence of likely errors in the model-building, has been presented in the literature. In addition

few such comparisons are available for framework regions. Since the model of protein 315 was constructed using the framework coordinates of protein 603 (Padlan et al., 1976a) it is important to determine the influence of this choice on the structure of the model. The construction of a model of a complete combining site, rather than of an individual domain, requires the further assumption that the mode of dimerization of two V-domains is conserved. The validity of this assumption must also be tested.

In this chapter, a quantitative comparison of the framework and hypervariable regions of four V_L domains is presented, using the most accurate coordinates of each structure available. Comparisons between homologous hypervariable loops are necessarily restricted to those of identical length. Only two structures of V_H domains are available, for proteins New and 603. A detailed comparison of their hypervariable regions is not possible, since only the short H_1 (first hypervariable) loops have the same lengths. The modes of dimerization of two V_LV_H pairs (proteins New and 603) and of two V_LV_L pairs (proteins REI and Mcg) are compared.

The comparisons of frameworks, hypervariable regions and modes of dimerization are also directed towards assessing the feasibility of predicting a structure for the combining site of the V_L dimer of protein 315, as an aid to the interpretation of the n.m.r. results presented in Chapter 5.

MATERIALS AND METHODS

Coordinates

Coordinates of the V_L dimer of protein REI (human κ-chain, 2.0 Å resolution) were kindly provided by Professor R. Huber.

The individual monomers of protein REI are almost identical in structure (Epp et al., 1975). Monomer 1 was used in the structure comparisons. Coordinates of the Fab fragment of protein 603 (mouse IgA/κ, 3.1 Å resolution) were kindly provided by Dr. D.R. Davies. Coordinates of the Fab' fragment of protein New (human IgG/λ, 2.0 Å resolution) and of the L-chain dimer of protein Mcg (human λ-chain, 2.3 Å resolution) were obtained from the Oxford and Cambridge data banks respectively. Monomer 2 of protein Mcg was used in the structure comparisons, since the conformation of this monomer mimics that of the L-chain in intact immunoglobulins (Schiffer et al., 1973). In addition, the combining site region of monomer 1 is distorted by interactions with a neighbouring molecule in the crystal (Edmundson et al., 1974b). The coordinates of the original model of protein 315 were kindly provided by Dr. E.A. Padlan.

Alignment of sequences

The amino acid sequences of the V_L domains of proteins REI, 603, New, Mcg and 315, aligned and numbered according to Kabat et al. (1976) are given in Table 4.1. The sequences of the V_H domains of proteins 603, New and 315 are given in Table 4.2. In this numbering system, the framework of the V_L domain is considered to include residues 1-23, 35-48, 57-88 and 98-106. The hypervariable regions of the V_L domains are formed by residues 24-34, 49-56 and 89-97. The hypervariable regions of the V_H domains include residues 31-35, 50-65 and 95-102. The numbering system of Kabat et al. (1976) is used in this chapter only, to simplify the comparison of the five structures.

The following positions were not included in the comparisons of the frameworks of the V_L domains:

Table 4.1 Alignment of V_L sequences

	1 10 20 23 27A B C D E F 28 30 35
REI	DIQMTQSPSSLSASVGDRVTITC*QASQ------DIIKYLN*W
McPC603	DIVMTQSPSSLSVSAGERVTMSC*KSSZSLLBSGBZKBFLA*W
New	XSVLTQP-PSVSGAPGQRVTISC*TGSS---SNIGAGNHVK*W
Mcg	PSALTQP-PSASGSLGQSVTISC*TGTS---SNVGGYNYVS*W
MOPC315	XAVVTQE-SALTTSPGGTVILTC*RSST---GAVTTSNYAN*W
	L_1

	40 48 50 57 60 70
REI	YQQTPGKAPKLLI*YEASNLQA*GVPSRFSGSGSGTDYTFT
McPC603	YZZKPGZPPKLLI*YGASTRES*GVPDRFTGSGSGTDFTLT
New	YQQLPGTAPKLLI*PHNNAR*-------FSVSKSGSSATLA
Mcg	YQQHAGKAPKVII*YEVNKRPS*GVPDRFSGSKSGNTASLT
MOPC315	IQEKPDHLFTGLI*GGTSDRAP*GVPVRFSGSLIGDKAALT
	L_2

	80 88 90 97B 98 100 106
REI	ISSLQPEDIATYYC*QQYQSLPYT*-FGQGTKLQI
McPC603	ISSVZAEDLAVYYC*QNDHSYPLT*-FGAGTKLEI
New	ITGLQAEDEADYYC*QSYDRSLRV*-FGGGTKLTV
Mcg	VSGLQAEDEADYYC*SSYEGSDNFV*FGTGTKVTV
MOPC315	ITGAQTEDDAMYFC*ALWFRBHFV*-FGGGTKVTV
	L_3

The sequences of proteins REI, 603, New and Mcg are those given with their coordinates. The original sequence of protein 315 (Dugan et al., 1973) has been updated at some glx and asx positions. There is also a change of glu for gln at position 6 (see Tonegawa et al., 1978).

Table 4.2 **Aligment of V_H sequences**

	1 10 20 30 35A 36
McPC603	EVKLVESGGGLVQPGGSLRLSCATSGFTFS*DFYM-E*W
New	ZVQLEQSGPGLVRPSQTLSLTCTVSGSTFS*NDYY-T*W
MOPC315	DVQLQESGPGLVKPSQSLSLTCSVTGYSIT*SGYFWN*W
	H_1

	40 49 52ABC 53 60 66
McPC603	VRQPPGKRLEWIA*ASRNKGNKYTTEYSASVKG*RFI
New	VRQPPGRGLEWIG*YVF---YHGTSDTDTPLRS*RVT
MOPC315	IRQFPGNKLEWLG*FIK---YDGSBYGBPSLKN*RVS
	H_2

	70 80 82ABC 83 90 100ABC 101
McPC603	VSRDTSQSILYLQMNALRAEDTAIYYCAR*NYYGSTWYFDV*W
New	MLVNTSKNQFSLRLSSVTAADTAVYYCAR*DLIAGCI--DV*W
MOPC315	ITRDTSENQFFLKLDSVTTZBTATYYCAG*DNDHLYF--DY*W
	H_3

	111
McPC603	GAGTTVTV
New	GQGSLVTV
MOPC315	GQGTTLTV

The sequences of proteins 603 and New are those given with their coordinates. The sequence of protein New differs at many positions from that reported in Kabat et al. (1976). The original sequence of protein 315 (Francis et al., 1974) has been altered by a change of trp for lys at position 35 (D. Givol, personal communication).

1. Position 8 of the two κ-chains. κ-chains contain one residue more than λ-chains at this position, but the deletion of this residue is not of great significance, since the distance between the alpha-carbon atoms of residues 7 and 9 is only 5.3 Å (Padlan et al., 1976a).

2. Positions 48 and 57-61 of all chains, except when stated otherwise. This deletion is required to make all four structures strictly comparable, since protein New has a deletion of residues 55-61. Although residue 48 is present in protein New, its position was found to be significantly different (>3 Å) from that of the homologous residue in all the other three structures, presumably as a direct result of the deletion.

3. The N-terminal positions 1-3. This segment is on the surface of the protein and does not appear to be an integral part of the framework.

Comparisons of homologous hypervariable loops were only made for loops of identical length. The first two residues of the L_1 loop and the first and last residues of the L_2 loop were not included, since coordinates of these residues do not exist for the present model of protein 315.

Method of structure comparisons

Alpha-carbon coordinates were compared using a FORTRAN IV program SUPERB, written for the Oxford ICL 1906A computer by Dr. J. Thornton, and made available by Dr. K. Wilson, Dept. of Biophysics, Oxford.

The program compares pairs of structures by attempting to superimpose one set of coordinates on the other, using a non-linear least squares method. One set of coordinates is held

fixed in space during this process, and the other is moved. Maximum convergence is obtained when the sum of the squares of the distances between homologous atoms of the two structures is minimized. An overall measure of structural similarity, the r.m.s. value, may then be defined as:

$$\text{r.m.s. value,} \quad R = \sqrt{\frac{\Sigma\, d_i^{\,2}}{n}}$$

where d is the distance between the ith pair of n pairs of atoms.

Superposition of two structures requires the calculation of three angles (the Euler angles, about which axial rotation occurs) and three distances (the x, y and z components of the translation vector). A minimum of six atomic positions is therefore required in any structure comparison. The rotation may be expressed as a 3 x 3 rotation matrix, M, and the translation as a 1 x 3 translation vector, V, such that:

$$\begin{pmatrix} x_1 \\ y_1 \\ z_1 \end{pmatrix} = M \begin{pmatrix} x_2 \\ y_2 \\ z_2 \end{pmatrix} + V$$

where x_1, y_1, z_1 and x_2, y_2, z_2 are the coordinates of a given atom in the structure fixed in space, and in the structure moved, respectively.

The program did not always find the minimum r.m.s. value when small numbers of atoms were compared. All comparisons using less than 50 atoms were therefore calculated twice, keeping first one set of coordinates fixed and then the other.

RESULTS AND DISCUSSION

Comparison of framework regions of V_L domains

The six comparisons of the four framework regions, and the corresponding r.m.s. deviations, are shown in Figure 4.1. The r.m.s. values range from 0.92 Å to 1.57 Å. It is therefore clear that all the structures are very similar, as previously documented (Padlan and Davies, 1975; Poljak, 1975; Padlan, 1977). It is, however, very difficult to estimate the errors in the atomic coordinates themselves, and therefore to decide when deviations between structures become significant. The accuracy of the coordinates depends on many factors, including the nominal resolution, the degree of disorder of the molecules in the crystal, the accuracy of the intensity measurements and the isomorphism of heavy atom derivatives (Blundell and Johnson, 1976). The degree of refinement of a protein structure is generally expressed as an R-factor, which is a measure of the difference between observed and calculated structure factor amplitudes. A theoretical relationship between the R-factor, resolution and error in atomic coordinates has been derived (Luzzatti, 1952). An alternative measure of accuracy, using the residual and curvature of the electron density at the atomic position is due to Cruickshank (1949). Epp et al. (1975) used a different approach to estimate the accuracy of the REI coordinates. Cruickshank's formula gave a standard deviation of 0.09 Å (errors estimated by Cruickshank's method are smaller than those estimated by Luzzatti's method; Blundell and Johnson, 1976). However, the mean deviation of the main-chain atoms of internal segments in the two halves of the dimer was found to be 0.22 Å. This was assumed to be an upper limit of the error, since small

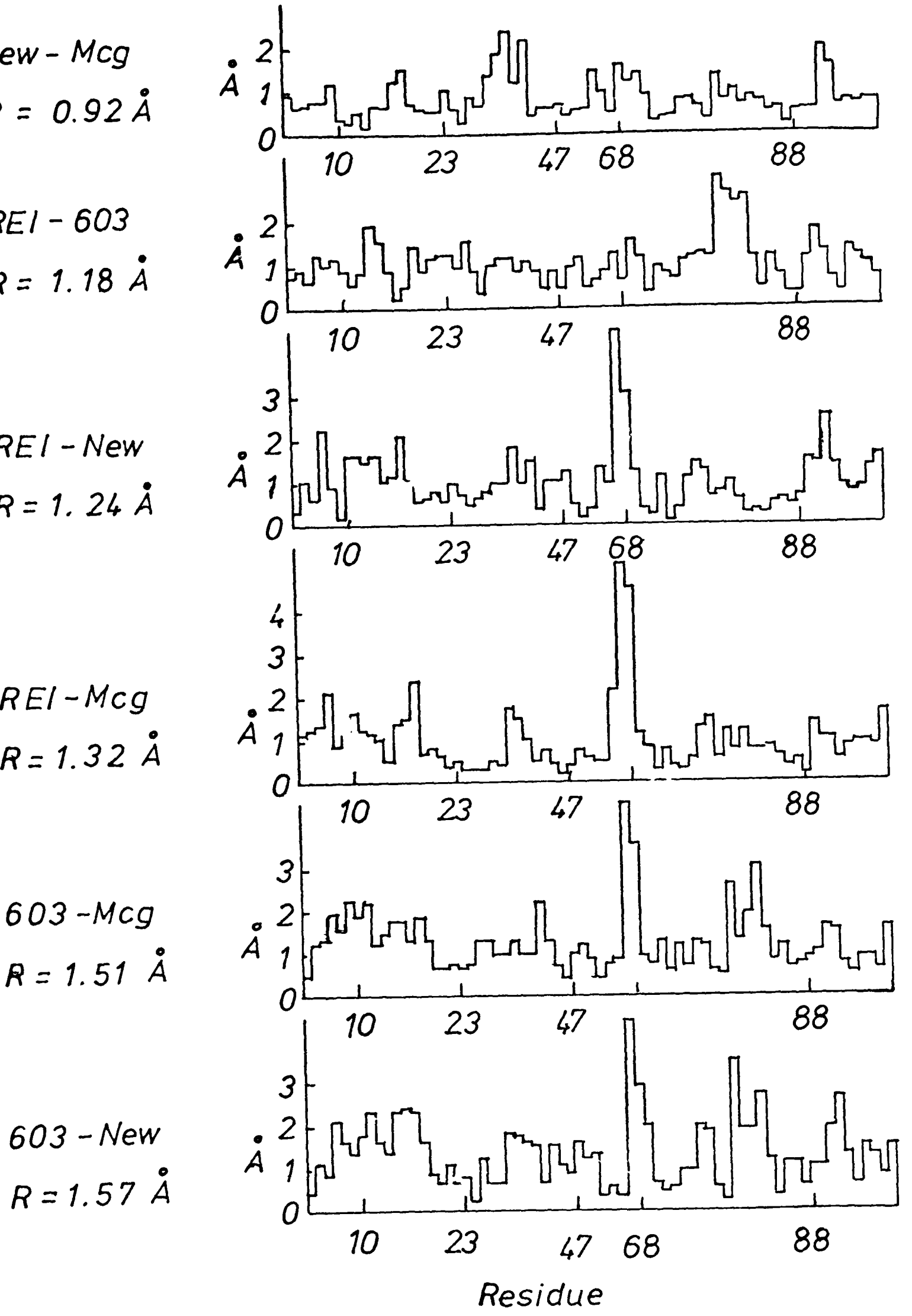

Figure 4.1 Comparisons between framework regions of V_L domains

The framework alpha-carbon positions compared are 4-7, 9-23, 35-47, 62-88 and 98-106. The distances in A between homologous atoms at the best superposition are plotted against the residue numbers. R is the r.m.s. difference between two structures.

structural alterations may occur on dimerization. However, the mean deviation of all atoms was 0.47 Å, with several solvent-facing segments deviating significantly from the local symmetry. Since the difference Fourier map was featureless in these regions, it was concluded that the deviations represented real alternative configurations. A mean deviation of the order of 0.5 Å is therefore the lower limit for the error of the model-building process, since model-building necessarily involves the selection of one of the many possible conformations. Errors of up to 0.5 Å can arise simply from the measurement of coordinates from wire models (Levitt, 1974).

The closest similarity is observed between the two λ-chains or the two κ-chains (Figure 4.1). The greater similarity between the two λ-chains as opposed to the two κ-chains may reflect the species of origin of the chains. Both λ-chains are of human origin, whereas one κ-chain is of human and one of murine origin. The human κ-chain and mouse κ-chain are more similar to each other than the human κ-chain is to either human λ-chain. This is consistent with the evolutionary divergence of κ and λ before mouse and man. The structures of two proteins AU and ROY, differing in sequence from protein REI at only 16 and 18 positions respectively, have been determined by comparing their X-ray data with that of protein REI using the Patterson search method (Fehlhammer et al., 1975; Colman et al., 1977). The positions of the backbone and internal side-chain atoms of protein AU (2.5 Å resolution) were found to be indistinguishable from those of protein REI. The structure of protein ROY (3.0 Å resolution) was also very similar. The structure of another V_L dimer, that of protein Rhe, has recently been reported (Wang et al., 1979). This structure differs from that of all the other six V_L domains

in a framework region between the first and second hypervariable loops. There is a difference of 7 Å between this region and the equivalent region of protein REI, with a corresponding difference in the modes of dimerization of the two proteins. The reason for the difference is not clear. It is essential, both for an understanding of the production of antibody combining sites, and for model-building, to determine whether the difference is an artefact of the dimerization of two identical domains or whether similar effects are to be expected occasionally for $V_L V_H$ pairs.

Inspection of Figure 4.1 shows that very few homologous atoms of the four V_L domains differ in position by more than 2 Å at the best superpositions of any of the structures. The largest difference between structures, about 4.5 Å, is seen at positions 67 and 68. This difference is observed when chains of different type are compared, but not when chains of the same type are compared. There is therefore a major difference between κ-chains and λ-chains at these positions, which has not been remarked upon before. The residues involved are part of a solvent-exposed loop, and would not be expected to have a significant effect on the conformations of the hypervariable loops. Residues 79-82 are in similar positions in all the structures except for protein 603. These residues are part of a long solvent-exposed loop distant from the combining site. Differences greater than 2 Å but less than 3 Å are observed in some comparisons at the following positions: (a) positions 41 and 43, part of a solvent-exposed β-bend; (b) positions 11 and 14-17, also an exposed loop; and (c) positions 7 and 9 in comparisons between κ-chains and λ-chains, as a result of the extra residue 8 in κ-chains.

The general validity of the model-building method is established by the comparisons described above, although it is not

yet possible to evaluate the significance of the difference shown by protein Rhe. The assumptions may be put to a more stringent test by comparing the variability of the six points of attachment of the hypervariable loops to the framework, and by comparing the structures of the hypervariable loops themselves.

Comparisons of framework attachment points for the hypervariable loops of the V_L domains

The six framework residues to which the three hypervariable loops are attached are defined as residues 23, 35, 48, 57, 88 and 98 (Kabat et al., 1976). Since residue 57 is deleted from protein New, comparisons were made between the other three structures. The r.m.s. deviations of the frameworks (residues 4-7, 9-23, 35-48, 57-88 and 98-106) are given in Table 4.3, together with the corresponding r.m.s. deviations of the six attachment points, calculated from the same comparisons. In all three cases, the r.m.s. differences between the attachment points are less than those between the whole frameworks. This implies that the attachment points are, on average, more conserved in position than the rest of the framework residues. The same conclusion was reached by comparing the attachment points of the L_1 and L_3 hypervariable loops of protein New with those of the other three structures. In addition, the r.m.s. differences of the attachment points are very small ($\sim$0.8 Å). The choice of a particular framework structure is therefore not expected to be a critical factor in the building of models of antibody combining sites. The choice should be dictated primarily by the accuracy of available coordinates.

Table 4.3 R.m.s. differences between framework attachment points for hypervariable loops

Framework residues compared are 4-7, 9-23, 35-48, 57-88 and 98-106. Attachment points are residues 23, 35, 48, 57, 88 and 98 (see Table 4.1)

Comparison	R.m.s. difference (Å)	
	Frameworks	Attachment points
REI-603	1.07	0.71
Mcg-REI	1.18	0.85
Mcg-603	1.47	0.89

Comparisons of hypervariable loops

The length of a hypervariable loop is particularly important in determining its structure (Padlan, 1977). It is therefore fortunate that each of the three hypervariable loops of the V_L domain has the same length in at least two of the four structures. Similarly, each hypervariable loop of the V_L domain of protein 315 has the same length as that of either two or three of the known structures. Comparisons of the L_1, L_2 and L_3 loops are shown in Figures 4.2. 4.3 and 4.4, respectively, with the corresponding r.m.s. differences. The same r.m.s. value for a given comparison was generally obtained regardless of which set of coordinates was held fixed by the superposition program, indicating the reaching of a true minimum. When r.m.s. values differed for the same comparison, the lowest value was assumed to be the true minimum. The only comparisons possible between hypervariable loops of the V_H domains are those between the H_1 loops of proteins New and 603, and between the H_2 and H_3 loops of protein New and the model of protein 315. These comparisons are shown in Figure 4.5. For the comparison of the H_1 loops, the carbon atoms of the main-chain carbonyl groups were included with the alpha-carbon atoms. The r.m.s. differences, given in Figures 4.2 to 4.5, range from 0.53 $\mathring{A}$ to 1.84 $\mathring{A}$, with an average of about 1.1 $\mathring{A}$.

L_1 loop: The L_1 loop of the original model of protein 315 was built using the coordinates of protein Mcg (Padlan et al., 1976a). It is therefore not surprising that the L_1 loop of the present model is more similar to the L_1 loop of protein Mcg than it is to that of protein New. However, the difference between the L_1 loops of the present model of protein 315 and of protein New is almost identical in magnitude to that between the L_1 loops of

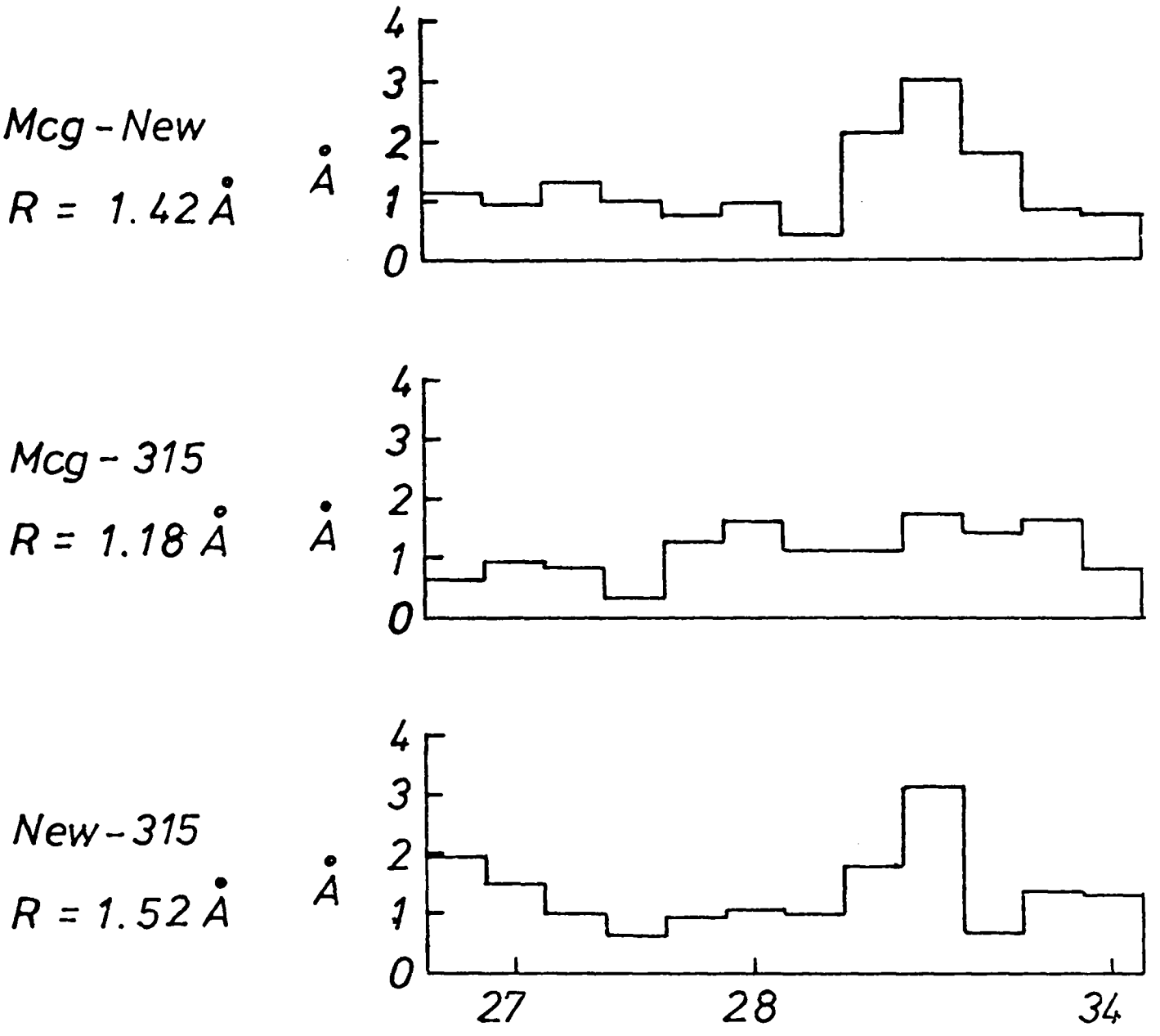

Figure 4.2 Comparisons between L_1 hypervariable loops

The alpha-carbon positions compared are 26, 27, 27D, 27E, 27F and 28-34. The distances in Å between homologous atoms at the best superposition are plotted against the residue numbers.

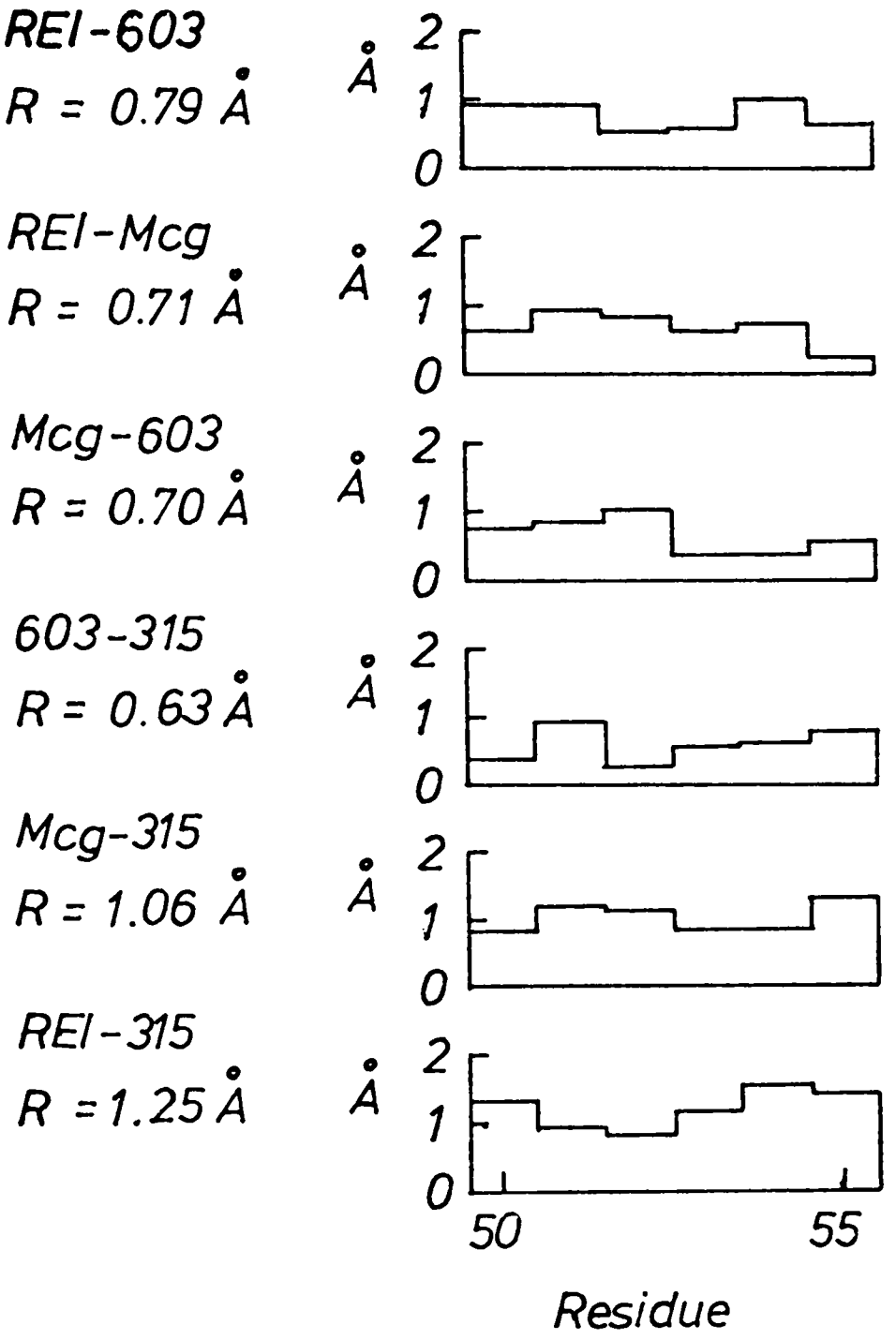

Figure 4.3 Comparisons between L_2 hypervariable loops

The alpha-carbon positions compared are 50-55. The distances in Å between homologous atoms at the best superposition are plotted against the residue numbers.

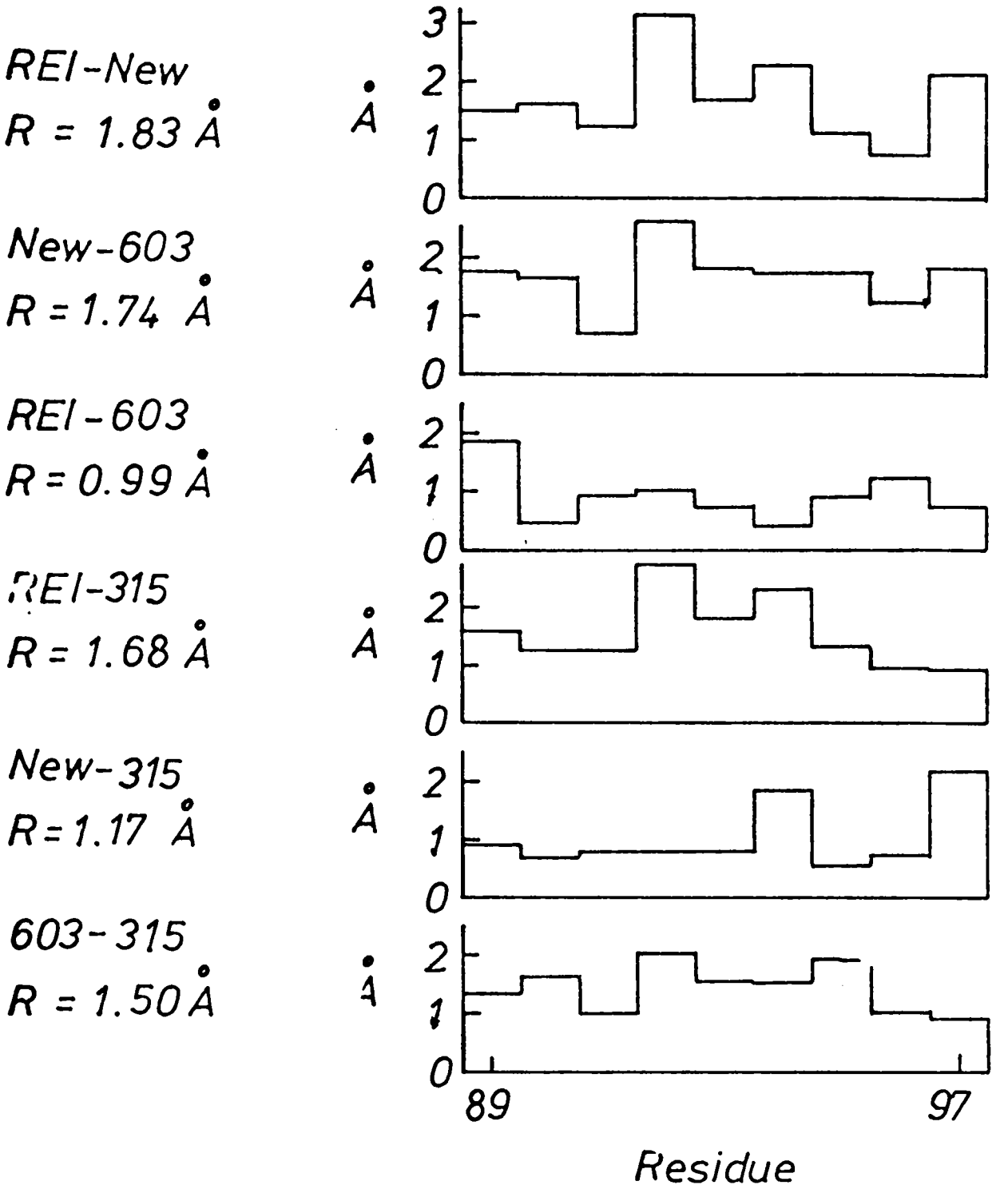

Figure 4.4 Comparisons between L_3 hypervariable loops

The alpha-carbon positions compared are 89-97. The distances in Å between homologous atoms at the best superposition are plotted against the residue numbers.

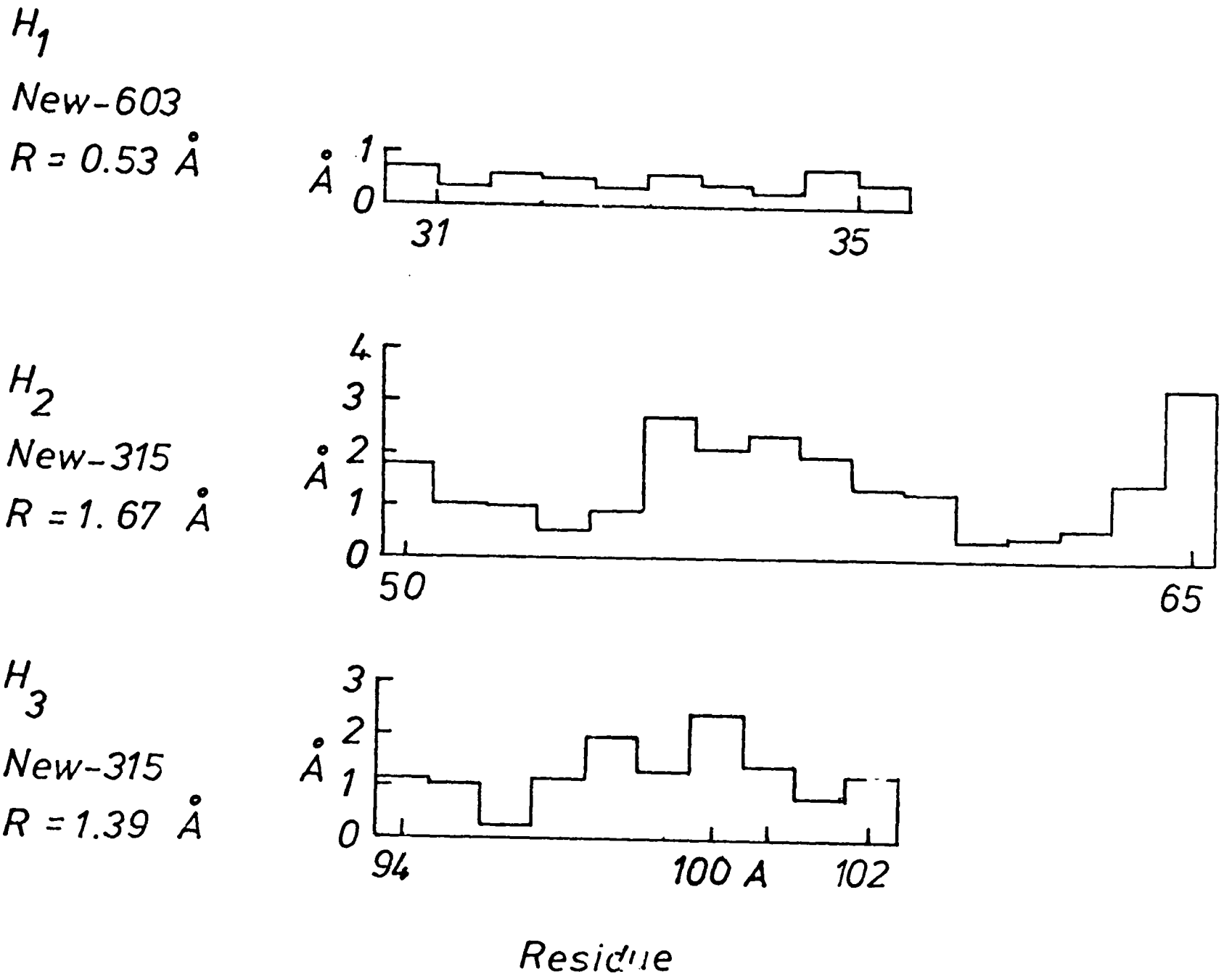

Figure 4.5 Comparisons between H_1, H_2 and H_3 hypervariable loops

For the H_1 loops, both the alpha-carbon and carbonyl-carbon positions of residues 30-35 are included. For the H_2 loops, the alpha-carbon positions compared are 50-65. For the H_3 loop they are 94-100, 100A, 101 and 102. The distances in Å between homologous atoms at the best superposition are plotted against the residue numbers.

proteins New and Mcg. The structure of the L_1 loop of protein 315 is therefore representative of the range of likely L_1 loop structures. The L_1 loop is probably of particular importance in determining the conformation of the combining site, since it is the most variable in length of the three hypervariable loops of the V_L domain (Potter et al., 1976). The H_3 loop is also of importance, for the same reason (Poljak, 1978).

L_2 loop: The L_2 loops of proteins REI, New and Mcg are clearly quite similar in structure to each other and to the L_2 loop of the model of protein 315. The L_2 loop is probably of minor importance in determining the specificities of antibodies, since it is generally shielded by the H_3 loop from forming contacts with ligands in the combining site.

L_3 loop: Both proteins REI and McPC603 contain a proline at position 95, absent in proteins New and 315. The similarity between the L_3 loops of the two κ-chains is very close, and greater than the similarity between the L_3 loop of protein New and that of either κ-chain, possibly as a result of the proline residue. The L_3 loop of the original model of protein 315 was built as an extended β-pleated sheet, although the coordinates of protein New were not used (Padlan et al., 1976a). The assumption of this type of structure is clearly reasonable, since the L_3 loop of the model of protein 315 is more similar to protein New than it is to proteins REI and 603.

H_1 loop: This loop is very short, and of similar length to the L_2 loop. Like the latter, it is highly conserved in structure, with an r.m.s. difference between proteins New and 603 of only 0.53 Å, compared with about 0.7 Å to 1 Å for the L_2 loops.

H_2 loop: No comparison of crystallographically determined structures is possible. However, the r.m.s. deviation of 1.67 Å between the H_2 loops of protein New and the model of protein 315 is in the expected range of 0.5 Å to 1.8 Å.

H_3 loop: Again, no comparison of crystallographically determined structures is possible. The r.m.s. deviation of 1.39 Å between the H_3 loops of protein New and the model of protein 315 is in the expected range of 0.5 Å to 1.8 Å.

While the above discussion shows that homologous hypervariable loops have similar structures, it does not show that the spatial relationships of these loops to each other and to the framework are also conserved. A measure of this conservation of spatial relationships may be obtained by calculating the r.m.s. differences between homologous loops when included in their entire frameworks. The r.m.s. differences between all the atoms in such comparisons (the framework and one hypervariable loop) are given in Table 4.4. The r.m.s. differences between the atoms of the hypervariable loops, calculated from the same comparisons, are also given in Table 4.4, with the data for the hypervariable loops compared independently of the frameworks (taken from Figures 4.2, 4.3 and 4.4). The effect of constraining the comparison of the hypervariable loops by attaching them to an extra 70-75 atoms is only to increase the r.m.s. differences by about 30%. Indeed, it is apparent from Table 4.4 that the L_2 loops are as conserved in position as the framework atoms. The r.m.s. differences between hypervariable loops included in the framework give a direct quantitative measure of the likely errors of the model-building. This error is of the order of 1 Å to 2 Å for alpha-carbon atoms.

Table 4.4 Effect of framework residues on r.m.s. differences between hypervariable loops

Framework residues compared are 4-7, 9-23, 35-48, 57-88 and 98-106 (proteins REI, Mcg and 603) or 4-7, 9-23, 35-47, 62-88 and 100-108 (protein New). Hypervariable loop residues are 26-34 (L_1), 50-55 (L_2) and 89-97 (L_3).

Comparison	R.m.s. difference (Å)		
	Framework and loop	Loop in framework	Isolated loop
L_1 New-Mcg	1.19	1.79	1.42
L_2 REI-603	1.05	0.87	0.79
L_2 REI-Mcg	1.21	1.21	0.71
L_2 603-Mcg	1.45	1.14	0.70
L_3 REI-603	1.10	1.31	0.99
L_3 REI-New	1.43	2.36	1.83
L_3 603-New	1.72	2.51	1.74

Dimerization of variable domains

It has already been shown that the hypervariable loops of V-domains bear very similar relationships both with respect to each other and to their frameworks. However, the diversity of antibody combining sites, and the difficulty of model-building, would be greatly increased by differences in the mode of dimerization of V-domains. The relative orientations of the V_H and V_L domains of proteins New and 603 were compared by using the coordinates of the H_1 loops with those of the frameworks of the V_L domains. The comparison will be almost entirely determined by the positions of the framework atoms and any difference in the mode of dimerization should be reflected in an unusually large difference between the positions of the H_1 loops at the best superposition. A similar comparison was made for proteins REI and Mcg, using the coordinates of the L_2 loop of one monomer with those of the framework of the other monomer. The r.m.s. values for the two comparisons, and for the H_1 and L_2 loops, calculated from the same comparisons, are given in Table 4.5. The modes of dimerization of the two V_LV_H pairs are very similar, since the r.m.s. difference between the positions of the H_1 loops is actually less than the average for the entire structures. There is a small difference between the modes of dimerization of the V_LV_L pairs, since the r.m.s. difference of 1.7 Å for the L_2 loops is greater than the value of 1.21 Å obtained between L_2 loops when included in the framework of the same monomer, rather than the other monomer (Table 4.4). Formation of the V_L dimer of protein Rhe is also different (Wang et al., 1979). There are, therefore, differences in the mode of dimerization of V_L domains, but it is not yet clear whether or not this extends to the V_LV_H pairs, since only two structures

Table 4.5 Comparisons between the modes of dimerization of the V_L and V_H domains of proteins New and 603, and between the V_L domains of proteins REI and Mcg

For the two Fab fragments, the residues compared were the H_1 loops (30-35) and the V_L frameworks (4-7, 9-23, 35-47, 62-88, 98-106). For the V_L dimer and L-chain dimer, the residues compared were the L_2 loops of one monomer (50-55) and the frameworks of the other monomer (4-7, 9-23, 35-48, 61-88, 98-106).

Comparison	R.m.s. difference (Å)	
	Framework and loop	Loop in framework
New-603	1.51	0.92
REI-Mcg	1.26	1.70

are available. It is possible that the light chain type has some influence on this process, since residues contacting the V_H domain are more conserved in κ-chains than in λ-chains (Padlan, 1979). The solution of further structures by crystallography is required to distinguish between these possibilities.

Extent of alteration of the original model of protein 315

Comparisons of the coordinates of the L_1, L_2 and L_3 hypervariable loops of the present model with those of the original model are shown in Figure 4.6. A comparison of the complete structures has been given by Dower (1979). Alterations made on the basis of spectroscopic data are small compared with the limits set by the differences between other structures. However, spectroscopic techniques only report on the interactions between a few atoms in the structure, and generally only on side-chain atoms. Several different positions of side-chain atoms may be consistent with very similar alpha-carbon positions. An example is the alteration in position of Tyr-49 between the structures of proteins REI, AU and ROY, all of which have very similar backbone conformations (Fehlhammer et al., 1975; Colman et al., 1977). Spectroscopic techniques are not capable of providing the extensive structural information given by X-ray diffraction. The power of spectroscopic methods lies in their ability, in conjunction with the knowledge of structures determined by X-ray crystallography or model-building, to define the nature of the interactions which are responsible for the specificity of the protein. Consideration of the r.m.s. values obtained in the above comparisons (1 Å to 2 Å for hypervariable loops) suggests that the model-building will not produce a misleading picture of the combining site. A full assessment of the potential of model-

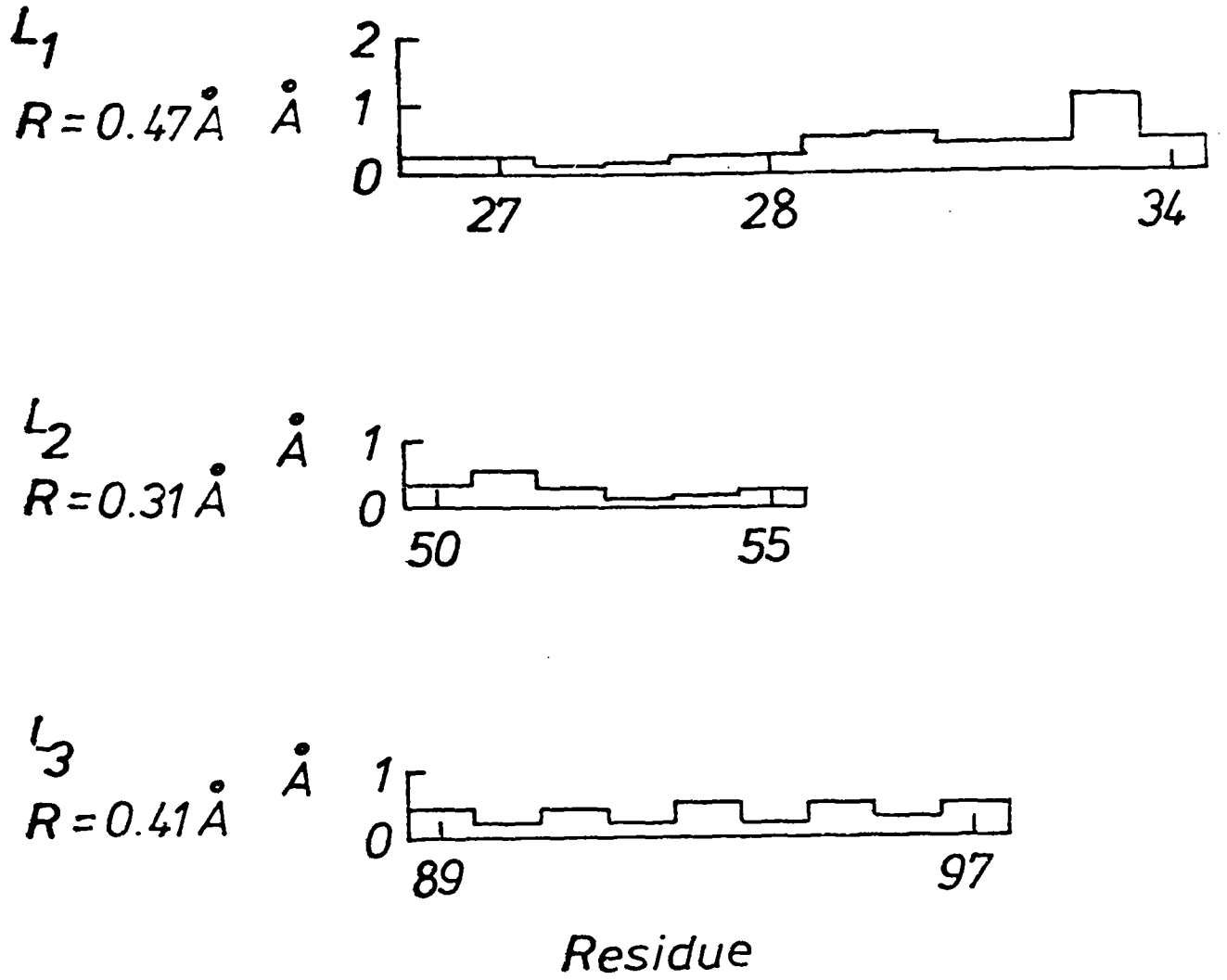

Figure 4.6 Comparisons between the original and modified models of the V_L domain of protein 315

The alpha-carbon positions compared are the same as those given in Figures 4.2, 4.3 and 4.4. The distances in Å between homologous atoms at the best superposition are plotted against the residue numbers.

building will have to await the accurate solution by X-ray diffraction of a structure for which a model has already been proposed.

Construction of a model of the combining site of the V_L dimer of protein 315

A model of the combining site of the V_L dimer of protein 315 was constructed by taking the coordinates of the V_L domain of the model of the Fv fragment, and applying to them the appropriate rotation and translation matrices relating the monomers of the REI or Mcg dimers. Because the coordinate systems of the three proteins are different, it is necessary first to transform the coordinate system of protein 315 into that of proteins REI or Mcg, using the SUPERB program. The matrices relating the coordinates of protein 315 to monomer 1 of protein REI were obtained by superimposing the homologous L_2 and L_3 loops. To relate the coordinates to monomer 2 of protein Mcg, the L_1 and L_2 loops were used. Since construction of the model relies on the homology between hypervariable loops, and since the mode of dimerization of V_L domains is not invariant, the model must be regarded only as a qualitative aid to the interpretation of subsequent n.m.r. data (Chapter 5). In particular, no check has been made for unallowed interdomain contacts. The important features of the combining site are shown in Figure 4.7, with the corresponding region of the Fv fragment for comparison. The combining site is expected to be a large cavity, lined with aromatic residues. The 'sides' of the site are formed by the side-chains of Trp-93_L, approximately 8.5 Å apart, while the 'floor' and 'ceiling' are provided by the Tyr-34 residues, approximately 11 Å to 14 Å apart. The site is therefore

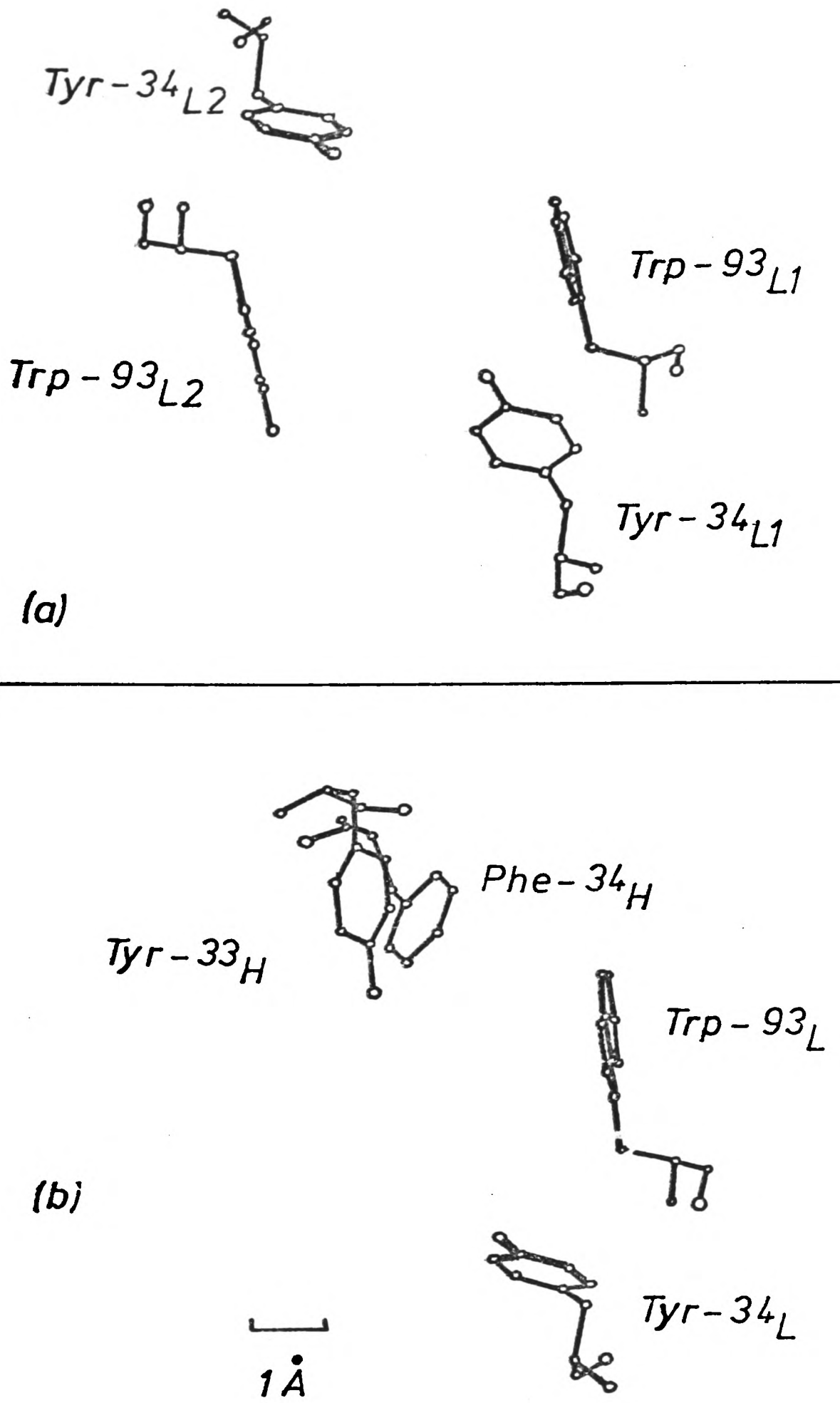

Figure 4.7 (a) The combining site of the V_L dimer of protein 315

The model was constructed using the coordinates of protein REI, as described in the text. The side-chains of Tyr-34_L point out towards the viewer.

(b) The combining site of the Fv fragment of protein 315

The model is taken from Dower et al. (1977). The side-chains of Tyr-34_L and Tyr-33_H point out towards the viewer, whereas that of Phe-34_H points back into the site.

much larger than that of the Fv fragment, although it resembles the site of the Fv fragment in being highly aromatic. The similarity between the two sites is evident from Figure 4.7. In particular, Tyr-34_L of one monomer of the V_L dimer occupies a position equivalent to that of Tyr-33_H in the intact Fv fragment. The complete coordinates of the model are given on microfiche at the back of the thesis.

CHAPTER 5

THE STRUCTURE, SPECIFICITY AND CONFORMATIONAL PROPERTIES OF THE V_L DIMER AND OF THE L-CHAIN DIMER OF PROTEIN 315

INTRODUCTION

According to the current model of the combining site of protein 315 (Dwek et al., 1977), several specific interactions of the ligand with the protein occur with residues from the L-chain. In particular, it is proposed that there is a stacking interaction of the DNP group with Trp-93_L, and hydrogen bonds between the 2-NO_2 group and Tyr-34_L, and between the 4-NO_2 group and Asn-36_L. It was therefore of interest to discover that the L-chain dimer and the V_L dimer of protein 315 retain affinity for the DNP group (Schechter et al., 1976; Gavish et al., 1977). The idea that the L-chain is important in determining the specificity of protein 315 was initially not easy to accept. Retention of specificity, including specificity for the DNP group, has often been observed in isolated H-chains, but rarely in L-chains (reviewed by Nisonoff et al., 1975). It has also been suggested that L-chains are particularly able to form a cavity capable of binding nonpolar molecules (Stevenson, 1974). The binding of such haptens to isolated L-chains would therefore be largely fortuitous. This possibility is illustrated by the binding of nitrophenyl and similar compounds to the L-chain dimer of protein Mcg (Edmundson et al., 1974b). The parent IgG_1 molecule does not bind DNP detectably (Firca et al., 1978). Recent partial sequencing of the V_H and V_L regions of a large number of mouse myeloma proteins with particular specificities revealed a

marked correlation between specificity and V_H, rather than V_L, sequence (Barstad et al., 1978). Indeed, the three DNP-binding myeloma proteins 315, 460 and 25 have closely related V_H regions but different V_L regions.

It therefore became important, both as a test of the model of protein 315 and for the more general reasons outlined above, to determine whether the binding of DNP compounds to the V_L dimer is fortuitous, or whether it reflects the retention of structural features required for the binding of nitrophenyl compounds to the Fv fragment. High resolution ^1H n.m.r. studies, similar to those previously carried out with the Fv fragment (Dower et al., 1978) were initially directed towards answering this question. It was also hoped that the n.m.r. analyses would simplify the interpretation of the spectrum of the Fv fragment, and allow some assignment of resonances to be made.

The studies were extended to investigate the possibility of differences between the combining sites of the V_L dimer and the L-chain dimer, due to the presence of the C-domains in the latter molecule. Previous studies with protein 315 have shown that there is no effect of the C-domains on the structure of the combining site (Kooistra and Richards, 1978; Morris et al., 1978).

Finally, an analysis of the kinetic parameters characterizing the pH-dependent conformational change of the V_L dimer is presented. The structural extent of this conformational change is investigated by ^1H n.m.r.

RESULTS AND DISCUSSION

Dimeric structure of the V_L dimer

Many L-chains exist as mixtures of monomers and dimers at concentrations of ~1 mg/ml and neutral pH (Bernier and Putnam,

1963; Green, 1973). Formation of monomers is particularly noticeable with κ-chains. λ-chains often exist as dimers covalently linked by a disulphide bridge between the C-domains (Solomon, 1976). Both the L-chain (λ_2-type) and V_L domain of protein 315 form stable non-covalently linked dimers at neutral pH (Lancet et al., 1977; Gavish et al., 1977). The V_L domains also dimerize at pH 4.8, which is the pH at which most of the n.m.r. studies reported below were carried out (M. Gavish, personal communication).

Since the V_L dimer (MW = 24,000) has a similar molecular weight to the Fv fragment (MW = 25,000) and the L-chain dimer (MW = 45,000) has a similar molecular weight to the Fab fragment (MW = 50,000), the ^1H resonances of the V_L dimer and Fv fragment or of the L-chain dimer and Fab fragment should be comparably broad. The spectra are shown in Figure 5.1, and confirm the dimeric nature of both the V_L domain and L-chain. Although L-chain dimers are generally readily dissociated by exposure to low pH, no change in the linewidths of the resonances of the V_L domain could be detected even at pH 1.

Binding properties of the V_L dimer

The binding properties of the V_L dimer are complex. The protein undergoes a pH-dependent conformational change between a form binding one hapten per dimer at pH 5 and two per dimer at pH 8 (Gavish et al., 1978). A difference in the environment of the DNP ring at the two pH values is indicated by differences between the absorption difference spectra and the induced CD spectra of the ligands.

The binding of DNP-aspartate and DNP-glycine to the V_L dimer at pH4.8 was measured by equilibrium dialysis, since these two ligands were used for the detailed n.m.r. studies described below.

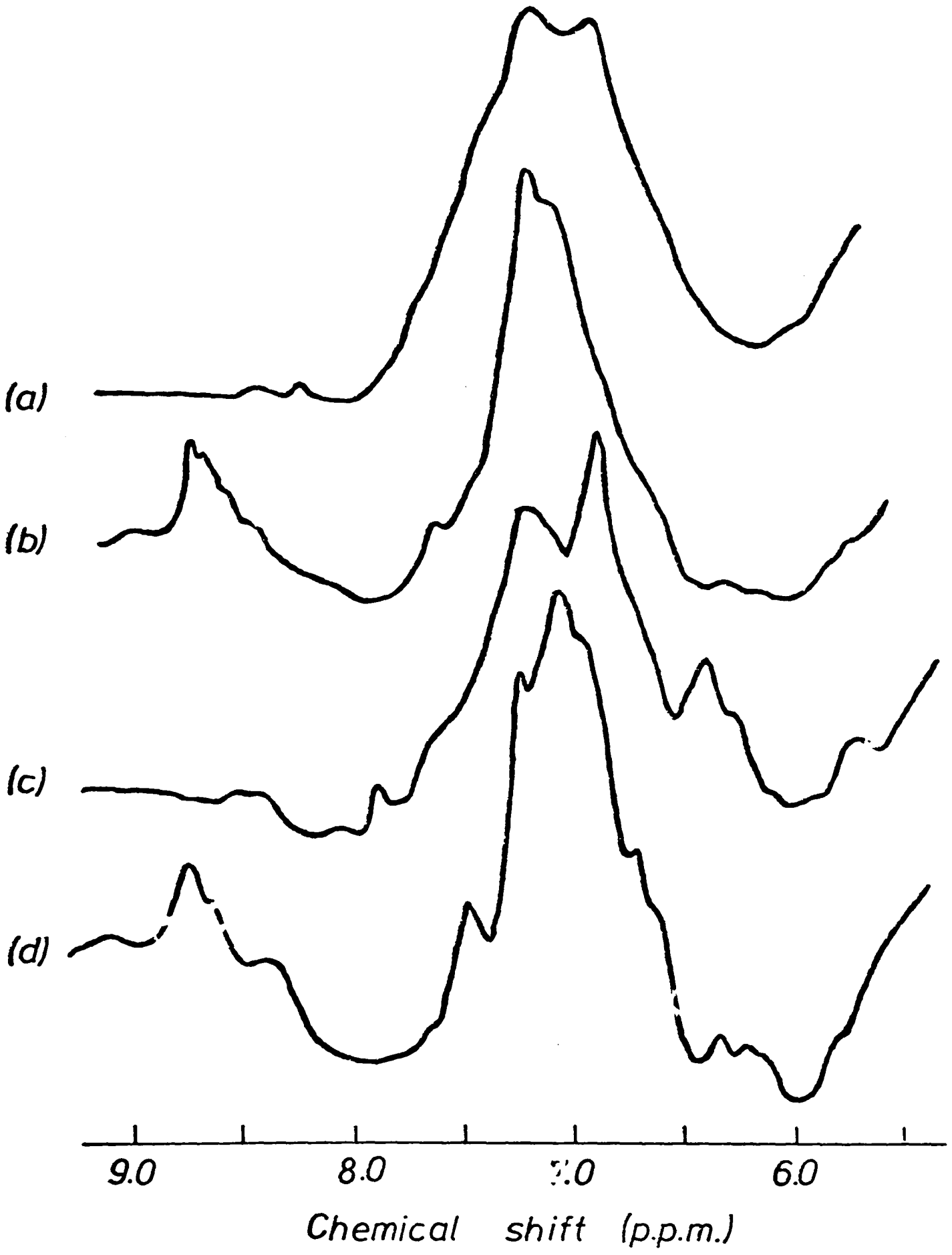

Figure 5.1 Comparison of the aromatic regions of the 270 MHz ^{1}H n.m.r. spectra of some immunoglobulin fragments

(a) Fab fragment of protein 25 (1.51 mM), MW = 50,000; 2000 scans with a solution in $^{2}H_2O$, 0.15M NaCl, pH* 7, T = 303K. (b) L-chain dimer of protein 315 (0.35 mM), MW = 45,000; 2000 scans with a solution in $^{2}H_2O$, 0.025M ^{2}H-acetate, pH* 4.3, T = 298K. (c) Fv fragment of protein 315 (0.84 mM), MW = 25,000; 2000 scans with a solution in $^{2}H_2O$, 0.15M NaCl, pH* 8.0, T = 303K. (d) V_L dimer of protein 315 (0.85 mM), MW = 24,000; 2000 scans with a solution in $^{2}H_2O$, 0.025M ^{2}H-acetate, pH* 4.3, T = 298K.

The conditions used were as close as possible to those of the n.m.r. experiments, and the results are shown in Figure 5.2. Similar results were obtained in $^{1}H_2O$ rather than $^{2}H_2O$ (M. Gavish, personal communication). Binding to more than one site per dimer is detected under these conditions by equilibrium dialysis. However, analysis of the n.m.r. data, described in detail below, shows clearly that only one site is detected by n.m.r. The dotted curves in Figure 5.2, which are asymptotic to the experimental curves, are calculated from parameters which give good fits to the n.m.r. data. It appears, therefore, that low affinity sites detected by equilibrium dialysis are not detected by n.m.r. These results demonstrate the difficulty of characterizing the binding of ligands such as DNP compounds to proteins. These ligands would be expected to associate weakly with apolar regions of the protein, and such interactions may not significantly affect a given spectroscopic parameter. A similar problem of binding of DNP-lysine to low affinity sites on the L-chain dimer was reported (Schechter et al., 1976). Such sites were not apparently detected when binding was measured spectroscopically (Lancet et al., 1977). The apparent discrepancy between the results presented in Figure 5.2 and those of Gavish et al. (1978) may reflect the higher protein and ligand concentrations used for the experiments reported here. Increased concentrations would increase the chance of detecting low affinity sites. The change of buffer conditions and temperature may also affect the binding. When the experiments were repeated using the conditions of Gavish et al. (1978), only one site was detected at pH 5 (see Figure 6.15).

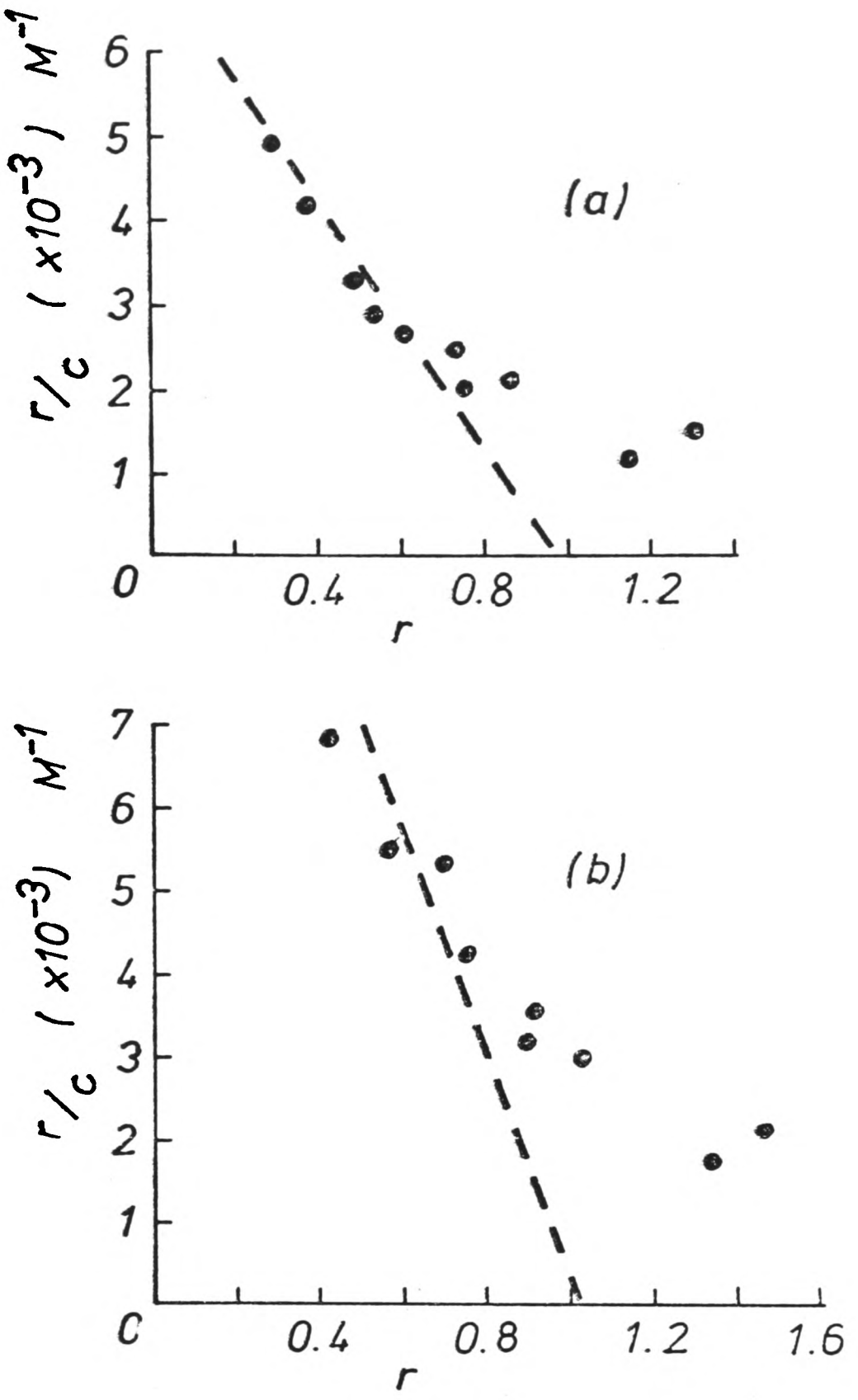

Figure 5.2 Scatchard plots for the binding of DNP-aspartate and DNP-glycine to the V_L dimer

Measurements were made by equilibrium dialysis at T = 298K, with solutions in ^2H_2O, 0.025M ^{2}H-acetate, pH* 4.8. The concentration of the V_L dimer was 2.16×10^{-4}M. Initial hapten concentrations ranged between 10^{-4}M and 2×10^{-3}M. (a) Binding of DNP-aspartate; the dashed line is calculated with the parameters K_D = 0.12 mM and n = 0.98. (b) Binding of DNP-glycine; the dashed line is calculated with the parameters K_D = 0.07 mM and n = 1.01.

High resolution ^1H n.m.r. studies of the V_L dimer

1. Effect of salt

At the protein concentrations required for the n.m.r. experiments (~16 mg/ml) the V_L dimer precipitates slowly in the presence of salt, or at a pH* above 5.0 (pH* is the measured pH of a solution in ^2H_2O). For these reasons, most of the experiments described here were carried out in the presence of 0.025M acetate at pH* 4.8. Since the experiments on the Fv fragment were carried out in the presence of 0.15M NaCl, it is necessary, for the purpose of comparing the results, to show that this salt concentration has no significant effect on the structure of the V_L dimer. The spectra of the V_L dimer in the absence and presence of 0.15M NaCl are shown in Figure 5.3. The latter spectrum was collected before precipitation could be seen. The difference between the two spectra is very small, presumably reflecting the perturbation of ionizable surface groups. No gross change of conformation is observed. Although the n.m.r. studies on the Fv fragment were usually carried out at pH 7, it has previously been shown that the change to pH 5 has no effect on the mode of ligand binding (S.K. Dower, personal communication). The results obtained with the V_L dimer should therefore be directly comparable to those obtained with the Fv fragment.

2. Binding of DNP-aspartate

DNP-aspartate was chosen as the initial ligand for the n.m.r. experiments, since the most extensive analysis of binding to the Fv fragment concerned this ligand (Dower et al., 1977).

The 270 MHz ^1H n.m.r. spectra of the V_L dimer in the absence of ligand or saturated with DNP-aspartate, and the resulting difference spectrum, are shown in Figure 5.4. The difference is

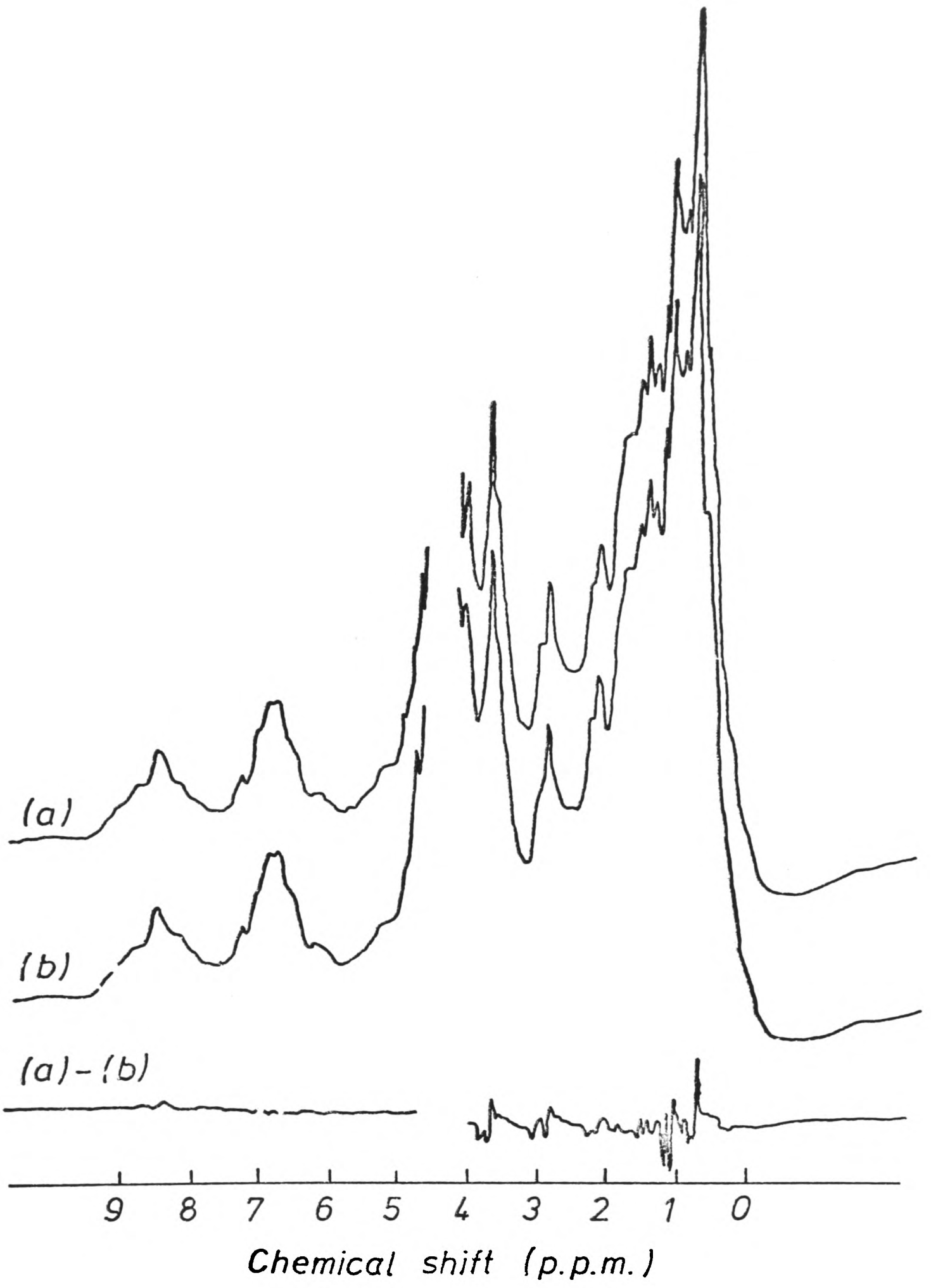

Figure 5.3 Effect of salt on the 270 MHz ^{1}H n.m.r. spectrum of the V_L dimer

2000 scans were recorded at T = 298K, with solutions in $^{2}H_2O$, 0.025M ^{2}H-acetate. The concentration of the V_L dimer was 0.69 mM. (a) Spectrum in the absence of NaCl. (b) Spectrum in the presence of 0.15M NaCl.

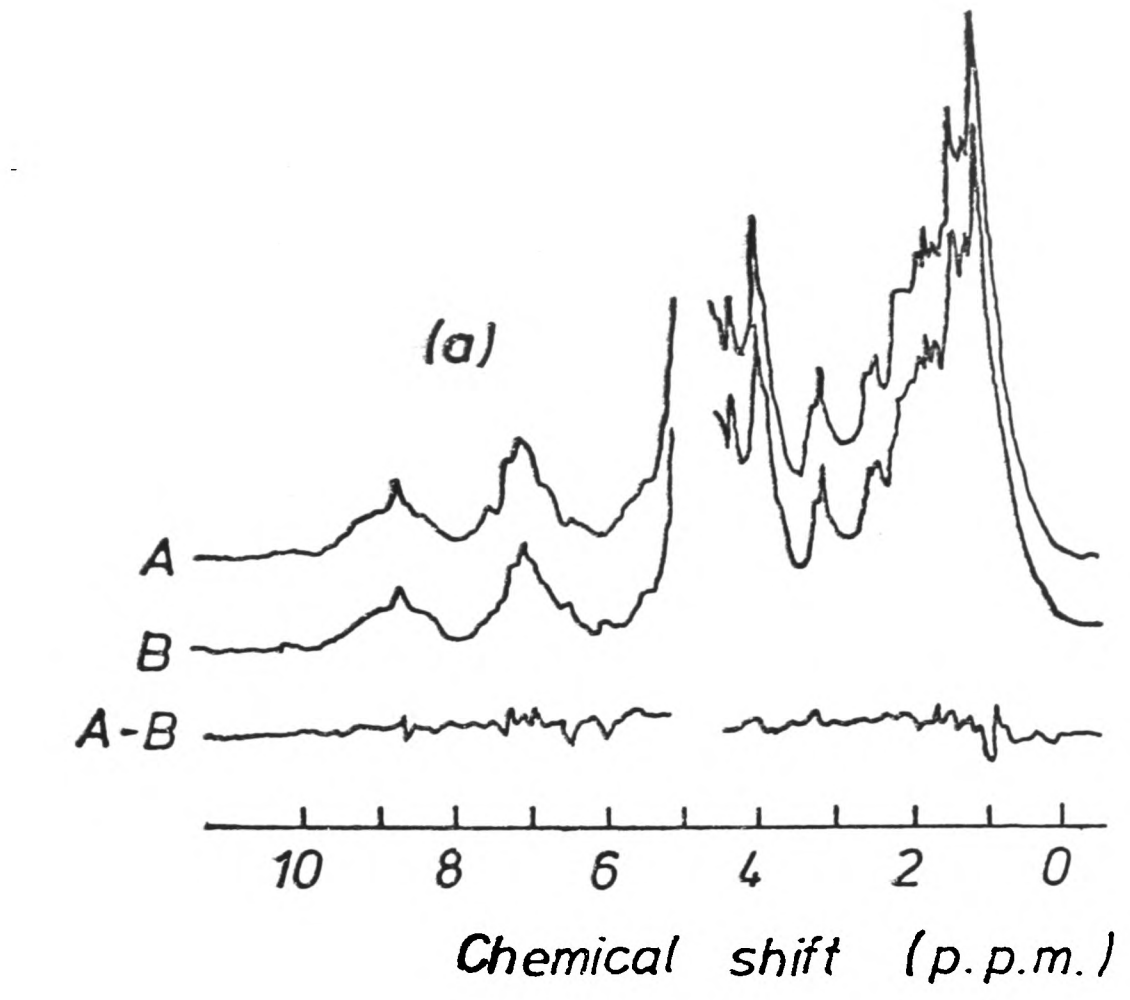

Figure 5.4 The effect of the binding of DNP-aspartate on the 270 MHz ^{1}H n.m.r. spectrum of the V_L dimer.

2000 scans were recorded at T = 298K with solutions in $^{2}H_2O$, 0.025M ^{2}H-acetate. (a) Whole spectrum. (b) Aromatic region. A - V_L dimer alone (0.85 mM). B - V_L dimer (0.80 mM) with equimolar DNP-aspartate.

only ~2-3% of the total intensity, with approximately equal perturbations of the aromatic and aliphatic regions, despite the presence of ~1100 unexchangeable aliphatic ^{1}H nuclei compared with 104 aromatic ^{1}H nuclei per dimer. The small intensity of the difference spectrum, and the proportionately large perturbation of aromatic rather than aliphatic resonances is also observed on ligand binding to the Fv fragment (Dower et al., 1977). The small intensity of the difference spectrum implies that any conformational changes on binding are limited to the combining site. It is in marked contrast to large changes observed on the binding of ligands to some proteins, for example N-acetylglucosamine to lysozyme (Dwek, 1977). The difference spectrum of the aromatic region (Figure 5.4b), representing about 20 out of 104 resonances, suggests a combining site containing several aromatic residues.

The titration behaviour of protein and ligand resonances may be followed by taking differences between spectra obtained after successive additions of ligand. Once the protein is saturated, only ligand resonances continue to titrate. The change in chemical shifts of the ligand resonances may then be calculated, and used to provide information on the local environments of the corresponding nuclei. The titration of the three aromatic resonances of DNP-aspartate may be seen in Figure 5.5. The titration curves of the aromatic protein and ligand resonances are shown in Figure 5.6, and the titration behaviour of the protein resonances is summarized in Table 5.1. Inspection of Figure 5.6 shows that at equimolar concentrations of V_L dimer and of ligand, the chemical shift changes of all the protein resonances are 70-80% of their total chemical shift changes. This demonstrates that binding at only one site per V_L dimer is affecting the protein resonances. If binding were occurring at

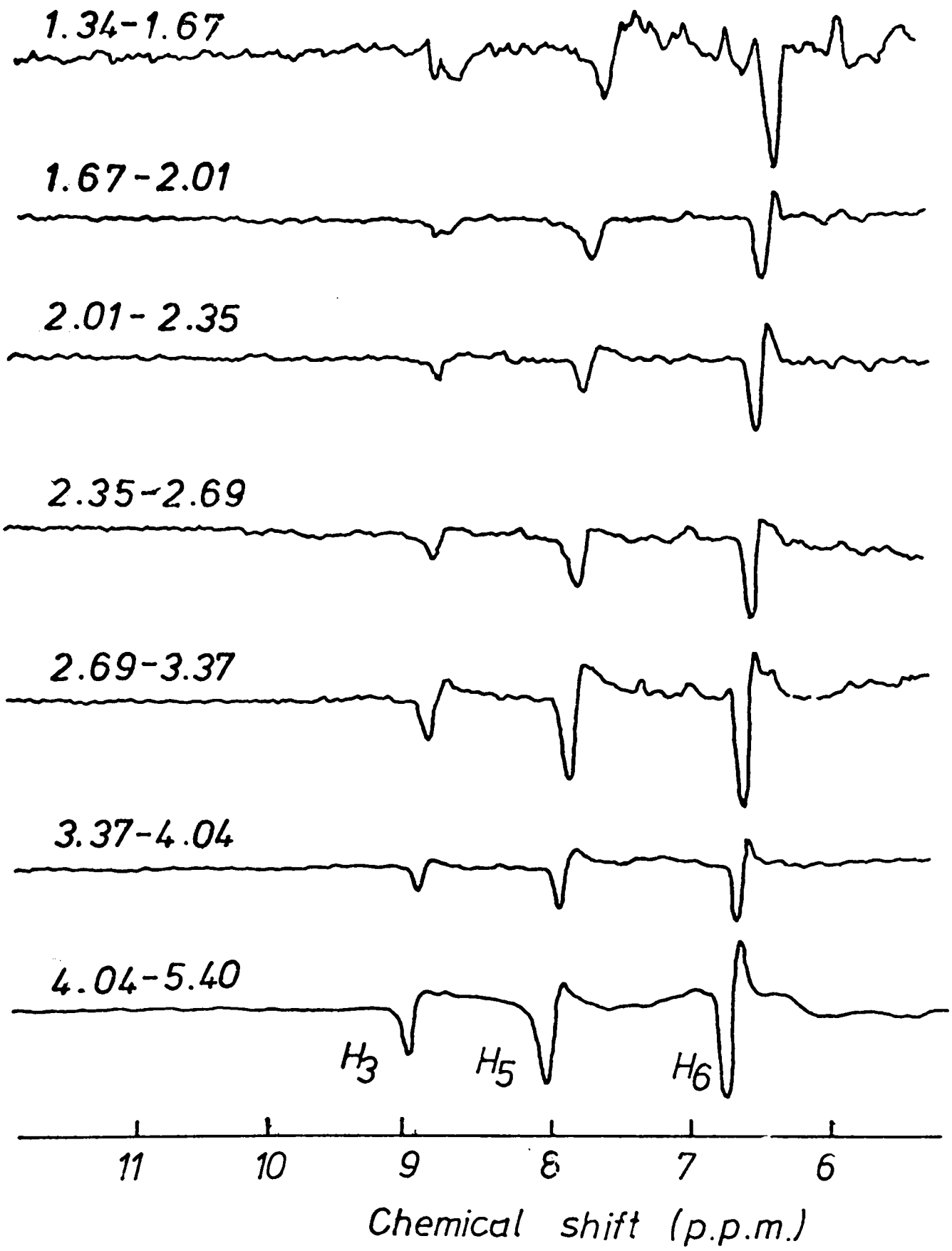

Figure 5.5 Chemical shift changes of the resonances of the aromatic ^{1}H nuclei of DNP-aspartate following binding to the V_L dimer

Measurements were made at 270 MHz, T = 298K, with solutions in $^{2}H_2O$, 0.025M ^{2}H-acetate, pH* 4.8. The protein concentrations were ~0.75 mM. The differences were taken between successive additions of hapten. The chemical shifts of the resonances of the free ligand are: H_3, 9.12 p.p.m.; H_5, 8.29 p.p.m.; H_6, 6.97 p.p.m.

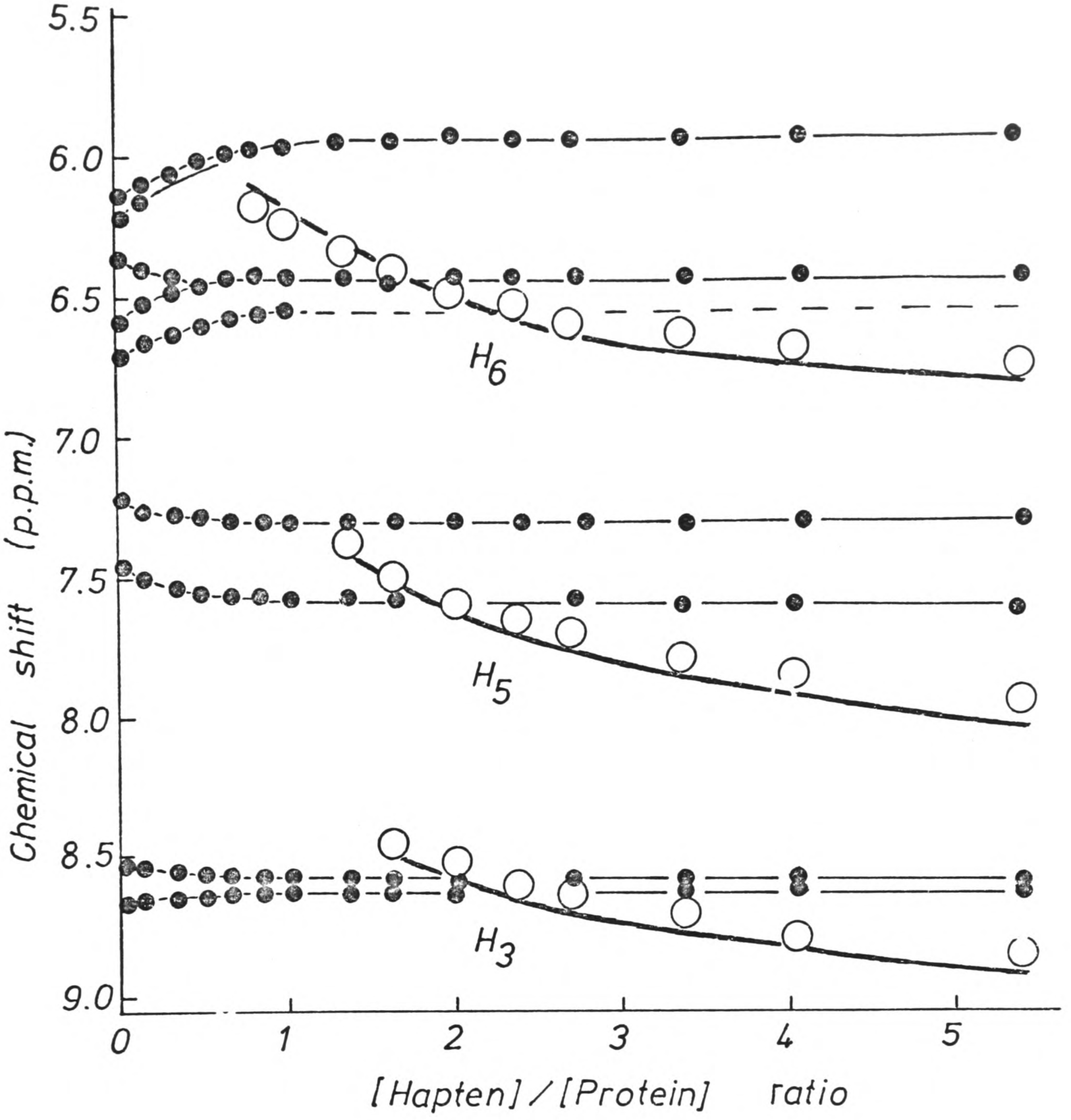

Figure 5.6 Chemical shift changes of the resonances of aromatic ^1H nuclei following the binding of DNP-aspartate to the V_L dimer

Measurements were made at 270 MHz, T = 298K, with solutions in ^2H_2O, 0.025M ^2H-acetate, pH* 4.8. The initial protein concentration was 0.85 mM. The chemical shifts of the resonances of the free ligand are: H_3, 9.12 p.p.m.; H_5, 8.29 p.p.m.; H_6, 6.97 p.p.m. The solid curves for the ligand resonances were calculated assuming K_D = 0.05 mM, n = 1.0 and the chemical shift changes given in Table 5.2.

Table 5.1 Chemical shifts (δ) and the changes in chemical shifts ($\Delta\delta$) of protein resonances perturbed on the binding of ligands to the Fv fragment of protein 315 and to the V_L dimer

Measurements were made at 270 MHz in ^2H_2O. Solutions of the V_L dimer contained 0.025M sodium acetate, T = 298K. Protein concentrations were ~0.8 mM. Solutions of the Fv fragment contained 0.15M NaCl, T = 303K. Protein concentrations were ~1.3 mM. pH* values are given in the Table. Shifts were measured from DSS, used as an external standard. + and - denote upfield and downfield shift changes respectively. Assignments to His-H_2 resonances and probable assignments to His-H_4 resonances are given in the Table. Blank positions in the Table do not imply a clear absence of perturbation.

V_L + DNP-aspartate pH* = 4.8		V_L + TNP-glycine pH* = 4.8		V_L + DNP-glycine pH* = 4.8		Fv + (a) DNP-aspartate pH* = 6.9		Fv + (b) TNP-glycine pH* = 6.7		Fv + (b) TNP-aspartate pH* = 7.05		
δ(p.p.m)	$\Delta\delta$(p.p.m)	δ(p.p.m)	$\Delta\delta$(p.p.m)	δ(p.p.m)	$\Delta\delta$(p.p.m)	δ(p.p.m)	$\Delta\delta$(p.p.m)	δ(p.p.m)	$\Delta\delta$(p.p.m)	δ(p.p.m)	$\Delta\delta$(p.p.m)	
		5.63	+0.18	5.64	-0.13					5.65	-0.13	
6.15	+0.23	6.17	+0.30	6.14	+0.27	6.16	+0.25	6.20	+0.14	6.20	+0.07	
6.23	+0.30	6.24	+0.37	6.21	+0.36	6.33	+0.17	6.31	+0.15	6.31	+0.05	
6.36	-0.08	6.36	-0.12	6.38	-0.11	6.37	-0.29	6.35	-0.17	6.35	-0.22	
6.58	+0.16	6.62	+0.14	6.62	+0.55	6.62	-0.08					
6.73	+0.18	6.75	broadens?	6.72	broadens?							
6.90	<+0.15 or broadens	6.94	broadens?	6.87	broadens?	6.90	+0.19	6.88	+0.15	6.88	+0.20	
								6.43	-0.05			
						His-102_H		6.95	+0.07	6.93	<+0.05	
7.06	<+0.15 or broadens	7.07	broadens?	7.04	-0.17?	7.00	broadens	7.04	broadens	7.04	broadens	
		7.22	+0.07	7.22	+ ?	7.20	decreases	7.23	decreases	7.23	decreases	
7.22	-0.10	7.22	-0.11	7.22	-0.16							
7.45	-0.15	7.46	no shift	7.45	-0.20	7.42	increases	7.43	increases	7.43	increases	
		7.64	+0.14	7.63	+0.13							
8.53	-0.06	8.56	broadens	8.55	-0.21	His-97_L						
8.67	+0.03	8.68	+0.07	8.67	+0.03	"						
						"		7.82	+0.06	7.76	<+0.05	
						His-102_H				8.07	no shift	
										8.07	-0.07	

(a) Data from Dower et al., 1977 (b) Data from Dower et al., 1978

two sites, many or all of the protein resonances would have titrated over less than 50% of their total range. The presence of only one site is also indicated by the constancy of the ratios of the chemical shift changes of the ligand resonances during the titration, although this does not exclude the possibility of independent identical sites. The number of binding sites and dissociation constants for the binding of DNP-aspartate were obtained from the titration curve of the resonance at 6.23 p.p.m., using the best-fit procedure described in Appendix 2.1. The analysis gave n = 1.03 and K_D = 0.05 mM, similar to the values n = 0.98 and K_D = 0.13 mM which characterize the theoretical curve shown in Figure 5.2a. It may also be seen from Figure 5.6 that the chemical shift changes of the ligand resonances are large and upfield. Calculation of the chemical shift changes of the ligand resonances on binding to the V_L dimer is, however, more difficult than for those to the Fv fragment, because the binding parameters are less well defined. The chemical shift change of the H_6 resonance can be estimated from the observed shift of the resonance when the concentration of ligand is less than that of the protein. Since the protein concentration (0.8 mM) is much greater than the value of the dissociation constant (~0.05 mM), it is possible to obtain a good estimate of the fraction of ligand bound. The observed chemical shift change of the H_6 resonance under conditions when approximately 75% of the hapten is bound gives an extrapolated chemical shift change of ~1.1 p.p.m. The chemical shift changes of the remaining resonances may then be calculated from their ratios relative to the H_6 resonance. The theoretical curves generated by using the calculated values (given in Table 5.2) and a K_D of 0.05 mM are superimposed on the data given in Figure 5.6. They clearly

provide acceptable fits to the data.

Table 5.2 Upfield chemical shift changes of the ^1H resonances of DNP-glycine and DNP-aspartate on binding to the V_L dimer of protein 315

Measurements were made at 270 MHz, T = 298 in ^2H_2O containing 0.025M ^2H-acetate, pH* = 4.8. Estimated errors are $\pm$ 10% on the values given.

	Chemical shift change (p.p.m.)	
Resonance	DNP-glycine	DNP-aspartate
H_3	1.6	1.2
H_5	2.7	1.5
H_6	3.0	1.1
αCH_2	1.2	-

Detailed interpretation of the n.m.r. data is presented in Sections 5 to 9.

3. Binding of DNP-glycine

The choice of DNP-glycine as a ligand was dictated by two considerations. Firstly, the resonance of the side-chain (αCH_2) ^1H nuclei is easily observable, and hence can provide information on protein residues interacting with the ligand side-chain. On binding to the Fv fragment, this resonance was observed to shift upfield by 1 p.p.m. (Dower et al., 1977). This chemical shift change was attributed to an interaction with Tyr-33_H. Tyr-33_H would, of course, be absent from the V_L dimer. However, the model-building study described in Chapter 4 suggests that Tyr-34_L from one monomer of the V_L dimer may occupy an equivalent position to Tyr-33_H (Figure 4.7.). Secondly, DNP ligands with

different side-chains bind with very similar affinities to the V_L dimer and L-chain dimer (Gavish et al., 1977). By contrast, the affinities of such ligands to the Fv fragment vary over three orders of magnitude. The n.m.r. studies should show whether or not the similarity in affinities of ligands for the V_L dimer is reflected by a conserved mode of binding of the DNP group.

The aromatic regions of the ^1H n.m.r. spectra at 270 MHz of the V_L dimer in the absence of ligand or saturated with DNP-glycine, and the resultant difference spectrum, are shown in Figure 5.7. For comparison, the difference with DNP-aspartate is also shown. It is clear from the two difference spectra that the ligands are not affecting the protein resonances in identical manners. The titration curves of the affected resonances are shown in Figure 5.8, and the data are summarized in Tables 5.1 and 5.2. Blank positions in Table 5.1. do not imply that the resonances are not perturbed, since resonance overlap often makes the titration of resonances difficult to follow. It may be seen from Table 5.1 that most, if not all, of the resonances perturbed by the binding of one ligand are perturbed by the other. However, there are significant differences between the chemical shift changes observed for the same resonances. This implies a difference in the modes of binding of the ligands, despite the similarity in their affinities. Examination of the titration curves of the protein resonances again showed that only one binding site per V_L dimer was detectable. The best-fit procedure gave $n = 0.97$ and $K_D = 0.07$ mM, compared with the values of $n = 1.02$ and $K_D = 0.07$ mM which characterize the theoretical curve shown in Figure 5.2b. The difference between the binding of DNP-glycine and DNP-aspartate is particularly noticeable if

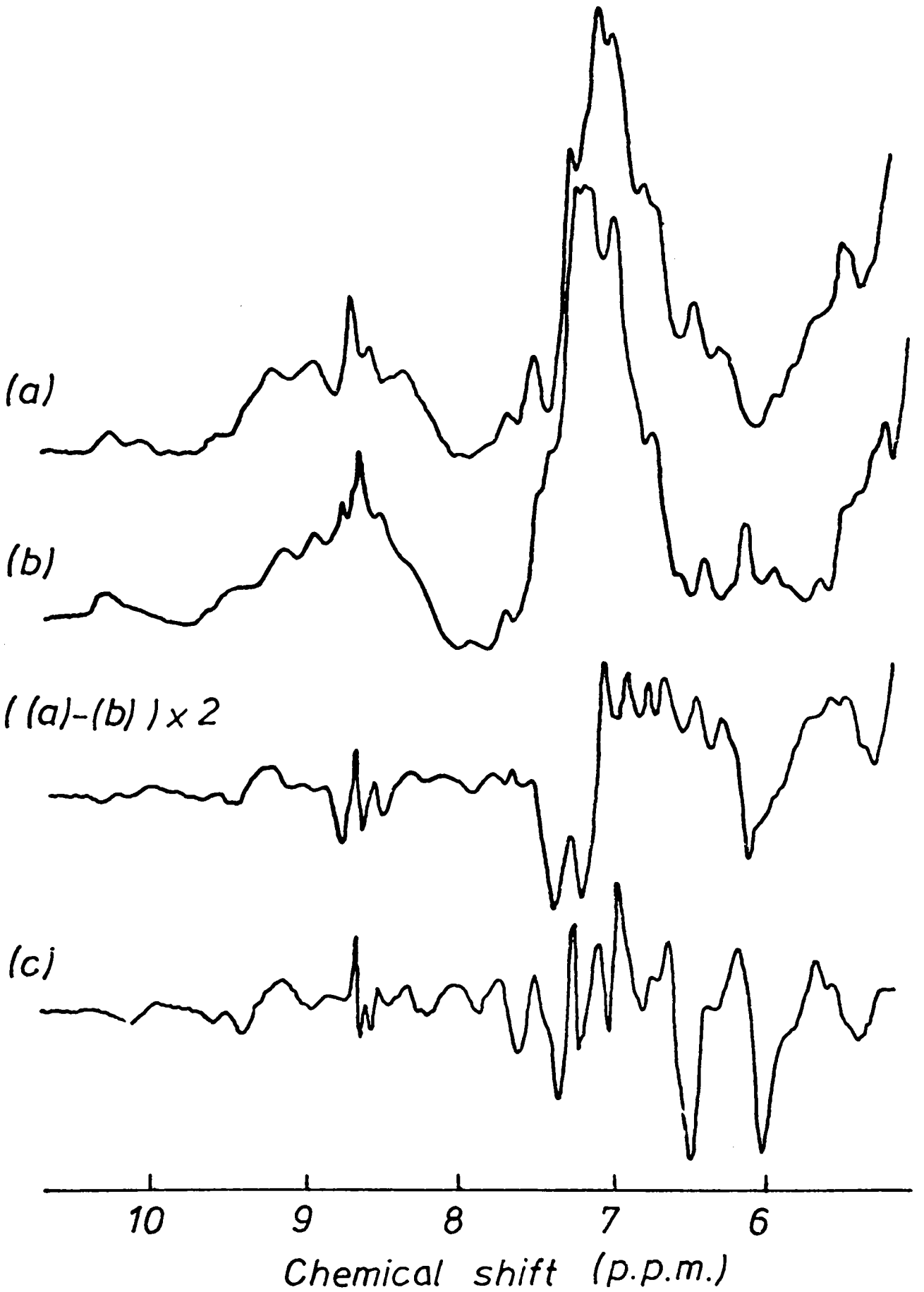

Figure 5.7 Comparison of the effects of the binding of DNP-glycine and DNP-aspartate on the aromatic region of the 270 MHz ^{1}H n.m.r. spectrum of the V_L dimer

2000 scans were recorded at T = 298K, with solutions in $^{2}H_2O$, 0.025M ^{2}H-acetate, pH* 4.8. (a) V_L dimer (0.76 mM). (b) V_L dimer (0.70 mM) with approximately equimolar DNP-glycine. (c) Difference obtained with DNP-aspartate (as for Figure 5.4b).

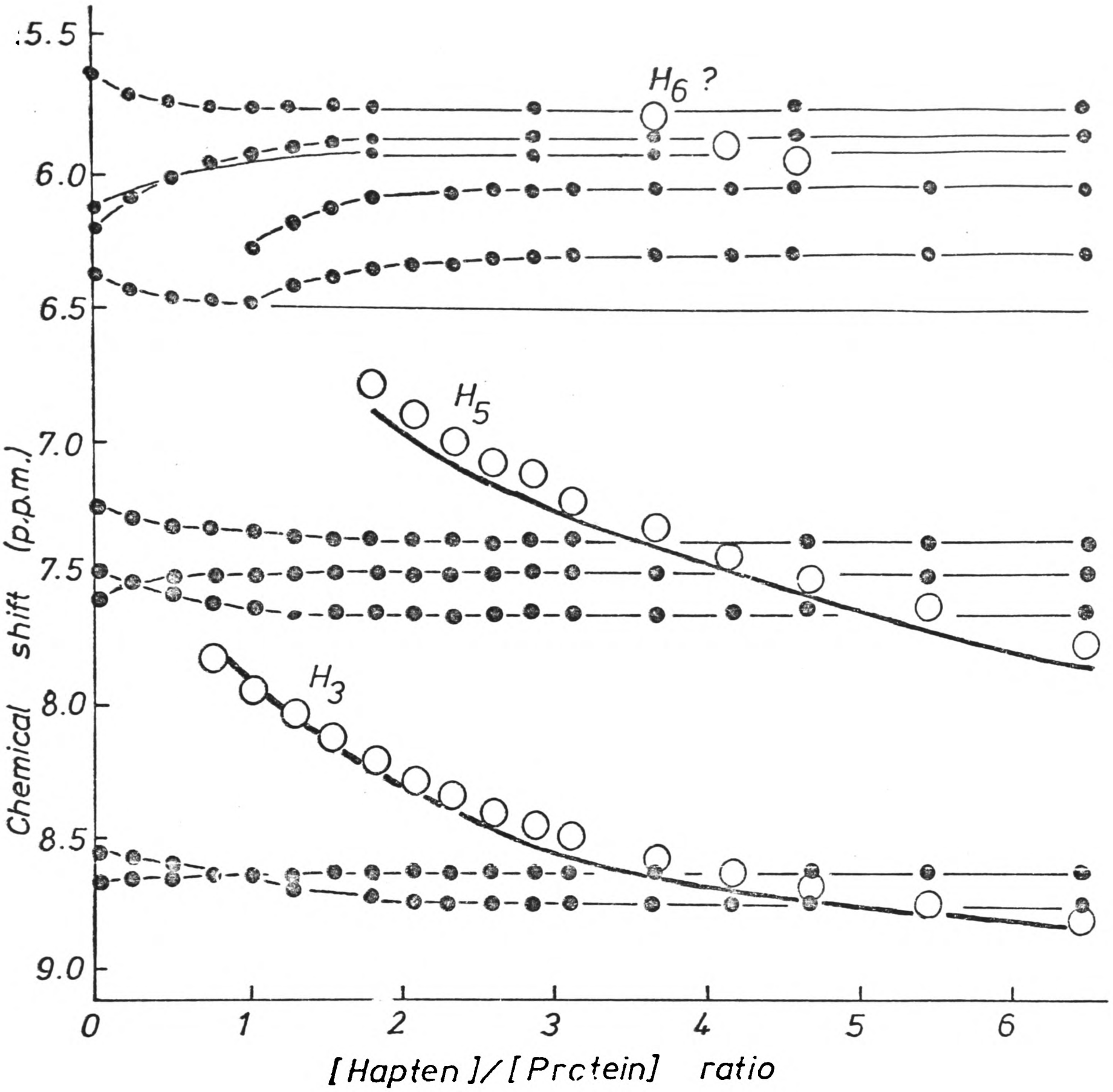

Figure 5.8 Chemical shift changes of the resonances of aromatic ^1H nuclei following the binding of DNP-glycine to the V_L dimer

Measurements were made at 270 MHz, T = 298K, with solutions in ^2H_2O, 0.025M ^2H-acetate, pH* 4.8. The initial protein concentration was 0.76 mM. The chemical shifts of the resonances of the free ligand are: H_3, 9.12 p.p.m.; H_5, 8.29 p.p.m.; H_6, 6.97 p.p.m. The solid curves for the ligand resonances were calculated assuming K_D = 0.07 mM, n = 1.0 and the chemical shift changes given in Table 5.2.

the chemical shift changes of the ligand resonances are compared (Table 5.2). The values for DNP-glycine were calculated as described above for DNP-aspartate. A chemical shift change of 1.3 p.p.m. is observed for the H_3 resonance when approximately 80% of the ligand is bound. The chemical shift change on binding may therefore be estimated at 1.6 p.p.m.. The theoretical curve calculated from this value, and a K_D of 0.07 mM is given in Figure 5.8. It is difficult to observe the titration of the H_5 and H_6 resonances, because their linewidths are large, and of the αCH_2 resonance because it is near the solvent peak. The chemical shift changes of these resonances were therefore confirmed by titrating a solution of the V_L dimer into a solution of DNP-glycine, and observing the ratios of the chemical shift changes relative to the H_3 resonance. The ratio for the H_5 resonance was used to calculate the curve given in Figure 5.8. Detailed interpretation of these chemical shift changes is given in Sections 5 to 9.

4. Binding of TNP-glycine

The data for TNP-glycine illustrate the effect of altering the nitrophenyl ring, and provide the best information available on the perturbation of the protein resonances.

The titration of the resonances of the aromatic region may be seen in Figure 5.9. The spectra illustrate very clearly the titration of the three high field resonances at 6.36 p.p.m., 6.24 p.p.m. and 6.17 p.p.m.. The first titrates downfield, and the other two titrate upfield. All the resonances in this region of the spectrum are perturbed, since no intensity remains in the spectrum of the saturated protein. The titration behaviour of the resonances is given in Table 5.1 for comparison with the behaviour observed with the other ligands. The chemical shift

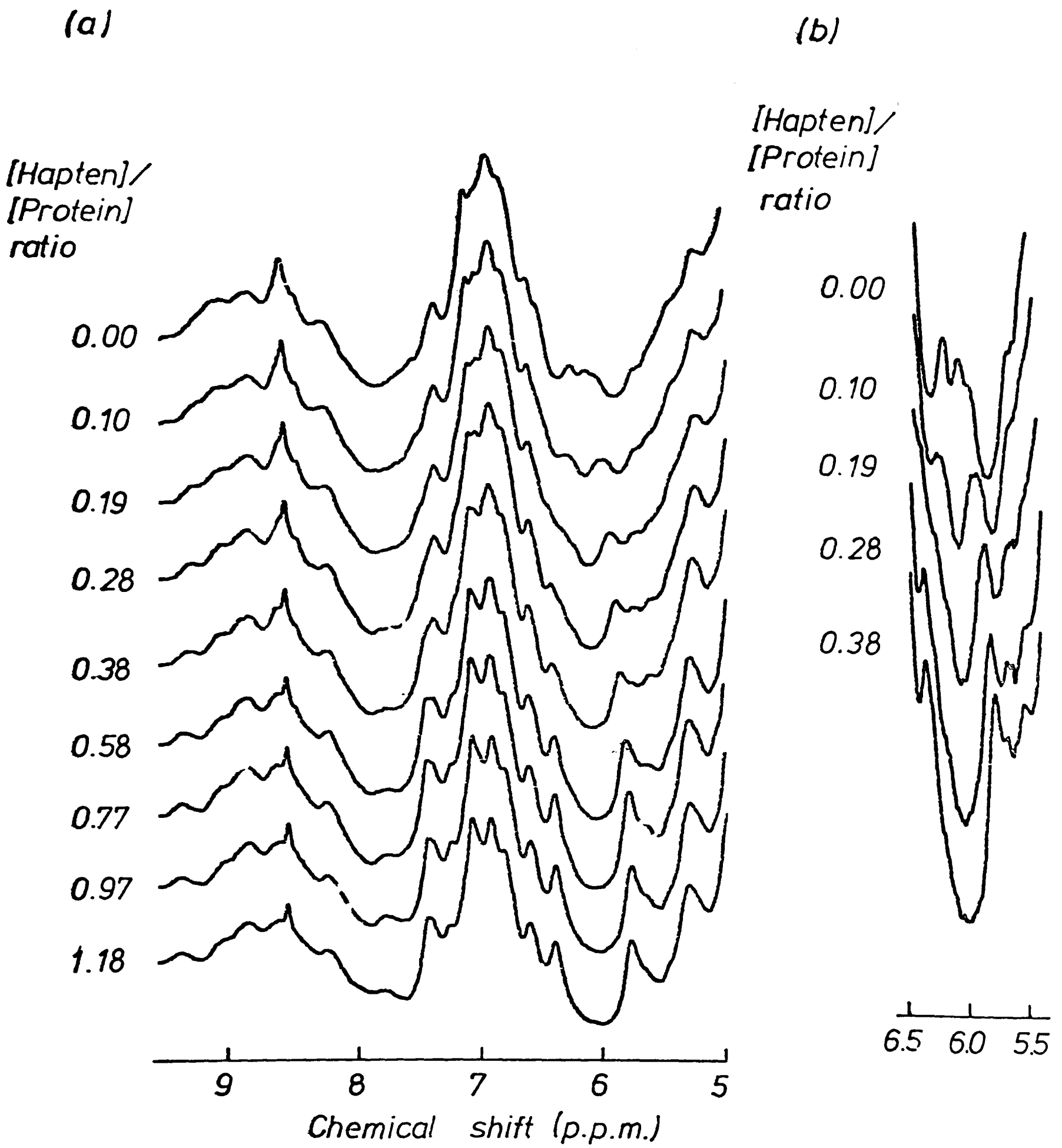

Figure 5.9 The effect of the binding of TNP-glycine on the aromatic region of the 270 MHz ^{1}H n.m.r. spectrum of the V_L dimer

2000 scans were recorded at T = 298K, with solutions in $^{2}H_2O$, 0.025M ^{2}H-acetate, pH* 4.8. The initial protein concentration was 0.85 mM. (a) Aromatic region. (b) High-field part of the aromatic region, showing the titration of the three high-field resonances.

changes differ again from those found with DNP-aspartate or DNP-glycine. However, the same resonances are perturbed, and the TNP derivative is clearly binding in the same region of the combining site as the DNP derivatives. The same conclusion was reached for the binding of these compounds to the Fv fragment (Dower et al., 1978). Measurement of the chemical shift changes of the ligand resonance was not possible, because of slight precipitation of the protein ir the presence of excess ligand.

5. Asymmetry of the V_L dimer

Small deviations from two-fold symmetry have been observed in crystallographic studies of the V_L dimer of protein REI. These deviations were confined to segments facing the solvent, including the first hypervariable loop (Epp et al., 1975). A larger deviation was observed in the combining site of the L-chain dimer of protein Mcg (Edmundson et al., 1974b). This is, however, due to a direct interaction between neighbouring molecules in the crystal.

Information on the symmetry properties of the V_L dimer may be obtained by observation of the histidine H_2 resonances, which are clearly resolved at 8.54 p.p.m. and 8.68 p.p.m. (see e. g. Figure 5.7.). Histidine H_2 resonances are sensitive monitors of the local protein conformation, since they are easily resolved and have narrow linewidths. The V_L dimer contains two histidine residues in each chain. His-44_L is a framework residue, and is distant from the combining site (Padlan et al., 1976a). His-97_L is a hypervariable residue in the region of the combining site, and is perturbed on the binding of hapten to the Fv fragment (Dower et al., 1977; Dower et al., 1978). If the histidines occupy symmetry-related positions, two histidine H_2 resonances of equal intensity should be observed. Instead, the

intensities of the resonances at 8.54 p.p.m. and 8.68 p.p.m. are in the approximate ratio of one to three. This difference is not a function of widely differing T_1 values, since the same ratio is maintained if the spectra are collected with a delay of 5 seconds between pulses. On hapten binding, the resonance at 8.54 p.p.m. and part of the resonance at 8.68 p.p.m. are observed to titrate (Table 5.1, Figure 5.6 and Figure 5.8). It is likely that both these resonances arise from the hypervariable residue His-97_L, and that the resonance at 8.68 p.p.m. associated with His-44_L remains unperturbed. There is therefore a deviation from the two-fold symmetry in the region of the combining site in solution. This deviation from symmetry may not be a widespread phenomenon, since no such deviation could be detected at histidine residues in the variable and constant domains of several Bence-Jones proteins (Arata and Shimuzu, 1979). The deviation is probably small and local, since the signal-to-noise ratio routinely obtained with solutions of the V_L dimer of ~0.8 mM is comparable to that obtained with solutions of the Fv fragment of twice that concentration.

6. Retention of combining site conformation in the separated V_L domain

The similarity in the folding pattern of V_L domains from V_L or L-chain dimers and from Fab fragments has been described in Chapter 4. It is therefore likely that the folding of the V_L domain of protein 315 will be very similar in both the V_L dimer and the Fv fragment. The retention of the conformation of the binding site has also been argued from thermodynamic data (Painter et al., 1972). The n.m.r. studies provide structural evidence on this point in the case of protein 315.

Comparison of the aromatic resonances perturbed on hapten

binding to the V_L dimer and to the Fv fragment reveals striking similarities (Table 5.1). Many perturbed resonances have almost the same chemical shifts in the spectra of both proteins. These equivalent resonances are often perturbed in a similar manner - either upfield or downfield - on hapten binding. Coincidences under the main aromatic envelope (6.5 p.p.m. to 7.4 p.p.m.) could well be fortuitous, but this is unlikely to be true of resonances outside the envelope. The clearest examples are provided by the resonance at 5.64 p.p.m. and the three resonances between 6.1 p.p.m. and 6.4 p.p.m. These resonances are all in very unusual positions. The resonances between 6.1 p.p.m. and 6.4 p.p.m. are almost certainly upfield-shifted aromatic resonances. The resonance at 5.64 p.p.m. could be an αCH resonance shifted downfield by ~1 p.p.m. It has been shown above (Section 4 and Figure 5.9) that the three resonances between 6.1 p.p.m. and 6.4 p.p.m. are the only resonances in this region of the spectrum. Resonances are infrequently observed at these positions in the spectra of proteins, and reflect specific tertiary structure interactions. The overall coincidence of the perturbed resonances leads to the conclusion that the conformation of the combining site residues of the V_L domain is largely maintained, regardless of the presence of either a V_H domain or of another V_L domain. This is an important conclusion in the light of suggestions that the binding of ligands such as DNP compounds by isolated chains may be predominantly fortuitous (Stevenson, 1974).

7. The possibility of assigning resonances in the spectrum of the Fv fragment to residues in the V_L domain

The coincidences of the chemical shifts of resonances affected by the binding of ligand to the Fv fragment and V_L

dimer imply that most of the affected resonances of the Fv fragment arise from amino acids in the V_L domain. It may also be concluded that the resonance positions arise from intrachain, rather than interchain, interactions, since the replacement of a V_H domain by another V_L domain has little effect on their positions. According to the current model of the combining site of the Fv fragment, the resonance positions of only four ^1H nuclei from aromatic residues in the hypervariable region of the V_L domain should be significantly affected by ring-current effects from aromatic residues in the hypervariable region of the V_H domain. Two of these resonances arise from an ortho and a meta ^1H nucleus of Tyr-34_L, and experience shifts of about -0.2 and +0.5 p.p.m. respectively from Tyr-104_H. The other two resonances are those of the H_5 and H_7 nuclei of Trp-93_L. These undergo very small shifts of about -0.1 p.p.m. and -0.2 p.p.m. respectively from Phe-34_H. The H_6 nucleus lies on the 'magic angle', resulting in no effect on the chemical shift. Resonances from the other Trp-93_L nuclei, and from Phe-98_L, Phe-94_L and His-97_L, should be unaffected. The independence of the chemical shifts of these resonances from the presence of the V_H domain provides a rationalization of the coincidences between chemical shifts of the Fv fragment and V_L dimer resonances. However, there is an apparent lack of many resonances which are affected by the binding of hapten to the Fv fragment and which may be attributed to residues from the V_H domain. It is possible, particularly in a highly aromatic environment, that resonances could be exchange-broadened and become unobservable. For example, slow motions, on a time-scale of 300-500 s^{-1} would cause broadening of the resonances of nuclei exchanging between environments differing by 0.2-0.3 p.p.m..

Precise analysis of the ^1H n.m.r. spectra of the Fv fragment and V_L dimer is made difficult by the lack of definite assignments of resonances other than those from histidines. The difficulty of making assignments is largely a function of the linewidths of the resonances, although it is complicated by severe overlap of resonances. The linewidths of the resonances both of the Fv fragment and V_L dimer (both of MW ~25,000) are sufficient to result in the disappearance of the multiplet structure of the resonances. Assignments cannot therefore be made by the spin-decoupling technique, nor by multiplet selection using the spin-echo method (Campbell et al., 1975). The availability of spectrometers operating at frequencies of 470 MHz or greater will decrease the overlap of resonances, but will not alleviate the problems caused by the large linewidths. Present attempts to assign resonances in the Fv fragment and V_L dimer are concentrated on chemical methods. Selective deuteration of the tryptophan ^1H nuclei in the Fv fragment has been achieved by P. Gettins, but at the time of writing, no firm assignments have emerged. It would be worth attempting this method on the V_L dimer, since the V_L domain only contains two tryptophan residues, compared with six in the Fv fragment. The results from the selective nitration of Tyr-34_L are presented in Chapter 6.

8. Possible structure of the DNP-binding site of the V_L dimer

The chemical shift changes of the ligand ^1H resonances on binding to the V_L dimer are all large and upfield (Table 5.2). Changes of similar magnitude were observed on binding to the Fv fragment (Dower et al., 1977). Chemical shift changes in proteins are believed to be dominated by the anisotropic shielding effects associated with delocalized systems of electrons, and particularly

by those of aromatic rings (see e.g. Perkins and Dwek, 1979). Significant shifts, of up to 1 p.p.m., may be produced by the carbonyl group (Pople, 1962; Jackman and Sternhell, 1969). However, only the carbonyl groups of Trp-93_L, Phe-94_L and the side-chain of Asn-36_L are oriented towards the combining site in the present model. They are all expected to be at least 4 Å from any ligand ^1H nucleus, causing shift changes of at most 0.1 p.p.m.. No carboxyl groups are positioned in the combining site.

The ring-current theory used to interpret the chemical shift changes is a modification of the Johnson-Bovey treatment (Johnson and Bovey, 1958), described by Perkins et al. (1977). One recent alteration to this treatment has been included. This involves increasing the strength of the ring-current field due to tryptophan. The rationale for this alteration has been described by Perkins and Dwek (1979). The effect of this alteration on the interpretation of the chemical shift changes is discussed in Section 9.

The proposed combining site of the V_L dimer is bounded by aromatic residues (Figure 4.7). The two parallel Trp-93_L side-chains form the 'sides' of the site, and the 'floor' and 'ceiling' are provided by the Tyr-34_L side-chains. Any proposed geometry of the combining site residues has to be able to explain both the very large upfield chemical shift changes observed for all four ^1H resonances of DNP-glycine, and the much smaller changes observed for DNP-aspartate (Table 5.2). It is expected that the DNP ring will stack between the two Trp-93_L residues. Evidence for a stacking interaction with a tryptophan in the combining site of the L-chain dimer has been obtained by CD (Freed et al., 1976) and by UV difference spectroscopy (Gavish et al., 1978). According to the model (Figure 4.7), the two Trp-93_L side-chains

are expected to be ~8 Å apart. The DNP ring cannot, therefore, be in van der Waals contact with both simultaneously, since the plane-to-plane distance for contact is 3.3 Å (Hanson, 1964; Gartland et al., 1974). Two possible orientations of the DNP ring relative to the two indole groups are shown in Figure 5.10. These may be regarded as the 'DNP-glycine' and 'DNP-aspartate' orientations. To obtain this structure from that of Figure 4.7, the indole side-chains are rotated 1 Å relative to each other. Many geometries close to those of Figure 5.10, allowing changes of about 1.5 Å in the relation positions of the tryptophan rings, can produce chemical shift changes very close to those given in Figure 5.10. One such possibility is shown in Figure 5.11. In these structures, the DNP ring is sandwiched between two indole rings, and is in van der Waals contact with both. The distance between the planes of the tryptophan rings is therefore 6.6 Å. The important conclusion from these calculations is that both the large chemical shift changes of the H_5 and H_6 resonances of DNP-glycine, and the much smaller changes for DNP-aspartate may be accommodated by moving the DNP ring about 1 Å relative to the indole rings. Two tryptophan rings alone, even in van der Waals contact with the ligand, are not sufficient to explain the chemical shift changes observed for the DNP-glycine H_3 and αCH_2 resonances. According to the structure given in Figure 5.10, a chemical shift change of 0.4 p.p.m. is produced on the H_3 resonance, compared with an experimental value of 1.6 p.p.m.. For the αCH_2 resonance, a chemical shift change of ~0.2 p.p.m. is produced, compared with the experimental value of 1.2 p.p.m.. Examination of the model (Figure 4.7) immediately suggests that Tyr-34_L is causing both these shift changes. The Tyr-34_L side-chain from one V_L domain (monomer 1) is in a

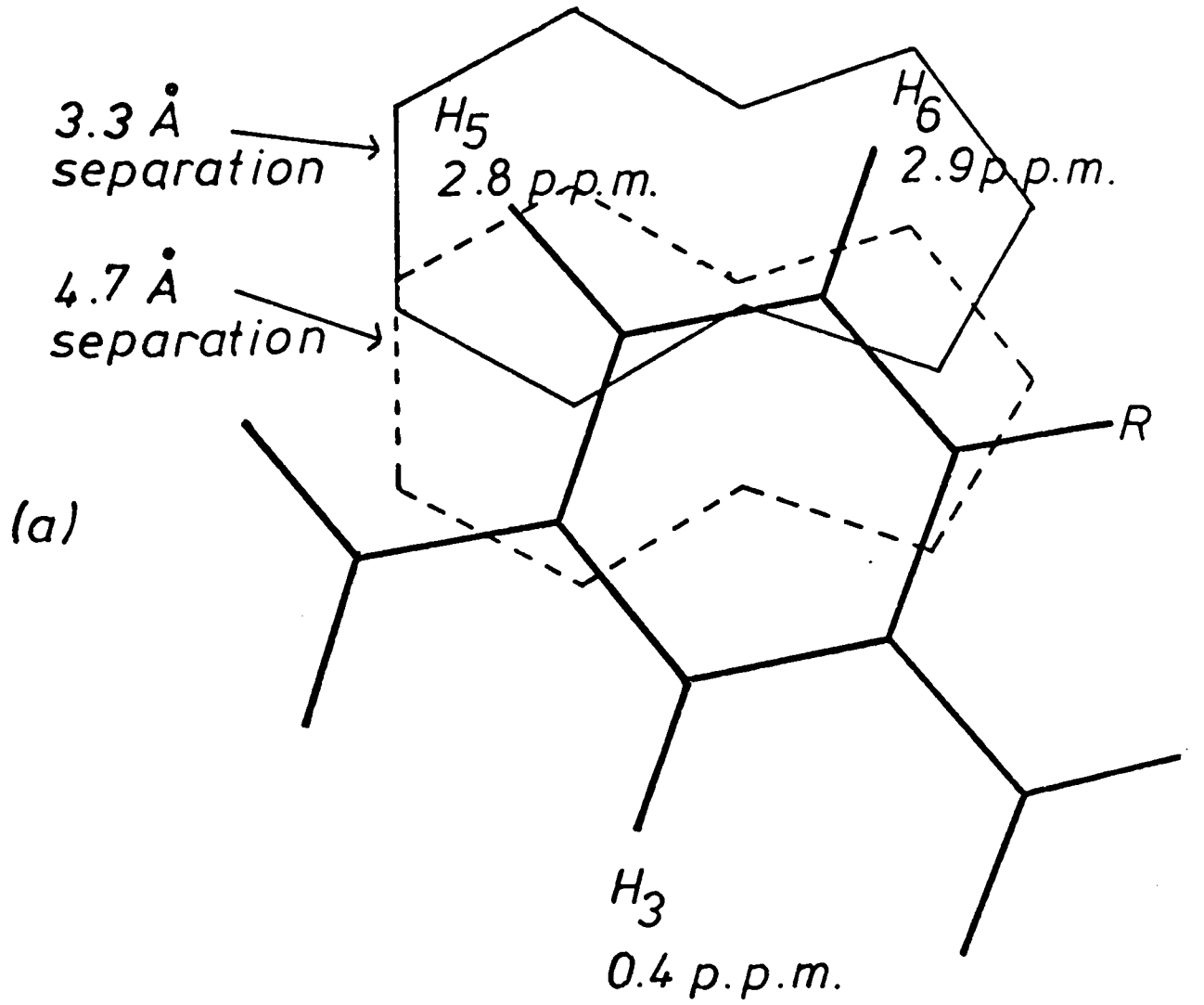

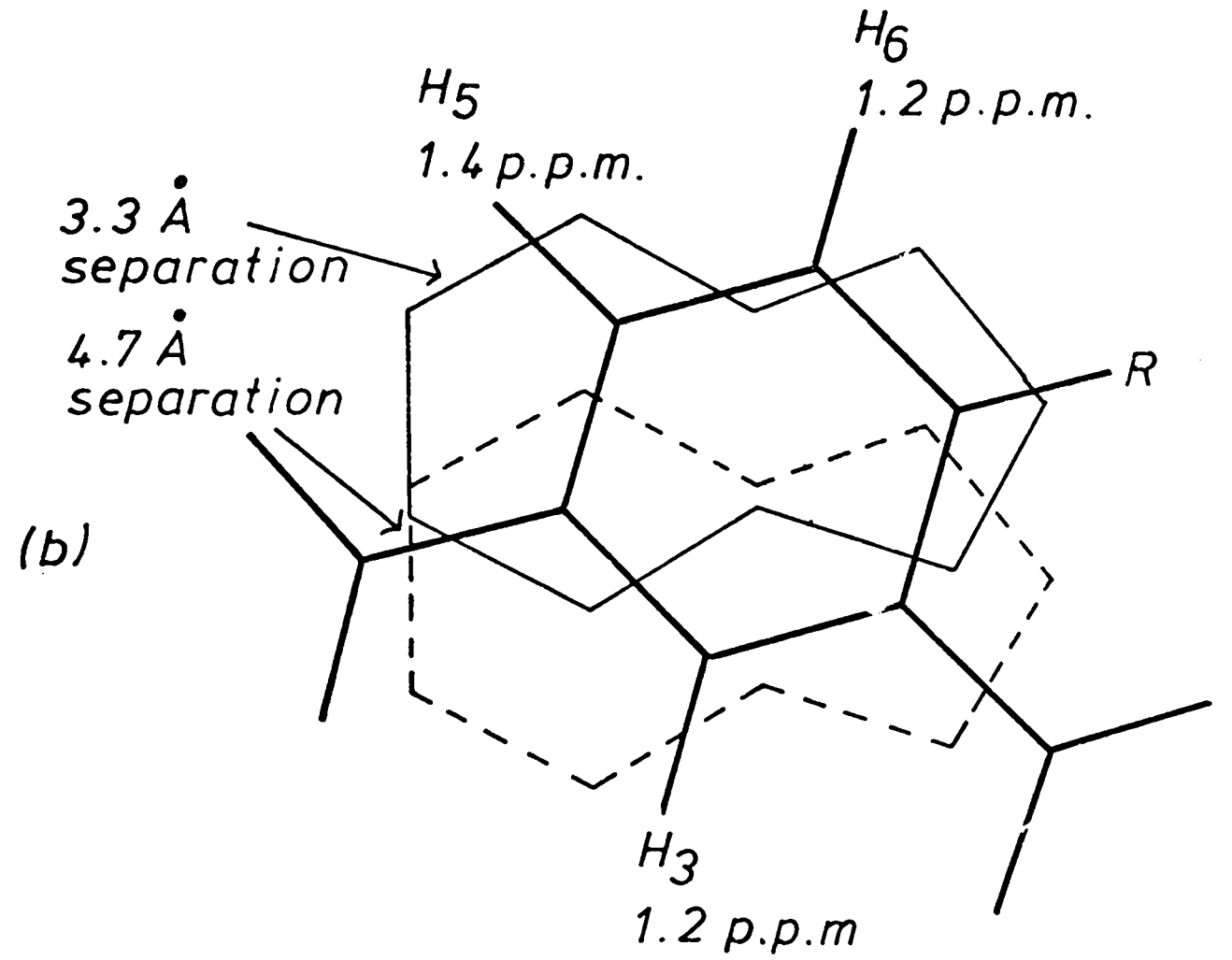

Figure 5.10 Possible geometries of the DNP ring relative to two tryptophan residues in the combining site of the V_L dimer

The planes of the rings are parallel. The tryptophan rings are separated by 3.3 Å and 4.7 Å from the DNP ring. (a) DNP-glycine structure. (b) DNP-aspartate structure.

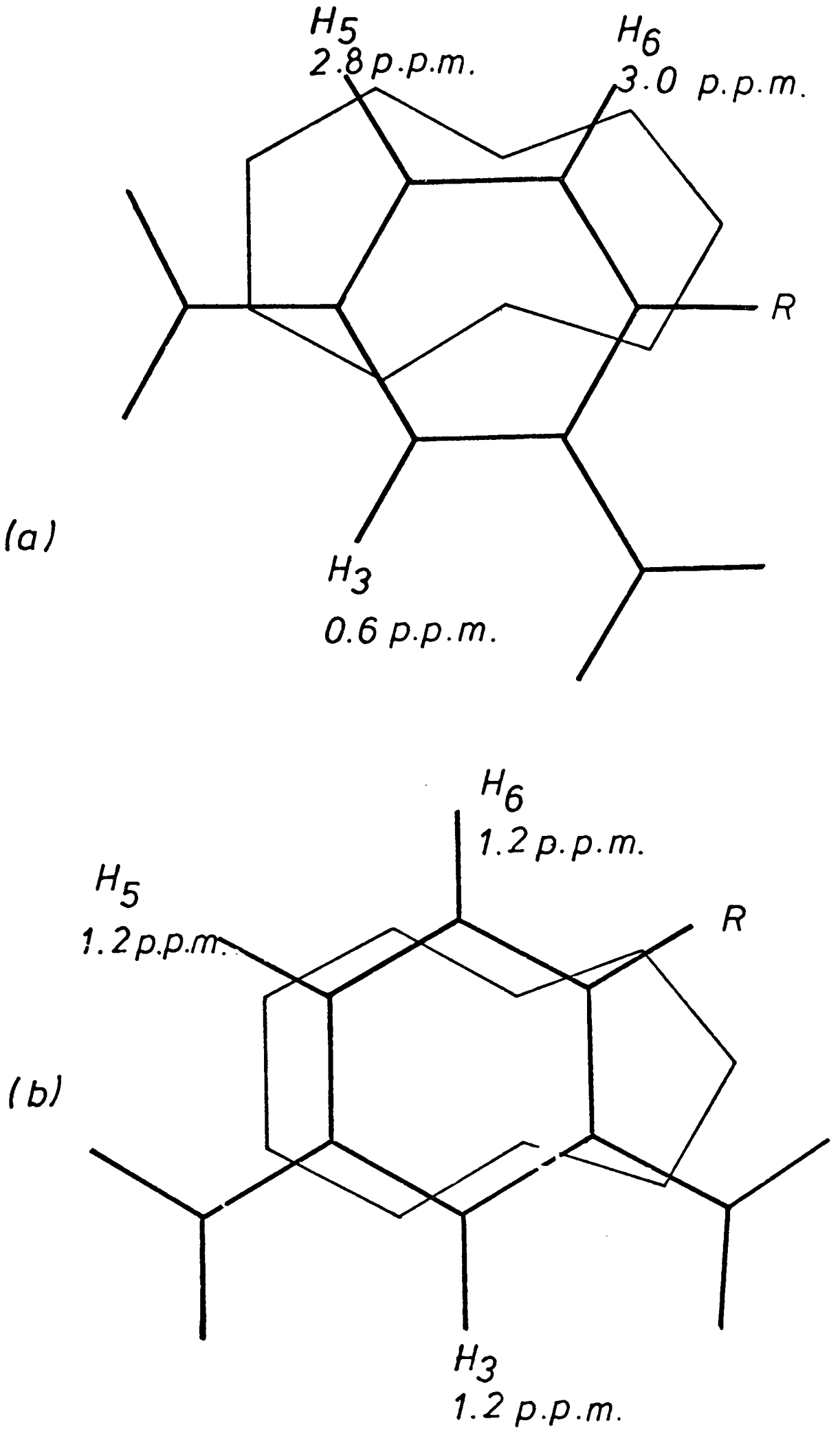

Figure 5.11 Possible geometries of the DNP ring relative to two tryptophan residues in the combining site of the V_L dimer

The planes of the rings are parallel. The tryptophan rings are both separated by 3.3 Å from the DNP rings, and are superimposed in this view. (a) DNP-glycine structure. (b) DNP-aspartate structure.

position to affect the H_3 resonance. To obtain the required chemical shift change, the residue is moved by 1 Å relative to its position in Figure 4.7. This movement is in the same sense as that of Trp-93_L. In other words, the two movements may be accommodated by a change of ~1 Å in the position of one V_L domain relative to the other. This movement is within the limits of the model-building study described in Chapter 4. A small movement, again ~1 Å, of the Tyr-34_L residue of monomer 2 of the V_L dimer is also required to explain the shift on the αCH_2 resonance. The experimentally determined values of the chemical shift changes for the DNP-glycine and DNP-aspartate resonances, and the theoretically calculated values, are given in Table 5.3.

Table 5.3 Experimental and calculated chemical shift changes of ligand ^1H resonances on binding to the V_L dimer

The orientations of the Trp-93_L residues in Figure 5.10 were used.

	DNP-glycine				DNP-aspartate		
Calculated shift change (p.p.m.)	H_3	H_5	H_6	αCH_2	H_3	H_5	H_6
Tyr-34_L (monomer 1)	1.2	-	-	-	0.2	-	-
Trp-93_L (monomer 1)	0.1	2.0	2.1	0.2	0.5	1.1	1.0
Tyr-34_L (monomer 2)	-	-	0.2	1.0	-	-	-
Trp-93_L (monomer 2)	0.3	0.8	0.8	-	0.7	0.3	0.2
	1.6	2.8	3.1	1.2	1.4	1.4	1.2
Experimental shift change (p.p.m.)	1.6	2.7	3.0	1.2	1.2	1.5	1.1

These semi-quantitative calculations are able to provide an excellent rationalization of the chemical shift changes observed on ligand binding to the V_L dimer. The same orientation of combining site residues is therefore able to explain both the

chemical shift changes of the ligand resonances on binding to the Fv fragment and to the V_L dimer.

9. Alteration of the theoretical treatment of the tryptophan ring-current field

The present treatment of Perkins and Dwek (1979), involving an increase of the ring-current field strength relative to the previous treatment (Perkins et al., 1977), is very similar to the original analysis of Sternlicht and Wilson (1967).

If the theory of Perkins et al. (1977) is used, it is not possible to explain the chemical shift changes of the H_5 and H_6 resonances of DNP-glycine on binding to the V_L dimer, unless both indole rings are in van der Waals contact with the ligand, and centrally placed over the H_5 and H_6 nuclei If the indole rings are about 8 Å apart, as expected from the model, the shift changes cannot be explained. This cannot, of course, be regarded as a serious test of the ring-current theory.

The effect of the alteration of the theory on the predicted chemical shift changes of the DNP-glycine resonances on binding to the Fv fragment is shown in Table 5.4. Although the effect of the change is to increase the calculated shift change by 0.3-0.5 p.p.m., there is still a requirement for the two additional rings, Tyr-34_L and Phe-34_H, to explain the observed chemical shift changes. The observed values may be explained by moving the rings of Tyr-34_L and Phe-34_H by ~0.5 Å. The result is therefore a small change in the position of combining site residues, but no qualitative alteration of the model.

Table 5.4 Predicted upfield chemical shift changes of the ^1H aromatic resonances of DNP-glycine arising from $Trp\text{-}93_L$ in the combining site of the Fv fragment. The effect of altering the theoretical treatment of the tryptophan ring-current field

The atomic coordinates of the model given in Dower et al. (1977) were used. The theoretical treatments of the tryptophan ring-current fields are given in Perkins et al. (1977) and Perkins and Dwek (1979)

Resonance	Upfield chemical shift change from $Trp\text{-}93_L$ (p.p.m.)	
	Perkins et al. (1977)	Perkins and Dwek (1979)
H_3	0.21	0.55
H_5	1.41	1.93
H_6	0.47	0.78

The significance of the different modes of binding of DNP-glycine and DNP-aspartate

It has been shown above (Section 8) that there is a difference of about 1 Å between the positions of the DNP rings of DNP-glycine and DNP-aspartate in the combining site of the V_L dimer. There are also differences in the positions of the DNP rings of DNP-aspartate, DNP-glycine and DNP-aminocaproate relative to the indole ring in the DNP/tryptophan complexes (Table 3.1), although these were not quantified. Both sets of results imply that a charge-transfer interaction is not the dominant force behind complex formation, even for the DNP/tryptophan interaction, since its magnitude will be dependent on the relative orientation of the appropriate transition dipoles. These can clearly change

without significantly affecting the affinity of the complex. Indeed, the difference between the modes of binding of the DNP rings to the protein suggests that the specificity of the protein for DNP ligands is provided not so much by discrete directional interactions, such as hydrogen bonds to the nitro groups or charge-transfer interactions, but by factors often considered to be non-specific. These would include the transfer of a relatively non-polar molecule from water to an aromatic combining site, i.e. 'hydrophobic' interactions, and the overall shape of the site in terms of its ability to provide effective van der Waals interactions with the ligand. The theoretical arguments outlined in Chapter 3 (p.51) suggest that 'hydrophobic' interactions may be important in determining the affinities both of complexes of DNP compounds with tryptophan and with antibody combining sites. Experimental evidence for this possibility has been obtained from a study of the thermodynamics of transfer of DNP-lysine from water to ethanol (Halsey and Biltonen, 1975). The authors suggested in particular that the large negative heat capacity changes measured for hapten-antibody reactions are predominantly the result of a reduction in water-hapten interactions. The use of DNP-lysine, with an associated chloride ion, for these experiments makes it difficult to analyse the contribution of the DNP group alone. Similar measurements using, for example, dinitroaniline would be very instructive.

It may be thought that generalizations on the basis of binding to a V_L dimer are unwarranted. However, examination of the data for the Fv fragment leads to the same conclusion. The CD spectra of DNP ligands induced on binding to the Fv fragment differ according to the nature of the side-chain (Rockey et al., 1972). This implies that there are differences in the relative

positions of the DNP and tryptophan rings. The resonance Raman bands associated with the nitro groups are also affected differently on binding (Kumar et al., 1978; Gettins, 1979). Although theoretical interpretation of these changes is difficult, the differences imply that particular interactions formed with a nitro group of one ligand may not be formed with the corresponding nitro group of a ligand with a different side-chain. The difference in ring positions giving rise to these changes may again be estimated from the variation in the chemical shift changes of the DNP ^{1}H resonances on binding. The variations amount to 0.3-0.5 p.p.m. (Dower et al., 1977), which may be explained by alterations in ring positions of ~0.5 Å.

The lack of any large conformational change on ligand binding, suggested by the low intensity of the ^{1}H n.m.r. difference spectra, implies that the binding site may be visualized as a rigid structure. Similarly low intensities of ^{1}H n.m.r. difference spectra are characteristically observed following the binding of haptens to antibodies (Gettins et al., 1977; Gettins, 1979). The specificity of antibodies for the nitrophenyl group may therefore largely be determined by the size and shape of a predominantly non-polar combining site. Clearly a stacking interaction of the DNP ring with an aromatic residue is likely to be favoured, since this will maximise the steric fit between the two species. It has been shown in Chapter 3 that the best interaction will be obtained with tryptophan side-chains, and that this interaction could contribute about a third of the binding energy of dinitroaniline for protein 315. An 'ideal' antibody will also maximise the use of specific directional interactions, including hydrogen bonds. The analysis of high-affinity anti-DNP antibodies, using the cell fusion technique, will help to define the relative importance of these forces

more precisely.

Implications of the DNP-binding activity of the V_L dimer for the mechanism of the generation of antibody diversity

It has been concluded from the n.m.r. experiments described in this chapter that the binding of DNP compounds to the V_L dimer is not fortuitous, but reflects the conservation of structural features of the L-chain of importance in determining the affinity of the intact protein 315 for the nitrophenyl group. A predominant role for either H-chain or L-chain in determining antibody specificity may not be a general feature of antibody diversity. Nevertheless, an extensive study of partial sequence data from mouse myeloma proteins with given specificities showed a distinct relationship between the binding specificity and the subgroup to which the V_H region could be assigned (Barstad et al., 1978). This relationship included the three DNP-binding proteins 315, 460 and 25. In the case of the phosphorylcholine-binding myeloma proteins, the relationship is explicable in structural terms, since contacts of the ligand with V_H residues of protein 603 are important (see Figure 1.4). The experiments reported here suggest that such correlations may occasionally be misleading. This conclusion is reinforced by the observation that antibodies containing L-chains of the uncommon λ_2 subtype, the same subtype as protein 315, are preferentially induced by DNP-KLH in BALB/c mice (Cotner and Eisen, 1978). The putative germ-line gene for the λ_2 V-region in BALB/c mice has been sequenced (Tonegawa et al., 1978). The predicted amino acid sequence differs at only four positions from the V_L sequence of protein 315. None of these changes, at positions 38 (Ile in protein 315 becomes Val), 94 (Phe-Tyr), 95 (Arg-Ser) and 96 (Asn-Thr) is expected greatly to alter the binding properties of

the V_L domain. It would therefore be expected that this putative λ_2 germ-line V-region gene, and closely related mutants, would frequently be represented in the anti-DNP response of BALB/c mice.

The rigidity of antibody combining sites, suggested by the present study and by others (Gettins et al., 1977) may be an important factor in the generation of antibody diversity. If the site formed by an individual domain is quite rigid, that domain may be associated with several different domains, or undergo limited amino acid substitutions without drastically altering its binding properties. Such a mechanism could increase the possibility of selection and maintenance of particular genes, and give the organism control over its ability to create slightly modified specificities by possible somatic mutational processes.

Comparison of the proposed binding site of the V_L dimer with those of proteins REI and Mcg

Both the V_L dimer of protein REI and the L-chain dimer of protein Mcg bind nitrophenyl compounds. The affinity of protein REI for DNP or TNP compounds is, however, only 10^1-10^2 M^{-1} (R. Huber, personal communication). The binding of bis-DNP compounds is 10^2-10^4 M^{-1} (Epp et al., 1975). The binding of bis-DNP compounds more tightly than mono-DNP compounds is found for the L-chain dimer of protein 315, as well as for protein REI (Licht et al., 1977). It is indicative of the large size and apolar nature of these combining sites. The structure of the combining site of protein REI, containing a bound TNP group is shown in Figure 5.12 (details provided by O. Epp and R. Huber). The nitrophenyl ring stacks between the two rings of Tyr-91 (equivalent to $Trp\text{-}93_L$ in protein 315), although it is not in close contact with either. There are groups capable of hydrogen bonding to all three nitro groups of the ligand (Asn-34, Tyr-96 and Tyr-296). Despite these apparently favourable interactions, the affinity is

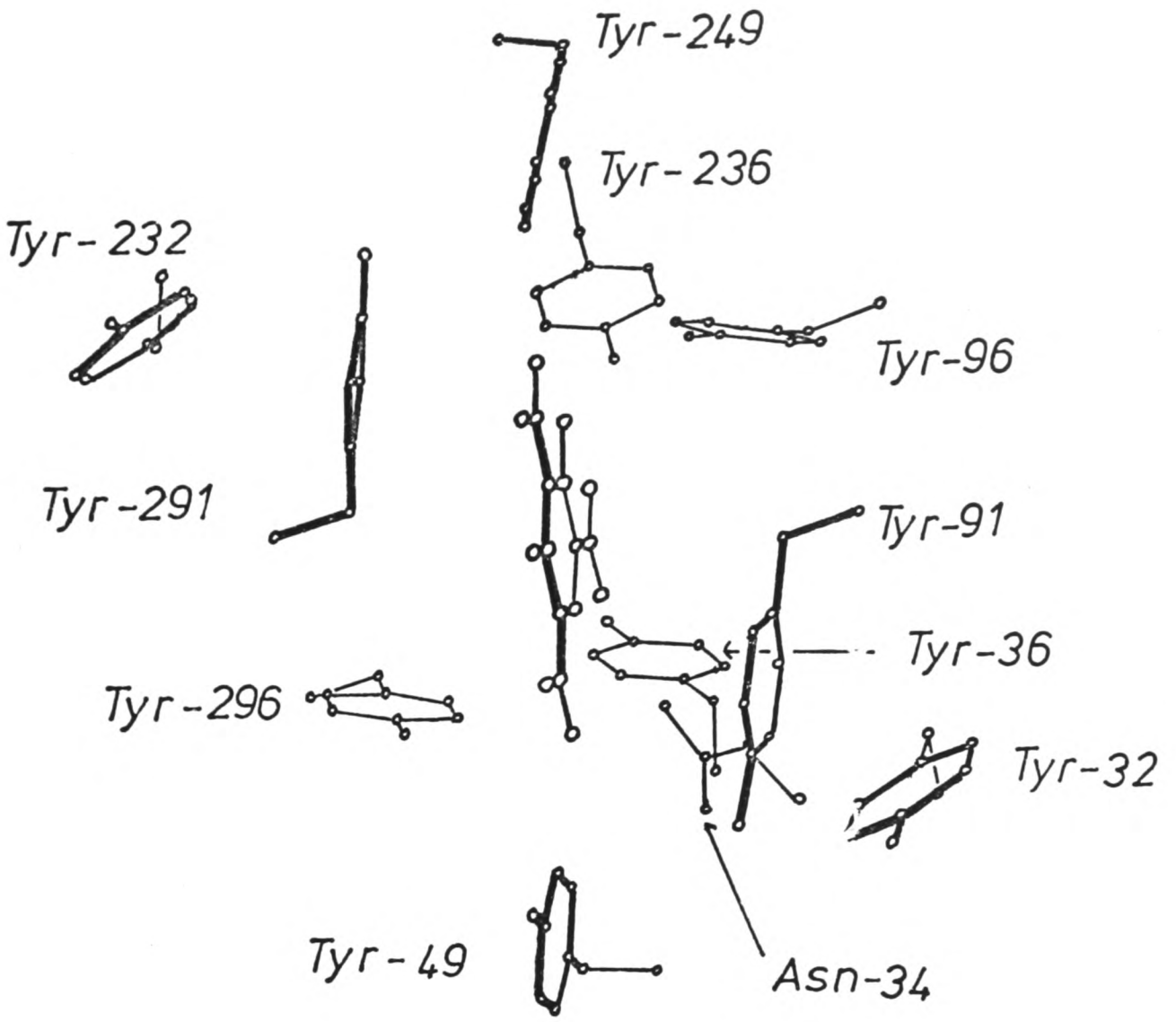

Figure 5.12 The combining site of the V_L dimer of protein REI containing a bound TNP group

This diagram was kindly provided by Dr. O. Epp and Professor R. Huber, Max-Planck Institute of Biochemistry, Munich.

very low. It is tempting to suggest that the presence of tryptophan rather than tyrosine at position 91 would result in a substantial increase in affinity. Movements of Tyr-36, Tyr-49, Tyr-96, Phe-98, Tyr-236, Tyr-249, Tyr-296 and Phe-298 of 0.1-0.7 Å are detected following binding. Similar small changes could contribute to the ^1H n.m.r. hapten difference spectra obtained with the V_L dimer.

The binding site of protein Mcg is a large cavity which can bind two bis-DNP-lysine molecules with an affinity of 3-4 x 10^4 M^{-1} (Firca et al., 1978). The affinities of mono-DNP or TNP compounds have not been reported, but would, by analogy with protein REI, be expected to be very low. There is no single site for the binding of aromatic molecules to protein Mcg (Edmundson et al., 1974b), and the parent IgG does not bind DNP (Firca et al., 1978), suggesting the fortuitous creation of a binding site for aromatic molecules. Indeed, some molecules (e.g. menadione and pyrimidine derivatives) bind in a site lined by framework residues (Firca et al., 1978). The major site is distorted by interactions between molecules in the crystal. However, Tyr-93 (equivalent to $Trp\text{-}93_L$ in protein 315) and Tyr-34 (equivalent to $Tyr\text{-}34_L$) are important contacts for the DNP groups of bis-DNP-lysine in this site (Firca et al., 1978). There are therefore considerable similarities between the combining sites of the V_L dimers of protein 315 and protein REI, and the L-chain dimer of protein Mcg. However, only the V_L dimer of protein 315 has been shown to have substantial affinity for mono-DNP compounds.

The pH-dependent conformational change of the V_L dimer

1. Kinetics

The intrinsic protein fluorescence of the V_L dimer is over 2-fold greater at pH 8 than at pH 6 (Gavish et al., 1978). This change was interpreted to reflect a transition from an 'open' conformer capable of binding two ligands, to a 'closed' conformer capable of binding one ligand. The pK_a of the transition was found to be 6.9.

The kinetic parameters of the conformational change were investigated using a pH jump technique at 25°C. The solutions of V_L dimer at pH 4.8 or pH 8.3 were diluted into buffer at pH 8.3 or pH 4.8 and mixed manually. The time courses of the fluorescence changes at 335 nm, after excitation at 285 nm, are shown in Figure 5.13 for a V_L dimer concentration of 3 μM. The jump from pH 4.8 to pH 8.3 is interpretable in terms of a single exponential (Figure 5.14a) with a time constant of 790s. The jump from pH 8.3 to pH 4.8 is biphasic (Figure 5.14b and c). The slow process has a time constant of 940s, similar to that characterizing the upward pH jump. The faster process has a time constant of 63s. It is unlikely that faster processes associated with fluorescence changes have been missed as a result of the long response time of the apparatus. This possibility may be tested by comparing the initial fluorescence intensities extrapolated from the curves given in Figure 5.14 with those measured after dilution of a stock solution of the V_L dimer into the buffer of the same pH. The extrapolated and measured values agreed within 5%. In order to rule out the possibility of a contribution from second-order processes, which could reflect dimerization, the experiments were repeated with V_L dimer concen-

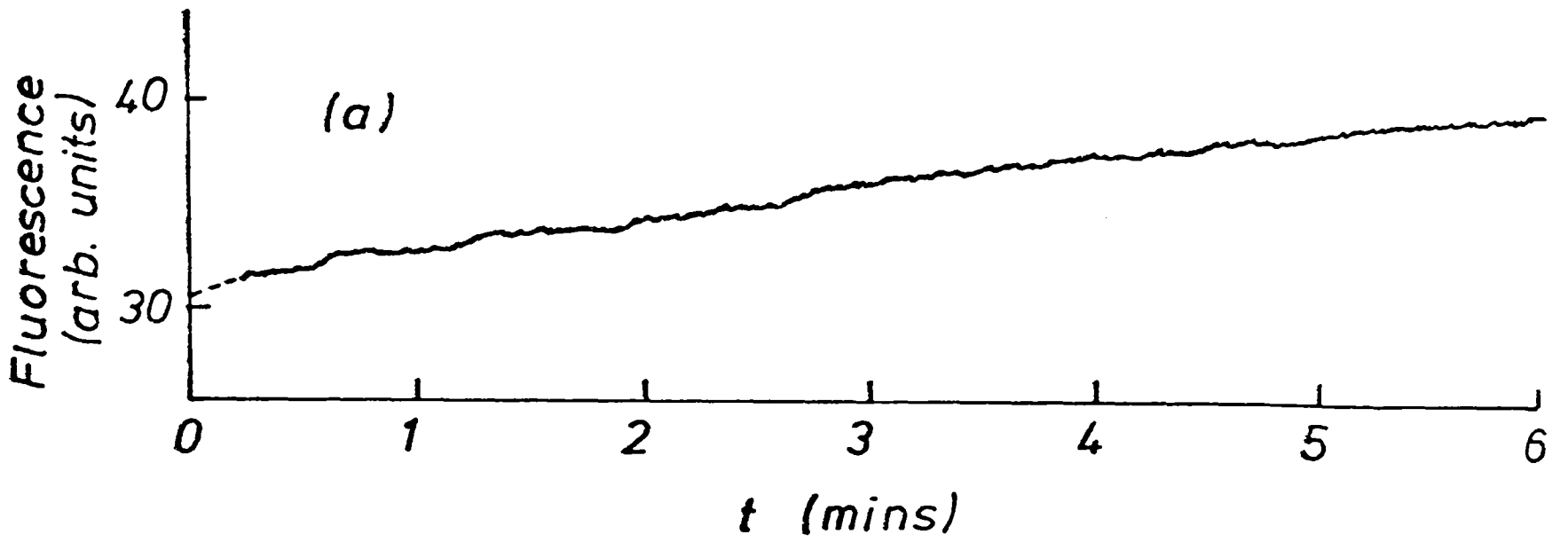

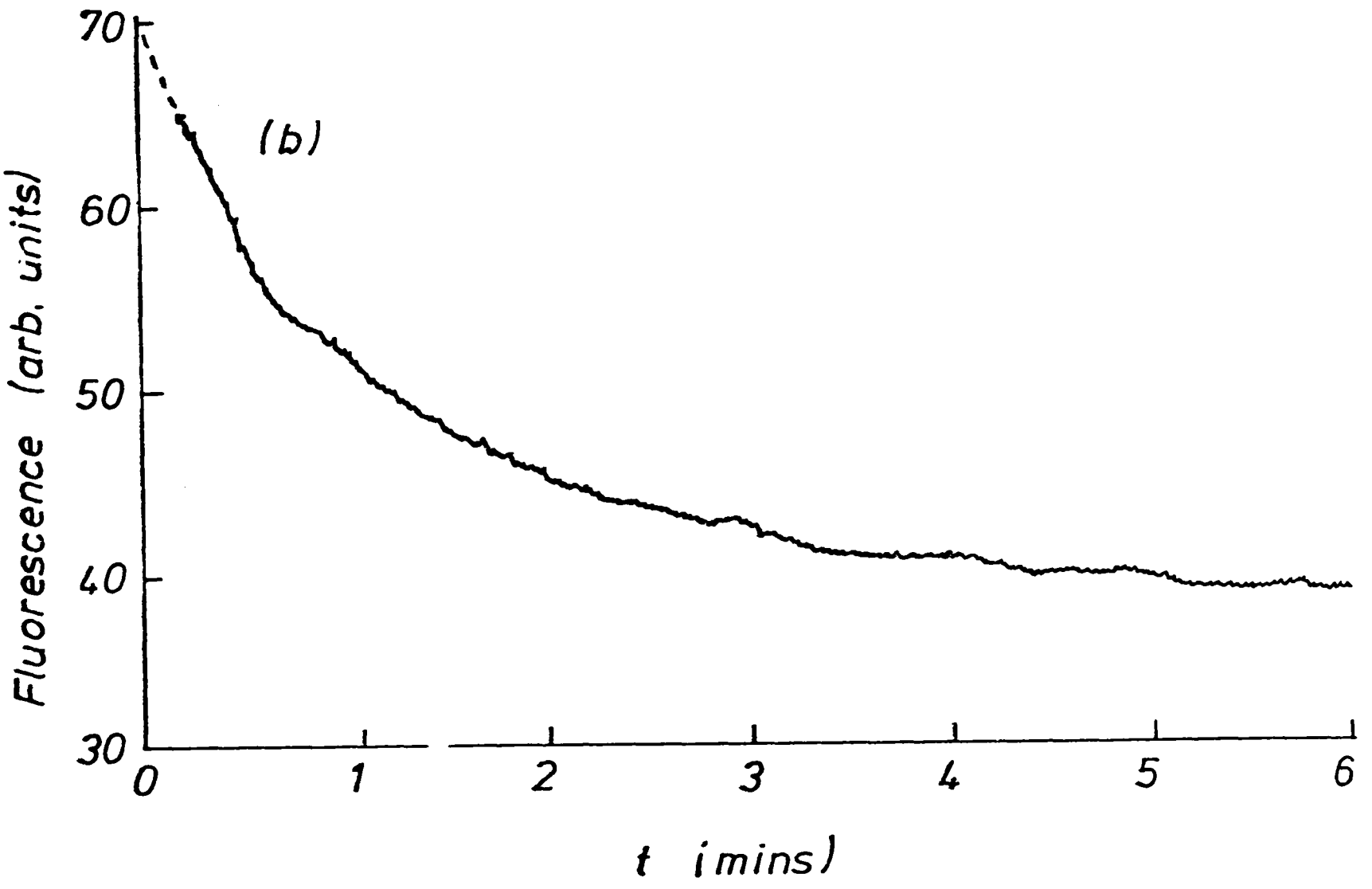

Figure 5.13 Time-dependent fluorescence changes of the V_L dimer following pH jumps

Measurements were made at T = 293K. The protein concentration was 3 μM. (a) Jump from pH 4.8 to pH 8.3. (b) Jump from pH 8.3 to pH 4.8.

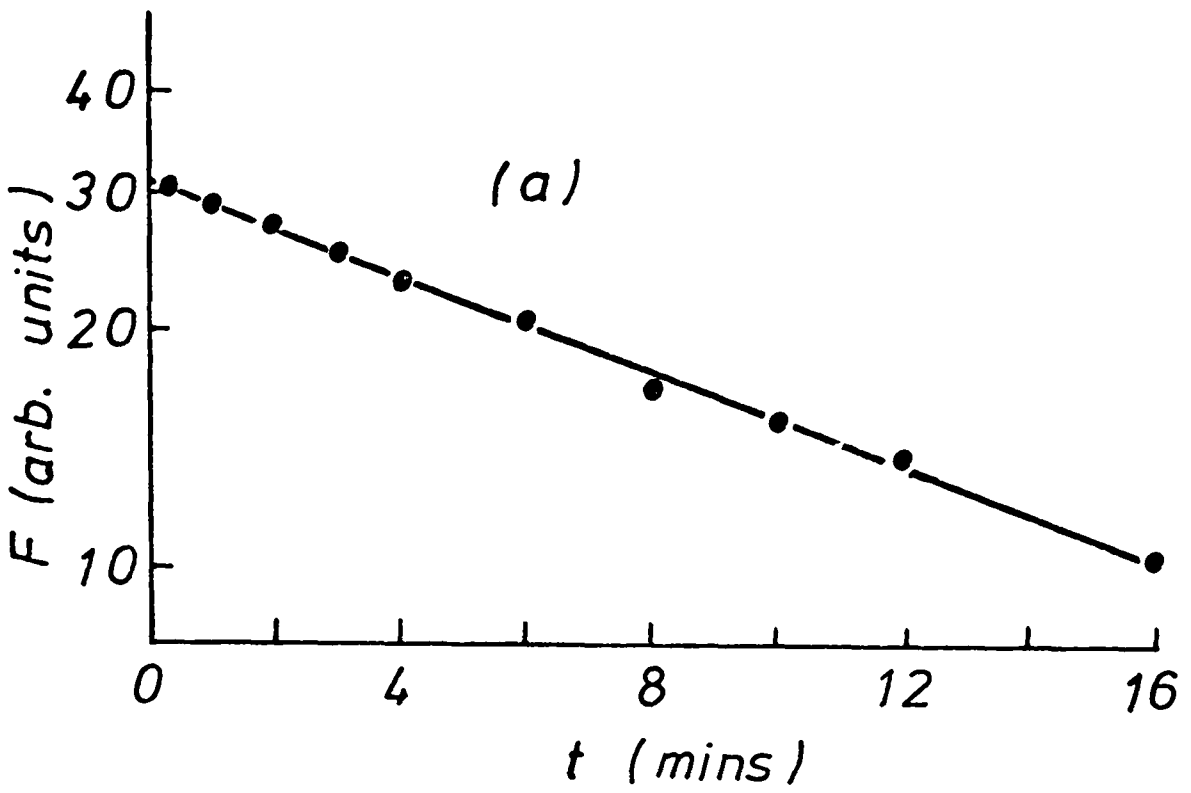

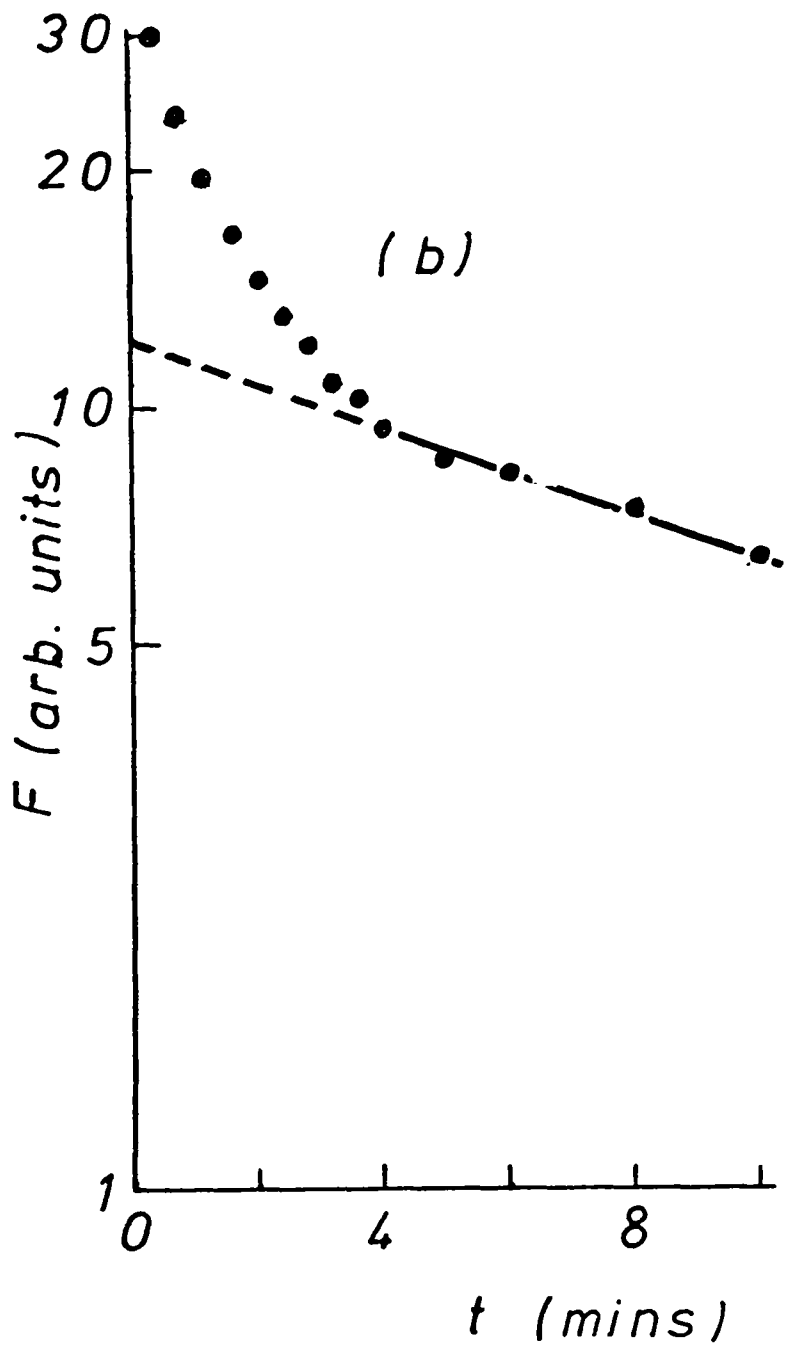

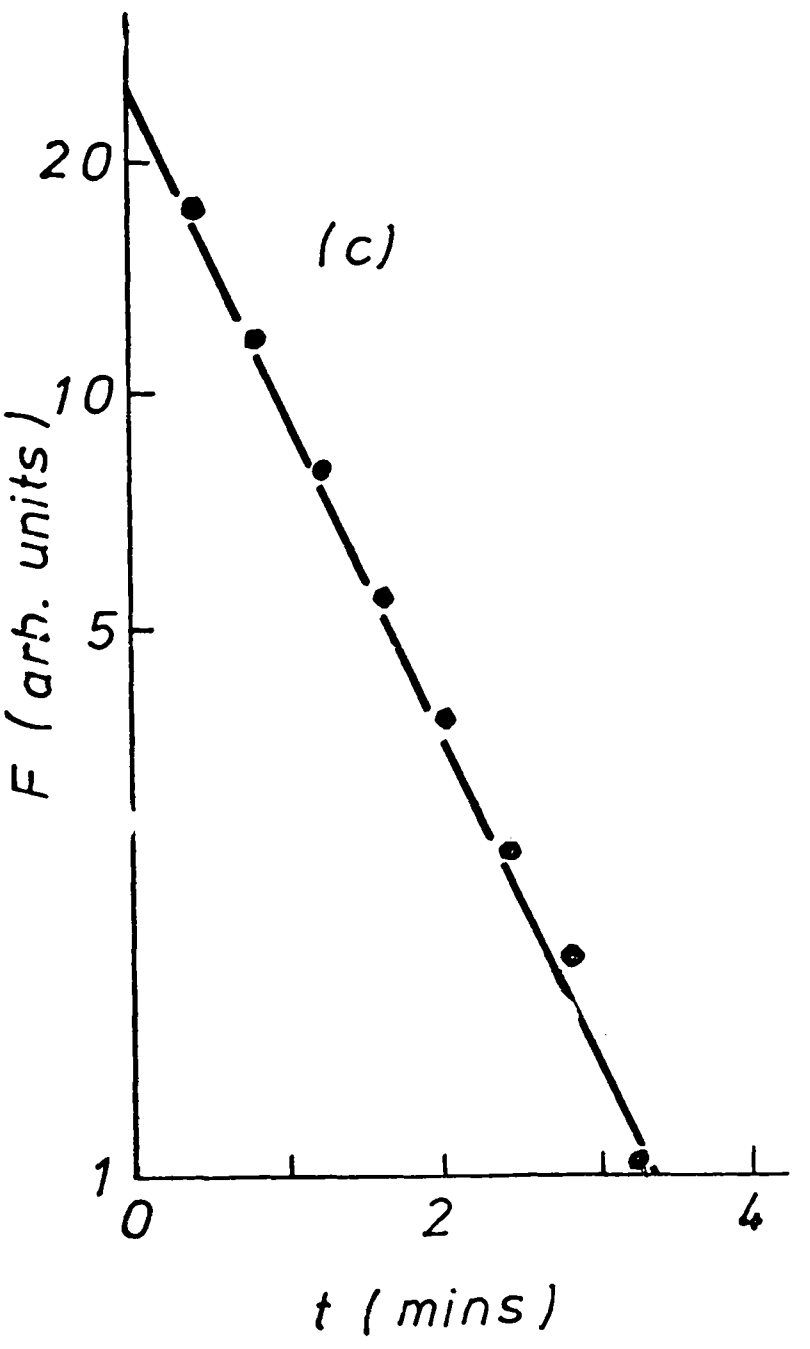

Figure 5.14 Analysis of the fluorescence changes of the V_L dimer

The protein concentration was 3 μM. (a) Jump from pH 4.8 to pH 8.3, $k = 1.27 \times 10^{-3}\ s^{-1}$. (b) Jump from pH 8.3 to pH 4.8, $k = 1.06 \times 10^{-3}\ s^{-1}$. (c) Jump from pH 8.3 to pH 4.8, $k = 1.59 \times 10^{-2}\ s^{-1}$.

trations of 1 μM and 0.3 μM. The kinetic parameters at all three concentrations are given in Table 5.5. There is no significant effect of the 10-fold change of concentration. Similar slow fluorescence changes were seen with the L-chain dimer but these were not characterized in detail.

The conformational change clearly does not proceed by a reversible one-step mechanism. The minimal mechanism requires one distinct intermediate (Ikai and Tanford, 1973), and is thus more complex than the concerted one-step mechanism proposed to account for the conformational change of protein 460 on ligand binding (Lancet and Pecht, 1976). The conformational change of the V_L dimer is further differentiated from that of protein 460 in that it occurs over a time-scale approximately three orders of magnitude more slowly. Indeed, the kinetic behaviour bears much more resemblance to the folding and unfolding processes of the pFc' fragment (Isenman et al., 1979) than to the ligand-induced change observed with protein 460.

2. Structural extent

The extent of the conformational change may be investigated by comparing the ^1H n.m.r. spectra of the V_L dimer at pH* 4.8 and pH* 8.3. Unfortunately, the low solubility of the V_L dimer at pH* 8.3 has prevented an extensive study of its ligand binding properties at high pH. Spectra were obtained with a solution of V_L dimer at 0.18 mM, collecting 16,000 transients, and are shown in Figure 5.15. The difference spectrum is of remarkably low intensity. Only 1-2% of the total intensity is represented in the difference, which is less than that of the hapten difference spectra (Figure 5.4). It may therefore be concluded that the conformational change is highly localized,

Table 5.5 Kinetic and fluorescence enhancement parameters for the conformational change of the V_L dimer of protein 315 in pH jump experiments

Measurements were made using solutions in 0.05M sodium acetate (pH 4.8) and 0.05M Tris (pH 8.3), T = 298K. Stock solutions of V_L dimer (2 mg/ml) were diluted into the appropriate buffer. Protein fluorescence was excited at 285 nm and measured at 335 nm, using excitation and emission slit widths of 7 nm. The enhancement parameter, ε , is defined as the ratio of the fluorescence intensity at high pH to that at low pH. It was calculated by taking the ratio of the observed fluorescence intensity at $t = \infty$ to the extrapolated intensity at $t = 0$, using the semi-log plots of Figure 5.14.

V_L dimer concentration (μM)	pH jump						
	4.8 to 8.3		8.3 to 4.8				
	k (s^{-1})	ε	k_{slow}(s^{-1})	k_{fast}(s^{-1})	$\varepsilon_{overall}$	ε_{slow}	ε_{fast}
3.0	1.27×10^{-3}	2.09	1.06×10^{-3}	1.59×10^{-2}	2.23	1.40	1.59
1.0	1.56×10^{-3}	2.20	0.99×10^{-3}	1.64×10^{-2}	2.24	1.31	1.71
0.3	1.85×10^{-3}	2.61	1.10×10^{-3}	1.40×10^{-2}	2.27	1.47	1.55

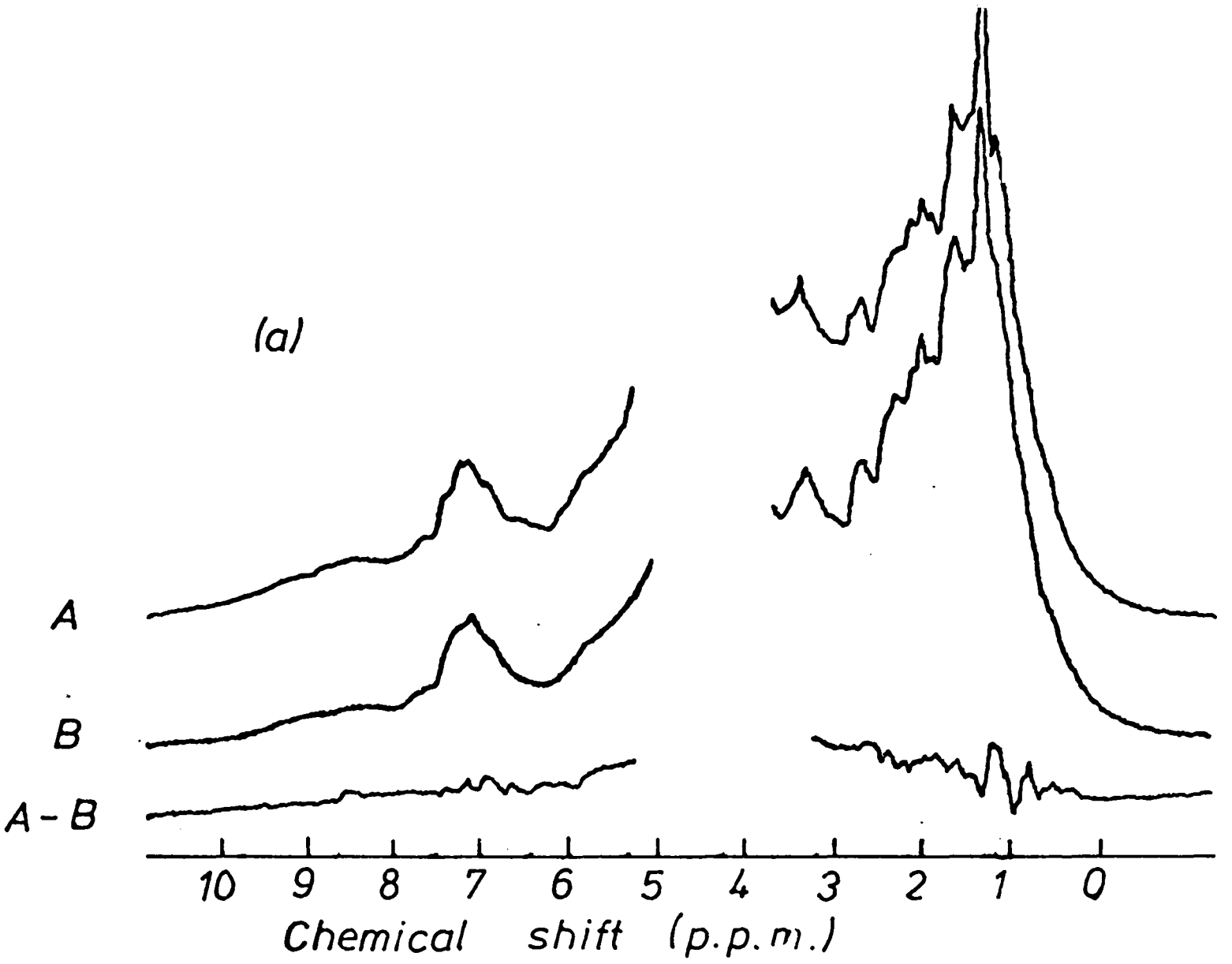

Figure 5.15 The effect of a change of pH on the 270 MHz ^{1}H n.m.r. spectrum of the V_L dimer

16,000 scans were collected at T = 298K, with solutions in $^{2}H_2O$, 0.025M ^{2}H-acetate. The protein concentration was 0.18 mM. (a) Whole spectrum. (b) Aromatic region. A - pH* 4.8. B - pH* 8.3.

despite the complexity and slowness of the kinetic behaviour. It has been suggested that conformational changes in immunoglobulins may involve changes in the relative positions of the chains (Schlessinger et al., 1975; Poljak et al., 1976; Lancet et al., 1977). Any such change in the V_L dimer should result in a substantial aromatic difference spectrum since, by analogy with the interdomain contacts of the REI dimer (Epp et al., 1975), six phenylalanine residues (Phe-46, Phe-89 and Phe-100) should be involved in such contacts in the V_L dimer of protein 315.

As discussed in Chapter 1, the significance of conformational changes in immunoglobulins is uncertain. This applies particularly to L-chain dimers, for which no physiological role is apparent, although they may reflect the conformational properties of the intact immunoglobulin. It has been pointed out by Gavish et al. (1978) that the dimerization constants of L-chains are about 10^5 M^{-1}, whereas those for the intact H-L pair are at least 10^9 M^{-1}. Conformational changes in L-chain dimers, either as a result of ligand binding or because of changing ionic conditions could then simply reflect the weak interactions between chains. However, no evidence for a large relative movement of the chains was detected in the present study.

The L-chain dimer of protein 315

The binding properties of the V_L dimer and L-chain dimer of protein 315 are reported to be very similar. In particular, both have very similar affinities for several DNP ligands (Gavish et al., 1977), and show the unusual pH-dependent binding properties (Gavish et al., 1978). Although the binding of two molecules of DNP-lysine to the L-chain dimer at pH 7.4 was

observed to exhibit positive cooperativity, whereas binding to the V_L dimer was not, the cooperativity is very weak and would often go undetected (Lancet et al., 1977). It would appear, therefore, that the presence of C-domains does not affect the binding properties of the V-domains.

The effect of the C-domains on the structure of the combining site may be determined by observing the changes of the ^1H n.m.r. spectrum of the L-chain dimer following ligand binding at pH* 4.3, and comparing the results with those obtained from the V_L dimer under similar conditions. The 270 MHz ^1H n.m.r. spectra of the L-chain dimer at pH* 4.3 in the absence of ligand and saturated with DNP-aspartate are shown in Figure 5.16. The low intensity of the difference spectrum can be accounted for entirely on the basis that perturbations are confined to V-region residues in the immediate vicinity of the bound ligand. It is unfortunate that this experiment cannot be carried out at pH 7.4, at which positive cooperativity in the binding to the L-chain dimer was observed (Lancet et al., 1977).

The similarity between the combining sites of the L-chain dimer and the V_L dimer of protein C15 may be seen more clearly by comparing the difference spectra of the aromatic regions of the protein spectra resulting from the binding of DNP-aspartate (Figure 5.17). Although both the signal-to-noise ratio and resolution of the L-chain spectra are poor, the conservation of the characteristic features of the difference spectrum may clearly be seen. A similar result was obtained with DNP-glycine. The technique of ^1H n.m.r. is therefore unable to detect any influence of the C-domains on the structure of the combining site, or of ligand binding on the structure of the C-domains. N.m.r. techniques have also been unable to detect any influence

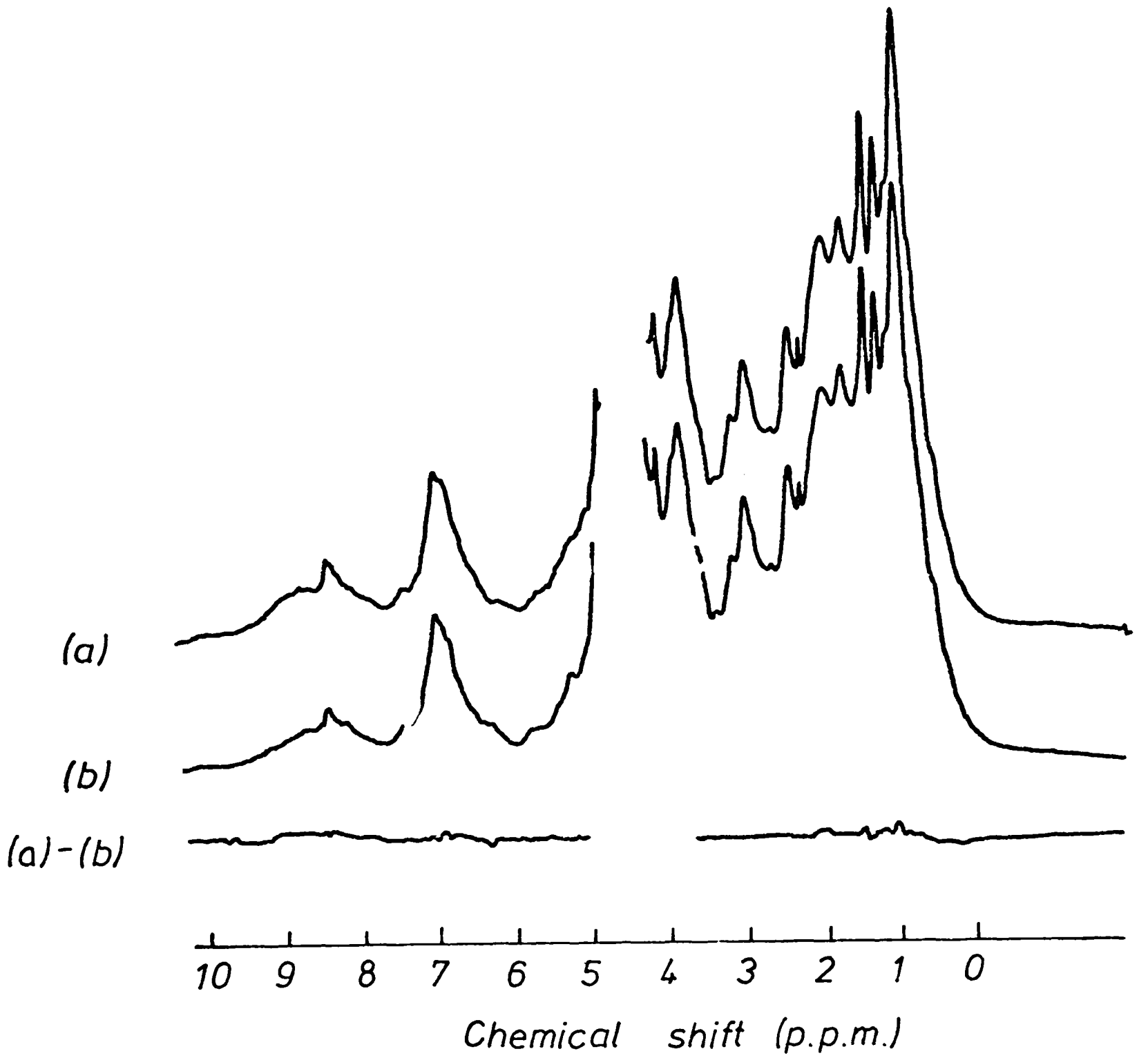

Figure 5.16 The effect of the binding of DNP-aspartate on the 270 MHz ^{1}H n.m.r. spectrum of the L-chain dimer

2000 scans were recorded at T = 298K, with solutions in $^{2}H_{2}O$, 0.025M ^{2}H-acetate, pH* 4.3. (a) L-chain dimer (0.36 mM). (b) L-chain dimer (0.33 mM) with approximately equimolar DNP-aspartate.

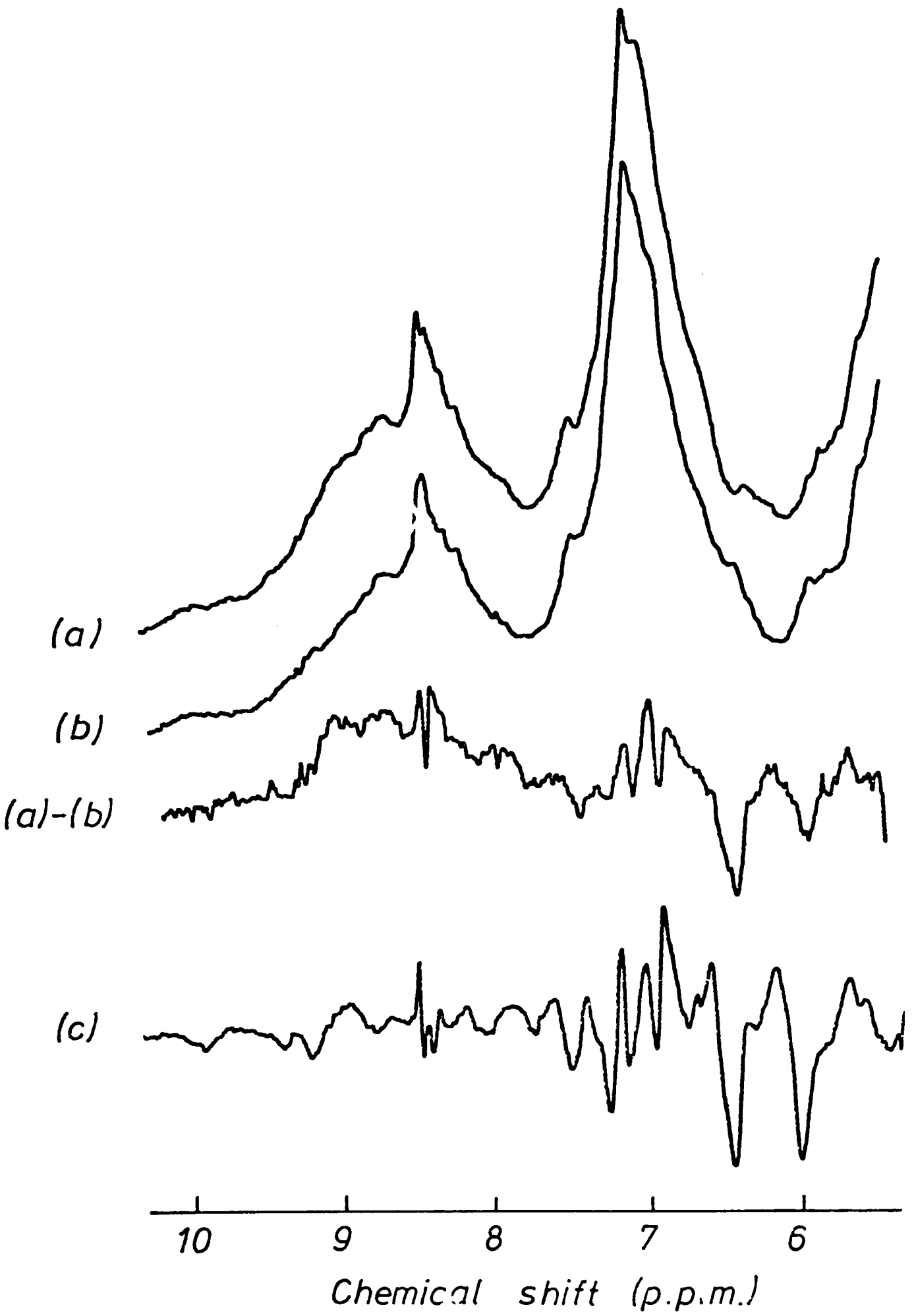

Figure 5.17 Comparison of the effects of the binding of DNP-aspartate on the aromatic regions of the 270 MHz ^{1}H n.m.r. spectra of the L-chain dimer and V_L dimer

2000 scans were recorded at T = 298K, with solutions in $^{2}H_2O$, 0.025M ^{2}H-acetate. (a) L-chain dimer (0.36 mM), pH* 4.3. (b) L-chain dimer (0.33 mM) with approximately equimolar DNP-aspartate. (c) Difference obtained from the binding of DNP-aspartate to the V_L dimer (as for Figure 5.4b).

of C-domains on the structure of the combining site of the Fv fragment (Kooistra and Richards, 1977; Morris et al., 1978).

Although there is no evidence from the n.m.r. spectra that C-region residues are perturbed on ligand binding, such perturbations, particularly if they were small in extent and did not involve aromatic residues, might be undetected. There is crystallographic and CD evidence that the binding of two bis-DNP-lysine molecules to the L-chain dimer of protein Mcg causes several changes at the interfaces of the V-domains and of the C-domains, which involve alterations of up to 2-3 Å (Ely et al., 1978). It is possible that the binding of two bulky bis-DNP ligands between two L-chains will cause more structural rearrangement than a single DNP group, and it would be instructive to examine the effect of ligand binding on the ^{1}H n.m.r. spectrum of protein Mcg.

CHAPTER 6

SPECIFIC NITRATION OF TYROSINE RESIDUES IN THE HYPERVARIABLE REGIONS OF PROTEIN 315

INTRODUCTION

According to the model of the combining site of protein 315 (Figure 1.5) two tyrosine residues, Tyr-34_L and Tyr-33_H, are positioned in the site and may form contacts with bound ligands. It has been proposed that Tyr-34_L is in contact with the DNP ring, and that a hydrogen bond is formed between the phenolic group and the 2-nitro group of the ligand. It has also been proposed that Tyr-33_H interacts with the side-chain of the ligand (Dower et al., 1977). The involvement of these two residues is investigated here by specific nitration. Nitration of the Fv fragment with tetranitromethane (TNM) results in an 80% modification of Tyr-33_H, with the remaining 20% on Tyr-34_L (R. Zakut and D. Givol, personal communication). It was subsequently found that Tyr-34_L could be specifically modified by separating the Fv fragment into its constituent V_L and V_H domains, nitrating the V_L dimer and reassociating the modified V_L domain with the V_H domain (Gavish et al., 1979). Nitration is a convenient method of modification of tyrosine residues, for several reasons: the modifying group is small, minimizing the possibility of large structural changes; the pK_a of the nitrotyrosine is about 7, allowing observation of the effect of the ionization of the phenolic group; the ionization of the phenolic group itself may be monitored spectrophotometrically, enabling perturbations of the pK_a to be followed; and the nitrotyrosine may be reduced to aminotyrosine, to provide a point for the attachment of other

spectroscopic probes.

Information on Tyr-34_L is also pertinent to the general problem of antibody specificity. According to Kabat et al. (1976), tyrosine occurs at the homologous position (position 32 in Table 4.1) in 50% (77 out of 154) of all L-chains. This tyrosine has been affinity-labelled in other antibodies (Franek, 1971; Chesbro and Metzger, 1972) as well as in protein 315 (Goetzl and Metzger, 1970b; Haimovich et al., 1970). Although the Fab fragments whose structures are known from X-ray crystallography do not contain tyrosine at this position (Phe in protein 603 and His in protein New), both protein Mcg and protein REI do contain it. The tyrosine is a contact residue for the DNP ring in protein Mcg (Firca et al., 1978). It is close to, but not in contact with, nitrophenyl ligands bound to protein REI (O. Epp, personal communication; see Figure 5.12).

At present, no firm assignments of resonances in the 270 MHz ^1H n.m.r. spectrum of the Fv fragment, other than those from the histidines, have been made. The specific nitration of a tyrosine residue affords the possibility of assignment (Snyder et al., 1975; Schmit-Aderjan et al., 1979).

METHODS

Nitration of Tyr-34_L

Nitration was carried out with TNM according to the method of Sokolovsky et al. (1966). A solution of the V_L dimer (5×10^{-5}M) in 0.1M Tris-HCl, pH 8.2, was reacted with TNM (5×10^{-4}M) for 1 hr at room temperature (Gavish et al., 1979). TNM was washed with water prior to use, and was added in ethanol solution. The final concentration of ethanol was 1% (v/v). The binding of ligands to the Fv fragment is not affected by ethanol

concentrations of less than 5% (Dwek et al., 1976). The reaction was terminated by passing the material through a Sephadex G-25 column in 0.1M NH_4HCO_3. The nitrated V_L (NO_2V_L) was further purified on a DNP-lysine-Sepharose column. The bound material was eluted with DNP-glycine (12.5 mg/ml, pH 7). 50% of the NO_2V_L did not bind to the column. This was attributed by Gavish et al. (1979) to the presence of covalently cross-linked molecules, which were detected by gel electrophoresis. Reassociation of NO_2V_L with V_H to produce the $NO_2V_LV_H$ fragment was performed as described by Hochman et al. (1973).

The V_L domain contains two tyrosine residues, $Tyr\text{-}34_L$ and $Tyr\text{-}86_L$ (Dugan et al., 1973). Amino acid and peptide analysis showed that the NO_2V_L contained one nitrotyrosine residue per chain, at position 34 (Gavish et al., 1979).

Nitration of $Tyr\text{-}33_H$

Nitration was performed by reacting the Fv fragment (4×10^{-5}M) in 0.1M Tris-HCl, pH 8.2, with TNM (2.8×10^{-4}M) for 1 hr at room temperature. The reaction was terminated by passing the material through a DNP-lysine-Sepharose column. The bound material was eluted with 0.05M NH_3 or with DNP-glycine (12.5 mg/ml, pH 7). These conditions gave a modification of 1 mole of nitrotyrosine per mole of Fv fragment, assuming $\varepsilon^{M}_{428} = 4100$ for nitrotyrosine at pH 10 (Riordan et al., 1967). It has previously been shown that 80% of the modification is on $Tyr\text{-}33_H$ and 20% is on $Tyr\text{-}34_L$ (R. Zakut and D. Givol, personal communication).

RESULTS AND DISCUSSION

Nitration of Tyr-34$_L$ in the Fv fragment

1. Effect on the protein structure of reassociating the Fv fragment

Since the specific nitration of Tyr-34$_L$ requires the separation and subsequent reassociation of the V_L and V_H domains, it is necessary to determine whether or not the reassociation affects the structure of the combining site. It has previously been shown that the affinity of the reconstituted Fv fragment (V_LV_H fragment) for DNP-lysine is the same as that of the native Fv fragment (Hochman et al., 1973), which implies that little, if any, structural alteration has occurred. The structure of the combining site of the V_LV_H fragment, and the mode of binding of the ligand, may be investigated by a 270 MHz ^1H n.m.r. experiment similar to those reported for the Fv fragment (Dower et al., 1977). This experiment also provides the control for the ^1H n.m.r. analysis of the binding of ligand to the $NO_2V_LV_H$ fragment. The titration was carried out with DNP-glycine, since the resonances of both the ring and side-chain ^1H nuclei are easily observable. The titration curves of the protein and ligand resonances are shown in Figure 6.1. The observed chemical shift changes of the protein resonances are given in Table 6.1. It may be seen from Table 6.1 that the chemical shifts of the affected protein resonances are the same in the V_LV_H fragment and Fv fragment, after allowing for the pH difference between the samples. The structure of the combining site is therefore the same in both cases. Confirmation of this conclusion is obtained from the behaviour of the ligand resonances (Table 6.2). The values were calculated assuming a value of 0.8 for the number of

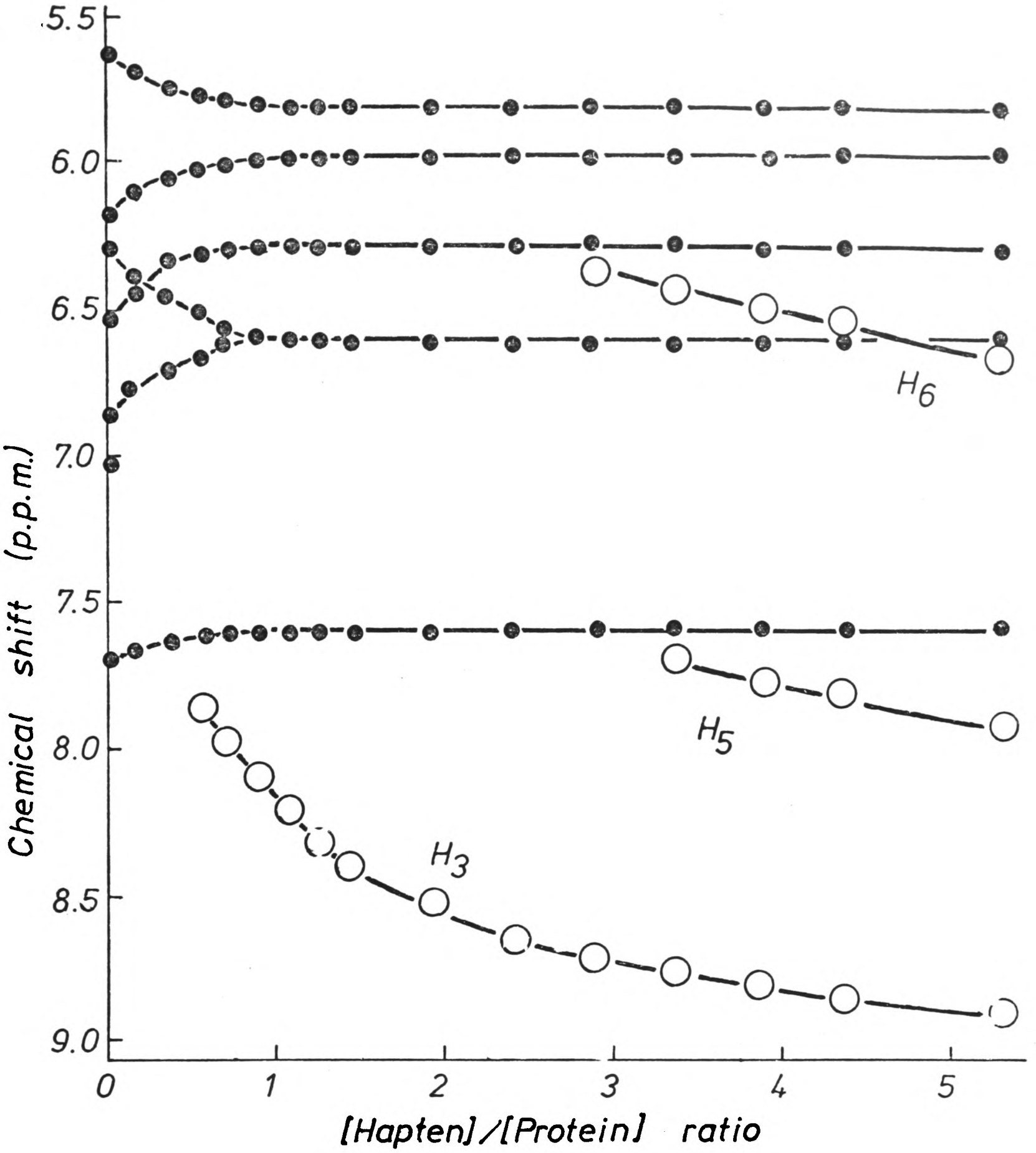

Figure 6.1 Chemical shift changes of the resonances of aromatic ^1H nuclei following the binding of DNP-glycine to the $V_L V_H$ fragment

Measurements were made at 270 MHz, T = 303K, with solutions in ^2H_2O, 0.15M NaCl pH* 8.0. The initial protein concentration was 0.79 mM. The chemical shifts of the resonances of the free ligand are: H_3, 9.12 p.p.m.; H_5, 8.29 p.p.m.; H_6, 6.92 p.p.m. The solid curves for the ligand resonances were calculated assuming K_D = 16 μM, n = 0.8 and the chemical shift changes given in Table 6.2.

Table 6.1 Chemical shifts (δ) and the changes in chemical shifts (Δδ) of protein resonances perturbed on the binding of ligands to the Fv fragment of protein 315, the V_LV_H fragment and the $NO_2V_LV_H$ fragment

Measurements were made at 270 MHz, T = 303K in ^2H_2O containing 0.15M NaCl. pH values are given in the Table. Shifts were measured from DSS, used as an external standard. + and - denote upfield and downfield shift changes respectively. Assignments to His-H_2 resonances and probable assignments to His-H_4 resonances are given in the Table. Blank positions in the Table do not imply a clear absence of perturbation.

$V_LV_H^+$ DNP-glycine pH* = 8.0 δ(p.p.m.)	Δδ(p.p.m.)	$NO_2V_LV_H^+$ DNP-glycine pH* = 8.0 δ(p.p.m.)	Δδ(p.p.m.)		Fv+ DNP-aspartate (a) pH* = 6.9 δ(p.p.m.)	Δδ(p.p.m.)	Fv+ TNP-aspartate (b) pH* = 7.05 δ(p.p.m.)	Δδ(p.p.m.)
							5.65	-0.13
5.64	-0.17	5.64	-0.17					
6.18	+0.19	5.90	+0.20		6.16	+0.25	6.20	+0.07
					6.33	+0.17	6.31	+0.05
6.29	-0.38	6.27	-0.36		6.37	-0.29	6.35	-0.22
6.52	-0.10	6.49	-0.10		6.62	-0.08		
6.79	small			$His\text{-}102_H$	6.95	+0.07	7.01	< +0.05
6.77	small	6.75	small	$His\text{-}97_L$				
6.88	+0.20	6.82	+0.19		6.90	+0.19	6.88	+0.20
7.03	broadens or < +0.15	7.02	broadens or < +0.15		7.00	broadens	7.04	broadens
7.20	broadens	7.20	broadens		7.20	decreases	7.23	decreases
7.42	increases	7.39	increases		7.42	increases	7.43	increases
7.54	decreases	7.54	decreases					
7.71	+0.05	7.66	± ?	$His\text{-}97_L$	7.82	+0.06	7.87	+0.06
7.75	+ ?	7.69	-0.05	$His\text{-}102_H$			8.07	-0.07

(a) Data from Dower et al. (1977); (b) Data from Dower et al. (1978)

Table 6.2 Upfield chemical shift changes of the ^1H resonances of DNP-glycine on binding to the Fv fragment of protein 315, the V_LV_H fragment and the $NO_2V_LV_H$ fragment

Measurements were made at 270 MHz, T = 303K in ^2H_2O containing 0.15M NaCl. pH* values were 6.8 (Fv fragment) and 8.0 (V_LV_H fragment and $NO_2V_LV_H$ fragment).

DNP-glycine resonance	Chemical shift change (p.p.m.)		
	Fv fragment(a)	V_LV_H fragment	$NO_2V_LV_H$ fragment
H_3	1.21	1.3	1.3
H_5	2.20	2.2	2.1
H_6	1.77	1.75	1.5
αCH_2	1.00	1.0	0.8

(a) Data from Dower et al. (1977).

sites, which was measured in the equilibrium dialysis experiments described in Section 3 below. A value of the dissociation constant of 16 μM was used. This value was obtained by a fluorescence titration, and is close to the value of 12 μM obtained under similar conditions for the Fv fragment (Dower et al., 1978). The curves calculated with these two parameters, and the chemical shift changes given in Table 6.2, are superimposed on the data given in Figure 6.1. Since there is no significant difference between the chemical shift changes of the ligand resonances on binding to the Fv fragment or to the $V_L V_H$ fragment, the modes of binding to each fragment are the same.

2. Effect of nitration on the ^1H n.m.r. spectrum of the $V_L V_H$ fragment

The extent of the structural perturbation caused by nitration can be measured by comparing the ^1H n.m.r. spectra of the native and nitrated proteins. The 270 MHz ^1H n.m.r. spectra of the $V_L V_H$ fragment and of the $NO_2 V_L V_H$ fragment at pH* 8 are shown in Figure 6.2, with the resulting difference spectrum. The difference spectrum only contains ~1-2% of the original spectral intensity. This small difference shows that the modification of Tyr-34_L has caused no perturbation of the protein structure beyond the immediate environment of the nitro group. The pH titration behaviour of the histidine resonances provides further evidence that any perturbations are limited. Two of the histidines, His-102_H and His-97_L, are constituents of hypervariable loops which are in contact with the loop containing Tyr-34_L. The pH titration curves, shown in Figure 6.3, are superimposable on those of the Fv fragment.

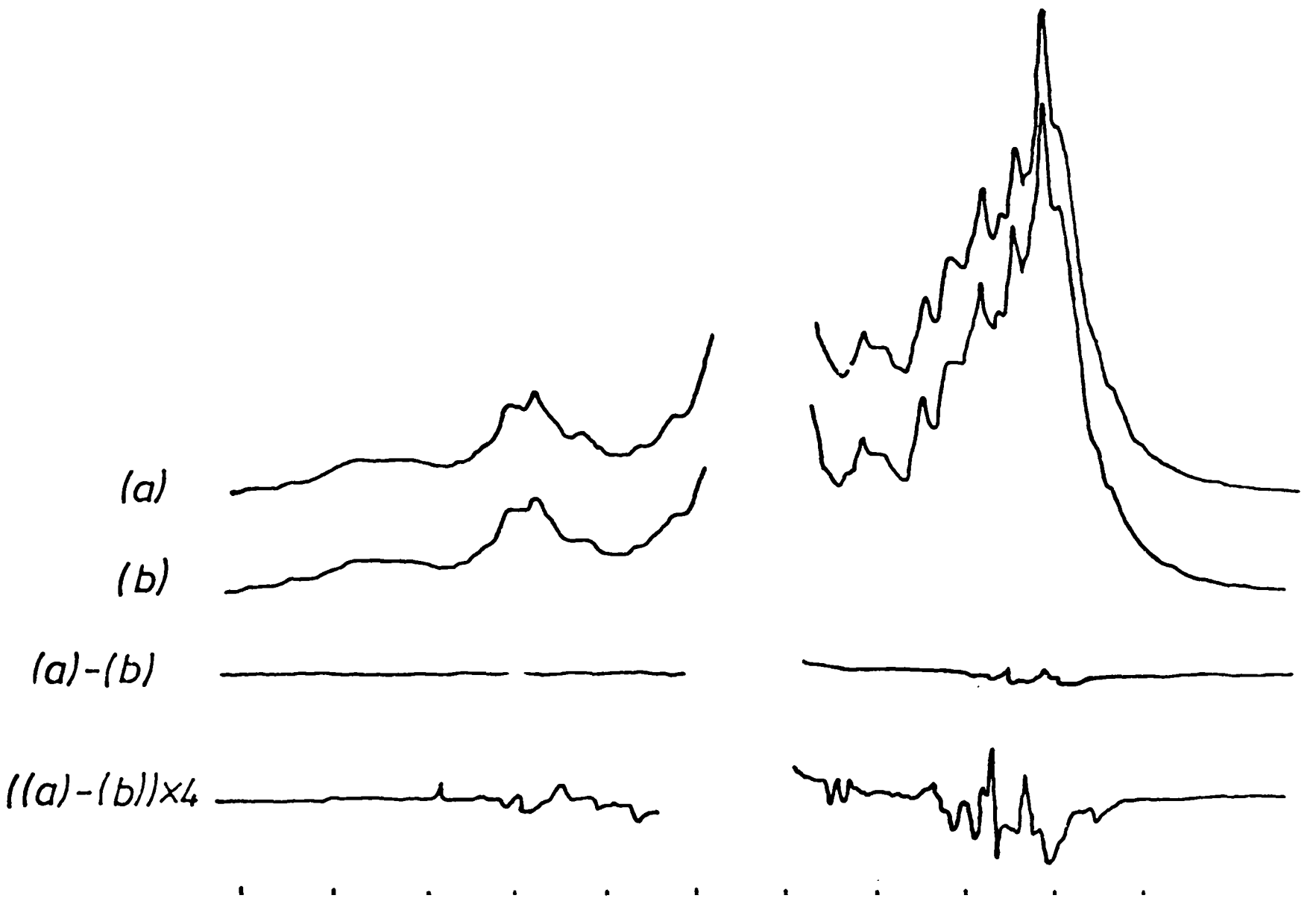

Figure 6.2 270 MHz ^{1}H n.m.r. spectra of the $V_L V_H$ fragment and the $NO_2 V_L V_H$ fragment

2000 scans were recorded at T = 303K with solutions in $^{2}H_2O$, 0.15M NaCl. (a) $V_L V_H$ fragment, 0.84 mM, pH* 8.05. (b) $NO_2 V_L V_H$ fragment, 0.84 mM, pH* 8.07.

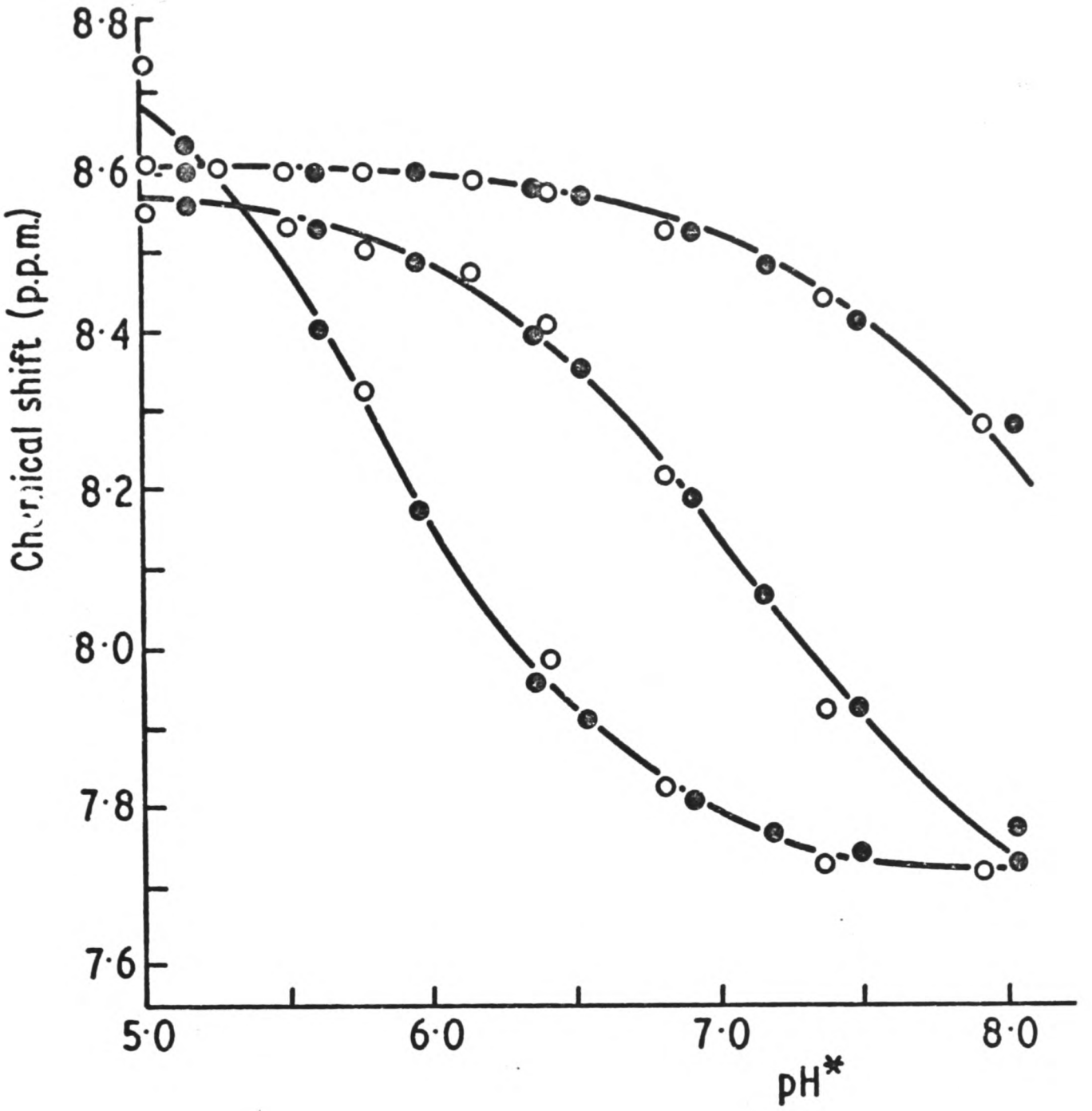

Figure 6.3 pH titration of the histidine H_2 resonances of the Fv fragment and $NO_2V_LV_H$ fragment

Measurements were made at 270 MHz, T = 303K, with solutions in ^2H_2O, 015M NaCl. o - Fv fragment, data of Wain-Hobson et al. (1977). • - $NO_2V_LV_H$ fragment. The solid curves were obtained by the non-linear least squares procedure given in Appendix 2.1. The pK_a values are 5.9, 6.9 and 8.2

Specific chemical modification is a potential method of assigning resonances in the ^1H n.m.r. spectra of proteins. Several tyrosine resonances in the 250 MHz ^1H n.m.r. spectrum of bovine pancreatic trypsin inhibitor were assigned by nitration (Snyder et al., 1975). Three approaches were used in an attempt to assign the resonances of Tyr-34_L: a comparison between the aromatic regions of the spectra of the V_LV_H and $NO_2V_LV_H$ fragments; a pH titration of the $NO_2V_LV_H$ fragment, since the NO_2Tyr-34_L has a pK_a of 6.6 (see Section 3 below); and a comparison between the effects of the binding of DNP-glycine on the spectra of the V_LV_H and $NO_2V_LV_H$ fragments. The aromatic region of the difference spectrum of the V_LV_H and $NO_2V_LV_H$ fragments at pH* 8 is shown in Figure 6.4. The major features are three positive peaks at 6.33 p.p.m., 6.8 p.p.m. and 7.25 p.p.m. (present in the V_LV_H fragment but not in the $NO_2V_LV_H$ fragment) and three negative peaks at 5.9 p.p.m., 6.7 p.p.m. and 6.95 p.p.m. (present in the $NO_2V_LV_H$ fragment but not in the V_LV_H fragment). The positive peak at 7.72 p.p.m. probably arises from His-102_H, as a result of a small pH difference between the two samples. If the three negative peaks correspond to the expected three resonances of the ionized nitrotyrosine, they should be observed to titrate with a pK_a of 6.6. However, no resonances other than those of the histidine H_2 and H_4 nuclei were observed to titrate over the pH range of 5.17 to 8.03. Instead, three resonances, at 6.54 p.p.m., 6.74 p.p.m. and 7.41 p.p.m., and possibly a fourth at 6.1 p.p.m., were observed to broaden as the pH was increased. Their behaviour may be seen in Figure 6.5. It is possible that three of these resonances arise from the unionized nitrotyrosine, and that the broadening results from a change of the mobility or of the position of the nitrotyrosine following ionization. No

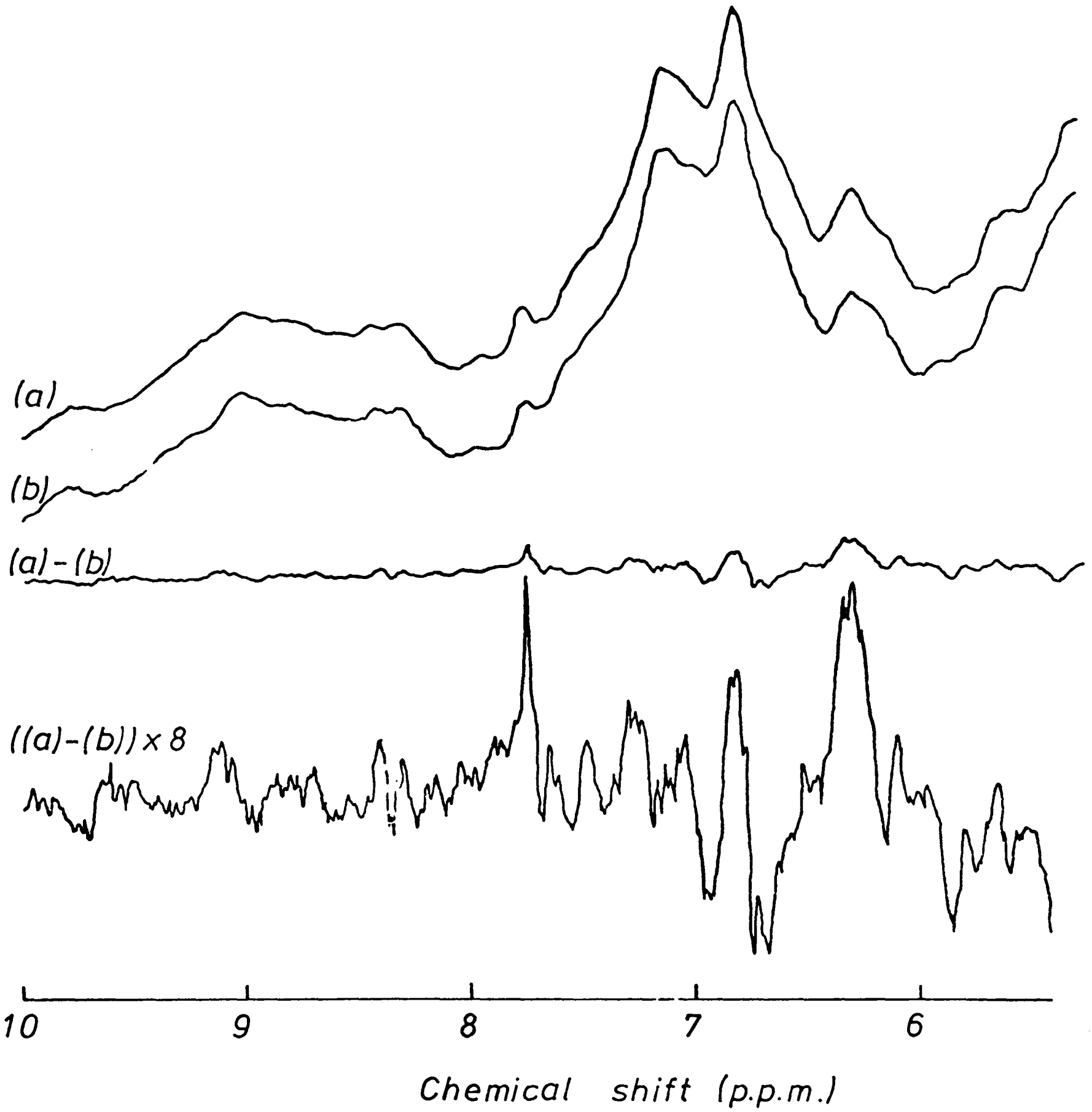

Figure 6.4 Aromatic regions of the 270 MHz ^{1}H n.m.r. spectra of the $V_L V_H$ fragment and $NO_2 V_L V_H$ fragment

2000 scans were recorded at T = 303K with solutions in $^{2}H_2O$, 0.15M NaCl. (a) $V_L V_H$ fragment, 0.84 mM, pH* 8.05. (b) $NO_2 V_L V_H$ fragment, 0.84 mM, pH* 8.07.

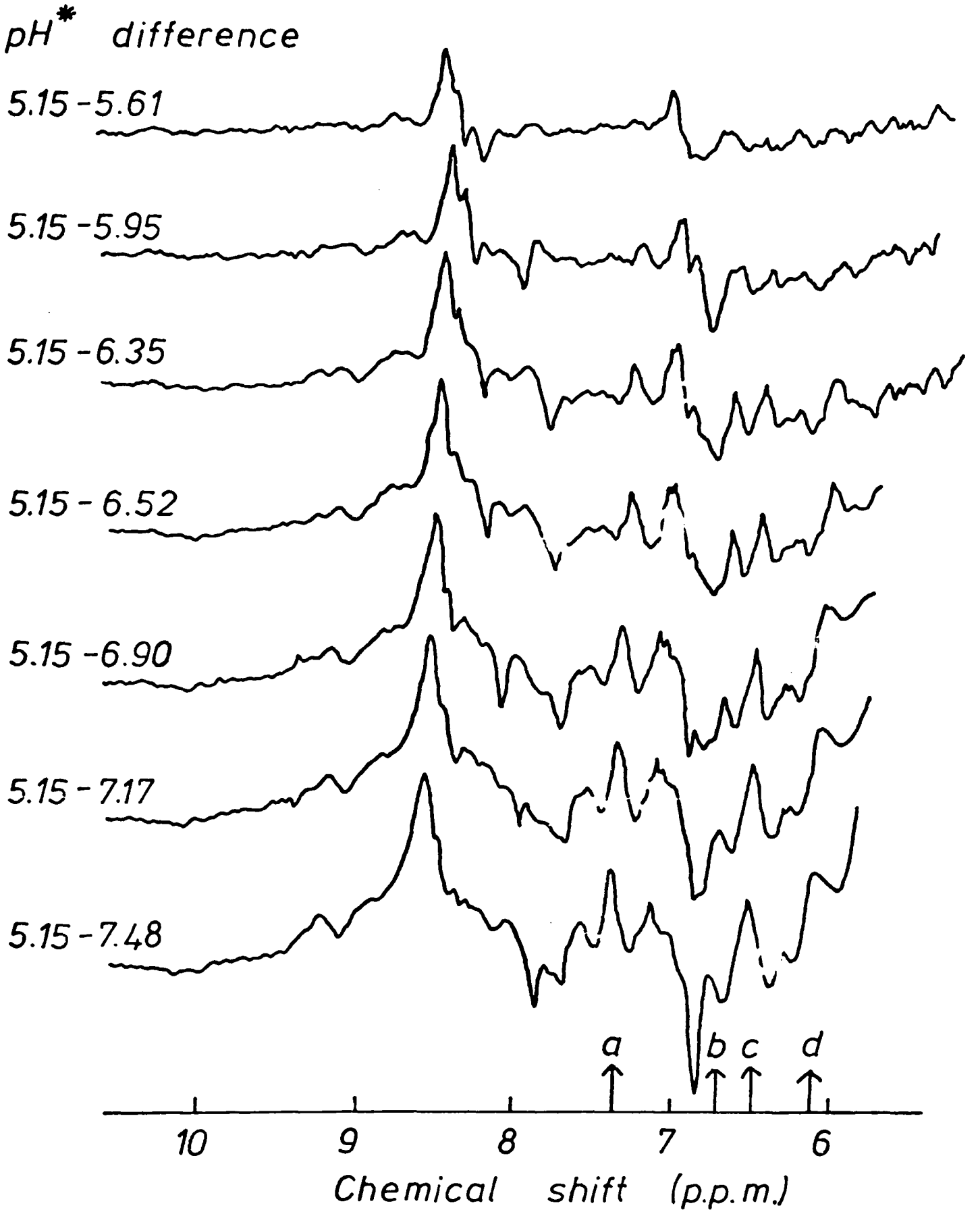

Figure 6.5 pH titration of the aromatic region of the 270 MHz ^1H n.m.r. spectrum of the $NO_2V_LV_H$ fragment

4000 scans were recorded at T = 303K with a solution in ^2H_2O, 0.15M NaCl. The protein concentration was 0.78 mM. The resonances marked a,b,c, and d can be observed to broaden on increasing the pH. Resonance b becomes obscured by the histidine H_4 resonances at the high pH values.

corresponding resonances attributable to the ionized nitrotyrosine could be observed. In particular, as the pH was increased there was no appearance of resonances at 5.9 p.p.m., 6.7 p.p.m. and 6.95 p.p.m., the positions of the negative peaks in Figure 6.4, although their presence might be obscured by the histidine H_4 resonances and the solvent resonance. No assignment is possible from these two sets of data, although it may be concluded that the nitrotyrosine is undergoing restricted motion. Further information can be obtained by comparing the perturbations of the resonances of the modified and unmodified proteins following the binding of DNP-glycine. The titration behaviour of the resonances of the $NO_2V_LV_H$ fragment is given in Table 6.1, for comparison with the effects on the V_LV_H fragment. The aromatic regions of the corresponding 270 MHz ^1H n.m.r. difference spectra, obtained with a saturating concentration of DNP-glycine at pH* 8, are shown in Figure 6.6. It is clear both from Table 6.1 and Figure 6.6 that the only difference between the two proteins in this experiment is the shift of a resonance from 6.18 p.p.m. in the spectrum of the V_LV_H fragment to 5.90 p.p.m. in the spectrum of the $NO_2V_LV_H$ fragment. This resonance is always perturbed by the binding of ligands to the Fv fragment. It has been tentatively suggested from a urea denaturation experiment that a resonance at 6.19 p.p.m. and one at 7.30 p.p.m. arise from a tyrosine residue in the combining site of the Fv fragment (P. Gettins, personal communication). It is therefore possible that the resonance at 5.90 p.p.m. is associated with the H_5 nucleus of the ionized $NO_2Tyr\text{-}34_L$, and that the resonance at 6.18 p.p.m. arises from the unionized $Tyr\text{-}34_L$. This conclusion must remain uncertain in the light of the difficulties of interpreting the pH titration data.

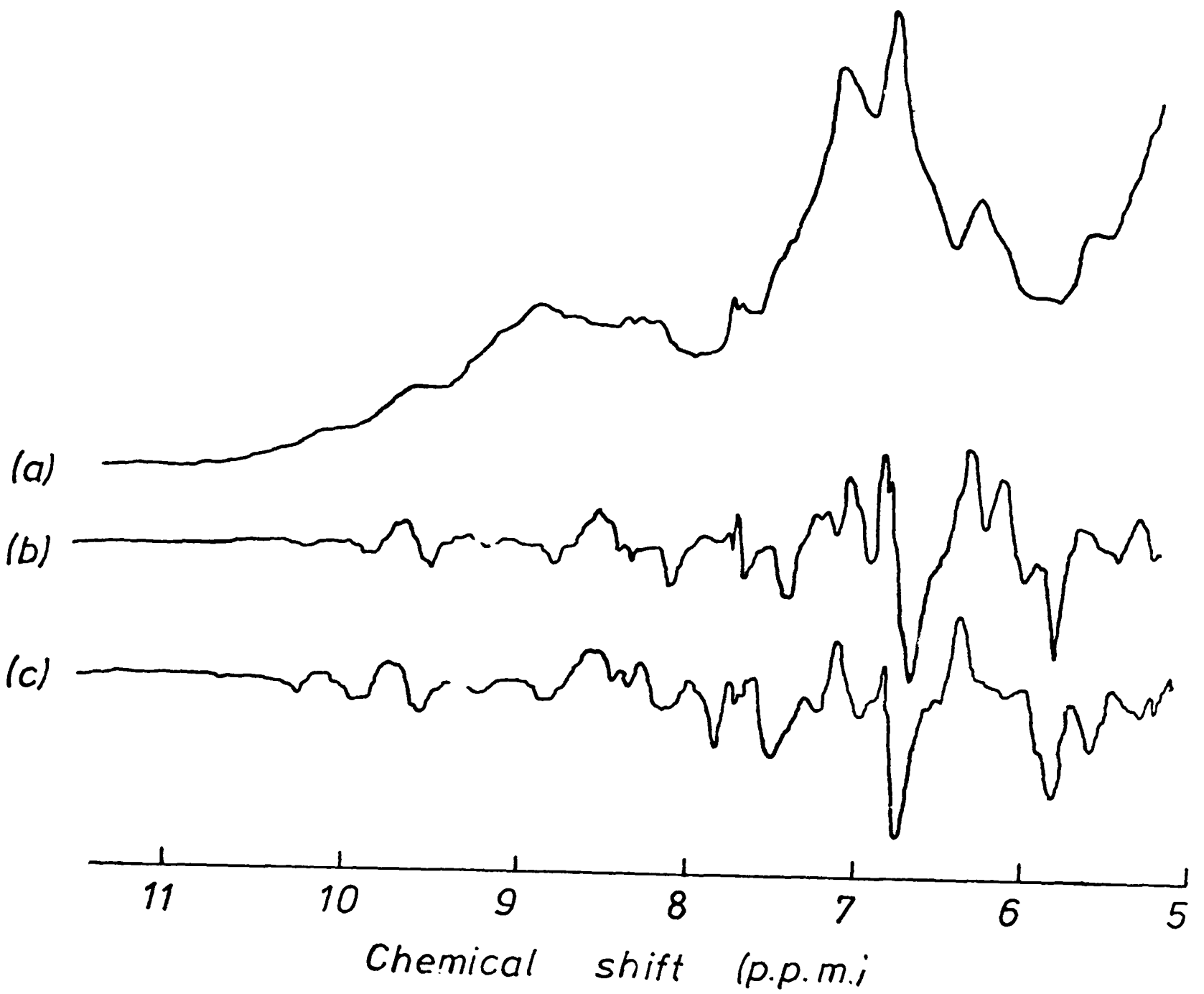

Figure 6.6 Comparison of the effects of the binding of DNP-glycine on the aromatic regions of the 270 MHz ^{1}H n.m.r. spectra of the $V_L V_H$ and $NO_2 V_L V_H$ fragments

2000 scans were recorded at T = 303K, with solutions in $^{2}H_2O$, 0.15M NaCl. (a) $V_L V_H$ fragment, 0.79 mM, pH* 8.05. (b) $V_L V_H$ fragment, difference obtained with approximately equimolar DNP-glycine. (c) $NO_2 V_L V_H$ fragment, pH* 8.07, difference obtained with approximately equimolar DNP-glycine.

3. Effect of nitration on the binding properties of the $V_L V_H$ fragment

The binding properties of the $NO_2V_LV_H$ fragment, both above and below the pK_a of the nitrotyrosine, were investigated by equilibrium dialysis. Scatchard plots of the data obtained for the binding of ^{3}H-DNP-lysine to the V_LV_H fragment and to the $NO_2V_LV_H$ fragment at pH 5 and pH 8 are shown in Figure 6.7. The binding parameters are given in Table 6.3. No difference between the two proteins was detected. There is therefore no steric effect of the introduction of the nitro group. It is also unlikely that a hydrogen bond is formed directly between the nitrotyrosine phenolic group and the ligand, since a decrease of the affinity for the ligand would be expected to follow the ionization of the group. However, it is possible that neither the ionized nor unionized nitrotyrosine forms a hydrogen bond to the ligand if the phenolic group forms an intramolecular hydrogen bond.

Table 6.3 Parameters characterizing the binding of ^{3}H-DNP-lysine to the V_LV_H fragment and the $NO_2V_LV_H$ fragment at pH 5 and pH 8

Measurements were made at 277K, in 0.05M sodium acetate, 0.15M NaCl (pH 5.0) or 0.05M Tris, 0.15M NaCl (pH 8.0). Protein concentration was 6.6×10^{-6}M.

	pH	Number of sites	Association constant ($M^{-1} \times 10^{-6}$)
V_LV_H	5.0	0.79	1.2
$NO_2V_LV_H$	5.0	0.78	0.83
V_LV_H	8.0	0.80	1.8
$NO_2V_LV_H$	8.0	0.85	1.9

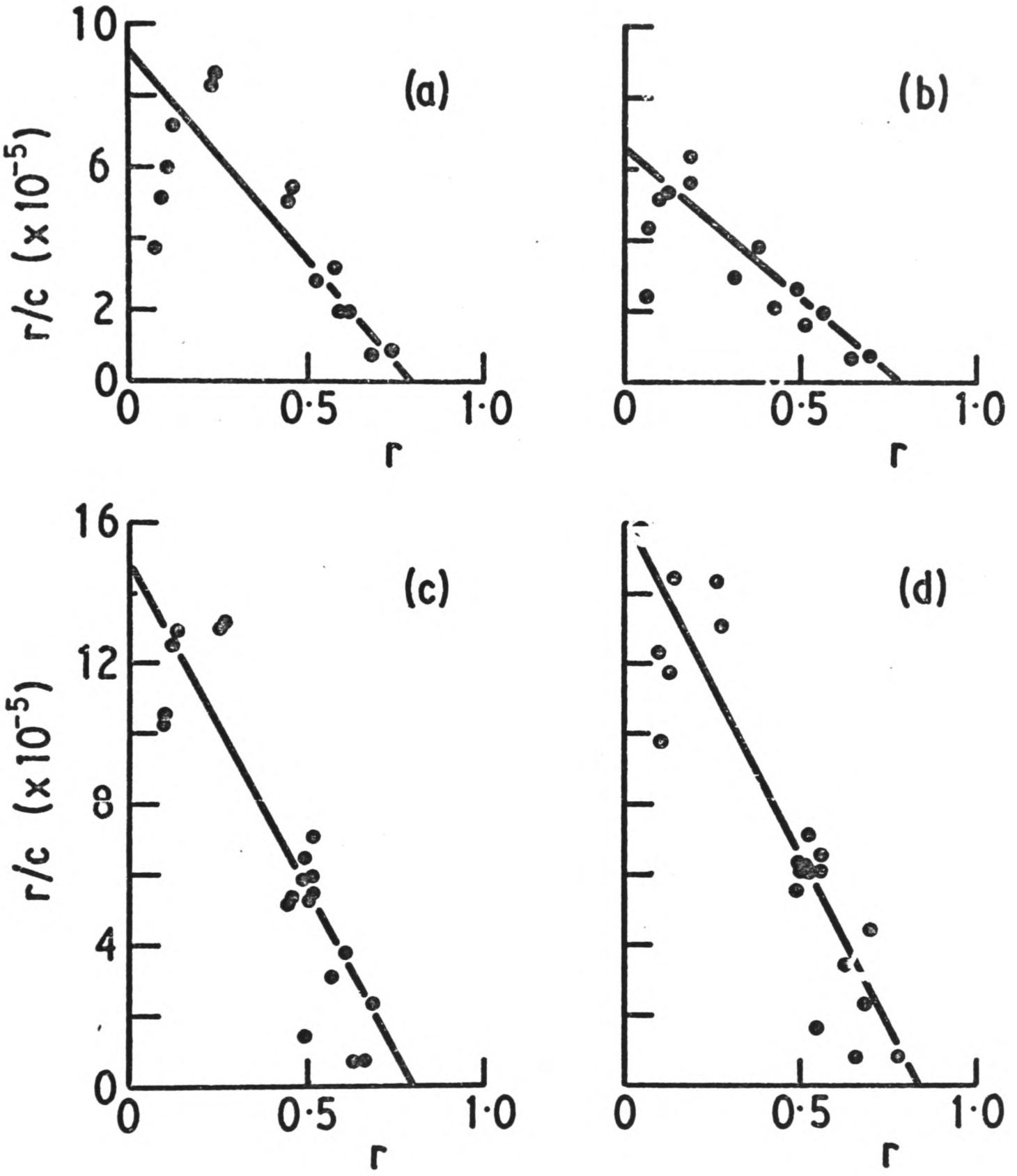

Figure 6.7 Scatchard plots for the binding of ^{3}H-DNP-lysine to the $V_L V_H$ and $NO_2 V_L V_H$ fragments at pH 5.0 and pH 8.0

Measurements were made by equilibrium dialysis at T = 277K with solutions in 0.05M sodium acetate, 0.1M NaCl, pH 8.0. The protein concentration was 5 μM. Initial hapten concentrations ranged between 0.75 μM and 25 μM. (a) $V_L V_H$ fragment, pH 5.0. (b) $NO_2 V_L V_H$ fragment, pH 5.0. (c) $V_L V_H$ fragment pH 8.0. (d) $NO_2 V_L V_H$ fragment, pH 8.0.

The possibility of direct hydrogen bonding to the phenolic group of the nitrotyrosine may be tested by measuring the pK_a of the nitrotyrosine in the absence and presence of ligand. If other effects are negligible, the pK_a should rise in the presence of ligand, by an amount corresponding to the strength of the hydrogen bond. The absorbance changes of the nitrotyrosine at 428 nm in the absence and presence of DNP-lysine are shown in Figure 6.8. The pK_a values are given in Table 6.4. The intrinsic pK_a of 6.6 is reduced slightly to 6.3, and not raised, in the presence of DNP-lysine, suggesting the absence of a hydrogen bond. Although the unionized nitrotyrosine may not form a hydrogen bond to the ligand, the lack of any difference between the affinities of the modified and unmodified proteins at either pH 5 or pH 8 suggests that no hydrogen bond is formed to Tyr-34_L in the V_LV_H fragment.

Table 6.4 The pK_a values of NO_2Tyr-34_L in the absence and presence of DNP-lysine

Measurements were made in 0.01M potassium phosphate, 0.15M NaCl, T = 293K. Protein concentrations were 60×10^{-6}M.

	pK_a		
	Expt. 1	Expt. 2	Average
$NO_2V_LV_H$	6.51	6.70	6.6
$NO_2V_LV_H$ + DNP-lysine	6.20	6.37	6.3

The importance of hydrogen bonding for the binding of ligands to protein 315 remains uncertain since, as discussed in Chapter 5, different haptens may bind in positions differing by ~0.5 Å. It is to be hoped that resonance Raman and ^{15}N n.m.r. studies of the nitro groups, initiated by P. Gettins, will help to answer this question.

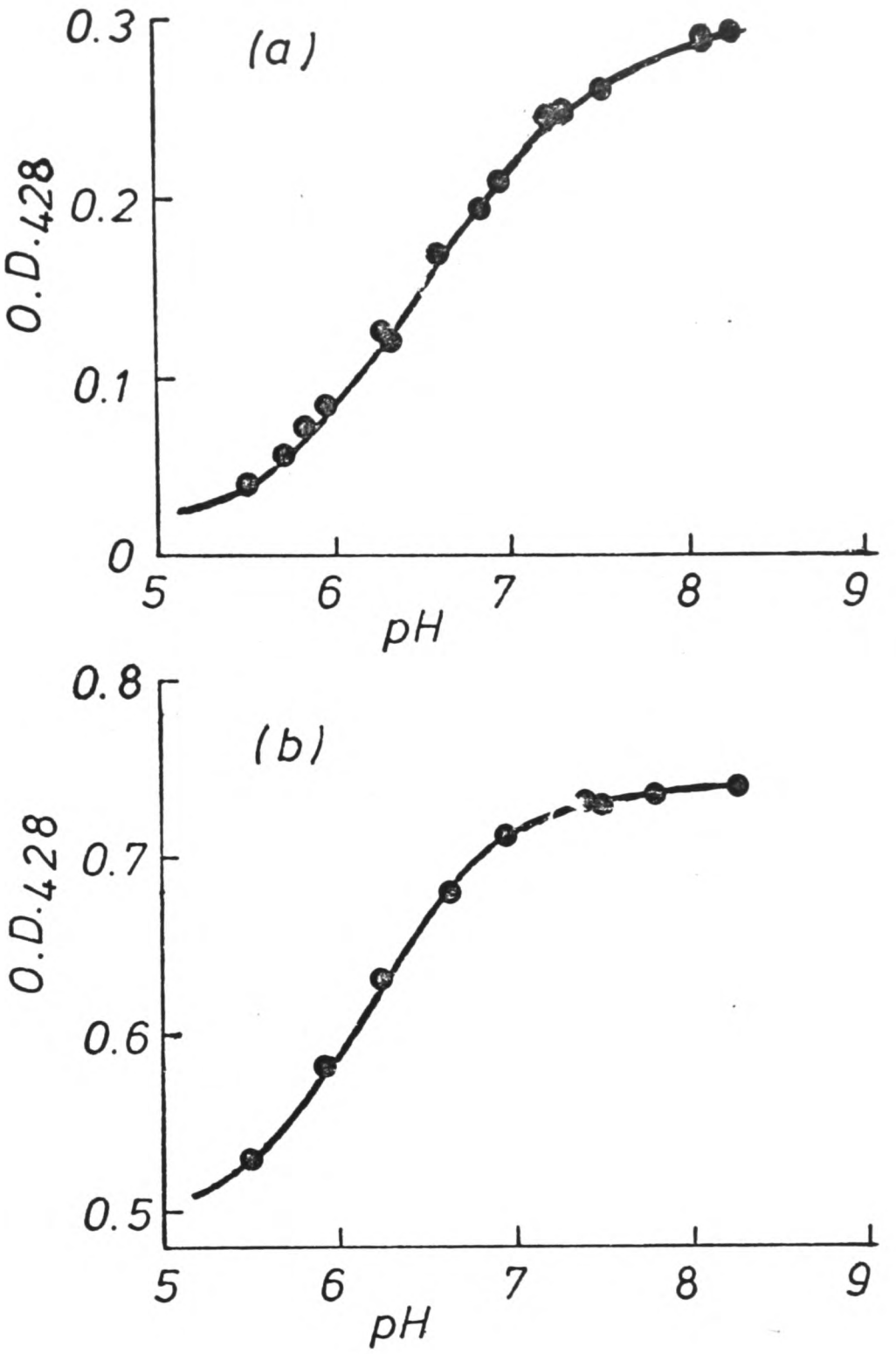

Figure 6.8 pH titration of $NO_2Tyr\text{-}34_L$ in the $NO_2V_LV_H$ fragment

Measurements were made at T = 293K with solutions in 0.005M potassium phosphate, 0.15M NaCl. The solid curves were obtained by the non-linear least squares procedure given in Appendix 2.1. (a) $NO_2V_LV_H$ fragment, 68 μM. (b) $NO_2V_LV_H$ fragment, 61 μM, with DNP-lysine, 63 μM.

The binding of three other ligands to the V_LV_H and $NO_2V_LV_H$ fragments was measured by competition with ^{3}H-DNP-lysine. The ligands TNP-aminocaproate, dinitrophenol and TNP-aminoethylamine were chosen to investigate the possibility of an interaction of the nitrotyrosine with the extra nitro group of TNP derivatives (TNP-aminocaproate) and with charged groups near the ring (dinitrophenol) or more distant from it (TNP-aminoethylamine). The association constants are given in Table 6.5. No effect of nitration was observed.

Table 6.5 Association constants for some nitrophenyl ligands with the V_LV_H fragment and $NO_2V_LV_H$ fragment

Measurements were made at 277K in 0.05M Tris, 0.15M NaCl, pH 8.0. The protein concentration was 6.6×10^{-6}M.

Ligand	Association constant (M^{-1})	
	V_LV_H fragment	$NO_2V_LV_H$ fragment
DNP-OH	1.6×10^3	0.71×10^3
TNP-$NH(CH_2)_5COO^-$	12.3×10^6	8.3×10^6
TNP-$NH(CH_2)_2NH_3^+$	6.6×10^6	4.6×10^6

The lack of any detectable effect of nitration on the affinity of protein 315 does not necessarily imply that the mode of binding of ligands is unaffected. Since the chemical shift changes of the DNP-glycine resonances provide sensitive monitors of the mode of binding of the ligand, this possibility may be tested. The titration of the chemical shift of the H_3 resonance following binding to the V_LV_H or $NO_2V_LV_H$ fragment, and the theoretical fits to the data, are shown in Figure 6.9. The theoretical fits were calculated assuming a value of 0.8 for the

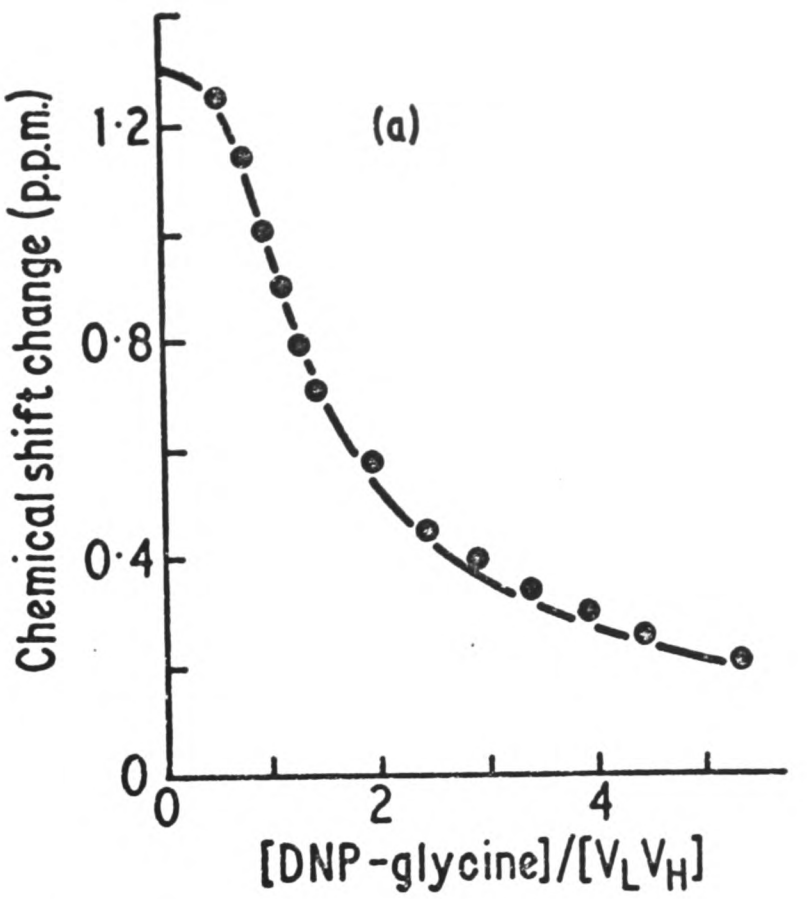

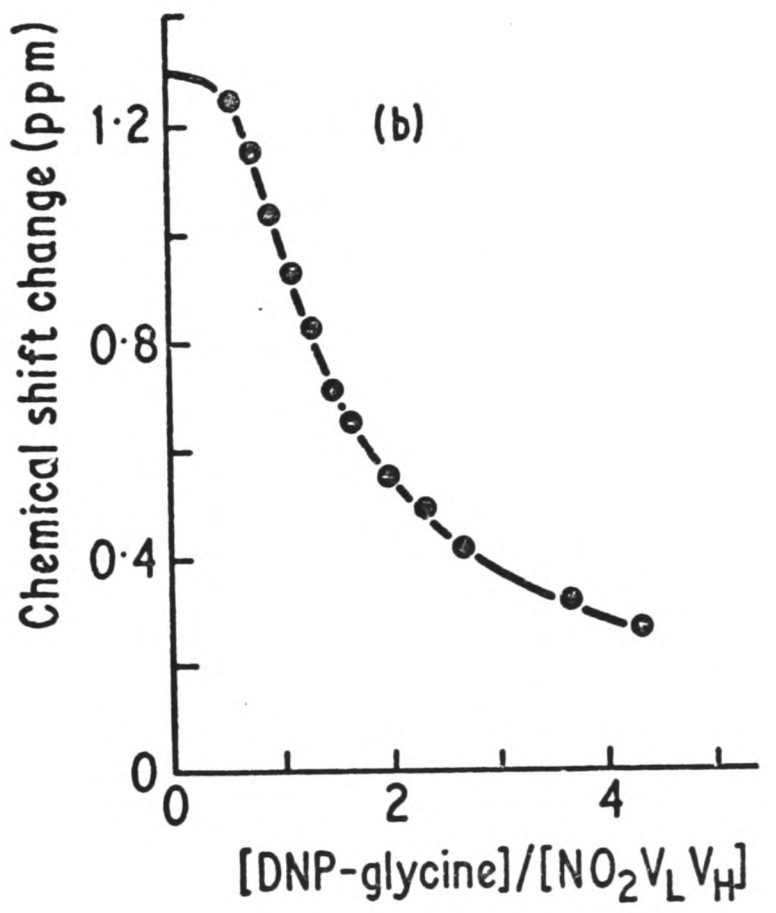

Figure 6.9 Chemical shift changes of the H_3 resonance of DNP-glycine following binding to the $V_L V_H$ and $NO_2 V_L V_H$ fragments

Measurements were made at 270 MHz, T = 303K, with solutions in ^2H_2O, 0.15M NaCl, pH* 8.0. (a) $V_L V_H$ fragment; the solid curve was calculated assuming K_D = 16 μM, n = 0.8 and a chemical shift change of 1.3 p.p.m. (b) $NO_2 V_L V_H$ fragment; the solid curve was calculated assuming K_D = 16 μM, n = 0.85 and a chemical shift change of 1.3 p.p.m.

number of sites (Figure 6.7) and 16 μM for the dissociation constants. The extrapolated chemical shift changes are given in Table 6.2. It is apparent that there is little difference between the binding of DNP-glycine to the Fv fragment, $V_L V_H$ fragment or $NO_2 V_L V_H$ fragment.

The lack of any effect of nitration of Tyr-34_L on the binding properties of the Fv fragment may be compared with the effects of other modifications of the same residue which are described in the literature. Modifications with m-nitrobenzene-diazonium-fluoroborate (Goetzl and Metzger, 1970a and b) or bromoacetyl-N-DNP-ethylenediamine (Haimovich et al., 1970) result in a 50-fold reduction in affinity or negligible affinity respectively. Both modifying groups are bulky, and would be expected to provide steric hindrance towards ligand molecules. However, both modifications show that Tyr-34_L is in, or close to, the combining site. Modification of Tyr-34_L by smaller groups reveals unexpected differences in their effects. Iodination results in a 20-fold reduction in affinity (Klostergaard et al., 1978), whereas both the aminotyrosine derivative (Hadler and Metzger, 1971) and the nitrotyrosine derivative described in this chapter are fully active. The results emphasize the difficulty of identifying contact residues by chemical modification, even when small groups are introduced.

The involvement of Tyr-34_L in the combining site of the Fv fragment is still strongly implicated by the model-building and n.m.r. studies, although there is at present no simple interpretation of the effects of the different chemical modifications.

Nitration of Tyr-34$_L$ in the V_L dimer

1. Effect of nitration on the ^1H n.m.r. spectrum of the V_L dimer

The 270 MHz ^1H n.m.r. spectra of the V_L dimer and the NO_2V_L dimer at pH* 4.8, and the resulting difference spectrum, are shown in Figure 6.10. The perturbations again represent only ~1-2% of the total intensity, and are therefore limited to the vicinities of the nitro groups. The aromatic region of the difference spectrum is seen more clearly in Figure 6.11. The difference is larger than that between the V_LV_H fragment and $NO_2V_LV_H$ fragment (Figure 6.4). However, the comparison is complicated by the fact that only one tyrosine residue of the V_LV_H fragment is modified, whereas two tyrosines, which may not be symmetrically related, are modified in the V_L dimer. It is also impracticable to examine the pH titration behaviour of the NO_2V_L dimer because of its low solubility at a pH greater than 5. The most striking difference between the spectra of the V_L dimer and NO_2V_L dimer occurs in the high-field part of the aromatic region, which is shown in Figure 6.12. It is clear that intensity is lost from this region after nitration. There are three resonances in this region of the spectrum of the V_L dimer, at 6.15 p.p.m., 6.23 p.p.m. and 6.36 p.p.m. All three are affected by the binding of ligands (Table 5.1). The first two resonances undergo upfield chemical shift changes of 0.2-0.3 p.p.m. and the third is shifted downfield by 0.1 p.p.m.. It appears from Figure 6.12 that one of these resonances is absent from spectrum of the NO_2V_L dimer. In order to determine which resonance is affected, and to explain the changes in the rest of the aromatic region, the binding of DNP-aspartate to the NO_2V_L dimer was investigated. The titration curves of the protein and

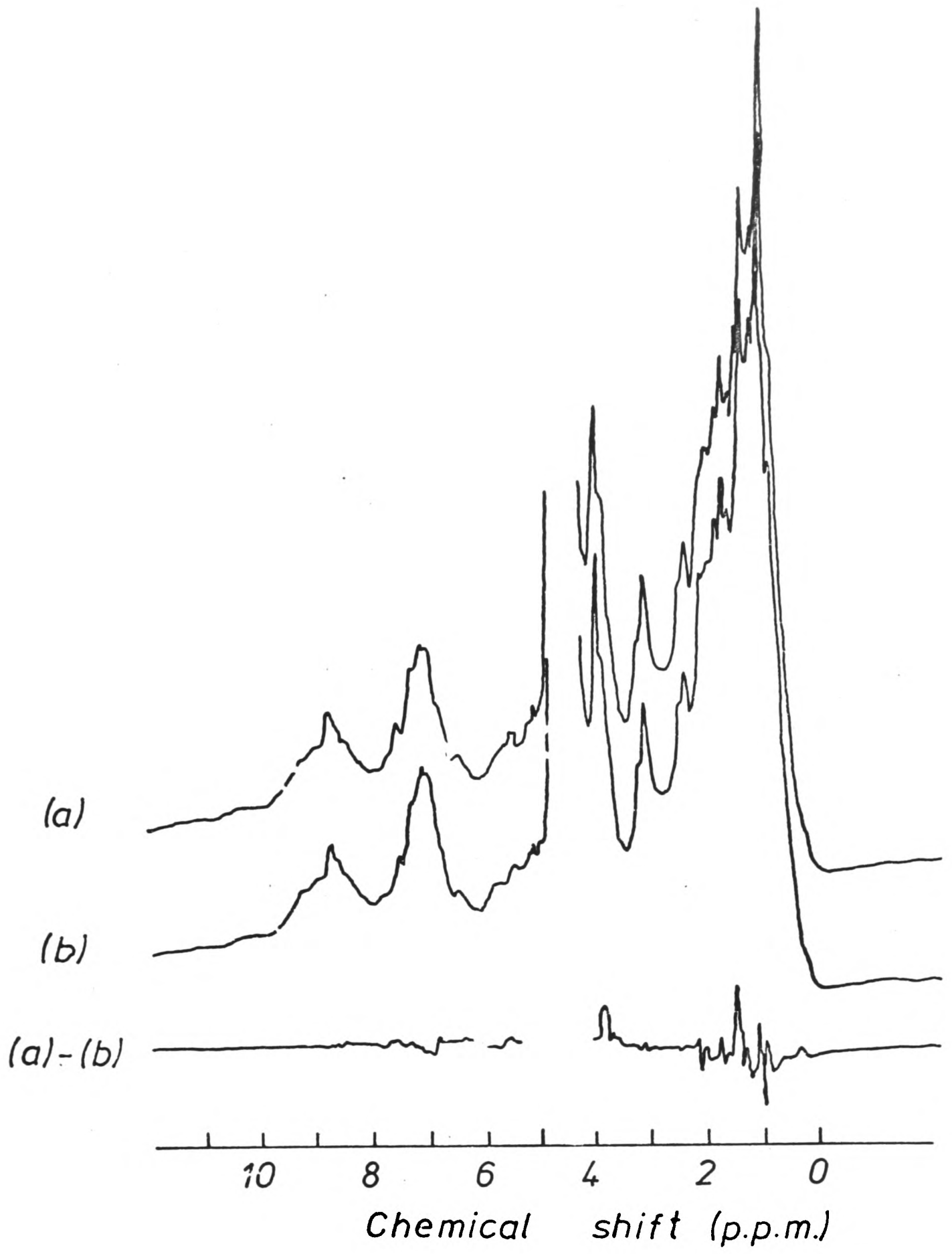

Figure 6.10 270 MHz ^{1}H n.m.r. spectra of the V_L dimer and NO_2V_L dimer

2000 scans were recorded at T = 298K with solutions in $^{2}H_2O$, 0.025M ^{2}H-acetate, pH* 4.8. (a) V_L dimer, 0.67 mM. (b) NO_2V_L dimer, 0.67 mM.

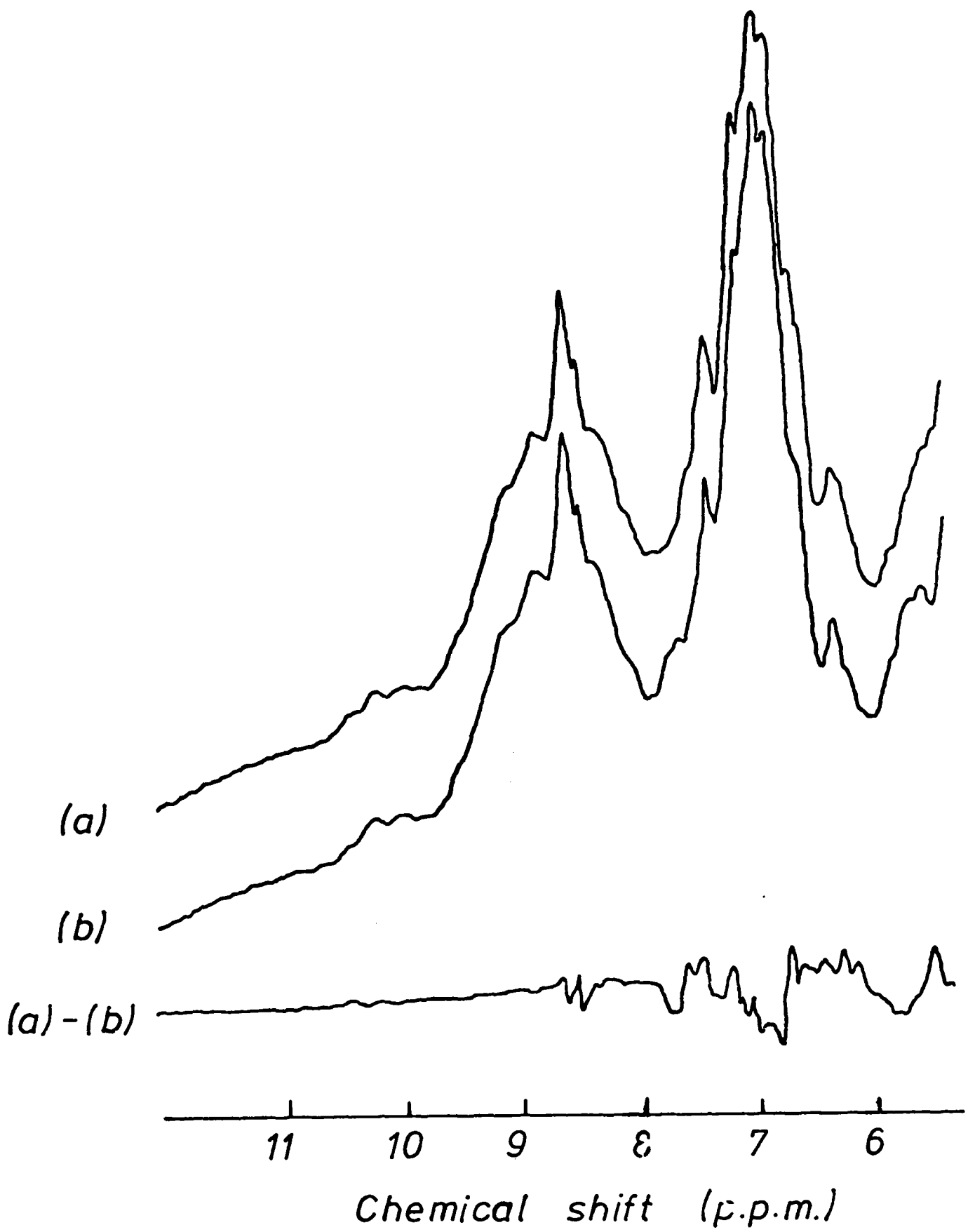

Figure 6.11 Aromatic region of the 270 MHz ^{1}H n.m.r. spectra of the V_L dimer and NO_2V_L dimer

2000 scans were recorded at T = 298K with solutions in $^{2}H_2O$, 0.025M ^{2}H-acetate, pH* 4.8. (a) V_L dimer, 0.67 mM. (b) NO_2V_L dimer, 0.67 mM.

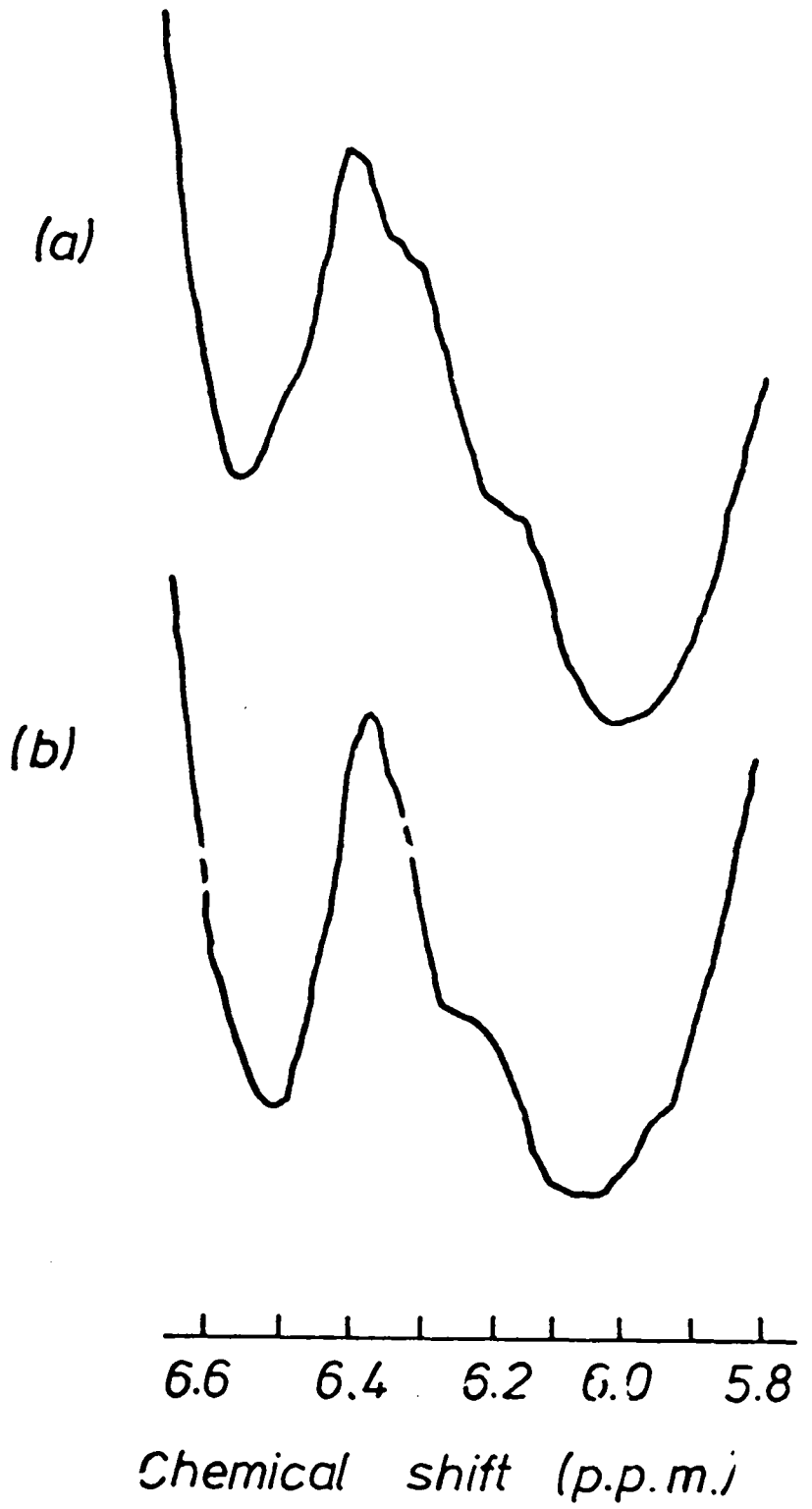

Figure 6.12 High-field aromatic resonances of the 270 MHz ^{1}H n.m.r. spectra of the V_L dimer and NO_2V_L dimer

2000 scans were recorded at T = 298K with solutions in $^{2}H_2O$, 0.025M ^{2}H-acetate, pH* 4.8. (a) V_L dimer, 0.67 mM. (b) NO_2V_L dimer, 0.67 mM.

ligand resonances are shown in Figure 6.13, and the effects are summarized in Table 6.6 for comparison with those obtained with the V_L dimer. In the high-field region of the spectrum of the NO_2V_L dimer, two resonances, at 6.25 p.p.m. and 6.36 p.p.m., titrate upfield. The titration of these resonances can be seen in Figure 6.14. No resonance can be seen to titrate downfield from this region. It is therefore concluded that the resonances at 6.15 p.p.m. and 6.23 p.p.m. in the spectrum of the V_L dimer are shifted to 6.25 p.p.m. and 6.36 p.p.m. respectively after nitration. A single shift of the resonance at 6.15 p.p.m. to 6.36 p.p.m., rather than shifts of both resonances, is less likely from a comparison of the line shapes of the resonances (Figure 6.12) and the changes of the chemical shifts of the resonances following the binding of the ligand (Table 6.6). The resonance at 6.36 p.p.m. in the spectrum of the V_L dimer, which titrates downfield, is apparently absent from the spectrum of the NO_2V_L dimer. The difference between the spectra of the aromatic regions of the V_LV_H and $NO_2V_LV_H$ fragments (Figure 6.4) also shows the presence of a resonance at 6.33 p.p.m. in the spectrum of the V_LV_H fragment which is absent from that of the $NO_2V_LV_H$ fragment. However, a resonance at this position in the spectrum of the $NO_2V_LV_H$ fragment is still observed to titrate downfield on the addition of DNP-glycine. Because there is more intensity in this region of the spectra of the Fv or V_LV_H fragments than of the V_L dimer, a clear intepretation of the data is not possible. No firm assignment of resonances to Tyr-34_L, neither in the spectra of the native nor of the nitrated proteins, is therefore feasible from these results. These findings emphasize the difficulties of assignment of these spectra, mentioned in Chapter 5. Despite the availability of a specific chemical

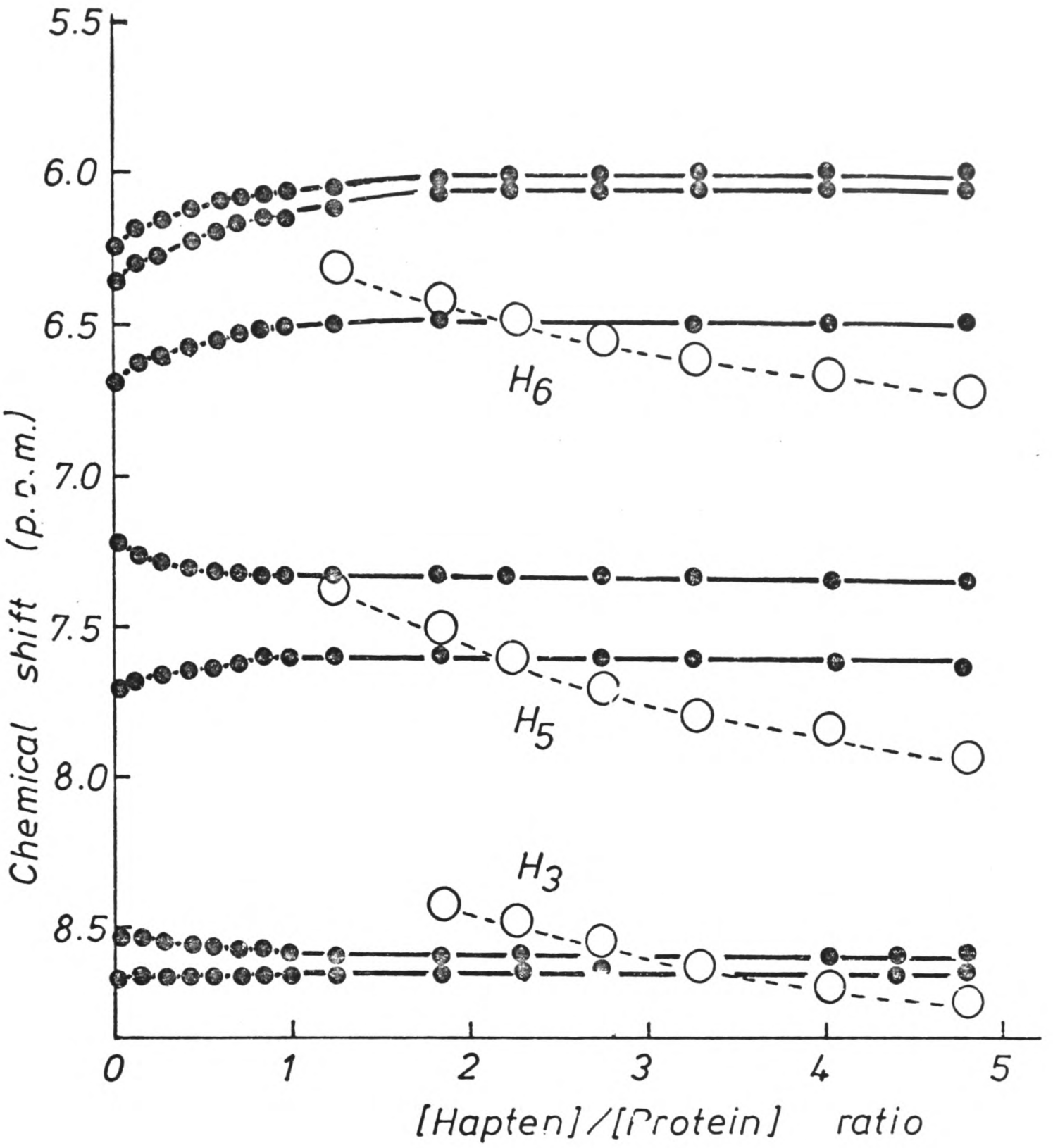

Figure 6.13 Chemical shift changes of the resonances of aromatic ^1H nuclei following the binding of DNP-aspartate to the NO_2V_L dimer

Measurements were made at 270 MHz, T = 298K, with solutions in ^2H_2O, 0.025M ^2H-acetate, pH* 4.8. The initial protein concentration was 0.67 mM. The chemical shifts of the resonances of the free ligand are: H_3, 9.12 p.p.m.; H_5, 8.29 p.p.m.; H_6, 6.97 p.p.m.

Table 6.6 Chemical shifts (δ) and the changes in chemical shifts (Δδ) of protein resonances perturbed on the binding of DNP-aspartate to the V_L dimer of protein 315 and the NO_2V_L dimer

Measurements were made at 270 MHz, T = 298K in ^2H_2O, 0.025M ^{2}H-acetate, pH* = 4.8. Shifts were measured from DSS, used as an external standard. + and - denote upfield and downfield shift changes respectively. Blank positions in the Table do not imply a clear absence of perturbation.

	V_L+ DNP-glycine (a)		V_L+ DNP-aspartate (a)		NO_2V_L + DNP-aspartate	
	δ(p.p.m.)	Δδ(p.p.m.)	δ(p.p.m.)	Δδ(p.p.m.)	δ(p.p.m.)	Δδ(p.p.m.)
	5.64	-0.13				
	6.14	+0.27	6.15	+0.23	6.25	+0.26
	6.21	+0.36	6.23	+0.30	6.36	+0.32
	6.38	-0.11	6.36	-0.08	probably absent	
	6.62	+0.55	6.58	+0.16	6.67	+0.24
	6.72	broadens ?	6.73	+0.18	6.85	?
	6.87	broadens ?	6.90	broadens or < +0.15	6.94	- ?
	7.04	-0.17 ?	7.06	broadens or < +0.15	7.11	+ ?
	7.22	-0.16	7.22	-0.10	7.23	-0.10
	7.45	-0.20	7.45	-0.15	7.45	- ?
	7.63	+0.13			7.71	+0.13
His-97_L	8.55	-0.21	8.53	-0.06	8.54	-0.07
His-97_L	8.67	+0.03	8.67	+0.03	8.68	+0.02

(a) Data from Table 5.1.

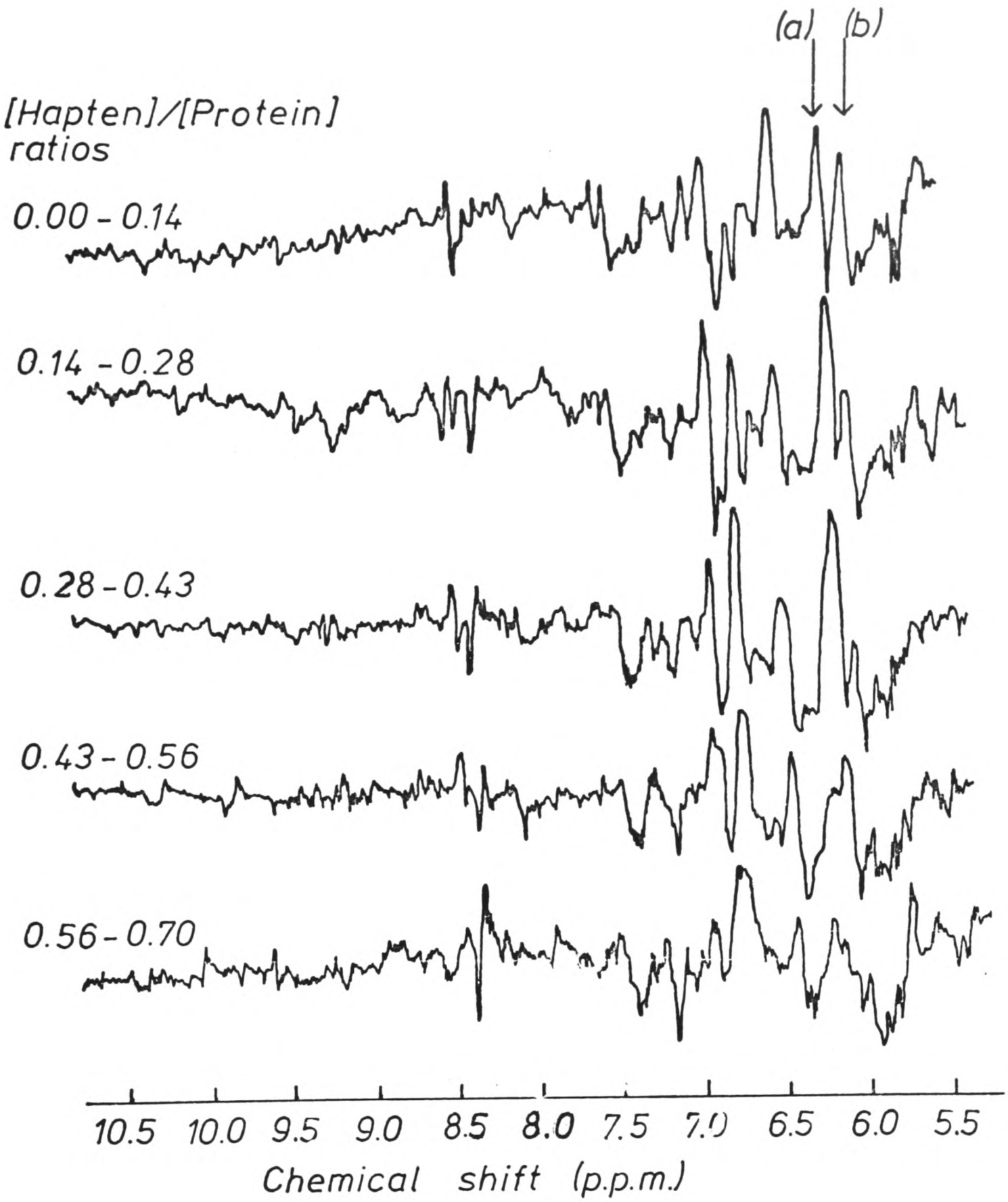

Figure 6.14 The effect of the binding of DNP-aspartate on the aromatic region of the 270 MHz ^{1}H n.m.r. spectrum of the NO_2V_L dimer

2000 scans were recorded at T = 298K, with solutions in $^{2}H_2O$, 0.025M ^{2}H-acetate, pH* 4.8. The initial protein concentration was 0.67 mM. The differences were taken between successive additions of hapten. Resonances (a) - 6.35 p.p.m. and (b) - 6.25 p.p.m. titrate upfield. No resonance at 6.35 p.p.m. is observed to titrate downfield.

modification, the general inapplicability of irradiation or pulse techniques to these sytems severely limits the information obtainable.

Comparison of the ligand titration of the NO_2V_L dimer with those of the V_L dimer reveals other differences outside the high-field part of the aromatic region (Table 6.6). The resonances at 6.58 p.p.m. and 7.64 p.p.m. in the spectrum of the V_L dimer are apparently shifted to 6.67 p.p.m. and 7.71 p.p.m. respectively. There may also be an effect of nitration on the resonance at 6.73 p.p.m. These changes account for the difference spectrum of the aromatic regions of the V_L dimer and NO_2V_L dimer shown in Figure 6.11. The effect of nitration on the positions of several resonances of the V_L dimer which are also perturbed by the binding of ligand, contrasts with the single obvious change observed with the V_LV_H fragment. However, the changes of position are very small (~0.1 p.p.m), and the observation that nitration affects predominantly those resonances which are also affected by the binding of ligands is further evidence that Tyr-34_L is a component of the combining site.

2. Effect of nitration on the binding properties of the V_L dimer

The data obtained by equilibrium dialysis for the binding of ^{3}H-DNP-lysine to the V_L dimer and NO_2V_L dimer at pH 5 and pH 8 are shown in Figure 6.15 in the form of Scatchard plots. The binding parameters are summarized in Table 6.7. There is no effect of the nitration either on the affinity or on the number of sites. However, there is a small effect on the mode of binding of DNP-aspartate. Any differences between the chemical shift changes of the ligand resonances following binding are most accurately measured by comparing the observed ratios rather than

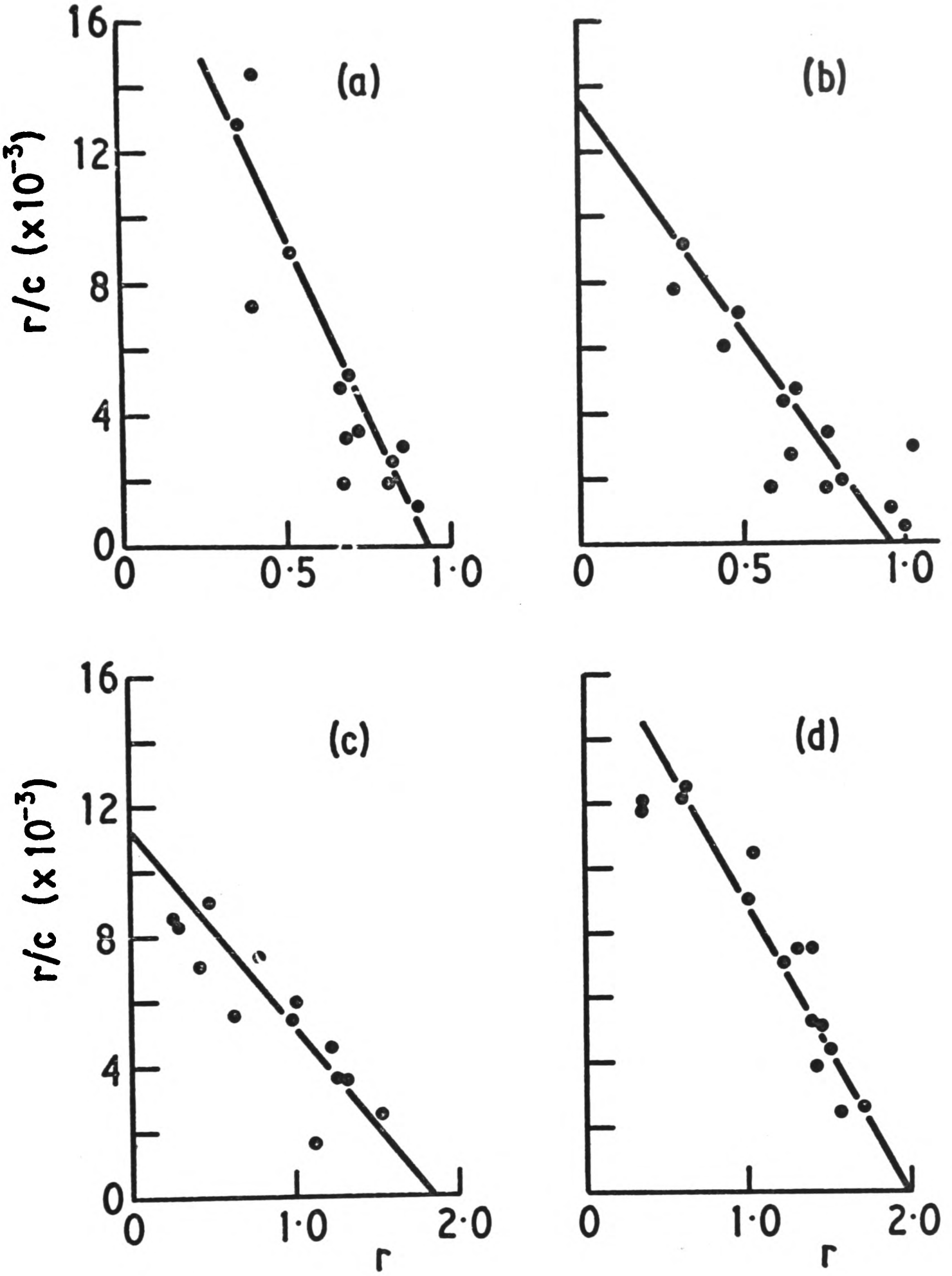

Figure 6.15 Scatchard plots for the binding of ^{3}H-DNP-lysine to the V_L dimer and NO_2V_L dimer at pH 5.0 and pH 8.0

Measurements were made by equilibrium dialysis at T = 277K with solutions in 0.05M sodium acetate, 0.1M NaCl, pH 5.0 or in 0.05M Tris-HCl, 0.1M NaCl, pH 8.0. The protein concentration was 1.1×10^{-4}M. Initial hapten concentrations ranged between 10^{-4}M and 1.7×10^{-3}M. (a) V_L dimer, pH 5.0. (b) NO_2V_L dimer, pH 5.0. (c) V_L dimer, pH 8.0. (d) NO_2V_L dimer, pH 8.0.

Table 6.7 Parameters characterizing the binding of ^{3}H-DNP-lysine to the V_L dimer of protein 315 and the NO_2V_L dimer

Measurements were made at 277K, in 0.05M sodium acetate, 0.15M NaCl (pH 5.0) or 0.05M Tris, 0.15M NaCl (pH 8.0). The protein concentration was 1.1×10^{-4}M.

	pH	Number of sites	Association constant ($M^{-1} \times 10^{-3}$)
V_L	5.0	0.93	22.0
NO_2V_L	5.0	0.96	14.0
V_L	8.0	1.86	6.0
NO_2V_L	8.0	1.99	8.6

the extrapolated values. The ratios of the chemical shift changes observed for the binding of DNP-aspartate to the V_L dimer and NO_2V_L dimer are given in Table 6.8. While the H_5 and H_6 resonances are unaffected, there is a significant difference between the chemical shift changes of the H_3 resonance.

Table 6.8 Ratios of the chemical shift changes of the ^{1}H aromatic resonances of DNP-aspartate on binding to the V_L dimer of protein 315 and the NO_2V_L dimer

Measurements were made at 270 MHz, T = 298K, in $^{2}H_2O$ containing 0.025M acetate, pH* = 4.8.

Protein	Shift ratio		
	H_5/H_3	H_6/H_3	H_5/H_6
V_L	1.30	0.92	1.41
NO_2V_L	1.03	0.74	1.39

The error in the values given in Table 6.8 is estimated to be $\pm$ 5%, since four titrations of the V_L dimer with DNP-aspartate

gave an H_5/H_3 ratio of 1.30 ± 0.07. Although nitration has influenced the precise mode of binding of DNP-aspartate, supporting the proposal that it is a residue in the combining site, the effect is very small. The difference in position is less than that between the orientations of DNP-aspartate and DNP-glycine in the binding site of the V_L dimer.

Nitration of Tyr-33_H in the Fv fragment

1. Purification of the NO_2Fv fragment

Nitration of tyrosine residues with TNM frequently results in the formation of covalently cross-linked products (Doyle et al., 1968; Boesel and Carpenter, 1970; Vincent et al., 1970). After nitration of Tyr-34_L, 50% of the V_L dimer of protein 315 is inactive, and occurs as covalently aggregated material (Gavish et al., 1979). Since the active monomeric species could be purified on a DNP-lysine-Sepharose column, the same method was used for purification of the NO_2Fv fragment. The column profile is shown in Figure 6.16. Approximately 30% of the material did not bind to the column. Both the active and inactive fractions were subjected to SDS-PAGE. The active material was indistinguishable from the Fv fragment, whereas the inactive material clearly contained covalent aggregates. It is therefore concluded that aggregation is responsible for the lack of affinity. Such a loss of affinity would be expected if cross-linking occurs through pairs of tyrosine residues which are in or near the combining site.

2. Perturbation of NO_2Tyr-33_H by ligands

The pH titration behaviour of the NO_2Fv fragment, monitored at 428 nm, is shown in Figure 6.17a. The pK_a is 7.4,

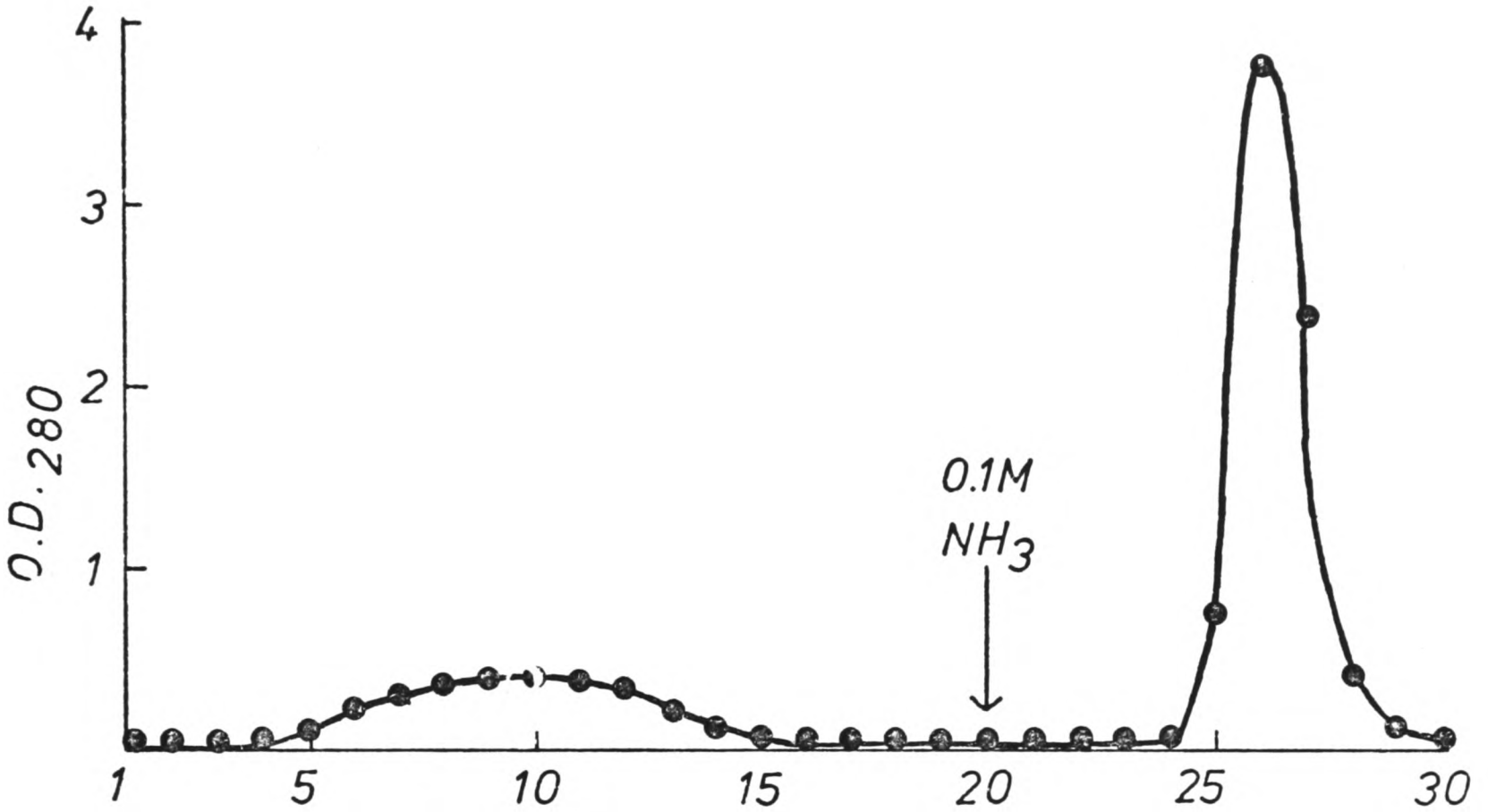

Figure 6.16 Affinity chromatography of the NO_2Fv fragment

10 ml of nitrated Fv fragment (1 mg/ml) were applied to a DNP-lysine-Sepharose column (1.5 x 4 cm) in 0.1M NH_4HCO_3. Bound material was eluted with 0.1M NH_3 as indicated. The fraction size was 1.5 ml.

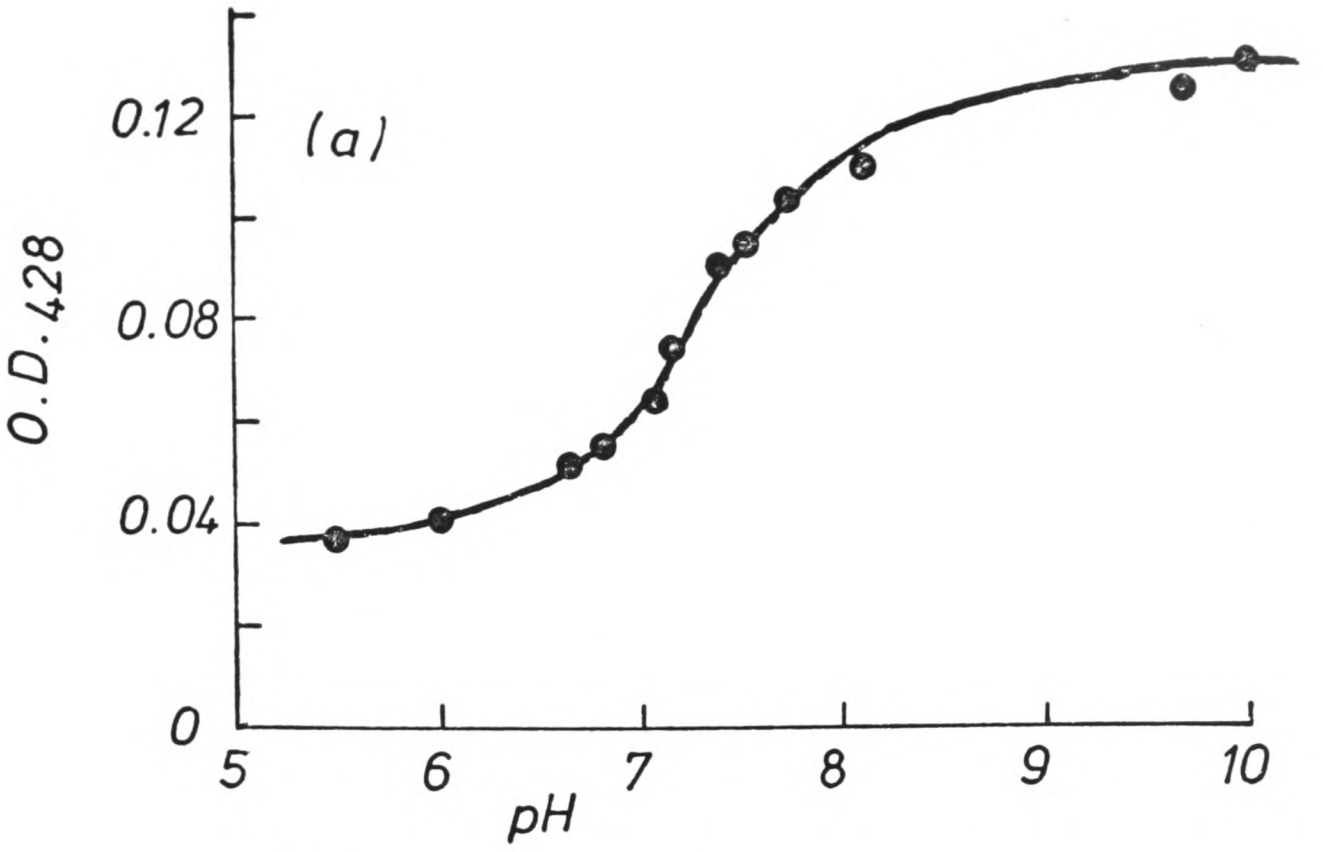

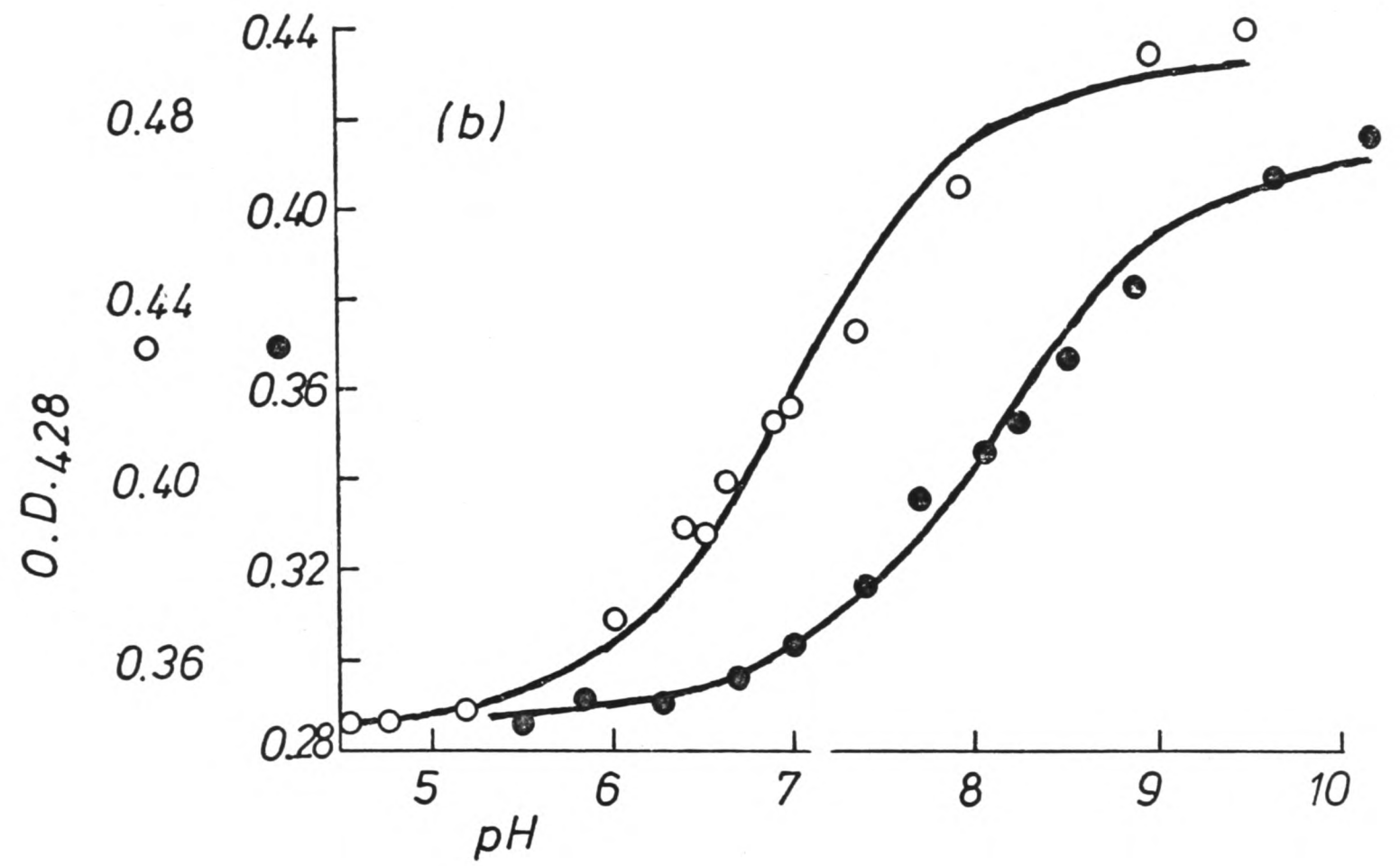

Figure 6.17 pH titration of $NO_2Tyr\text{-}33_H$ in the NO_2Fv fragment

Measurements were made at T = 293K with solutions in 0.005M potassium phosphate, 0.15M NaCl. The solid curves were obtained by the non-linear least squares procedure given in Appendix 2.1. (a) NO_2Fv fragment, 40 μM, pK_a 7.4. (b) o - NO_2Fv fragment, 50 μM, with DNP-lysine, 51 μM, pK_a 7.0; • - NO_2Fv fragment, 40 μM, with TNP-glycine, 42 μM, pK_a 8.2.

which is different from the value of 6.6 determined for $NO_2Tyr\text{-}34_L$. However, if 20% or less of the nitration occurs on $Tyr\text{-}34_L$ (Wain-Hobson, 1977) it would probably be undetected.

The effects of various ligands on the pK_a of the nitrotyrosine were determined by using protein concentrations of ~50 μM, with a slight excess of ligand. Titration curves for the ligands DNP-lysine and TNP-glycine are shown in Figure 6.17b. The titration parameters for all the ligands, in terms of the pK_a and extinction coefficient relative to that of the nitrotyrosine in the uncomplexed NO_2Fv fragment, are given in Table 6.9.

Table 6.9 The pK_a values and relative extinction coefficients of $NO_2Tyr\text{-}33_H$ in the absence and presence of various nitrophenyl ligands

Measurements were made in 0.01M potassium phosphate, 0.15M NaCl, T = 293K. The protein concentrations were ~50 x 10^{-6}M.

Ligand	pK_a	Relative change in extinction coefficient (428 nm)
None	7.4	1.0
$DNP\text{-}NH_2$	7.5	0.9
$TNP\text{-}NH_2$	7.5	1.15
$DNP\text{-}NH\text{-}CH_2\text{-}COO^-$	7.5	0.9
$TNP\text{-}NH\text{-}CH_2\text{-}COO^-$	8.1	1.5
$TNP\text{-}NH\text{-}CH_2\text{-}CH_2\text{-}NH_3^+$	7.7	2.15
$DNP\text{-}NH\text{-}(CH_2)_4\text{-}CH(NH_3^+)\text{-}COO^-$	7.0	1.25

Neither dinitroaniline nor trinitroaniline affects the ionization of $NO_2Tyr\text{-}33_H$. Any observed effect may therefore be attributed to the side-chain of the ligand. No such effect is seen with DNP-

glycine, but the presence of TNP-glycine causes an increase of the pK_a from 7.4 to 8.1, and a concomitant increase of the apparent extinction coefficient of the absorption band. An increase of the pK_a would be expected from the proximity of the negatively charged carboxyl group of the ligand side-chain. The difference between the effects of DNP-glycine and TNP-glycine may reflect either a difference in the modes of binding of the DNP and TNP rings (Dower et al., 1978) or a steric effect of the 6-nitro group on the conformation of the side-chain. The possibility that a simple charge effect is responsible for the perturbation may be tested by replacing the negatively charged side-chain with a positively charged one. The presence of TNP-aminoethylamine does result in a perturbation of the nitrotyrosine, since it changes the apparent extinction coefficient by more than 2-fold. However, it causes a small increase, and not a decrease, of the pK_a. The perturbations of the pK_a are therefore not caused solely by direct interactions between the ligand and the nitrotyrosine, but may also result from changes of the protein structure around the nitrotyrosine group. This conclusion is reinforced by the effect of DNP-lysine, which actually reduces the pK_a from 7.4 to 7.0. Regardless of the mechanisms by which the perturbations are mediated, the results are consistent with the proximity of Tyr-33_H to the side-chains of the ligands, as proposed in the model of the combining site.

Further analysis of the binding properties of the NO_2Fv fragment and of its ^1H n.m.r. spectrum should help to define the role of Tyr-33_H more precisely.

CHAPTER 7

SOME PROPERTIES OF THE DNP-BINDING MONOCLONAL ANTIBODY A3

INTRODUCTION

Information about the structure, specificity and secondary functions of antibodies has been obtained almost entirely from heterogeneous populations of immunoglobulins and from myeloma proteins. There are disadvantages associated with either approach, as discussed in Chapter 1. The major problem with heterogeneous preparations is that any measurable parameter is an ill-defined average value. Important differences between individual antibodies may easily be missed. Although the use of myeloma proteins alleviates this difficulty, it raises others. In particular, the binding properties of a myeloma protein have to be established by a laborious screening procedure. It is therefore difficult to make any systematic study of specificity, or of the effect of antigen-binding on other processes. The relationship of a myeloma protein to an antibody induced by an antigen is also not clear. Although there is much evidence for a connection between myeloma proteins and induced antibodies of the same specificity, the position of any myeloma protein in the development of the immune response remains uncertain. In addition, myeloma proteins can only be induced in a few strains of mice.

The development of the cell-fusion technique for producing monoclonal antibodies of defined specificity is therefore of great value. In this chapter, the recloning, purification and binding properties of one such protein, with specificity for the

DNP group, are described. The binding properties of this protein are compared with those of myeloma proteins and antisera with DNP-binding activity.

MATERIALS

Protein A3

The cell-line A3/3.3/3 producing protein A3, an IgG_1/κ, was kindly given by Dr. B.A. Askonas, National Institute for Medical Research, Mill Hill. Protein A3 is the product of a hybrid cell line obtained by fusing mouse spleen cells with the myeloma cell line P3/NSI/1-Ag4-1, according to the method of Köhler and Milstein (1975). The spleen cells were obtained from CBA mice, primed and boosted with DNP-keyhole limpet hemocyanin (DNP-KLH). The myeloma cell line is a nonsecreting variant of the BALB/c MOPC 21 line (Köhler et al., 1976). It synthesizes, but does not secrete, small amounts of L-chain. Very little of this L-chain could be detected with protein A3 (Askonas, private communication).

METHODS

Recloning of A3/3.3/3 cell line

The cell line was recloned by L. Hackfath (M.R.C. Immunology Unit, Oxford). Experimental details are given in Appendix 7.1.

Preparation of TNP-SRBC (Trinitrophenylated sheep red blood cells)

The method of Rittenberg and Pratt (1969) was used. 1 ml of packed SRBC (2.5×10^{10} cells), aged at least two weeks, was washed three times with cold veronal saline (VS) buffer (0.01M sodium barbitone, 0.15M NaCl, pH 7.2). Batches still showing

hemolysis after washing were discarded. Cells were added dropwise to 10 ml VS containing 1 mg/ml TNBS (trinitrobenzene sulphonic acid), and left at room temperature for 20 mins, stirring gently. After centrifugation (1000 r.p.m. for 5 mins), 8 ml cold VS containing 1 mg/ml glycylglycine were added to react with excess TNBS, and the cells were washed three times with cold VS. Cells prepared by this method were stable for at least 2-3 days at $4^{o}C$, and gave very low levels of background lysis in the sensitive slide assay for plaque-forming cells (Cunningham, 1965).

Extent of modification of TNP-SRBC

Since the TNP-glycylglycine molecule is a chromophore, an estimate of the extent of modification of SRBC may be obtained.

0.8 ml of SRBC (1.73×10^{10} cells) was added to one of two tubes, each containing 7.5 mg TNBS in 6 ml VS. After reaction at room temperature for 20 mins the $O.D._{340}$ of the supernatants were measured and 11 mg glycylglycine in 1 ml VS were added to each tube. 12% of the TNBS was found to have reacted, equivalent to a modification of 10^{3} TNP groups per SRBC.

Glutaraldehyde fixation of TNP-SRBC

TNP-SRBC were washed with VS buffer, resuspended at 2×10^{8} cells/ml and reacted with an equal volume of 0.25% glutaraldehyde at room temperature for 5 mins. The reaction was stopped by the addition of one tenth of the volume of 10% BSA. The cells were spun (1000 r.p.m. for 5 mins), filtered through cotton wool, spun again and resuspended in VS containing 10% BSA. The cells were passed through a syringe to avoid clumping, resuspended at 5×10^{8} cells/ml in VS containing 10% BSA and stored frozen in 1 ml vials.

Binding assay for antibody-producing cells

The method of Williams et al. (1977) was used. This is an indirect binding assay, which detects antibody bound to the target cells by means of a second ^{125}I-labelled rabbit anti-mouse IgG antiserum. 50 µl of culture supernatant were added to 50 µl of VS buffer, 0.5% BSA, containing 5 x 10^6 glutaraldehyde-fixed TNP-SRBC, and incubated at 4°C for 1 hr. The cells were washed twice with 1 ml VS buffer, 0.1% BSA. 50 µl of ^{125}I-rabbit anti-mouse IgG (300,000 c.p.m.) were added, and the cells were incubated at 4°C for a further 1 hr. The cells were washed twice before counting.

Farr assay

The method described is a modification of the original assay (Farr, 1958), developed by Miss E.M. Press for protein 315. It was used to measure the amount of antibody present in ascites fluid or in column fractions. Dilutions of ascites fluid or of column fractions were made with a 1 in 4 dilution of non-immune rabbit serum in borate buffered saline (BBS) (Boric acid 6.18 gm l^{-1}, borax 9.54 gm l^{-1}, 0.075M NaCl, pH 8.4). ^{3}H-DNP-lysine was used with a specific activity of 3 x 10^4 c.p.m./nmole.

0.1 ml of sample and 0.1 ml of ^{3}H-DNP-lysine (0.5 nmol) were left at 4°C for 1 hr. 0.5 ml of 75% saturated $(NH_4)_2SO_4$ was added, and the mixture was left at 4°C for a further 30 mins. 1 ml of 50% saturated $(NH_4)_2SO_4$ was added, the precipitate was pelleted (2500 r.p.m. for 20 mins) and the supernatant was removed. The precipitate was redissolved in 0.2 ml BBS with a drop of 5N HCl and counted. 0.5 nmol of ^{3}H-DNP-lysine was subsequently added to determine the extent of quenching of the radioactivity.

Maintenance of A3 cell line in vivo

5×10^6 cells in 0.5 ml of HAM medium were injected intraperitoneally into D2c/F_1 mice, which had received 0.5 ml pristane intraperitoneally at least 2 weeks previously. D2c/F_1 mice were used since they are closely related to the more suitable CBA×BALB/c strain, which is not available commercially. To avoid tumour suppression, the mice were exposed to 500 Rad of gamma radiation prior to injection of cells. Ascites fluid could be collected after about 2 weeks by draining the peritoneal cavity with a needle. The fluid was centrifuged immediately (1000 r.p.m. for 5 mins). Ascites cells were resuspended at 10^7/ml for transfer to further recipients. This method of propagation is much to be preferred over the passaging of cells into the flank to form a solid tumour, since it reduces the number of mice required. No problems with secondary infections were encountered.

Purification of protein A3 by ion-exchange chromatography

A saturated $(NH_4)_2SO_4$ solution was added dropwise, with continuous stirring, to an equal volume of ascites fluid, and the suspension was left to stand at 4°C for 2 hrs. The material was centrifuged at 2800 r.p.m. for 30 mins, and the precipitate was redissolved in Tris buffer (0.025M Tris, 0.020M NaCl, 0.02% NaN_3, pH 7.6). The solution was applied to a column of DEAE-cellulose (DE-52) and eluted with a shallow NaCl gradient (0.02M-0.05M) in an attempt to separate protein A3 from possible IgG contaminants.

Purification of protein A3 by affinity chromatography

The method described was devised by Dr. G.G.B. Klaus (Mill

Hill), and is at present unpublished (August, 1979).

2 gm of thiol-activated Sepharose 4B were swollen in PBS (0.015M potassium phosphate, 0.15M NaCl, 0.02% NaN_3, pH 7.0) and washed. The Sepharose was suspended in 20 ml dithioerythritol (0.01M) for 30 mins with continuous stirring, washed with Tris buffer (0.1M, pH 8.0), reacted with 20 ml di-DNP-cystine (1 mg/ml in Tris buffer) for 30 mins with continuous stirring, and washed with PBS. The material was packed in a column (1.6 x 5 cm), 10 ml of ascites fluid were applied, and the column was washed with PBS. 8 ml of cysteine (0.02M in Tris buffer) were run on, and the column was clamped off for 30 mins. After elution with PBS, yellow fractions were dialysed against PBS for 3 hrs, exchange dialysed twice against 100 ml dinitrophenol (0.1M in 0.1M NaOH, pH 7.0) and finally dialysed against PBS. Bound dinitrophenol was removed by a Dowex IX-8 column.

RESULTS AND DISCUSSION

Recloning of the A3/3.3/3 cell line

Although myeloma cell lines can apparently be propagated indefinitely from suitable stock, difficulties in the maintenance of a healthy line do occur. The myeloma MOPC 315 in Oxford has had to be obtained from fresh stock twice in the past three years. The A3 line, after arrival from London, grew well for two generations and then rapidly deteriorated. Problems with the line were experienced in London at the same time. A3 cells from the later transfers did not grow in culture, and it was necessary to use cells which had been frozen after the first transfer in Oxford, in order to reclone the line. It is clearly essential to freeze several vials of cells as early as possible.

The identification of culture wells containing positive

clones, both after the initial fusion and during cloning, requires a suitable assay. The cell-binding assay of Williams et al. (1977) should, in principle, be an excellent method, since it is rapid and since nitrophenyl groups can be coupled easily to a carrier cell. The standard curve obtained for the assay is shown in Figure 7.1. The culture well supernatants gave maximum readings of 2000 c.p.m. above the background level of 600 c.p.m. obtained with non-specific IgG. This contrasts with values of 10,000-20,000 c.p.m. obtained with antibodies to membrane antigens under similar conditions (Sunderland, private communication). There are several factors which could contribute to the low values obtained. A3 cells are low producers of antibody, and give only 2-3 mg/ml of antibody in ascites fluid, compared with 6-10 mg/ml for many other myeloma lines. The low values are probably also related to the density and distribution of antigenic determinants, and to the affinity and effective valency of the antibody. Experiments with monoclonal antibodies to rat thymocyte antigens showed that the majority of the antibodies bound monovalently, regardless of a change of site density from 1.5×10^4 to 10^6 determinants per cell (Mason and Williams, 1979). The anti-thymocyte antibodies had high affinities of about 4×10^9 M^{-1}. The correspondingly low off-rates prevented significant dissociation of the monovalent complexes during the washing procedure. The affinity of protein A3 for the TNP group is at least two orders of magnitude lower. Since the on-rates of antibody-antigen complexes are quite similar, and their lifetimes are generally directly related to their equilibrium constants (Froese, 1968), it is likely that only bivalent binding is being detected. It is necessary to bear these points in mind if this convenient assay is to be used in future for the

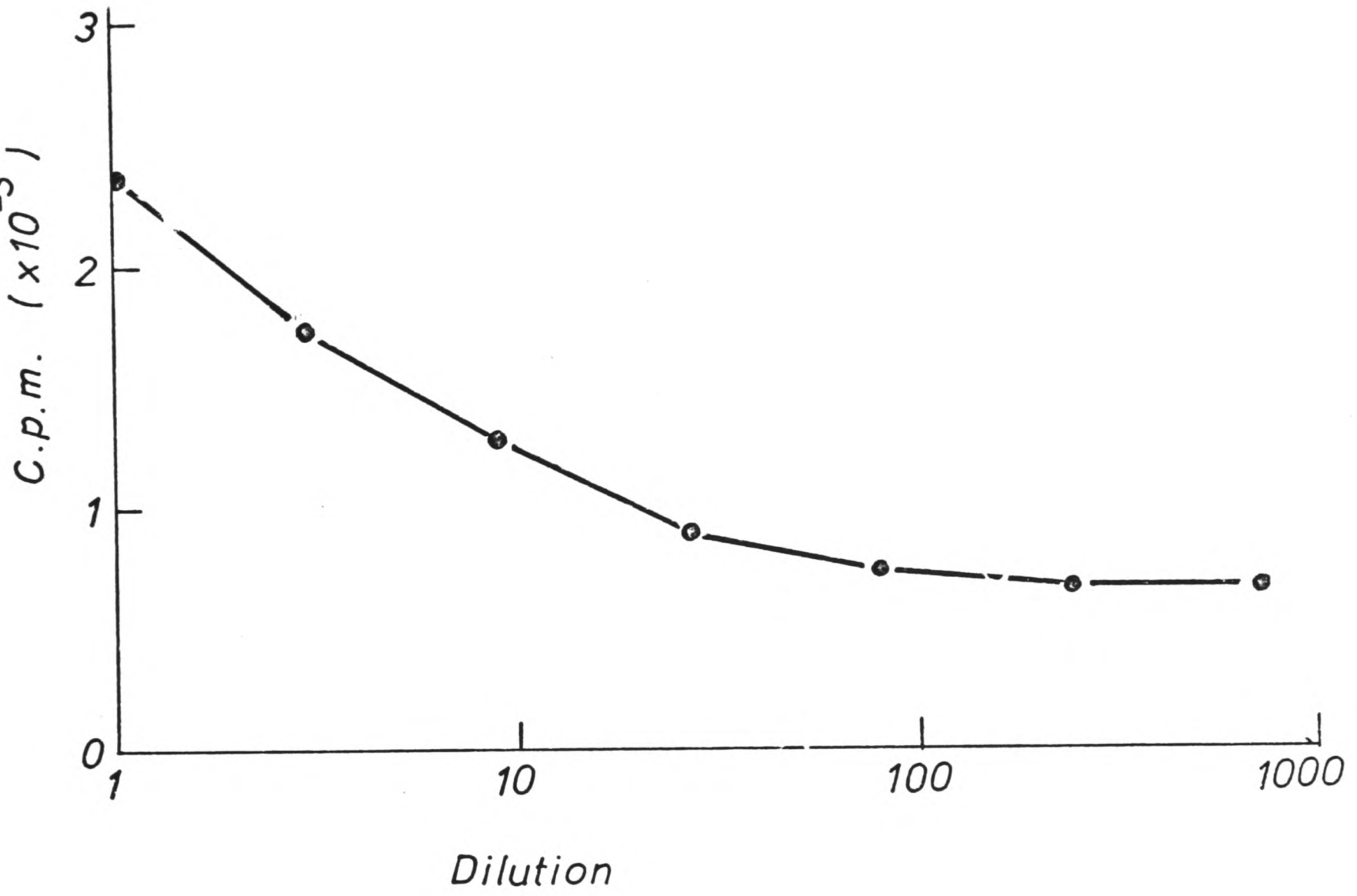

Figure 7.1 Standard curve for the indirect binding assay

The target cells were glutaraldehyde-fixed TNP-SRBC (5×10^6). 50 µl of dilutions of a purified sample of protein A3 (13 µg/ml) were assayed. The second antibody was ^{125}I-labelled rabbit anti-mouse IgG (50 µl, 300,000 c.p.m.).

selection of hybrid cells producing anti-nitrophenyl antibodies. Results may depend on the nature of the target cell used, and the sample may be biased towards antibodies with high affinities, or towards classes and subclasses which are particularly able to bind simultaneously to two or more sites.

Cells were initially grown in soft agar (Appendix 7.1) and assayed after 2 weeks. Excepting wells with the lowest number of cells initially (2,500 cells), which had undergone little growth, 23 of 24 wells were clearly positive. Single clones were picked from the best wells and grown for a further 2 weeks. 33 of the 34 wells were clearly positive. The negative well contained few cells, and no further cloning was considered necessary. Three clones were selected from the best wells and grown up for storage.

Preparation of protein A3

Since protein A3 has a high affinity for the DNP group, its purification by affinity chromatography is quite difficult. In order to prepare a sample of sufficient purity for the experiments described in this chapter, a standard method of preparing IgG using ion-exchange chromatography was used. The elution profile obtained from the DEAE-cellulose column is shown in Figure 7.2. SDS-PAGE patterns of the four fractions indicated in Figure 7.2 were identical, and consistent with the presence of IgG. Farr assays of each of the three apparent peaks were positive, and showed concentrations of antibody proportional to the heights of the peaks. It appears that the procedure detected microheterogeneity of the IgG, which has also been observed with human and mouse myeloma proteins (Owen et al., 1958; Askonas, 1961; Fahey, 1961), and did not resolve possible contaminants. A

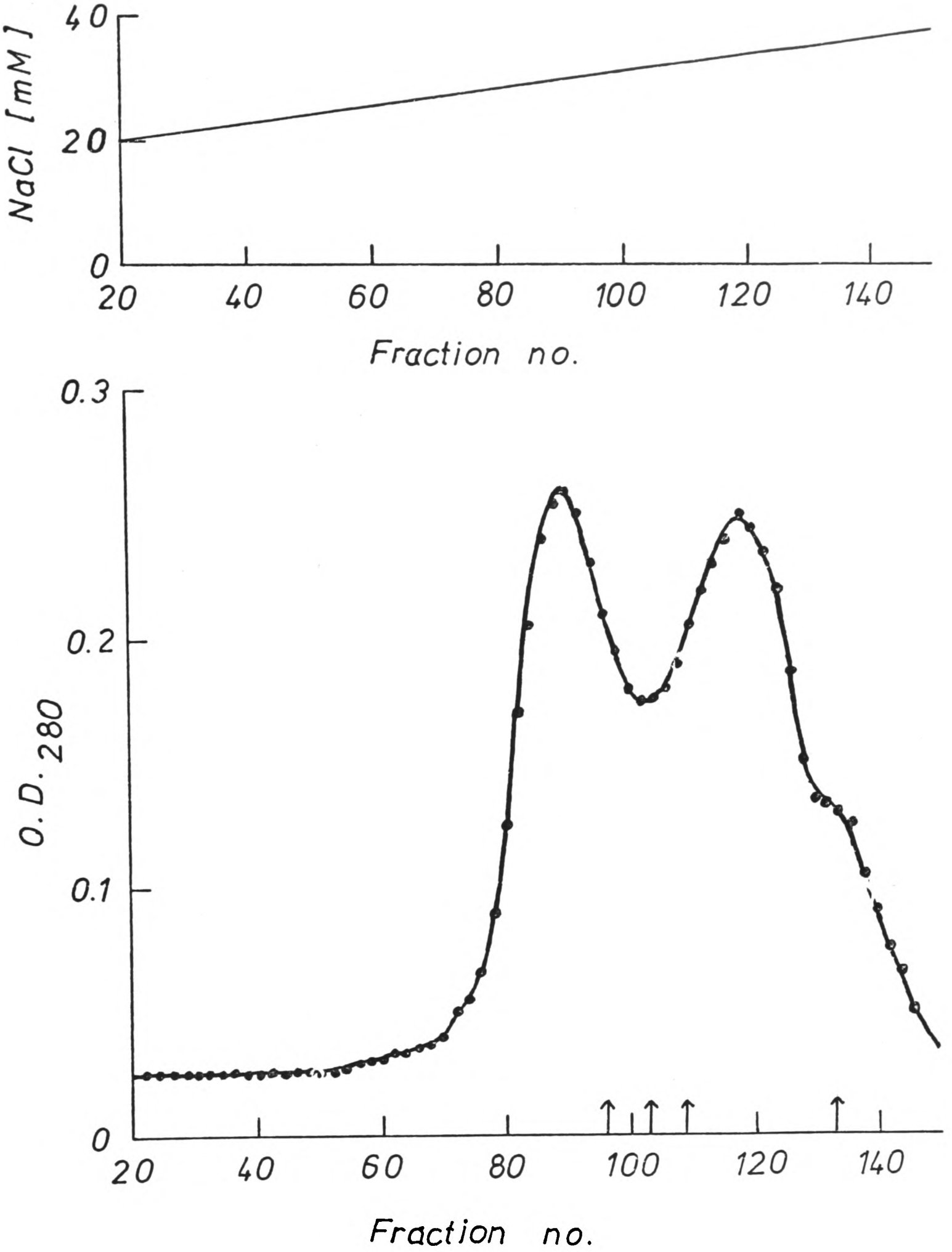

Figure 7.2 Elution profile of IgG from A3 ascites fluid

Protein precipitated by 50% $(NH_4)_2SO_4$ was redissolved in 0.025M Tris/0.02M NaCl/0.02% NaN_3/pH 7.6 and applied to a 3 x 7.5 cm column of DE-52. The column was developed at 40 ml/hr with a linear gradient of NaCl, shown above the column profile. Fractions of 2-3 ml were collected. The positions of the arrows indicate the fractions submitted to SDS-PAGE analysis. A single pool of fractions 73-141 was made.

small sample of the protein (1 O.D.) was tested for purity by applying it to a DNP-lysine-Sepharose column, and was found to contain 15% of non-binding material.

Although the material prepared by ion-exchange chromatography was sufficiently pure for the measurement of the affinity of the protein for ligands, a novel method of affinity chromatography was subsequently made available. A sample of protein was prepared by this method, for comparison with the protein prepared by ion-exchange chromatography. The method is not entirely satisfactory, since it involves the use of cysteine for the elution step. The concentration of cysteine is sufficient to reduce the disulphide bridges between the H-chains. Reoxidation of the molecules after removal of the reducing agent could lead to the production of cross-linked molecules. Covalently linked dimers and trimers were detected by gradient gel electrophoresis (Figure 7.3). A sedimentation velocity run at 52,000 r.p.m. showed a major band with a sedimentation coefficient of 7S, equivalent to monomeric IgG. However, the presence of faster sedimenting material was also detected.

Despite the presence of aggregates, the fluorescence quenching properties and binding constant for DNP-lysine of the protein purified by affinity chromatography were indistinguishable from those of the material purified by ion-exchange chromatography. The aggregation therefore does not significantly affect the binding sites of the antibody. The properties of the material obtained before and after recloning were also identical. The superposition of the three fluorescence quenching curves is shown in Figure 7.4.

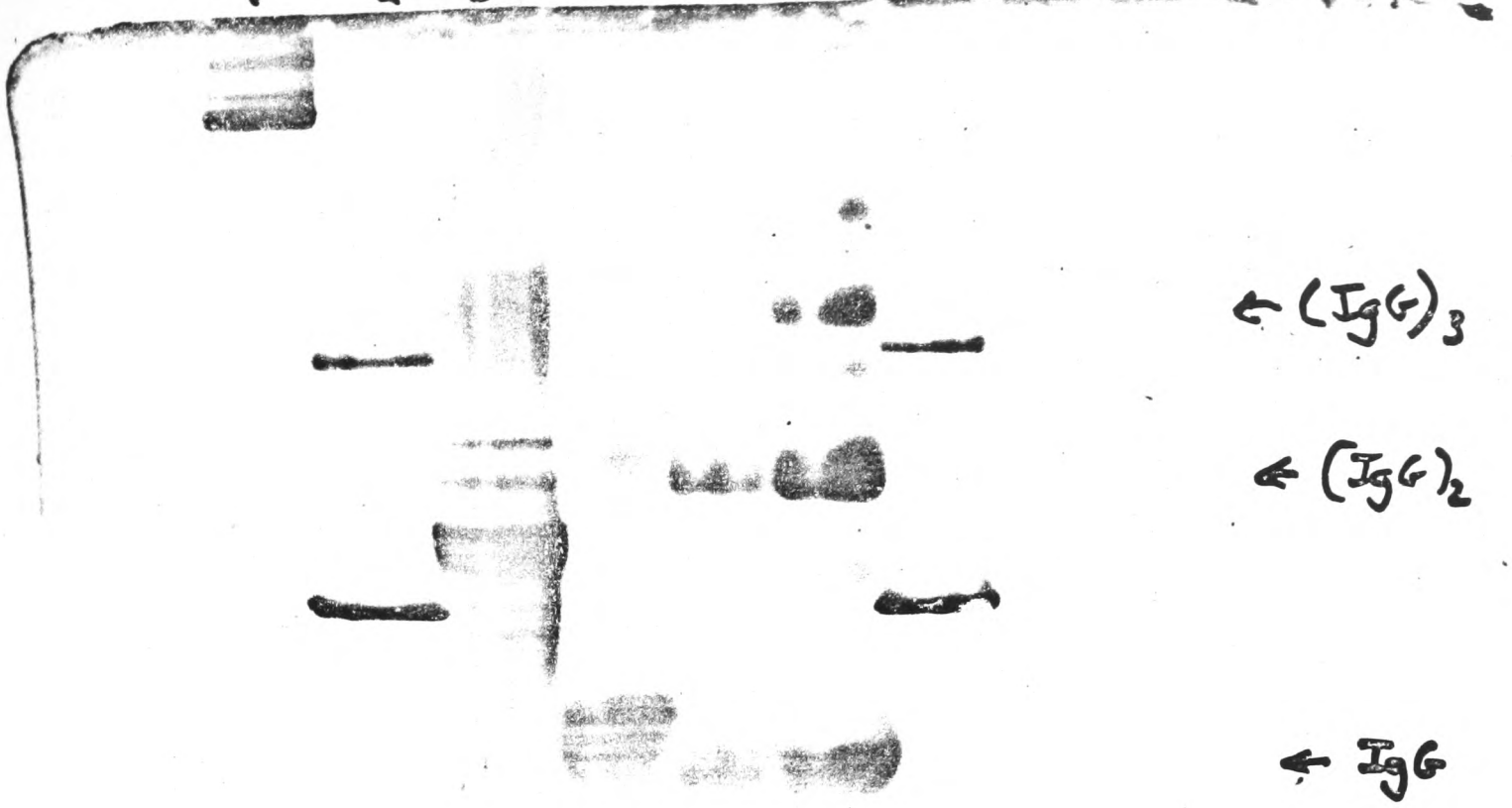

Figure 7.3 Gradient gel electrophoresis of protein A3 purified by affinity chromatography

Samples were applied to a gradient gel (Pharmacia, PAA 4/30) in 0.165M Tris/0.025M borate/0.007M EDTA, and run for 16 hrs at 125V. Protein bands were stained with 0.2% Coomassie Blue.
1. MOPC 104E, IgM; 2. Sheep ferritin; 3. Human tryptic $(Fc)_5$ (major band = 350,000 M.W.);
4. MOPC 21 IgG; 5 and 6. Protein A3; 7. Sheep ferritin.
This diagram was kindly provided by Dr. N. Richardson

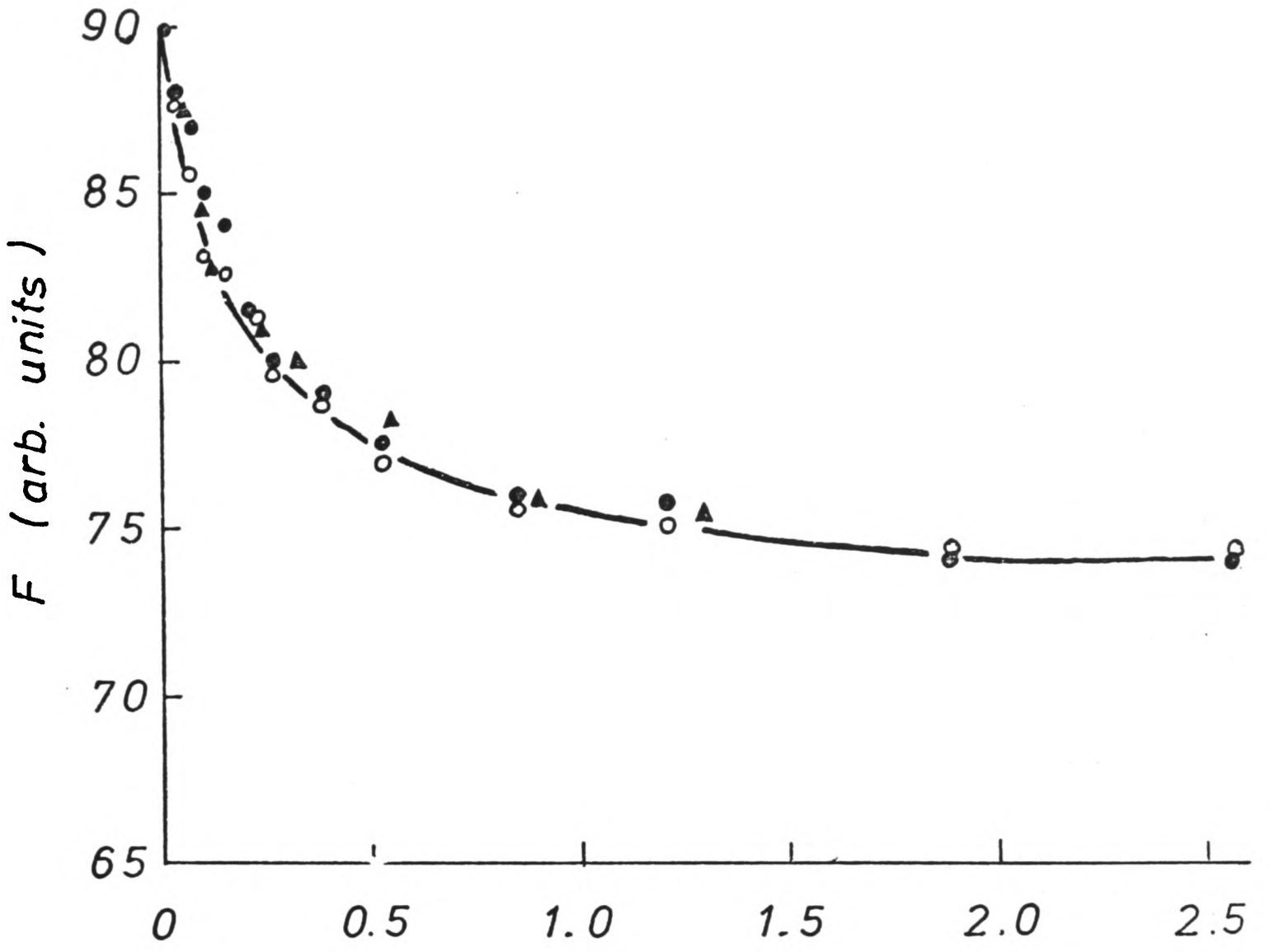

Figure 7.4 Fluorescence quenching curve for the binding of DNP-lysine to three preparations of protein A3

Measurements were made at 298K using IgG concentrations of 0.15 μM in 0.01M potassium phosphate/0.15M NaCl/pH 7.0. Protein fluorescence was excited at 295 nm and monitored at 340 nm. ● - material purified by ion-exchange before recloning; o - material purified by affinity chromatography before recloning; ▲ - material purified by ion-exchange after recloning.

Binding properties of protein A3

In the absence of the amino acid sequences of the V-regions of protein A3, and hence of a model of the combining site, it is clearly not possible to carry out the detailed structural analysis which has been applied to protein 315. However, it is possible to measure important parameters such as the size and shape of the site, and the ability of the antibody to distinguish between different ligands. The occurrence of a large red-shift of the absorption spectrum of DNP-lysine on binding to protein A3, characteristic of anti-DNP antibodies and indicative of a stacking interaction with tryptophan, has already been discussed in detail in Chapter 3.

The affinities of a series of nitrophenyl ligands and related compounds for protein A3 were measured by fluorescence quenching. The method of analysis of the data has been given in Chapter 2. The values of the association constants and Q_{max} (the percentage of intrinsic protein fluorescence quenched after saturation with ligand) are given in Table 7.1.

The affinity of protein A3 for DNP-lysine at $20^{o}C$ is $1.8 \times 10^{7}\ M^{-1}$. This value is in good agreement with the value of $3.1 \times 10^{7}\ M^{-1}$ determined at $4^{o}C$ by equilibrium dialysis (Askonas, private communication). This affinity is approximately an order of magnitude higher than that of protein 315 for DNP-lysine. The value of $2 \times 10^{7}\ M^{-1}$ is typical of that of IgG antibodies formed against DNP in a secondary immune response in rabbits (Johnston and Eisen, 1976). It is two orders of magnitude lower than the largest reported value of $3 \times 10^{9}\ M^{-1}$ for a rabbit antiserum (Haber et al., 1967).

Protein A3 has unusual fluorescence quenching properties. Q_{max} values of 20 were obtained with all the ligands used

Table 7.1 Association constants and Q_{max} values for the binding of ligands to protein A3, at 20°C in 0.01M potassium phosphate, 0.15M NaCl, pH 7.0

Ligand	Association constant (M^{-1})	Q_{max}
DNP-lysine	1.8×10^7	19
Dinitroaniline	1.3×10^6	18
DNP-glycine	3.3×10^6	21
2-chloro-4-nitrophenylglycine	8.3×10^5	16
4-chloro-2-nitrophenylglycine	4.4×10^5	12
TNP-glycine	1.7×10^6	21
Trinitroaniline	1.3×10^6	18
Dinitronaphthol	5.9×10^7	17
Flavianic acid	9.0×10^7	20
Menadione	8.3×10^4	18

(Table 7.1). This value is much lower than the values of 70-90 which are obtained with rabbit or guinea pig IgG antisera (Little and Eisen, 1966; Little and Eisen, 1969; Eisen et al., 1970), or with the IgA protein 315 (Eisen et al., 1968). Further analysis of mouse IgG antibodies would reveal whether this represents a species difference in the structure of anti-DNP antibodies, or variation within heterogeneous antisera.

Comparison of the binding energies of DNP-lysine and dinitroaniline shows that 87% of the binding energy of DNP-lysine is provided by the DNP ring. The value for protein 315 is also 87%. The difference between the affinities of the two ligands may be accounted for by a carrier effect of the alkyl side-chain. It is, of course, possible that the carrier effect extends over a larger region of the immunizing agent DNP-KLH, and that the affinities of the antibody for the true antigenic determinants are higher than the affinity for DNP-lysine.

The importance of the nitro groups may be evaluated by substituting them with chlorine (Gettins et al., 1978). This substitution affects three parameters. The stacking interaction with tryptophan, which may occur in the combining site, is reduced by a factor of 2 (Gettins, 1979). The chloro group has a smaller van der Waals radius (0.31 nm) than the nitro group (0.36 nm), which could result in decreased van der Waals interactions. Also, chlorine has a lower ability than oxygen to form hydrogen bonds. The substitution of either nitro group of DNP-glycine with chlorine results in decreases in affinity of factors of 5 to 10 (Table 7.1). This is similar to the values of 10-20 observed with protein 315 (Gettins et al., 1978). The decrease is not entirely accountable for in terms of a weakened stacking interaction, and presumably reflects additional small

differences in van der Waals or hydrogen bonding forces.

The contributions of the DNP ring and of the nitro groups to the total binding energy of protein A3 for DNP-lysine are therefore remarkably similar to those for protein 315. This provides further indirect evidence that protein 315 is representative of the naturally inducible pool of anti-DNP antibodies.

Protein A3 does not discriminate between DNP and TNP ligands. The binding constants of dinitroaniline and trinitroaniline, or of DNP-glycine and TNP-glycine are very similar (Table 7.1). In this property, protein A3 differs slightly from protein 315. Ligands such as trinitrophenol and trinitroaniline, in which the 6-nitro group is coplanar with the phenyl ring, bind approximately an order of magnitude more strongly to protein 315 than the dinitrophenyl analogues (Morris, 1979). However, there is little difference in the affinities of DNP ligands and the homologous TNP ligands with non-coplanar 6-nitro groups.

The ability of antisera to distinguish between structurally related ligands is an important feature of the immune response. It has been proposed that the heterogeneity of the antiserum and the absolute values of the affinities of the antibodies for any pair of ligands are the crucial parameters (Talmage, 1959; Johnston and Eisen, 1976). Protein A3 is able to bind the naphthoquinone ligand menadione with an affinity of 8×10^4 M^{-1} (Table 7.1), a decrease of about 200-fold from the affinity for DNP-lysine. Both the absolute value of this affinity and the difference between the affinities of menadione and DNP-lysine are very similar to the average values observed with anti-DNP antisera taken from late in the immune response in rabbits (Johnston and Eisen, 1976). If the heterogeneity of the anti-

serum is an important factor in determining its discriminatory ability, distinct antibodies from the same antiserum ought to have very different relative affinities for given pairs of ligands. A clear answer to this question can only be obtained by isolating several antibodies from a single immune response using the cell fusion technique. However, although the affinities of protein A3 for DNP-lysine and menadione are similar to the average values from an immune antiserum, those for DNP-lysine and dinitronaphthol are not. Dinitronaphthol, and the related compound flavianic acid, bind more tightly to protein A3 than does DNP-lysine (Table 7.1). Protein A3 may therefore be 'heteroclitic' (Mäkelä, 1965), since it was raised against DNP-KLH, and not against a dinitronaphthalene determinant. Dinitronaphthol was found to bind an order of magnitude more weakly than DNP-lysine to anti-DNP antibodies from guinea pigs (Michaelides and Eisen, 1974). The isolation of an antibody like protein A3 from such an antiserum would strongly support Talmage's theory.

The relative affinities of protein A3 for dinitronaphthol, DNP-lysine and menadione are similar to those of the myeloma protein 460, although the absolute magnitudes are much higher. It is therefore likely that the combining site of protein A3 is quite large, resembling that of protein 460 more than protein 315. It would be interesting to discover whether or not the V_H or V_L regions of the two proteins share substantial structural features.

Potential uses of the cell fusion technique

The cell fusion technique clearly has immense potential for the study of antibody specificity and function. As indicated in

the previous section, it will allow a more precise understanding of the role of heterogeneity and the occurrence of cross-reactivity in the immune response. The comparison of immunoglobulins of different subclasses, but with the same binding specificity, should greatly clarify our knowledge of the mechanism by which the secondary functions of antibodies are mediated. In addition, the study of several antibodies with differing affinities for the same ligand could be of interest for a detailed analysis of protein-ligand interactions, since the system is free from the complications of catalysis.

APPENDIX 7.1

Soft agar cloning

The soft agar medium contained 0.25% agar and 20% FCS (foetal calf serum) in HEPES 1640 (Flow R.P.M.I. 1640 with 10mM HEPES buffer, pH 7.35). Suitable dilutions of cells in 0.3 ml of soft agar medium were transferred to the wells of a Linbro plate. The wells initially contained 10000, 5000 or 2500 cells. The agar was left for 1 hr to set, and then 1.5 ml of R.P.M.I. 1640 containing 10% FCS were added to each well. The cells were incubated for 2 weeks, and the supernatants were then assayed. Single clones were picked from the lowest dilutions of cells giving antibody activity, and transferred with a Pasteur pipette to a micro-titre well. Approximately 30 clones were grown in 2 ml wells and then assayed.

REFERENCES

AMZEL, L.M., POLJAK, R.J., SAUL, F., VARGA, J.M. and RICHARDS, F.F. (1974). Proc. Nat. Acad. Sci. U.S.A. 71, 1427-1430.

ARATA, Y. and SHIMUZU, A. (1979). Biochemistry 18, 2513-2520.

ASHMAN, R.F. and METZGER, H. (1969). J. Biol. Chem. 244, 3405-3414.

ASKONAS, B.A. (1961). Biochem. J. 79, 33-43.

ASKONAS, B.A., WILLIAMSON, A.R. and WRIGHT, B.E.G. (1970). Proc. Nat. Acad. Sci. U.S.A. 67, 1398-1403.

BARISAS, B.G., STURTEVANT, J.M. and SINGER, S.J. (1971). Biochemistry, 10, 2816-2821.

BARISAS, B.G., SINGER, S.J. and STURTEVANT, J.M. (1972). Biochemistry 11, 2741-2744.

BARISAS, B.G., SINGER, S.J. and STURTEVANT, J.M. (1975). Immunochemistry 12, 411-421.

BARISAS, B.G., SINGER, S.J. and STURTEVANT, J.M. (1977). Immunochemistry 14, 247-252.

BARSTAD, P., HUBERT, J., HUNKAPILLER, M., GOETZE, A., SCHILLING, J., BLACK, B., EATON, B., RICHARDS, J., WEIGERT, M. and HOOD, L. (1978). Eur. J. Immunol. 8, 497-503.

BERNHARD, S.A., LEE, B.F. and TASHJIAN, Z.H. (1966). J. Mol. Biol. 18, 405-420.

BERNIER, G.M. and PUTNAM, F.W. (1963). Nature 200, 223-225.

BJÖRK, I. and TANFORD, C. (1971a). Biochemistry 10, 1271-1280.

BJÖRK, I. and TANFORD, C. (1971b). Biochemistry 10, 1280-1288.

BLASER, K. and EISEN, H.N. (1978). Proc. Nat. Acad. Sci. U.S.A. 75, 1495-1499.

BLUNDELL, T.L. and JOHNSON, L.N. (1976). Protein Crystallography, Academic Press.

BOESEL, R.W. and CARPENTER, F.H. (1970). Biochim. Biophys. Res. Commun. 38, 678-682.

BRIDGES, S.H. and LITTLE, J.R. (1972). Biochemistry 10, 2525-2530.

BURNET, F.M. (1959). The Clonal Selection Theory of Acquired Immunity, Camb. Univ. Press.

CAMPBELL, I.D., DOBSON, C.M., WILLIAMS, R.J.P. and WRIGHT, P.E. (1975). F.E.B.S. Lett. 57, 96-99.

CAREY, P.R., FROESE, A. and SCHNEIDER, H. (1973). Biochemistry 12, 2198-2208.

CARSTEN, M.E. and EISEN, H.N. (1953). J. Amer. Chem. Soc. 75, 4451-4456.

CARSTEN, M.E. and EISEN, H.N. (1955). J. Amer. Chem. Soc. 77, 1273-1277.

CHESBRO, B. and METZGER, H. (1972). Biochemistry 11, 766-771.

CHOTHIA, C. and JANIN, J. (1975). Nature 256, 705-708.

CLAFLIN, L. and MERCHANT, B. (1973). J. Immunol. 110, 252-261.

CLELAND, W.W. (1967). Adv. Enzymol. 29, 1-32.

COLMAN, P.M., DEISENHOFER, J., HUBER, R. and PALM, W. (1976). J. Mol. Biol. 100, 257-282.

COLMAN, P.M., SCHRAMM, H.J. and GUSS, J.M. (1977). J. Mol. Biol. 116, 73-79.

COTNER, T. and EISEN, H.N. (1978). J. Exp. Med. 148, 1388-1399.

CRUICKSHANK, D.W.J. (1949). Acta Cryst. 2, 65-82.

CUNNINGHAM, A.J. (1965). Nature 207, 1106-1107

DAVIE, J.M. and PAUL, W.E. (1972). J. Exp. Med. 135, 660-674.

DAVIES, D.R., PADLAN, E.A. and SEGAL, D.M. (1975a). Ann. Rev. Biochem. 44, 639-667.

DAVIES, D.R., PADLAN, E.A. and SEGAL, D.M. (1975b). Cont. Topics in Mol. Immunol. 4, 127-155.

DIMICOLI, J.L. and HÉLÈNE, C. (1973). J. Amer. Chem. Soc. 95, 1036-1044.

DINTZIS, H.M., DINTZIS, R.Z. and VOGELSTEIN, B. (1976). Proc. Nat. Acad. Sci. U.S.A. 73, 3671-3675.

DOWER, S.K. (1979). D.Phil. Thesis, Oxford.

DOWER, S.K., WAIN-HOBSON, S., GETTINS, P., GIVOL, D., JACKSON, W.R.C., PERKINS, S.J., SUNDERLAND, C.A., SUTTON, B.J., WRIGHT, C.E. and DWEK, R.A. (1977). Biochem. J. 165, 207-225.

DOWER, S.K., GETTINS, P., JACKSON, W.R.C., DWEK, R.A. and GIVOL, D. (1978). Biochem. J. 169, 179-188.

DOYLE, R.J., BELLO, J. and RICHOLT, O.A. (1968). Biochem. Biophys. Acta 160, 274-276.

DREYER, W.J. and BENNETT, J.C. (1965). Proc.Nat. Acad. Sci. U.S.A. 54, 864-869.

DUGAN, E.S., BRADSHAW, R.A., SIMMS, E.S. and EISEN, H.N. (1973). Biochemistry 12, 5400-5416.

DWEK, R.A. (1977). Cont. Topics in Mol. Immunol. 6, 1-52.

DWEK, R.A., GIVOL, D., JONES, R., McLAUGHLIN, A.C., WAIN-HOBSON, S., WHITE, A.I. and WRIGHT, C.E. (1976). Biochem. J. 155, 37-53.

DWEK, R.A., WAIN-HOBSON, S., DOWER, S.K., GETTINS, P., SUTTON, B.J., PERKINS, S.J. and GIVOL, D. (1977). Nature 266, 31-37.

EDELMAN, G.M. and POULIK, M.D. (1961). J. Exp. Med. 113, 861-884.

EDELMAN, G.M. and GALLY, J.A. (1962). J. Exp. Med. 116, 207-227.

EDELMAN, G.M., OLINS, D.E., GALLY, J.A. and ZINDER, N.D. (1963). Proc. Nat. Acad. Sci. U.S.A. 50, 753-761.

EDELMAN, G.M., CUNNINGHAM, B.A., GALL, W.E., GOTTLIEB, P.D., RUTISHAUSER, U. and WAXDEL, M.J. (1969). Proc. Nat. Acad. Sci. U.S.A. 63, 78-85.

EDMUNDSON, A.B., ELY, K.R., GIRLING, R.L., ABOLA, E.E., SCHIFFER, M. and WESTHOLM, F.A. (1974a). Prog. Immunol. II, 1, 103-113.

EDMUNDSON, A.B., ELY, K.R., GIRLING, R.L., ABOLA, E.E., SCHIFFER, M., WESTHOLM, F.A., FAUSCH, M.D. and DEUTSCH, H.F. (1974b). Biochemistry 13, 3816-3827.

EDMUNDSON, A.B., ELY, K.R., ABOLA, E.E., SCHIFFER, M. and PANAGIOTOPOULOS, N. (1975). Biochemistry 14, 3953-3961.

EISEN, H.N. and SISKIND, G.W. (1964). Biochemistry 3, 996-1008.

EISEN, H.N., LITTLE, J.R., OSTERLAND, C.K. and SIMMS, E.S. (1967). Cold Spring Harbour Symp. Quant. Biol. 32, 75-81.

EISEN, H.N., SIMMS, E.S. and POTTER, M. (1968). Biochemistry 7, 4126-4134.

EISEN, H.N., MICHAELIDES, M.C., UNDERDOWN, B.J., SCHULENBERG, E.P. and SIMMS, E.S. (1970). Fed. Proc. 29, 78-84.

ELY, K.R., FIRCA, J.R., WILLIAMS, K.J., ABOLA, E.E., FENTON, J.M., SCHIFFER, M., PANAGIOTOPOULOS, N.C. and EDMUNDSON, A.B. (1978). Biochemistry 17, 158-167.

EPP, O., LATTMAN, E.E., SCHIFFER, M., HUBER, R. and PALM, W. (1975). Biochemistry 14, 4943-4952.

ERWIN, P.M. and ALADJEM, F. (1976). Immunochemistry 13, 873-883.

FAHEY, J.L. (1961). J. Exp. Med. 114, 399-413.

FAHEY, J.L., CARBONE, P.P., ROWE, D.S. and BACHMAN, R. (1968). Amer. J. Med. 45, 373-380.

FARR, R.G. (1958). J. Infect. Dis. 103, 239-262.

FEHLHAMMER, H., SCHIFFER, M., EPP, O., COLMAN, P.M., LATTMAN, E.E., SCHWAGER, P., STEIGEMANN, W. and SCHRAMM, H.J. (1975). Biophys. Struct. Mech. 1, 139-146.

FEINSTEIN, A. and ROWE, A.J. (1965). Nature 205, 147-149.

FIRCA, J.R., ELY, K.R., KREMSER, P., WESTHOLM, F.A., DORRINGTON, K.J. and EDMUNDSON, A.B. (1978). Biochemistry 17, 148-157.

FLEISCHMAN, J.B., PAIN, R.H. and PORTER, R.R. (1962). Arch. Biochem. Biophys. Suppl. 1, 174-180.

FLEISCHMAN, J.B., PORTER, R.R. and PRESS, E.M. (1963). Biochem. J. 88, 220-228.

FOSTER, R. (1969). Organic Charge-Transfer Complexes, Academic Press.

FOSTER, R. and FYFE, C.A. (1965). Trans. Farad. Soc. 61, 1626-1631.

FRANCIS, S.H., LESLIE, R.G.Q., HOOD, L. and EISEN, H.N. (1974). Proc. Nat. Acad. Sci. U.S.A. 71, 1123-1127.

FRANEK, F. (1971). Eur. J. Biochem. 19, 176-183.

FREED, R.M., ROCKEY, J.H. and DAVIS, R.C. (1976). Immunochemistry 13, 509-515.

FROESE, A. (1968). Immunochemistry 5, 253-264.

FROESE, A. and SEHON, A.H. (1975). Cont. Topics in Mol. Immunol. 4, 23-54.

GARTLAND, G.L., FREEMAN, G.R. and BUGG, C.E. (1974). Acta Cryst. B30, 1841 1849.

GAVISH, M., DWEK, R.A. and GIVOL, D. (1977). Biochemistry 16, 3154-3159.

GAVISH, M., DWEK, P A. and GIVOL, D. (1978). Eur. J. Immunol. 8, 42-46.

GAVISH, M., BEN-NERIAH, Y., ZAKUT, R., GIVOL, D., DWEK, R.A. and JACKSON, W.R.C. (1979). Molec. Immunol. in press.

GETTINS, P. (1979). Thesis submitted for D.Phil., Oxford.

GETTINS, P., POTTER, M., RUDIKOFF, S. and DWEK, R.A. (1977). F.E.B.S. Lett. 84, 87-91.

GETTINS, P., GIVOL, D. and DWEK, R.A. (1978). Biochem. J. 173, 713-722.

GIVOL, D., STRAUSBACH, P.H., HURWITZ, E., WILCHEK, M., HAIMOVICH, J. and EISEN, H.N. (1971). Biochemistry 10, 3461-3466.

GLASER, A.N. (1970). Proc. Nat. Acad. Sci. U.S.A. 65, 1057-1063.

GLASER, M. and SINGER, S.J. (1971). Proc. Nat. Acad. Sci. U.S.A. 68, 2477-2479.

GOETZL, E.J. and METZGER, H. (1970a). Biochemistry 9, 1267-1278.

GOETZL, E.J. and METZGER, H. (1970b). Biochemistry 9, 3862-3871.

GOIDL, E.W., PAUL, G.W., SISKIND, G.W. and BENACERRAF, B. (1968). J. Immunol. 100, 371-375.

GOODMAN, J.W. and DONCH, J.J. (1965). Immunochemistry 2, 351-357.

GRANATO, D., BRAUN, D.G. and VASSILLI, P. (1974). J. Immunol. 113, 417-427.

GREEN, R.W. (1973). Biochemistry 12, 3225-3231.

GREY, H.M. and MANNIK, M. (1965). J. Exp. Med. 122, 619-632.

GRUBB, R. (1956). Acta Path. Microbiol. Scand. 39, 195-197.

GURNEY, R.W. (1953). Ionic Processes in Solution, McGraw-Hill, p.90.

HABER, E. and RICHARDS, F.F. (1966). Proc. Roy. Soc. Ser. B. 166 176-187.

HABER, E., RICHARDS, F.F., SPRAGG, J., AUSTEN, K.F., VALLOTTON, M. and PAGE, C.B. (1967). Cold Spring Harbour Symp. Quant. Biol. 32, 299-310.

HADLER, N.M. and METZGER, H. (1971). Proc. Nat. Acad. Sci. U.S.A. 68, 1421-1424.

HAIMOVICH, J. and du PASQUIER, L. (1973). Proc. Nat. Acad. Sci. U.S.A. 70, 1898-1902.

HAIMOVICH, J., GIVOL, D. and EISEN, H.N. (1970). Proc. Nat Acad. Sci. U.S.A. 67, 1656-1661.

HALSEY, J.F. and BILTONEN, R.L. (1975). J. Soln. Chem. 4, 275-283.

HANNA, M.W. and ASHBAUGH, A.L. (1964). J. Phys. Chem. Ithaca 68, 811-816.

HANSON, A.W. (1964). Acta Cryst. 17, 559-568.

HARDY, R.R. and RICHARDS, J.H. (1978). Biochemistry 17, 3866-3871.

HASELKORN, D., FRIEDMAN, S., GIVOL, D. and PECHT, I. (1974). Biochemistry 13, 2210-2222.

HELMAN, M., SCHREIER, I. and GIVOL, D. (1976). J. Immunol. 117, 1933-1937.

HILSCHMAN, N. and CRAIG, L.C. (1965). Proc. Nat. Acad. Sci. U.S.A. 53, 1403-1409.

HOCHMAN, J., INBAR, D. and GIVOL, D. (1973). Biochemistry 12, 1130-1135.

HONG, R. and NISONOFF, A. (1966). J. Immunol. 96, 622-628.

HOOKER, S.B. and BOYD, U.C. (1933). J. Immunol. 25, 61-69.

HSIA, J.C. and PIETTE, L.H. (1969). Arch. Biochem. Biophys. 129, 296-307.

IKAI, A. and TANFORD, C. (1973). J. Mol. Biol. 73, 145-163.

INBAR, D., HOCHMAN, J. and GIVOL, D. (1972). Proc. Nat. Acad. Sci. U.S.A. 69, 2659-2662.

INMAN, J.K. (1973). Fed. Proc. 32, 957 (No. 4141).

ISENMAN, D.E., LANCET, D. and PECHT, I. (1979). Biochemistry in press.

JACKMAN, L.M. and STERNHELL, S. (1969). Applications of nuclear magnetic resonance spectroscopy in organic chemistry, Pergamon Press, pp.88-92.

JANEWAY, C.A., WIGZELL, H. and BINZ, H. (1976). Scand. J. Immunol. 5, 993-1001.

JANIN, J. and CHOTHIA, C. (1976). J. Mol. Biol. 100, 197-211.

JANIN, J. and CHOTHIA, C. (1978). Biochemistry 17, 2943-2948.

JENCKS, W.P. (1969). Catalysis in Chemistry and Enzymology, McGraw-Hill, p.421.

JENSENIUS, J.C., WILLIAMS, A.F. and MOLE, L.E. (1977). Eur. J. Immunol. 7, 104-110.

JOHNSON, C.E. and BOVEY, F.A. (1958). J. Chem. Phys. 29, 1012-1014.

JOHNSTON, M.F.M. and EISEN, H.N. (1976). J. Immunol. 117, 1189-1196.

JOHNSTON, M.F.M., BARISAS, B.G. and STURTEVANT, J.M. (1974). Biochemistry 13, 390-396.

JONES, H.B. (1848). Phil. Trans. Roy. Soc. 138, 55-62.

KABAT, E.A. (1960). J. Immunol. 84, 82-85.

KABAT, E A. and WU, T.T. (1971). Ann. N.Y. Acad. Sci. 190, 382-393.

KABAT, E.A., WU, T.T. and BILOVSKY, H. (1976). Variable Region Sequences of Immunoglobulin Chains, Medical Computer Systems, Bolt Beranek and Newman, Inc., Cambridge, Mass.

KARUSH, F. (1962). Adv. in Immunol. 2, 1-40.

KAUZMANN, W. (1959). Adv. in Prot. Chem. 14, 1-63.

KECK, K., GROSSBERG, A.L. and PRESSMAN, D. (1973). Immunochemistry 10, 331-335.

KLINMAN, N.R. (1971). J. Immunol. 106, 1330-1337.

KLINMAN, N.R. (1972). J. Exp. Med. 136, 241-260.

KLINMAN, N.R. and PRESS, J.L. (1975a). J. Exp. Med. 141, 1133-1146.

KLINMAN, N.R. and PRESS, J.L. (1975b). Trans. Rev. 24, 41-83.

KLINMAN, N.R., PRESS, J.L. and SEGAL, G.P. (1973). J. Exp. Med. 138, 1276-1281.

KLOSTERGAARD, J., MAYERS, G.L., GROSSBERG, A.L. and PRESSMAN, D. (1978). Immunochemistry 15, 225-230.

KÖHLER, G. and MILSTEIN, C. (1975). Nature 256, 495-497.

KÖHLER, G., HOWE, S.C. and MILSTEIN, C. (1976). Eur. J. Immunol. 6, 292-301.

KOOISTRA, D.A. and RICHARDS, J.H. (1978). Biochemistry 17, 345-351.

KRETH, H.W. and WILLIAMSON, A.R. (1973). Eur. J. Immunol. 3, 141-147,

KUMAR, K., PHELPS, D.J., CAREY, P.R. and YOUNG, N.M. (1978). Biochem. J. 175, 727-735.

KUNKEL, H.G. (1970). Fed. Proc. 29, 55-58.

LANCET, D. and PECHT, I. (1976). Proc. Nat. Acad. Sci. U.S.A. 73, 3549-3553.

LANCET, D., LICHT, A., SCHECHTER, I. and PECHT, I. (1977). Nature 269, 827-829.

LANDAUER, J. and McCONNELL, H. (1952). J. Amer. Chem. Soc. 74, 1221-1224.

LANDSTEINER, K. (1945). The Specificity of Serological Reactions, Harvard Univ. Press.

LEVITT, M. (1974). J. Mol. Biol. 82, 393-420.

LICHT, A. LANCET, D., SCHECHTER, I. and PECHT, I. (1977). F.E.B.S. Letts 78, 211-215.

LITTLE, J.R. and EISEN, H.N. (1966). Biochemistry 5, 3385-3393.

LITTLE, J.R. and EISEN, H.N. (1967). Biochemistry 6, 3119-3125.

LITTLE, J.R. and EISEN, H.N. (1969). J. Exp. Med. 129, 247-265.

LUZZATTI, P.V. (1952). Acta Cryst. 5, 802-810.

MACARIO, A.J.L. and CONWAY de MACARIO, E. (1973). Nature 245, 263-264.

MÄKELÄ, O. (1965). J. Immunol. 95, 378-381.

MANJULA, B.N., RICHARDS, F.F. and ROSENSTEIN, R.W. (1976). Immunochemistry 13, 929-937.

MASON, D.W. and WILLIAMS, A.F. (1979). submitted to Biochem. J.

McGUIGAN, J.E. and EISEN, H.N. (1968). Biochemistry 7, 1919-1928.

MELCHER, U. and UHR, J.W. (1976). J. Immunol. 116, 409-415.

MELCHER, U., VITETTA, E.S., McWILLIAMS, M., LAMM, M.E., PHILLIPS-QUAGLIATA, J.M. and UHR, J.W. (1974). J. Exp. Med. 140, 1427-1431.

METZGER, H. (1978). Cont. Topics in Mol. Immunol. 7, 119-152.

MICHAELIDES, M.C. and EISEN, H.N. (1974). J. Exp. Med. 140, 687-702.

MONTGOMERY, P.C., ROCKEY, J.H., KAHN, R.L. and SKANDON, C.A. (1975). J. Immunol. 115, 904-910.

MORRIS, A.T. (1979). Thesis submitted for D.Phil., Oxford.

MORRIS, A.T., GIVOL, D. and DWEK, R.A. (1978). Immunochemistry 15, 519-522.

NIALL, H.D. and EDMAN, P. (1967). Nature 216, 262-263.

NISONOFF, A., HOPPER, J.E. and SPRING, S.B. (1975). The Antibody Molecule, Academic Press.

ORIN, G.B., DAVIS, R.C., FREED, R.M. and ROCKEY, J.H. (1976). Immunochemistry 13, 517-523.

OSTERLAND, C.K., MILLER, E.J., KARAKAWA, W.W. and KRAUSE, R.M. (1966). J. Exp. Med. 123, 599-614.

OUDIN, J. (1956). C.R. Acad. Sci. Paris 242, 2489-2490.

OUDIN, J. (1966). Proc. Roy. Soc. Ser. B 166, 207-219.

OWEN, J.A., GOT, C. and SILBERMAN, H.J. (1958). Clin. Chem. Acta 3, 605-607.

PADLAN, E.A. (1977). Quart Rev. Biophys. 10, 35-65.

PADLAN, E.A. (1979). Molec. Immunol. 16, 287-296.

PADLAN, E.A. and DAVIES, D.R. (1975). Proc. Nat. Acad. Sci. U.S.A. 72, 819-823.

PADLAN, E.A., DAVIES, D.R., PECHT, I., GIVOL, D. and WRIGHT, C.E. (1976a). Cold Spring Harbour Symp. Quant. Biol. 41, 627-637.

PADLAN, E.A., DAVIES, D.R., RUDIKOFF, S. and POTTER, M. (1976b). Immunochemistry 13, 945-949.

PAGE, M.I. and JENCKS, W.P. (1971). Proc. Nat. Acad. Sci. U.S.A. 68, 1678-1683.

PAINTER, R.G., SAGE, H.J. and TANFORD, C. (1972). Biochemistry, 11, 1327-1337.

PARKER, C.W. and OSTERLAND, C.K. (1970). Biochemistry 9, 1074-1082.

PAUL, W.E., YOSHIDA, T. and BENACERRAF, B. (1970). J. Immunol. 105, 314-321.

PERKINS, S.J. and DWEK, R.A. (1979). Biochemistry, in press.

PERKINS, S.J., DOWER, S.K., GETTINS, P., WAIN-HOBSON, S. and DWEK, R.A. (1977). Biochem. J. 165, 223-225.

PERNIS, B., CHIAPPINO, G., KELUS, A.S. and GELL, P.G.H. (1965). J. Exp. Med. 122, 853-876.

PINK, J.R.L. and ASKONAS, B.A. (1974). Eur. J. Immunol. 4, 426-430.

POLJAK, R.J. (1975). Adv. in Immunol. 21, 1-33.

POLJAK, R.J. (1978). Comprehensive Immunology 5, 1-36.

POLJAK, R.J., AMZEL, L.M., AVEY, H.P., CHEN, B.L., PHIZACKERLEY, R.P. and SAUL, F. (1973). Proc. Nat. Acad. Sci. U.S.A. 70, 3305-3310.

POLJAK, R.J., AMZEL, L.M., CHEN, B.L., PHIZACKERLEY, R.P. and SAUL, F. (1974). Proc. Nat. Acad. Sci. U.S.A. 71, 3440-3444.

POLJAK, R.J., AMZEL, L.M. and PHIZACKERLEY, R.P. (1976). Prog. Biophys. Molec. Biol. 31, 67-93.

POPLE, J.A. (1962). J. Chem. Phys. 37, 60-66.

PORTER, R.R. (1959a). Biochem. J. 73, 119-126.

PORTER, R.R. (1959b). Methods in Medical Research, Gerard, R.W. (ed.) Year Book, Chicago 3, 256-271.

POTTER, M. (1972). Phys. Rev. 52, 631-719.

POTTER, M., PADLAN, E. and RUDIKOFF, S. (1976). J. Immunol. 117, 626-629.

RAYNAUD, M. and MANGALO, R. (1967). Ann. Inst. Pasteur, Paris 113, 549-567.

RICHARDS, F.F., KONIGSBERG, W.H., ROSENSTEIN, R.W. and VARGA, J.M. (1975). Science 187, 130-137.

RIESEN, W.F. and JATON, J.-C. (1976). Biochemistry 15, 3829-3833.

RIESEN, W.F., BRAUN, D.G. and JATON, J.-C. (1976). Proc. Nat. Acad. Sci. U.S.A. 73, 2096-2100.

RIORDAN, J.F., SOKOLOVSKY, M. and VALLEE, B.C. (1967). Biochemistry 6, 358-361.

RITTENBERG, M.B. and PRATT, R.L. (1969). Proc. Exp. Soc. Biol. Med. 132, 575-581.

ROCKEY, J.H., MONTGOMERY, P.C., UNDERDOWN, B.J. and DORRINGTON, K.J. (1972). Biochemistry 11, 3172-3181.

ROHOLT, O.A., RADZIMSKI, G. and PRESSMAN, D. (1965). Science 147, 613-615.

ROSENSTEIN, R.W. and RICHARDS, F.F. (1976). Immunochemistry 13, 939-943.

ROSS, S.D. and LABES, M.M. (1957). J. Amer. Chem. Soc. 79, 76-80.

RUDIKOFF, S. and CLAFLIN, J.L. (1976). J. Exp. Med. 144, 1294-1304

SARMA, V.R., SILVERTON, E.W., DAVIES, D.R. and TERRY, W.D. (1971). J. Biol. Chem. 246, 3753-3759.

SAUL, F.A., AMZEL, L.M. and POLJAK, R.J. (1978). J. Biol. Chem. 253, 585-597.

SCHALCH, W., WRIGHT, J.K., RODKEY, L.S. and BRAUN, D.G. (1979). J. Exp. Med. 150, 923-937.

SCHECHTER, B., SCHECHTER, I. and SELA, M. (1970). J. Biol. Chem. 245, 1438-1447.

SCHECHTER, I., SCHECHTER, B. and SELA, M. (1966). Biochim. Biophys Acta 127, 438-456.

SCHECHTER, I.. ZIV, E. and LICHT, A. (1976). Biochemistry 15, 2785-2790.

SCHIFFER, M., GIRLING, R.L., ELY, K.R. and EDMUNDSON, A.B. (1973). Biochemistry 12, 4620-4631.

SCHLESSINGER, J., STEINBERG, I.Z., GIVOL, D., HOCHMAN, J. and PECHT, I. (1975). Proc. Nat. Acad. Sci. U.S.A. 72, 2775-2779.

SCHMIT-ADERJAN, U., RÖSCH, P., FRANK, R. and HENGSTENBERG, W. (1979). Eur. J. Biochem. 96, 43-48.

SCHUBERT, W.M., STEADLY, H. and CRAVEN, J.M. (1960). J. Amer. Chem. Soc. 82, 1353-1356.

SEGAL, D.M., PADLAN E.A., COHEN, G.H., RUDIKOFF, S., POTTER, M. and DAVIES, D.R. (1974). Proc. Nat. Acad. Sci. U.S.A. 71, 4298-4302.

SIRISINHA, S. and EISEN, H.N. (1971). Proc. Nat. Acad. Sci. U.S.A. 68, 3130-3135.

SNYDER, G.H., ROWAN, R., KARPLUS, S. and SYKES, B.D. (1975). Biochemistry 14, 3765-3777.

SOKOLOVSKY, M., RIORDAN, J.F. and VALLEE, B.L. (1966). Biochemistry 5, 3582-3589.

SOLOMON, A. (1976). N. Engl. J. Med. 294, 17-23.

SOLOMON, A. and McLAUGHLIN, C.L. (1969). J. Biol. Chem. 244, 3393-3404.

STEINER, L.A. and EISEN, H.N. (1967). J. Exp. Med. 126, 1143-1183.

STERNLICHT, H. and WILSON, D. (1967). Biochemistry 6, 2881-2892.

STEVENSON, G.T. (1974). Biochem. J. 139, 369-374.

SZENT-GYÖRGI, A. (1960). Introduction to Submolecular Biology, Academic Press.

SZEWZUK, M.R. and MUKKUR, T.K.S. (1977). Immunol. 32, 111-119.

TALMAGE, D.W. (1959). Science 129, 1643-1648.

TONEGAWA, S., MAXAM, A.M., TIZARD, R., BERNHARD, O. and GILBERT, W. (1978). Proc. Nat. Acad. Sci. U.S.A. 75, 1485-1489.

UTSUMI, S. and KARUSH, F. (1964). Biochemistry 3, 1329-1338.

VALENTINE, R.C. and GREEN, N.M. (1967). J. Mol. Biol. 27, 615-617.

VARGA, J.M., KONIGSBERG, W.H. and RICHARDS, F.F. (1973). Proc. Nat. Acad. Sci. U.S.A. 70, 3269-3274.

VELICK, S.F., PARKER, C.W. and EISEN, H.N. (1960). Proc. Nat. Acad. Sci. U.S.A. 46, 1470-1482.

VINCENT, J.P., LAZDUNSKI, M. and DELAAGE, M. (1970). Eur. J. Biochem. 12, 250-257.

VOSS, E.W. and EISEN, H.N. (1968). Fed. Proc. 27, 684 (No. 2631).

VOSS, E.W. and WATT, R.M. (1977). Immunochemistry 14, 237-246.

WAIN-HOBSON, S. (1977). D.Phil. Thesis, Oxford.

WAIN-HOBSON, S., DOWER, S.K., GETTINS, P., GIVOL, D., McLAUGHLIN, A.C., PECHT, I., SUNDERLAND, C.A. and DWEK, R.A. (1977). Biochem. J. 165, 227-235.

WANG, B.-C., YOO, C.S. and SAX, M. (1979). J. Mol. Biol. 129, 657-674.

WELLS, J.V., FUDENBERG, H.H. and GIVOL, D. (1973). Proc. Nat. Acad. Sci. U.S.A. 70, 1585-1587.

WERBLIN, T.P. and SISKIND, G.W. (1972). Immunochemistry 9, 987-1011.

WILDER, R.L., GREEN, G. and SCHUMAKER, V.N. (1975). Immunochemistry 12, 55-60.

WILLIAMS, A.F., GALFRÈ , G. and MILSTEIN, C. (1977). Cell 12, 663-673.

WILLIAMSON, A.R. and ASKONAS, B.A. (1972). Nature 238, 337-339.

WU, T.T. and KABAT, E.A. (1970). J. Exp. Med. 132, 211-250.

YGUERABIDE, J., EPSTEIN, H.F. and STRYER, L. (1970). J. Mol. Biol. 51, 573-590.

YOO, T.J., ROHOLT, O.A. and PRESSMAN, D. (1967). Science 157, 707-709.

YOSHIDA, T., PAUL, W.E. and BENACERRAF, B. (1970). J. Immunol. 105, 306-313.

Table 5.5 Kinetic and fluorescence enhancement parameters for the conformational change of the V_L dimer of protein 315 in pH jump experiments

Measurements were made using solutions in 0.05M sodium acetate (pH 4.8) and 0.05M Tris (pH 8.3), T = 298K. Stock solutions of V_L dimer (2 mg/ml) were diluted into the appropriate buffer. Protein fluorescence was excited at 285 nm and measured at 335 nm, using excitation and emission slit widths of 7 nm. The enhancement parameter, ε, is defined as the ratio of the fluorescence intensity at high pH to that at low pH. It was calculated by taking the ratio of the observed fluorescence intensity at $t = \infty$ to the extrapolated intensity at $t = 0$, using the semi-log plots of Figure 5.14.

V_L dimer concentration (μM)	pH jump						
	4.8 to 8.3		8.3 to 4.8				
	k (s^{-1})	ε	k_{slow}(s^{-1})	k_{fast}(s^{-1})	$\varepsilon_{overall}$	ε_{slow}	ε_{fast}
3.0	1.27×10^{-3}	2.09	1.06×10^{-3}	1.59×10^{-2}	2.23	1.40	1.59
1.0	1.56×10^{-3}	2.20	0.99×10^{-3}	1.64×10^{-2}	2.24	1.31	1.71
0.3	1.85×10^{-3}	2.61	1.10×10^{-3}	1.40×10^{-2}	2.27	1.47	1.55